Remote Sensing of Natural Scots Pine Regeneration

David Shaw

Ph.D.

The University of Edinburgh

2001

ABSTRACT

The regeneration of native Scots pine forest has become an important objective of conservation management within Scotland. Management practices are being employed to encourage regeneration by natural means, but quantitatively monitoring progress is difficult to achieve on the ground. The study explores the potential application of optical remote sensing to monitoring natural regeneration. However, there is currently a lack of understanding of the detailed spectral and spatial properties of such semi-natural landscapes. The study addresses this problem through detailed analysis of the spectral and spatial properties of regions of natural regeneration at Inshriach and Rothiemurcus in the Cairngorms National Nature Reserve, Scotland.

High-spectral resolution field-spectroradiometeric data (400 - 2500 nm) were collected over the growing seasons of 1997 and 1998 over sample plots. A method was developed to measure Leaf Area Index (LAI) within the sample plots and correlation analysis was used to assess the relationship of both LAI and percentage cover (PC) with reflectance and first-derivative reflectance. LAI and PC correlated most strongly with reflectance indices involving red and NIR wavelengths, such as the Simple Ratio (SR), NDVI and R_{752}/R_{722}. Derivative indices involving the red-edge (D_{730}/D_{700} and D_{719}/D_{703}), the green-edges (D_{520} and D_{570}), and the NIR at D_{1150}, also correlated strongly with LAI and PC. Two peaks were identified on the derivative red-edge feature (D_{719} and D_{703}), with D_{719} becoming more prominent with increasing LAI and PC. Red-edge position correlated more strongly with PC than with LAI, but a sudden switching of REP to longer wavelengths was identified with increasing sapling amount, rather than a smooth progression. These relationships were unaffected by seasonal changes in the heather understorey reflectance at the sites investigated.

A hybrid geometric-optical canopy reflectance model (FLIGHT) was used to simulate the canopy reflectance of the sample plots. Model scenarios were run to account for changing LAI, PC and crown needle density. A method was developed and tested in order to measure the optical properties of Scots pine needles (400 - 1000 nm), which were used as model input data. Mean seasonal reflectance (MSR) of the sample plots was well represented by the modelled spectra, with the greatest variance occurring in the blue and NIR wavelength regions. This was attributed to fine-scale crown structure not accounted for within the model. Derivative modelled spectra corresponded well with MSR derivative spectra as a descriptor of reflectance spectra shape. The model confirmed the sensitivity of reflectance indices in the NIR and red-edge derivative indices to canopy LAI and PC, whilst also confirming the insensitivity of the REP to PC. Crown density was less influential on both reflectance and derivative reflectance than LAI or PC.

Geostatistical analysis of digitized aerial photographs using the semivariogram was used to characterise the textural properties of different stages of regeneration. Directional perpendicular (to the Sun's rays) semivariograms from H-resolution images were recommended for estimating within-plot structural variables, such as mean crown size. An optimal spatial resolution of between 1.0 and 2.0 m was recommended for separation of regeneration stage.

The study highlights the need for detailed ground-based studies that take into account the information requirement of forest managers, the range of remote sensing research techniques available and current research issues within landscape ecology. Digitised aerial photography was recommended for inventory and mapping of regeneration sites, whilst the reflectance and derivative indices proposed for measuring pine sapling amount need to be tested using hyperspectral airborne imagery.

DECLARATION

I declare that this thesis has been composed by myself and the work presented and described is my own, unless otherwise stated.

David Shaw, November 2001

ACKNOWLEDGEMENTS

This study was supported and funded by the UK National Environment Research Council (NERC) as a CASE studentship (GT04/97/84/EO), with Scottish Natural Heritage (SNH).

I gratefully acknowledge the assistance of a number of people in completing this work. David Duncan (SNH, Aviemore Area Office) and Dr John Kupiec (formerly at SNH) for their discussions, advice and access to Inshriach. Fieldwork would not have been possible without the assistance of Lennart Beringer, John Watson, Evanthia Karpouzli, Jurgen Holzner and Alex Jackson, who made the radiometer stand. I am particularly grateful to Nick Hardy for his help with fieldwork and laboratory measurements, and to David Emery (former manager of the NERC Equipment Pool of Spectroscopy) for his technical support. GPS equipment and support was supplied by the NERC Geophysical Equipment Pool.

Assistance was also provided at the Dept of Geography, University of Edinburgh, by Anona Lyons (map production), Chris Place (technical support), Dr Andrew Grout (digital camera work) and Dr Richard Hedger whose knowledge of geostatistics was invaluable. Dr Peter North (formerly ITE, Monkswood, now of Geography, University of Wales, Swansea) supplied his FLIGHT model and advice. Finally, completion of this thesis would not have been possible without the support of Andrew. I especially acknowledge the time, professional assistance and direction given by my supervisor, Dr Tim Malthus; his input has been instrumental to every stage of this thesis, from conception to the final draft.

TABLE OF CONTENTS

LIST OF FIGURES

LIST OF TABLES

LIST OF PLATES

1.0 INTRODUCTION

1.1 Rationale

The potential advantages of applying remote sensing data to monitoring vegetation change are well rehearsed in the literature. The advantages of optical remote sensing data over field survey and aerial photographic interpretation include the provision of quantitative, timely and synoptic data at a lower per hectare cost. However, these advantages have largely not been realised in the application of remote sensing to monitoring semi-natural landscapes. This study identifies the problems associated with using optical remote sensing to monitor natural regeneration of Scots pine in Scotland. A greater understanding of the particular requirements of remotely sensed data is achieved through the application of a range of current techniques within remote sensing research. These include the analysis of high-spectral resolution data, detailed optical measurements of pine needles, geostatistical techniques for spatial analysis of image texture and a physical modelling approach.

Quantitative data are provided through the relation between measured reflectance and vegetation canopy biophysical properties. For example, relationships have been established between visible and near infrared (NIR) wavelengths and vegetation characteristics (e.g. Knipling, 1970; Tucker, 1979). Whilst much work has explored these relationships for forest cover, there is a lack of information relating the spectral properties of saplings in semi-natural environments to typical vegetation variables, such as percentage cover or Leaf Area Index (LAI). Pitt *et al.* (1997) identify a need for discovery and definition of spectral signatures for young crop and non-crop forest plants. This becomes more important for semi-natural environments where a more complex mix of species conspire to confuse the signal of interest. For sensors with a lower spectral resolution, any quantitative relation between the vegetation element of

interest and measured reflectance becomes increasingly uncertain. Consequently, applications of remotely sensed data to conservation in Scotland using Landsat TM data, for example, have been confined to mapping broad habitat types (e.g. Hubbard and Wright, 1982; Belward *et al.*, 1990).

The problem of spectral inseparability may be addressed by analysing finer spectral resolution data, thereby increasing the potential for information extraction (Curran and Kupiec, 1995). There is evidence that the application of such high-spectral resolution data through imaging spectroscopy is becoming recognized as a tool in ecological investigations (e.g. Ustin, 1991; Vane and Goetz, 1993). High-spectral resolution data also enable the employment of background noise reduction techniques, such as derivative spectroscopy (Demetriades-Shah *et al.*, 1990). Fine-scale spectral features, such as the derivative red-edge peak, may also aid species discrimination (Gong *et al.*, 1997) and can be related to canopy variables such as LAI (Danson and Plummer, 1995). Zarco-Tejada and Miller (1999) point out that there is a paucity of field data for studying the sensitivity of red-edge parameters to canopy structure, especially for open conifer canopies.

Having established relationships between measured reflectance and canopy variables, there often remains further unanswered questions on the nature of these relationships under the highly complex range of data acquisition and environmental conditions that exist, particularly for semi-natural systems. Canopy reflectance models have developed rapidly in type and complexity and offer a potential solution to unravelling some of this complexity. A need has been identified for research in the area of modelling reflectance of coniferous species (e.g. Myneni *et al.*, 1995).

Timely data are easily provided by most remote sensing platforms. Monitoring of ecological processes is defined by Hellawell (1991) as 'surveillance carried out in order to ascertain the extent of compliance with a predetermined standard of degree of deviation from an expected norm'. Monitoring by remote sensing is therefore concerned with change detection from a defined and understood baseline. Varying rates of environmental change may undermine change detection and this is

particularly true for semi-natural vegetation where, seasonal, phenological and longer-term environmental change may be measured concurrently. For example, the monitoring of Scots pine regeneration is relatively long-term in comparison with seasonal change and it is therefore important to predetermine any seasonal effects before the change of interest can be ascertained. There is currently a lack of information on the magnitude of seasonal changes to longer-term changes for many vegetation types at a range of scales (Lambin, 1996).

Synoptic data are provided through the superior spatial coverage of remotely sensed data, particularly over ground-based survey methods. In general, spatial resolution is reduced as spatial coverage increases. For detailed landscape monitoring, it is now widely accepted that the utility of remotely sensed data for ecological applications is related to scale (e.g. Woodcock and Strahler, 1987; Curran and Williamson, 1987; 1988; Davis, *et al.*, 1991; Weiler and Stow, 1991 and Hyppänen, 1996). Spatial resolution has therefore become a primary consideration because ecological pattern and process information changes with scale (Wickland, 1989) and an optimal scale of observation will exist for different applications. Furthermore, when appropriate spatial resolution imagery is employed, it may be possible to relate statistical measures of image texture to the size, orientation and shape of the landscape elements of interest (e.g. St-Onge and Cavayas, 1995; 1997; Coops and Culvenor, 2000).

1.2 Context

Data for monitoring natural regeneration are required by forest mangers to meet the increasing emphasis on ecosystem management (e.g. Ratcliffe *et al.*, 1997) and legislative demands for improved reporting of progress (Kupiec, 1997). For example, Article 11 of the EC Habitats and Species Directive requires surveillance of the conservation status of habitats in the newly designated European Natura 2000 sites, of which the Cairngorms is one such site. Article 17 requires evaluation and reporting of the impact of conservation measures undertaken to protect and enhance the network.

Forest regeneration management is seen as an essential part of current forestry practice, which is moving away from large-scale, clear-cut and replant methods towards a continuous growth philosophy. Natural forest regeneration may take place within areas of clearcut managed forestry or within semi-natural landscapes. Sufficient inventory data may already exist, but there may also be a lack of inventory data in the form of geo-referenced base maps depicting each element of the semi-natural or silvicultural landscape mosaic. A first step is therefore an inventory of current areas of regeneration and/or sites suitable for establishment. This may involve a range of environmental data such as soil, relief and vegetation community data, ideally within a GIS environment. A next step might be the identification of regeneration establishment at the seedling stage (< 0.5 m). In a UK context, inventory and mapping to identify and measure the extent of regeneration is perhaps less important to forest managers, since the location of sites is generally known.

Management is often required, however, to assist establishment by controlling competition and browsing pressures. Information may therefore be required on species composition and cover, tree height and health, and stage of regeneration. It is this within-stand level of information requirement that provides a context for this research. For example, Scots pine regeneration is considered safe from browsing pressure once a tree height over 2 m is reached. Identification of species may also

required to assess ecological diversity. The information requirement therefore focusses on the monitoring of progress, which may be tackled in remote sensing terms as a problem of measuring vegetation type and amount at appropriate spatial and temporal scales.

Ideally, such data will take advantage of technological advances, such as GIS and improvements in computer software and hardware, but must also be cost-effective, timely, objective, quantitative and spatially accurate, as discussed in the previous section. Remotely sensed data (satellite, airborne optical, radar and laser sensors) largely meet these requirements. However, such data have not been utilized for forest regeneration management (Pitt *et al.*, 1997). This study seeks to address this problem by matching the information requirement for monitoring natural Scots pine regeneration with current methods of optical high-spectral resolution remote sensing and geostatistical methods of image textural analysis.

1.3 Aims and Objectives

The study takes a ground-based approach in order to characterise the spatial and spectral properties of Scots pine regeneration with a view to defining a remote sensing system to monitor regeneration. Often, applied research in remote sensing takes the opposite approach; take some available imagery and explore its potential for a chosen application using well-established techniques. A problem with the latter approach is that whilst it can help to inform the remote-sensing researcher about the merits of his/her data, it may not assist the forest manager or ecologist in providing the information they need. As the range of sensor types available increases, it is the responsibility of the remote-sensing researcher to fully understand the nature of the information requirement on the ground in order to select the appropriate techniques and sources of data.

Often this information requirement necessitates tackling research issues that overlap disciplines. For example, the research issues relating to scale in landscape ecology are essentially the same in remote sensing. The landscape ecologist may ask; what is the appropriate landscape scale to monitor natural regeneration? The remote-sensing researcher may ask; what is the appropriate ground pixel resolution for monitoring natural regeneration? The questions are essentially the same. This kind of overlap is important in remote-sensing research, which is in danger of being regarded purely in terms of a technology with little practical purpose in forest management (e.g. Meyer and Werth, 1990; Holmgren and Thuresson, 1998).

The study therefore sets out with no preconception that a particular remote-sensing system will provide all the necessary information for regeneration management. However, it is beyond the scope of a single study to consider all sensor types. Radar and lidar systems will no doubt have a role to play in the mapping and inventory of forest structure and tree height. The objective of this study is to address the current lack of information on the spectral and spatial properties of natural Scots pine regeneration through the following specific aims:

1) To use *in situ* hyper-spectral reflectance data to propose wavelengths most suitable for monitoring Scots pine regeneration.
2) To investigate seasonal changes in reflectance and their effect on established relations between measured reflectance and canopy parameters, LAI and percentage cover.
3) To measure the optical properties of Scots pine needles for model input data.
4) To understand the role of LAI, percentage cover, and tree crown needle density on measured reflectance using a canopy reflectance model.
5) To relate geostatistical measures of image texture to the spatial properties of different stages of Scots pine regeneration.
6) To propose an optimal spatial resolution for monitoring natural Scots pine regeneration using remote sensing.

The characteristics of the study area are described and illustrated in Chapter 2, and details of the sample plots used are given. Chapter 3 serves to clarify work undertaken prior to the present study, but also indicates the key research questions raised through the earlier study. Therefore, Chapter 3 is not just a brief summary of earlier work, but provides an important base of understanding and a context in which to formulate focussed research questions for the present study. Chapter 4 begins by reviewing the literature on relating measured reflectance to the biophysical properties of vegetation canopies and the problems in obtaining accurate measures of LAI in the field. Results of correlation analysis are presented and discussed along with the effects of seasonal changes in understorey reflectance. Chapter 5 describes the method developed to carry out laboratory measurements of reflectance and transmittance of needles and presents the results of the measurements made. Types of canopy reflectance model are reviewed in Chapter 6. The role of LAI, percentage cover and crown needle density on canopy reflectance is explored using a hybrid geometric-optical model (FLIGHT). The use of geostatistical analysis of images using the semivariogram is reviewed in Chapter 7 and the results of this method for digitized, orthorectified colour aerial photographs of natural Scots pine regeneration are presented and discussed. Finally, Chapter 8 draws the principal outcomes of the

study together in the context of both remote sensing research and monitoring of Scots pine regeneration.

1.4 References

BELWARD, A. S., TAYLOR, J. C., STUTTARD, M. J., BIGNAL, E., MATHEWS, J., and CURTIS, D., 1990, An unsupervised approach to the classification of semi-natural vegetation from Landsat Thematic Mapper data: a pilot study on Islay. *International Journal of Remote Sensing*, **11**, 429-445.

CURRAN, P. J., and KUPIEC, J. A., 1995, Imaging Spectroscopy: a new tool for ecology. In *Advances in Environmental Remote Sensing*, edited by F. M. Danson and S. E. Plummer, (Chichester: Wiley & Sons), pp. 71-88.

CURRAN, P. J., and WILLIAMSON, H. D., 1987, Airborne MSS data to estimate GLAI. *International Journal of Remote Sensing*, **8**, 57-74.

CURRAN, P. J., and WILLIAMSON, H. D., 1988, Selecting a spatial resolution for estimation of per-field green leaf area index. *International Journal of Remote Sensing,* **9**, 1243-1250.

COOPS, N., and CULVENOR, D., 2000, Utilizing local variance of simulated high spatial resolution imagery to predict spatial pattern of forest stands. *Remote Sensing of Environment* **71**, 248-260.

DANSON, F. M., and PLUMMER, S. E., 1995, Red-edge response to forest leaf area index. *International Journal of Remote Sensing*, **16**, 183-188.

DAVIS, F. W., QUATTROCHI, D. A., RIDD, M. K., LAM, N. S-N., WALSH, S. J., MICHAELSEN, J. C., FRANKLIN, J., STOW, D. A., JOHANNSEN, C. J., and JOHNSTON, C. A., 1991, Environmental analysis using integrated GIS and remotely sensed data: some research needs and priorities. *Photogrammetric Engineering and Remote Sensing*, **57**, 689-697.

DEMETRIADES-SHAH, T. H., STEVEN, M. D., and CLARK, J. A., 1990, High resolution derivative spectra in remote sensing. *Remote Sensing of Environment*, **33**, 55-64.

GONG, P., RUILIANG, P, and YU, B., 1997, Conifer species regognition: an exploratory analysis of *in situ* hyperspectral data. *Remote Sensing of Environment*, **62**, 189-200.

HELLAWELL, J. M., 1991, Development of a rationale for monitoring. In *Monitoring for Conservation and Ecology*, edited by F. B. Goldsmith (London: Chapman & Hall), pp. 1-14.

HOLMGREN, P., and THURESSON, T., 1998, Satellite remote sensing for forestry planning - a review. *Scandinavian Journal of Forest Research*, **13**, 90-110.

HUBBARD, N. K., and WRIGHT, R., 1982, A semi-automated approach to land cover classification of Scotland from Landsat. *Proceedings of the Annual Conference of the Remote Sensing Society, Liverpool, 15-17 December, 1982*, (Durham: Remote Sensing Society), pp. 212-221.

HYPPÄNEN, H., 1996, Spatial autocorrelation and optimal spatial resolution of optical remote sensing data in boreal forest environment. *International Journal of Remote Sensing*, **17**, 3441-3452.

KNIPLING, E. B., 1970, Physical and physiological basis for the reflectance of visible and near-infrared radiation from vegetation. *Remote Sensing of Environment*, **1**, 115-159.

KUPIEC, J., 1997, Earth Observation for Natura 2000; customer requirement document. *Draft SNH document* (Edinburgh: Scottish Natural Heritage).

LAMBIN, E. F., 1996, Change detection at multiple temporal scales: seasonal and annual variations in landscape variables. *Photogrammetric Engineering and Remote Sensing*, **62**, 931-938.

MEYER, M., and WERTH, L., 1990, Satellite data: management panacea or potential problem? *Journal of Forestry*, **88**, 10-13.

MYNENI, R. B., MAGGION, S., IAQUINTA, J., PRIVETTE, J. L., GOBRON, N., PINTY, B., KIMES, D. S., VERSTRAETE, M. M., and WILLIAMS, D. L., 1995, Optical remote sensing of vegetation: modeling, caveats, and algorithms. *Remote Sensing of Environment* **51**, 169-188.

PITT, D. G., WAGNER, R. G., HALL, R. J., KING, D. J., LECKIE, D. G., and RUNESSON, U., 1997, Use of remote sensing for forest vegetation management: a problem analysis. *The Forestry Chronicle*, **73**, 459-477.

RATCLIFFE, P. R., PETERKEN, G. F., and HAMPSON, A., 1997, A Forest Habitat Network for the Cairngorms. *Unpublished report to Scottish Natural Heritage.* SNH Contract no: RASD/107/97 CNG.

St-ONGE, B. A., and CAVAYAS, F., 1995, Estimating forest stand structure from high resolution imagery using the directional variogram. *International Journal of Remote Sensing*, **16**, 1999-2021.

St-ONGE, B. A., and CAVAYAS, F., 1997, Automated forest structure mapping from high resolution imagery based on directional semivariogram estimates. *Remote Sensing of Environment*, **61**, 82-95.

TUCKER, C. J., 1979, Red and infrared linear combinations for monitoring vegetation. *Remote Sensing of Environment*, **8**, 127-150.

USTIN, S. L., WESSMAN, C. A., CURTISS, B., KASISCHKE, E., WAY, J., and VANDERBILT, V. C., 1991, Opportunities for using the EOS imaging spectrometers and synthetic aperture radar in ecological models, *Ecology*, **72**, 1934-1945.

VANE, G., and GOETZ, A. F. H., 1993, Terrestrial imaging spectrometry: current status, future trends. *Remote Sensing of Environment*, **44**, 117-126.

WICKLAND, D. E., 1989, Future directions for remote sensing in terrestrial ecological research. In *Theory and Applications of Optical Remote Sensing*, edited by A. Asrar (New York: Wiley & Sons), pp. 691-724.

WEILER, J. M. N., and STOW, D. A., 1991, Spatial analysis of land cover patterns and corresponding remotely-sensed image brightness. *International Journal of Remote Sensing*, **12**, 2237-2257.

WOODCOCK, C. E., and STRAHLER, A. H., 1987, The Factor of Scale in Remote Sensing. *Remote Sensing of Environment*, **21**, 311-332.

ZARCO-TEJADA, P. J., and MILLER, J. R., 1999, Land cover mapping at BOREAS using red edge spectral parameters from CASI imagery. *Journal of Geophysical Research*, **104**, No. D22, 27,921-27933.

2.0 THE STUDY AREA

2.1 Site Description

2.1.1 Location, Geology and Soils

Inshriach and Rothiemurcus (Grid ref. NH 8805 and NH 9309) lie about 4 km apart at about 280 m altitude in the Spey valley just south of Aviemore on the northwest margin of the Cairngorm National Nature Reserve. The Cairngorms lie in the northeast part of the Grampian Mountains and are formed largely of pink granite intrusions into Caledonian schists. Inshriach and Rothiemurcus, however, are parallel to the western flank of the Cairngorm range and are underlain by coarse glacial meltwater deposits. Inshriach is the smaller of the two sites covering about 2 km^2 of heather moorland with scattered mature Scots pine, clumps of regeneration and the occasional mature birch tree. The study area within the Rothiemurcus estate is larger (about 4 km^2) and the vegetation composition is very similar; an open area of heather moorland, with scattered mature Scots pines, clumps of regeneration, and bounded by mature Caledonian woodland. The local topography is characterised by ridges and hummocks orientated in the direction of the fluvio-glacial flow. On this freely drained granitic and siliceous parent material, the cool climate contributes to the formation of podzolic soils. At Inshriach, there is evidence from an eroded bank of leaching and iron deposition, whilst the organic horizon is characteristically dark and peaty, but shallow. Under such nutrient impoverished conditions, these soils are suitable for pine regeneration because of reduced competition from the field layer species (Steven and Carlisle, 1959). Figure 2.1 illustrates the location of the study sites within Scotland, together with the remaining significant areas of native Caledonian woodland.

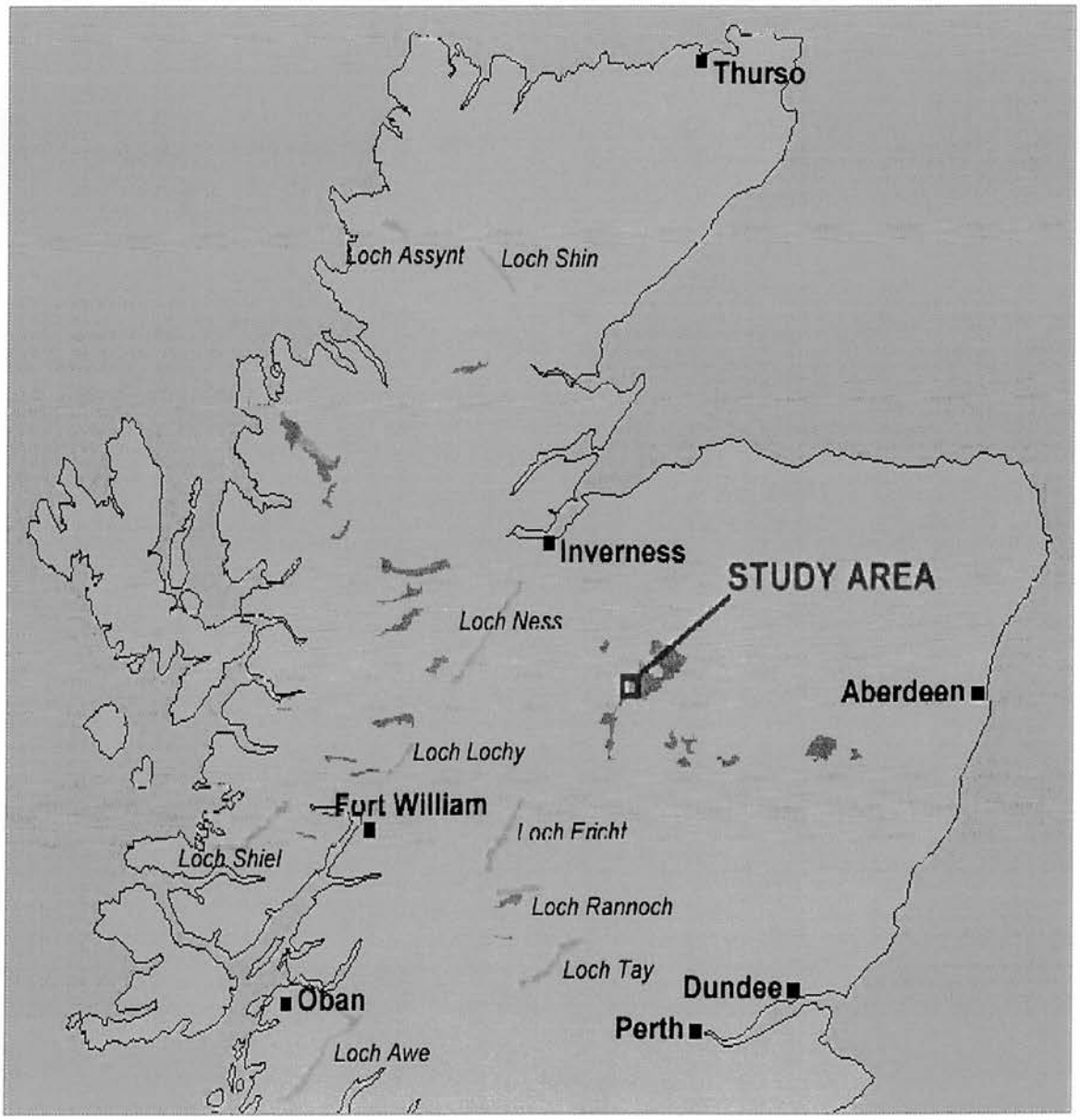

Figure 2.1 The location of the study area and the current extent of Caledonian pinewood (in dark grey).

Source: Redrawn from the Caledonian Pinewood Inventory 1998, Forestry Commission.

2.1.2 Vegetation and Management History

Following the end of the last ice age, warmer conditions led to the spread of Caledonian forests across central Scotland. These forests consisted of *Pinus sylvestris* (Scots pine) as the dominant species of the region, but locally other species such as *Sorbus aucuparia* (Rowan), *Prunus padus* (Bird cherry) and *Salix* spp. (Willow), were dominant (NCC, 1989), depending on the soil conditions. The Caledonian forests were therefore a rich mosaic of woodland types, each with their own associated plant communities. The study area at Inshriach and Rothiemurcus were covered by native Scots pine forest, some remnants of which still remain and stretch up to 600 m on Creag Fhiaclach, which bounds Inshriach to the east (James *et al.*, 1994).

The impact of man on the native forests stretches back to the Bronze Age (Steven and Carlisle, 1959) although major exploitation of the timber did not occur until the nineteenth century. The last major felling episode in the area was following World War II when the valley floor and the lower slopes of Creag Fhiaclach were cleared (D. Duncan, pers. comm., 1997). The vegetation in the cleared areas reverted to *Calluna vulgaris* (Ling heather) moorland, although some remnant species of the native pine forest understorey linger incongruously in places, such as *Juniperus communis* (Juniper). The *Calluna* heathland was maintained by rotational burning mainly for the benefit of the red deer (*Cervus elaphus*) in the 'deer forest' estates (Thompson *et al.*, 1995).

Inshriach is bounded to the west by a 30-year-old Scots pine plantation, to the south and east by native Scots pine forest and to the north by Loch Gamhna. The study area at Rothiemurcus is bounded primarily by mature native Scots pine forest and some plantation to the east. The plant species that have been identified within the dryer areas of the *Calluna* heathland, where regeneration is taking place at both sites, are listed in Table 2.1. The list is not compiled from a formal vegetation sampling scheme, but rather from those species simply identified within the study areas. Based on this, the heathland most closely resembles, the Arctostaphyleto-Callunetum

community described by McVean and Ratcliffe (1962) as having its 'headquarters in Speyside'. This community is particularly species-poor and is best described as the National Vegetation Classification H16; *Calluna vulgaris-Arctostaphylos uva-ursi* heath (Rodwell, 1991). It is likely that the sub-community H16 c (*Cladonia* spp. sub-community) is also represented, particularly at the top of exposed hummocks where there is a noticeable absence of any herb species.

Table 2.1 Species identified within areas of pine regeneration at the study sites.

Scientific name	Common name	Scientific name	Common name
Calluna vulgaris	Ling heather	*Deschampsia flexuosa*	Wavy hair-grass
Artostaphylos uva-ursi	Bearberry	*Nardus stricta*	Mat-grass
Vaccinium vitis-idaea	Cowberry	*Molinia caerulea*	Purple moor-grass
Vaccinium myrtillus	Bilberry/Blaeberry		
Genista anglica	Needle whin	*Hypnum jutlandicum*	Mosses
Erica cinerea	Bell heather	*Pluerozium schreberi*	
Potentilla erecta	Tormentil	*Dicranum scoparium*	
Lotus corniculatus	Com. Bird's-foot-trefoil		
Galium saxatile	Heath bedstraw	*Cladonia impexa*	Lichens
Viola riviniana	Common Dog-violet	*Hypogymnia physodes*	
Juniperus communis	Juniper		
B. pubescens seedling	Downy birch	*Pteridium aquilinum*	Bracken

Calluna exhibits a cyclical growth process in heathlands that has four identifiable phases over the lifespan of a single plant. These phases have been described as pioneer, building, mature and degenerate (Gimmingham, 1972, *sensu* Watt, 1955). The *Calluna* at the study sites resembles the late building to degenerate phases, which puts the age of the plants at about 25 years (Gimmingham, 1972). At this stage, there is much less green biomass production each year than in the pioneer or building phases, and more of the ground is visible. It is clearly important that where remote sensing studies are carried out involving such communities, the age of the *Calluna* is reported since the spectral response will differ between the phases. This has been shown by other workers in remote sensing studies involving *Calluna* heathland (e.g. Wardley *et al.*, 1987; Emery and Milton, 1996).

Following the period of felling after the Second World War, there is some evidence that regeneration of native Scots pine was thought desirable. Although still privately owned, conservation within the Inshriach and Rothiemurcus estates was steered by the management committee of the Cairngorms NNR. Their report of February 1958 commented on the lack of regeneration at Inshriach compared to the neighbouring Rothiemurcus estate, which they attributed to 'much recent burning in places' (Arbuthnott and Roger, 1958). These authors also reported that extensive burning took place at Inshriach 'inadvertently' in 1957 and recommended that natural regeneration of pine must not be endangered by heather burning. Ten years later, the 1968 management plan shows little evidence that earlier recommendations had been followed. It is reported that 'no serious attempt has been made to assist regeneration because the lower ground here is valuable wintering ground for deer. Nevertheless, protection from burning is enforced as far as possible where regeneration might occur' (Roger and Matthew, 1968). Clearly, the estates such as Inshriach and Rothiemurcus continued burning in order to keep deer populations as high as possible during this period and there was little incentive to aid pine regeneration.

However, in 1970, Inshriach was purchased by the Nature Conservancy Council (now Scottish Natural Heritage) in 1970. Rothiemurcus remains privately owned but conservation management agreements exist between the estate and SNH. Deer have been culled by a combination of SNH staff and sport shooting, the revenue from which has gone to the estate. It is assumed that heather burning has not taken place since the early 1970s, which would agree with the estimate of the age of the heather suggested above. Tree regeneration at Inshriach has been monitored by SNH by measurements made along transects, although no detailed records of this work were available. Some aerial photography of regions of regeneration exists for the Rothiemurcus site from 1994 (1:5,000) and 1995 (1:10,000). Inshriach has become an experimental area for natural regeneration through control of the deer population rather than by enclosure and recent research by ground-survey indicates that this strategy is a successful one (Palmer *et al.*, 1996).

2.2 Sample Plots

Nine 5 x 5 m sample plots were marked out at Inshriach for the purpose of measuring spectral response over the 1997 and 1998 growing seasons using a field spectroradiometer (Chapters 3 and 4). The location of each sapling stem was recorded within each plot. Figure 2.2 illustrates the number and distribution of the saplings within each of these plots. Measurements recorded for each sapling included sapling height, basal crown width and number of whorls (equal to age in years). These statistics are summarized in Table 2.2. Figure 2.3 illustrates the location of the sample plots at Inshriach. Plates are also included at the end of this chapter to illustrate the study sites and reflectance measurements over the sample plots.

Table 2.2 Sapling statistics within the sample plots at Inshriach, May 1997.

	No. Saplings	% cover	Sapling height (m)		Sapling width (m)		No. Whorls (age)	
			Mean	Std. Dev	Mean	Std. Dev	Mean	Std. Dev
Plot 1	0	0	0	0	0	0	0	0
Plot 2	16	2	0.28	0.12	0.16	0.09	3	1.5
Plot 3	26	13	0.39	0.25	0.31	0.25	5	2.5
Plot 4	44	19	0.71	0.29	0.33	0.19	6	2.0
Plot 5	99	51	0.95	0.30	0.38	0.17	7	1.0
Plot 6	32	29	0.97	0.36	0.49	0.22	7	1.0
Plot 7	14	29	1.58	0.30	0.77	0.24	13	1.4
Plot 8	26	37	1.19	0.45	0.60	0.29	10	2.0
Plot 9	22	15	0.85	0.36	0.42	0.22	8	1.7

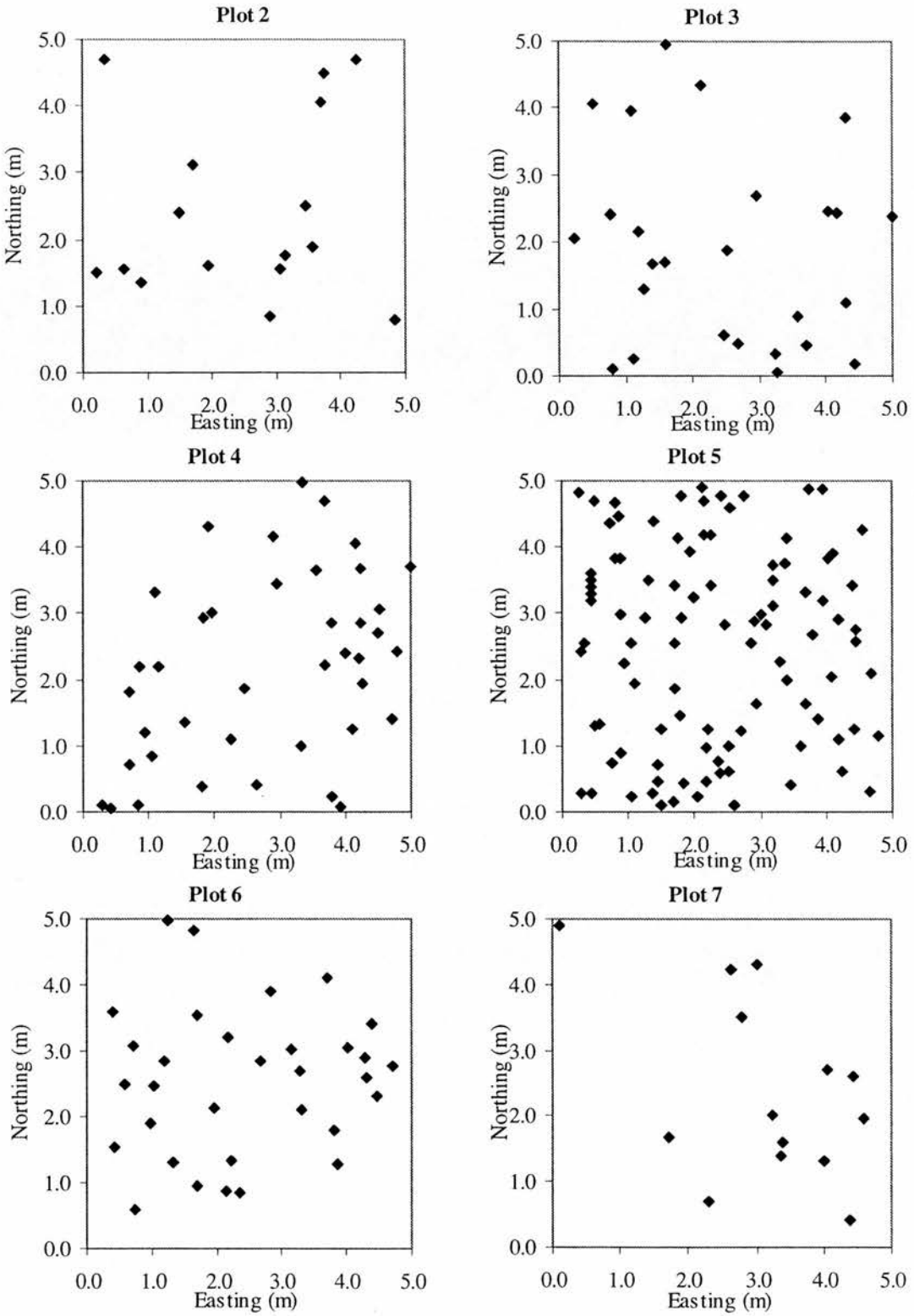

Figure 2.2 The distribution of sapling stems (crown centres) within the sample plots (contd.....\over)

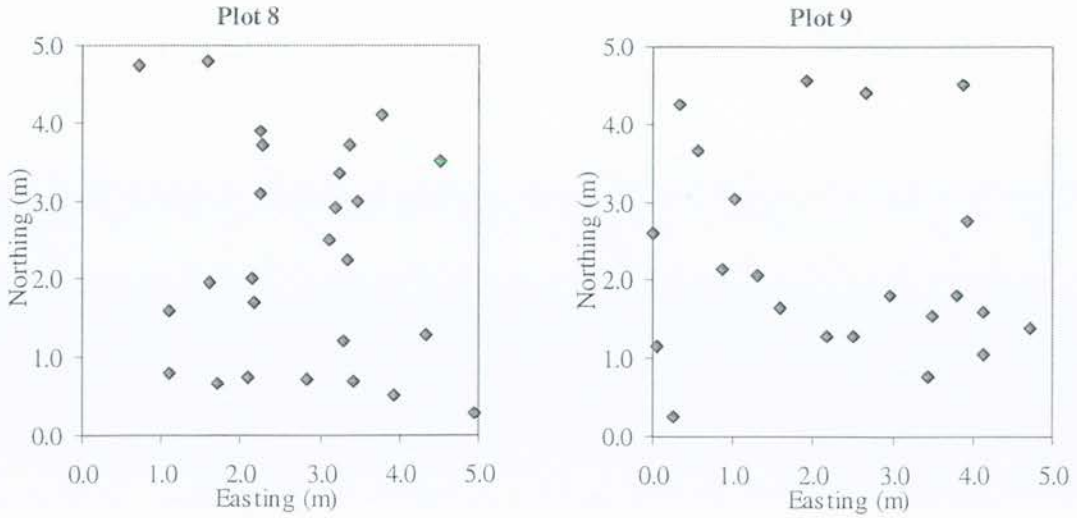

Figure 2.2 (contd.) The distribution of sapling stems (crown centres) within the sample plots.

Plate 2.1 Dense regeneration within sample plot 5 at Inshriach

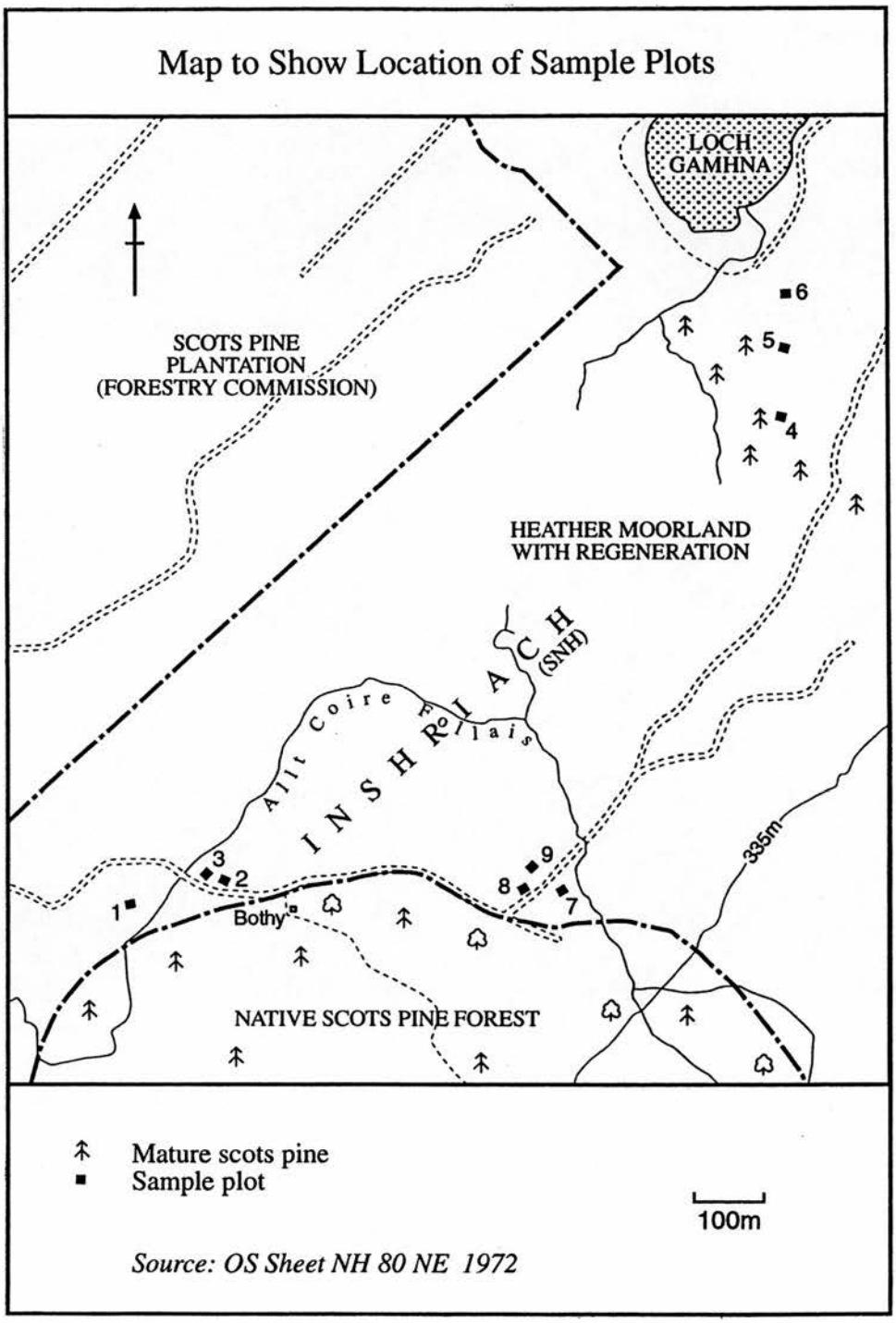

Figure 2.3 The location of sample plots at Inshriach

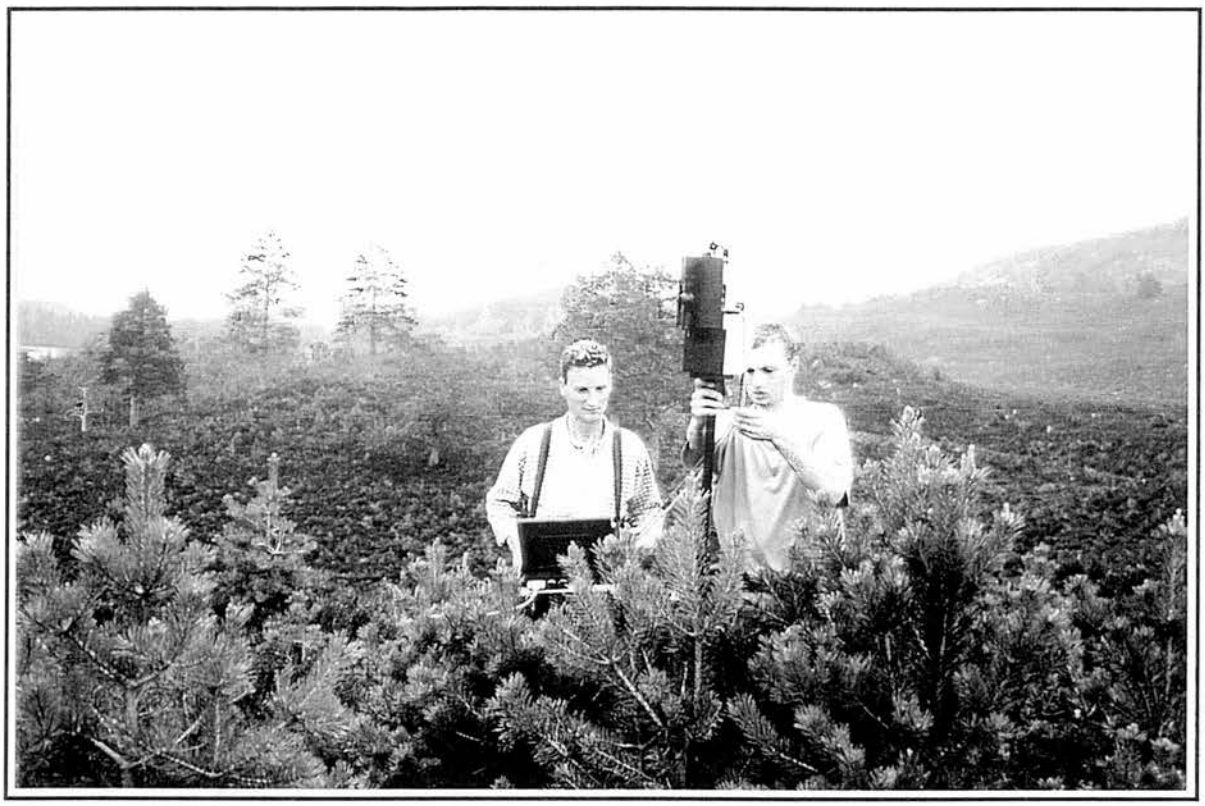

Plate 2.2 The GER 3700™ field spectroradiometer in use at Inshriach.

2.3 References

ARBUTHNOTT, J. C., and ROGER, J. G., 1958, *Cairngorms NNR Management Plan* (Edinburgh: The Scottish Committee).

EMERY, D. R., and MILTON, E. J., 1996, Seasonal and episodic variations in the strength of the relationship between NDVI and plant canopy variables for lowland heath. *Proceedings of the 22nd Annual Conference of the Remote Sensing Society*, (Durham: Remote Sensing Society), pp. 274-280.

GIMMINGHAM, C. H., 1972, *Ecology of Heathlands*. London: Chapman and Hall.

JAMES, J. C., GRACE, J., and HOAD, S. P., 1994, Growth and photosynthesis of *Pinus sylvestris* at its altitudinal limit in Scotland. *Journal of Ecology*, **82**, 297-306.

McVEAN, D. N., and RATCLIFFE, D. A., 1962, *Plant Communities of the Scottish Highlands. Monographs of the Nature Conservancy, 1* (London: HMSO).

NATURE CONSERVANCY COUNCIL, 1989, *Cairngorms NNR: Trees and dwarf shrubs* (Aberdeen: NCC).

PALMER, S. C. T., PATERSON, I. S., MARQUISS, M., and STAINES, B. W., 1996, Scots pine regeneration in the presence of deer. *Institute of Terrestrial Ecology (ITE) Project T08093d5.* Report to the Caledonian Partnership under the EU LIFE programme.

RODWELL, J. S., editor, 1991, *British Plant Communities 2: Mires and Heaths.* (Cambridge: Cambridge University Press).

ROGER, J. G., and MATTHEW, E. M., 1968, *Cairngorms NNR Management Plan* (Edinburgh: The Scottish Committee).

STEVEN, H. M., and CARLISLE, A., 1959, *The Native Pinewoods of Scotland* (Cornwall: Hartnolls Ltd.).

THOMPSON, D. B. A., MacDONALD, A. J., MARSDEN, J. H., and GALBRAITH, C. A., 1995, Upland heather moorland in Great Britain: a review of international importance, vegetation change and some objectives for nature conservation. *Biological Conservation*, **71**, 163-178.

WARDLEY, N. W., MILTON, E. J., and HILL, C. T., 1987, Remote sensing of structurally complex semi-natural vegetation – an example from heathland. *International Journal of Remote Sensing*, **8**, 31-42.

3.0 SUMMARY OF MRes.

3.1 Introduction

This chapter briefly details work carried out prior to the present study that contributed to a separate Master of Research (MRes.) degree and published in Shaw *et al.* (1998) (Appendix A). The MRes. field work was carried out between March and July 1997, involving primarily field spectral data collected over the 1997 growing season for the nine sample plots at Inshriach, and some data analysis. The data collection for the present study commenced in September 1997, following the same methods, and was therefore a direct continuation of the MRes. study. Some of the results presented in the following chapters relating to sample plot spectra include data collected during the earlier study. The purpose of this chapter is to provide a clear statement of work completed prior to the commencement of the present study.

The MRes. study had two primary aims;

1. To propose wavelengths or combinations or wavelengths most suitable for monitoring crown closure of saplings (as measured by percentage cover)

2. To determine the degree of seasonal variation in understorey vegetation reflectance and its influence on the estimation of crown closure using measured reflectance.

3.2 Methods

Nine 5 x 5 m plots with varying amounts of sapling cover were measured for reflectance using a GER 1500™ spectroradiometer. Twenty-five measurements were recorded over each plot in a systematic grid-sampling pattern (see 4.3 Fig. 4.1), and the measurements were repeated in March, May, June and July 1997. The GER 1500™ instrument measures reflectance relative to a Spectralon™ standard in 512 channels from the visible (300 nm) to NIR (1100 nm) wavelengths, with a spectral resolution of 3 nm. Further details on the data acquisition are given in Shaw (1997).

Percentage cover is the most commonly measured structural variable for forest stands in vegetation management and is defined as the 'area of ground occupied by the vertical projection of plant material growing above the ground onto a horizontal plane' (Ferris-Kaan and Patterson, 1992). The diameter of each tree was measured across the base of its crown and crown base area was calculated as though the base of each crown was circular. Plot percentage cover was estimated by simply summing the crown base areas of each tree within the plot to give an approximation of the vertical projection of plant material. The plot statistics are presented in the following chapter.

The twenty-five plot spectra were processed to absolute reflectance before averaging in each wavelength to give mean overall reflectance spectra for each plot on each sampling date. The relationships between percentage cover and both reflectance and first-order derivative spectra were investigated using the Pearson product-moment correlation coefficient (r), with the t-statistic to assess the significance. In addition to the correlation of reflectance at individual wavelengths with percentage cover, correlations with spectral indices were also considered. These included the established Normalized Difference Vegetation Index (NDVI) and the Simple Vegetation Ratio (SVR). A two-dimensional correlogram matrix enabled further wavelength ratios of reflectance and derivative reflectance to be identified for their strong correlation with percentage cover.

3.3 Results and Discussion

Results of the spectral data collected for the MRes. study were used to characterise the reflectance from the vegetation at the study site, consider seasonal changes in reflectance, and to explore the relation with percentage cover. Figure 3.1 compares the spectra of the different vegetation elements at the study site and traces the changes in grass reflectance through the growing season.

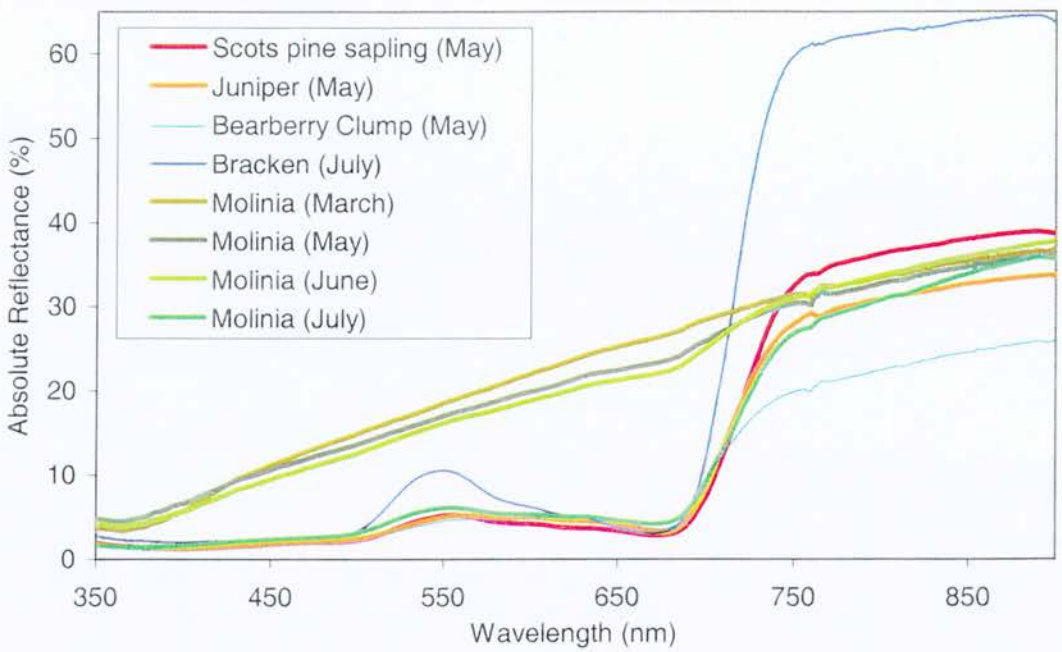

Figure 3.1 Mean reflectance spectra of different species at Inshriach in 1997 (n=10)

The rough grass *Molinia caerulea* (Purple moor-grass) was spectrally very flat earlier in the season but by July the new green leaves dominated the reflectance resulting in stronger absorption through the visible wavelengths. The Juniper signal was very similar to that of the Scots pine sapling, which was thought to be due to the structural similarity of the two canopy types, as much as to leaf chemistry. The bracken signal was conspicuous in July by its strong reflectance at the green and NIR wavelengths.

It was concluded that the pine signal may be masked by other species within the vegetation community at the study site during the height of summer in July. The reflectance spectra of bracken, juniper and any grass species present are particularly likely to mask the pine signal. However, in general, pine regeneration takes place almost exclusively within the dominant heather community, such that areas of bracken and grass should be distinct within higher spatial resolution data. The influence of these neighbouring species would be greater on measurements collected with lower spatial resolution sensors, such as Landsat TM, due to mixed pixels.

Linear correlation analysis was carried out for selected indices for both reflectance and derivative data in relation to percentage cover. Table 3.1 summarizes the strength of these relationships using the correlation coefficient (r), and tested for significance using the t-statistic.

Table 3.1 Linear correlation coefficients (r) between percentage cover of pine and plot mean reflectance for selected indices (from Shaw *et al.*, 1998).

Wavelength (nm)	March	May	June	July
Reflectance				
R_{550}	0.4 n.s.	0.4 n.s.	-0.22 n.s.	0.65 n.s.
R_{670}	-0.86**	-0.78**	-0.85**	-0.57 n.s.
R_{800}	0.81**	0.66*	0.76**	0.87**
SVR	0.97***	0.88***	0.97***	0.95***
NDVI	0.97***	0.93***	0.97***	0.93***
R_{757}/R_{722}	0.97***	0.97***	0.97***	0.97***
1st Derivative				
REP	0.73*	0.90***	0.82**	0.67*
D_{520}†	0.96***	0.89***	0.83**	0.89***
D_{570}†	-0.98***	-0.94***	-0.92***	-0.93***
D_{719}	0.92***	0.85**	0.91***	0.90***
D_{703}	0.65*	0.59*	0.76**	0.82**
D_{719}/D_{703}	0.95***	0.99***	0.97***	0.96***
D_{730}/D_{700}	0.98***	0.99***	0.99***	0.96***

*=p<0.05; **=p<0.01; ***=p<0.001; n.s. = not significant at the p<0.05 confidence level
†Maximum and minimum values derived irrespective of wavelength but at approximately 520 and 570 nm respectively.
n = 9 in each case.

The SVR (NIR_{800}/Red_{670}) and NDVI [(NIR_{800} - Red_{670})/(NIR_{800} + Red_{670})] indices both correlated strongly with percentage cover of pine, but the strongest correlation with the reflectance indices was with the ratio R_{757}/R_{722}. Table 3.1 illustrates that the reflectance indices that combine different wavelengths correlate more strongly with pine cover than the single wavelength indices (R_{670} and R_{800}). One reason for the stronger correlation for combinations of wavelengths is likely to be because such indices may reduce background variability in absolute reflectance (e.g. Malthus *et al.* 1993).

Table 3.1 also illustrates a strong correlation between first-derivative indices and percentage cover of pine. A strong correlation was found throughout the sampling period for red-edge indices, particularly for the red-edge peak ratio D_{719}/D_{703}, and for the ratio D_{730}/D_{700}. The red-edge region was characterised by two peaks, one at longer wavelengths, D_{719}, and one centred at D_{703} (Figure 3.2).

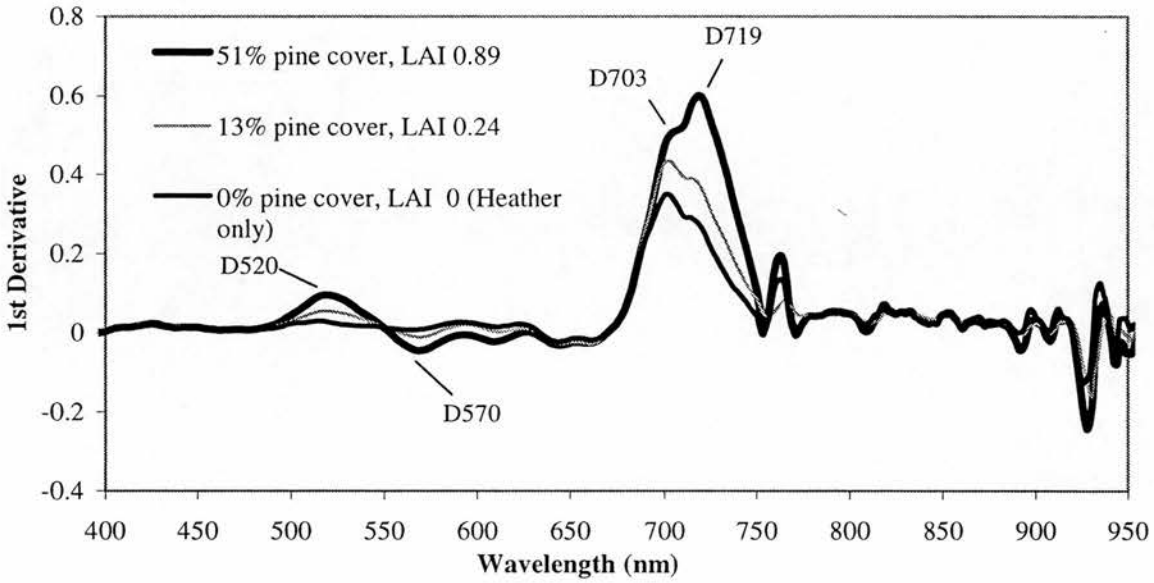

Figure 3.2 Mean plot first-order derivative spectra (for three plots in March 1997)

Since reflectance at D_{719} correlated more strongly with percentage cover of pine, it was suggested that this peak was more sensitive to the pine canopy. Previous workers have suggested that the peak at shorter wavelengths is controlled primarily by chlorophyll concentration, whilst the peak at longer wavelengths is controlled by both chlorophyll concentration and depth of the green canopy component (Horler *et al.*, 1983; Ferns *et al.*, 1984; Boochs *et al.*, 1990; Filella and Peñuelas, 1994).

The slopes of the green reflectance peak are represented by the derivative maximum at D_{520} and the minimum at D_{570}. The minimum at D_{570}, which represents the descending limb of the green reflectance peak, had a slightly stronger correlation than D_{520}, which represents the ascending curve.

Another vegetation index that has been shown to relate to pine canopy amount, measured as LAI, is the red-edge position (REP). For example, LAI for coniferous plantations was reported to relate strongly to REP by Danson and Plummer (1995). However, since the red-edge feature displayed two peaks for the heather/pine canopy, which switched in dominance according to the amount of pine cover, the idea of tracing the movement of a single peak towards longer wavelengths with increasing cover of pine was discounted. It was concluded that the relative proportion of the two peaks, described by the ratio D_{719}/D_{703}, would hold more information about the relative proportion of the species in this bimodal canopy than the REP. Horler *et al.* (1983) came to a similar conclusion, stating that the interpretation of the red-edge peak maximum only, is limited because 'it does not describe spectral shape and only refers to one or other of the two identifiable first derivative components'.

Figure 3.2 formalises the relation between the red-edge peak ratio as a simple empirical model using linear regression. A similar relationship was observed for the D_{730}/D_{700} ratio, which represents the shoulders on either side of the derivative peaks.

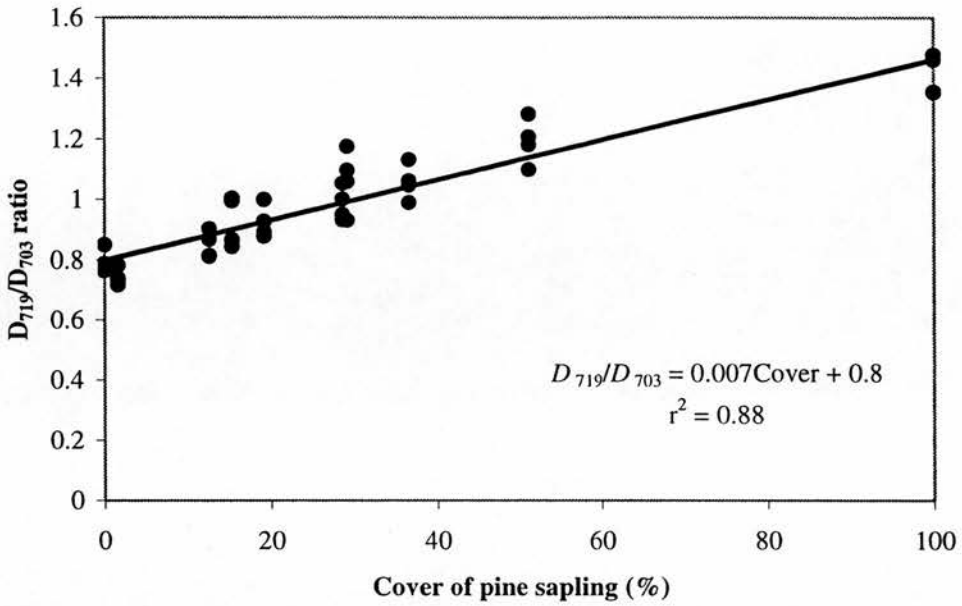

Figure 3.3 Relation between sapling cover and the D_{719}/D_{703} *derivative red-edge peak ratio, with a linear regression model fitted. Data from March, May, June and July 1997 included. 100% cover was simulated using a mean of repeated measurements over a single healthy sapling on each sampling date.*

3.4 Conclusions and Future Work

This section summarizes the main conclusions drawn from the MRes. study and highlights the key areas for future work.

3.4.1 Seasonal Change

Correlation between selected indices and percentage cover of pine remained very similar for each of the four sampling dates between March and July 1997. Any changes in the colour of the heather-dominated understorey did not influence the strength of the correlations. This may be due to the late growth phase of the heather and its associated low productivity. The aim of future work was to complete the set of seasonal measurements beyond July to the end of the growing season. In particular, it was considered important to sample during late August or early September when the heather canopy would be flowering. The greatest seasonal change in understorey canopy colour may occur at this time.

For the young pine canopy itself, the greatest seasonal change was observed in July when the present year's growth undergoes rapid shoot extension. This flush of growth may explain the dramatic change in the correlation coefficient of R_{550} in July (Table 1). Reflectance at this wavelength is dominated by green plant pigments which will be at their maximum during a growth flush. Other indices however, appeared unaffected by any changes in the understorey, or the pine canopy over the sampling period.

Measured reflectance of other species at the study site included bracken, purple-moor grass, bearberry and juniper. Strong vegetation spectra were measured for bracken and grass during July in particular, whilst the evergreen juniper, had a similar reflectance spectrum to Scots pine (Figure 3.1). Although these species rarely occurred in close association with regenerating pine saplings at Inshriach, it was

suggested that they could significantly influence the measured signals from lower spatial resolution sensors, particularly in mid-summer. Defining the optimum spatial resolution for monitoring natural pine regeneration is therefore a requirement for future work. This is a fundamental issue, not least because it defines the type of sensors that may be sensibly used for the purpose.

3.4.2 Measuring Percentage Cover

Using linear correlation analysis and correlograms, it was possible to highlight wavelength regions and combinations of wavelengths where measured reflectance may be used to predict percentage cover of pine. Simple empirical models were used to summarise the relation between percentage cover of pine and measured reflectance using linear regression. These regression models produced high correlation coefficients, suggesting that they could be inverted to predict percentage cover of pine with some confidence. In practice, however, there would be difficulties with this approach since such models do not account for many of the factors that contribute to measured reflectance, such as sun-sensor geometry, depth of canopy, site-specific factors and many others. There are two possible solutions to this common remote sensing problem; one is to attempt to account for as many of these factors as possible by exhaustive measurements in the field, and the other is to model the relationship with greater complexity to account for the real complexity of canopy reflectance as accurately as possible. Whilst complex physical models may not be directly invertible to retrieve canopy variables such as percentage cover, this approach does allow for greater understanding of the influences on canopy reflectance. Their particular advantage is in the ability to vary a single parameter, whilst keeping all others constant; something that is rarely achievable in practical field data collection. It also allows extension of the work to older regeneration stages, beyond those that are physically possible to measure in the field.

The relation between red-edge indices and percentage cover was explained, in part, by the increase in chlorophyll as pine cover increased. This resulted in a noticeable

shift in REP to longer wavelengths. The shift was observed to be a switching of dominance from the peak at shorter wavelengths to the peak at longer wavelengths, rather than a regular progression. For this reason, it was suggested that the derivative red-edge ratio was a more reliable measure of the relative amounts of pine and heather understorey. However, percentage cover does not accurately describe the amount of pine within the sample area since it is restricted to two dimensions. In other words, it does not account for canopy depth, or crown density. Since D_{719} and the NIR wavelengths used in the SVI and NDVI indices are sensitive to canopy structure, Leaf Area Index (LAI) may be a more meaningful canopy variable to compare with measured canopy reflectance. Furthermore, the MRes. study did not distinguish between the possible distribution of sapling amount within a given area. For example, for a given area, a few large individual trees may have the same LAI as many smaller individuals with a smaller crown depth. The subsequent question of whether these two scenarios produce similar, or distinguishable, measured reflectance has obvious implications for monitoring the state of pine regeneration. It is clearly important to be able to distinguish between different stages of regeneration with different canopy physiology. This type of problem is most suited to the physical canopy modelling approach by keeping LAI constant whilst varying other canopy structural variables. In summary, the following points were recommended for future work:

- An extension of the wavelength range beyond the NIR.
- Measurement of LAI within the sample plots.
- Consideration of the effects of the heather canopy flowering season.
- Physical canopy reflectance modelling to further explore the relation between reflectance and pine sapling amount, including LAI as a canopy variable, and further exploring the validity of the indices proposed.
- Determination of appropriate spatial scales for monitoring pine regeneration, and the application of spatial statistics.

The first three of these points are considered in the following chapter, whilst the latter two are the subjects of subsequent chapters.

3.5 References

BOOCHS, F., KUPFER, G., DOCKTER, K., and KÜHBAUCH, W., 1990, Shape of the red edge as vitality indicator of plants. *International Journal of Remote Sensing*, **11**, 1741-1753.

DANSON, F. M. and PUMMER, S. E., 1995, Red-edge response to forest leaf area index. *International Journal of Remote Sensing*, **16**, 183-188.

FILELLA, I., and PEÑUELAS, J., 1994, The red edge position and shape as indicators of plant chlorphyll content, biomass and hydric status. *International Journal of Remote Sensing*, **15**, 1459-1470.

FERNS, D. C., ZARA, S. J., and BARBER, J., 1984, Application of high resolution spectroradiometry to vegetation, *Photogrammetric Engineering and Remote Sensing*, **50**, 1725-1735.

FERRIS-KAAN, R., and PATTERSON, G. S., 1992, Monitoring vegetation changes in conservation management of forests. *Forestry Commission Bulletin 108* (London: HMSO).

HORLER, D. N. H., DOCKRAY, M., and BARBER, J., 1983, The red edge of plant leaf relectance. *International Journal of Remote Sensing*, **4**, 273-288.

MALTHUS, T. J., AMDRIEU, B., DANSON, F. M., JAGGARD, K. W. and STEVEN, M. D., 1993, Candidate high spectral resolution infrared indices for crop cover. *Remote Sensing of Environment*, **46**, 204-212.

SHAW, D. T., 1997, Remote sensing for monitoring natural regeneration of Scots Pine (*Pinus sylvestris*) in the Cairngorms. Unpublished M Res. thesis, Department of Geography, University of Edinburgh.

SHAW, D. T., MALTHUS, T. J., and KUPIEC, J. A., 1998, High-spectral resolution data for monitoring Scots pine (*Pinus sylvestris* L.) regeneration. *International Journal of Remote Sensing*, **19**, 2601-2608.

4.0 FIELD SPECTRAL ANALYSIS

4.1 Introduction

The monitoring of semi-natural environments using remote sensing techniques is complicated by the spectral inseparability of components within the heterogeneous landscape. Since the measurement of a single component, such as Scots pine saplings, requires a target-specific signal, it was considered necessary to characterise the reflectance of regions of regeneration. A second step was to relate the measured reflectance to pine sapling amount. Leaf Area Index (LAI) is a commonly used measure of vegetation amount since it provides an estimate of photosynthetically active material in the canopy layer. This chapter begins by reviewing the literature in relation to characterising vegetation reflectance, and in relation to measuring LAI. Methods used for spectral data acquisition, analysis and LAI measurement are then described, followed by presentation of results and discussion. The conclusion summarizes the work and draws together the main points in relation to monitoring pine regeneration.

4.2 Previous Work

4.2.1 Measuring Spectral Response From Vegetation

According to Guyot *et al.* (1992) the spectral response of individual biophysical attributes of the ground surface occurs in narrow bands, which explains the poor performance of broad-band sensors in analysing the attributes of more complex canopies. For example, broad wavelength band imagery has only successfully been used for broader landscape classification in the U. K. (e.g. Hubbard and Wright, 1982; Belward *et al.*, 1990). When applied to the measurement of forested stands using the NDVI, Teillet *et al.* (1997) found that broad-band sensors underestimated 'true' NDVI values. This was attributed to the inability of such sensors to maximise the difference between the narrow red-absorption feature at around 670 nm and the NIR. Nel *et al.* (1994) used Thematic Mapper imagery to explore the spectral differences between old and young spruce-fir stands in Colorado. NDVI and SVR (Simple Vegetation Ratio; NIR/Red) images were successful in differentiating between old growth and the younger post-fire stands, but it was concluded that results could be improved by higher spectral and spatial resolution imagery, particularly for more fragmented heterogeneous areas. Chen (1996) used bands 3 (red) and 4 (NIR) from Landsat-5 TM images to explore the relation between a range of standard vegetation indices and LAI for boreal forest. It was concluded that the NDVI and SVR and his own Modified Simple Ratio (MSR) correlated most strongly with LAI and Fraction of Photosynthetically Active Radiation. Chen also concluded that 'the major problem in using the vegetation indices obtained from red and near infrared bands is the small sensitivity to overstorey vegetation conditions'. Even when soil, or background reflectance adjusted broad band indices are applied, there is the problem of decreased sensitivity to changes in the forest canopy reflectance.

In order to characterise these narrow spectral band features of different vegetation types, an increasingly available and well-used research tool for this purpose is the

field spectroradiometer (Malthus, 1995). The utility of such data to the application of remote sensing for ecological assessment is the contribution of detailed knowledge about reflectance characteristics of the vegetation type of interest. The spectral response from vegetation has been well documented, but has focussed primarily on relatively homogeneous agricultural or silvicultural stands (e.g. Curran, 1983; Malthus and Madeira, 1993; Malthus *et al.*, 1993; Danson and Curran, 1993 and many others). The study of seminatural vegetation has been less consistent and has often been for the purpose of classification, rather than quantitative ecological assessment (Weaver, 1987; Jones and Wyatt, 1988; Foody, 1990; Treitz *et al.*, 1992; Trodd, 1993). Several studies have had a primarily ecological purpose, such as monitoring the spread of bracken in Australia (Taylor, 1993); quantifying tundra vegetation biomass in Alaska (Hope *et al.*, 1993) and separation of heathland vegetation types (Wardley *et al.*, 1987).

The use of high-resolution spectra has led to the proposal of a range of reflectance indices that utilize specific wavelengths. For example, for the estimation of leaf chlorophyll content the reflectance ratios R_{NIR}/R_{700} and R_{NIR}/R_{550} were suggested (Gitelson and Merzlyak, 1994, 1997; Gitelson *et al.*, 1996; Lichtenthaler *et al.*, 1996). Carter and Miller (1994) proposed similar wavelengths in combination, as the ratio R_{694}/R_{760}, for plant stress detection. Moran *et al.* (2000) identified reflectance at 698 nm to be most sensitive to different nitrogen treatments for conifer seedlings and recommended the ratio R_{698}/R_{760} for inferring plant physiological status from spectral reflectance measurements. R_{760} is chosen as the denominator in these studies because the NIR is considered insensitive to changes in chlorophyll concentration. Other authors recommend 800 or 850 nm wavelengths; being further from the red-edge region and associated sensitivity to pigment absorption, but not too close to water absorption features at about 940 nm (Datt, 1999).

One problem with high-resolution spectra, however, can be in relating the increased number of narrow bands to the particular vegetation variable of interest in the

presence of unwanted background signals. For example, most spectra collected in the field contain contributions from soil and other targets in the view of the sensor. Demetriades-Shah *et al.* (1990) described the use of derivative spectroscopy as a technique used in analytical chemistry to suppress low frequency background noise by differentiation. These workers suggested that derivatives of reflectance spectra should be used to counter the problems of low frequency background noise and interference from other overlapping spectral signals. A number of detailed studies have come to a similar conclusion (e.g. Horler *et al.*, 1983; Vogelmann *et al.*, 1993).

Within higher-order derivative spectra, sloping regions within the zero-order reflectance spectra are amplified. Most notable is the so-called red-edge region, defined as the wavelength region of the reflectance spectrum between 670 nm and 800 nm (Gates *et al.*, 1965). The red-edge position (REP) is defined as the wavelength of maximum slope of the reflectance spectrum over this range, or the peak on the derivative curve. This region has been shown to be sensitive to chlorophyll concentration within leaves (e.g. Horler *et al.*, 1983).

Blackburn (1998) investigated the effectiveness of hyperspectral approaches for estimating concentrations of pigments at plant and canopy scales for bracken. He concluded that narrow band reflectance indices could be developed which have strong relationships with the concentration per unit area of individual pigments at the canopy scale. However, since LAI was used to scale-up the leaf measurments to the canopy scale it is unclear how much these indices actually relate to LAI rather than the canopy pigment concentrations. Spectral derivative approaches were also closely related to canopy pigment concentration per unit area and were more useful for estimates at both canopy and leaf scales.

For higher density coniferous forest compartments, Danson and Plummer (1995) compared red-edge position (REP) with LAI. They found the REP more sensitive to LAI than the NDVI, although only relatively high LAI values were used. These workers concluded that the REP may be controlled by leaf amount, as measured by

LAI, as well as by the chlorophyll content of the foliage. However, Shaw *et al.* (1998) found the REP to be problematic for lower density stands with other canopy components due to the presence of two peaks at the red-edge (see previous chapter), although only percentage cover was considered. REP has the benefit of being relatively insensitive to variations in pixel brightness caused by variations in canopy geometry and illumination direction (Bonham-Carter, 1988) because it is measured in wavelength units rather than reflectance units (Lucas *et al.*, 2000). However, recent studies have suggested that REP has higher estimation errors in relation to leaf chlorophyll content than a red-edge first derivative ratio (Datt, 1999). Whilst the relation between leaf chlorophyll content and red-edge, and between canopy LAI and red-edge may not be directly comparable, it is generally accepted that canopy LAI is a surrogate for canopy chlorophyll content, since the two are closely related (e.g. Lucas *et al.*, 2000).

Cochrane (2000) demonstrated that red-edge first derivative values could be used to discriminate between native Brazilian tree species using high resolution spectroradiometer measurements of needles and whole branches. He concluded that the red-edge region contained the most important wavelengths for species discrimination. Other workers have also reported that red-edge indices may be used to improve forest species classifications (Gong *et al.* 1997; Martin *et al.* 1998). Zarco-Tejada and Miller (1999) used red-edge parameters derived from CASI imagery to assess their potential for land clover classification in the BOREAS project study region of Canada. They concluded that the use of the red-edge could improve classification accuracy to 61% from 47% and 42% for classification with 16 channnel CASI data and TM-based classification, respectively. These authors also concluded that provided seasonal variations could be accounted for, shifts in the red-edge could be used to monitor changes in cover or species.

4.2.2 The Potential Use Of Short-Wave Infrared (SWIR; 1300 - 2500 nm)

The purpose of this section is to examine the role of SWIR wavelengths for determining leaf, plant and canopy biophysical characteristics. The interest in this part of the spectrum for monitoring pine comes from the results of an MSc. study of Landsat TM data in relation to regeneration at Inshriach and Rothiemurcus (McCoy, 1997). The study highlighted a correspondence between the Landsat TM band 5 (1560 - 1680 nm) and pine regeneration.

Vegetation has a relatively low reflectance in the SWIR region because of strong absorption by water (e. g. Knipling, 1970). The interaction of light with the leaf at these wavelengths is therefore governed by leaf water content, with increased reflectance for non-succulent leaves (Gausman *et al.*, 1978). However, the morphology of leaf internal structure also affects reflectance due to changes in refractive index (Woolley, 1971). Variations between the reflectance of leaves throughout the infrared region will therefore be governed by variations in water content and intercellular air spaces and their morphology. Aldakheel and Danson (1997) concluded that changes in leaf internal structure in C4 plants affected reflectance across the whole spectrum due to changes in cell wall air interface of both palisade and spongy mesophyll layers.

At the canopy level, there is some evidence that reflectance at SWIR wavelengths is sensitive not just to water content but also to structural variations within the canopy. This has confounded attempts to relate leaf water content directly to forest canopy reflectance (e.g. Hunt and Rock, 1989; Pierce *et al.*, 1990; Riggs and Running, 1991). Horler and Ahern (1986) noted that as forests regenerate, TM 4 (NIR) and TM 5 and 7 (SWIR) reflectance decreases. However, the SWIR has an added advantage because atmospheric scattering is much less variable in this region compared with the visible part of the spectrum. These workers conclude that the SWIR is sensitive to forest density, especially in the early stages of regeneration. They also suggest that because of the near absence of diffuse sky illumination in this region, it is reasonable to postulate that shadowing may play an important role in

reflectance. This would seem to explain why the SWIR is sensitive to vegetation density rather than leaf moisture content alone. Horler and Ahern (1986) caution against the use of the term 'wetness' to describe the contrast between SWIR and NIR/VIS since this appears to be an oversimplification of the causes of SWIR reflectance.

The contrast between the SWIR (TM5 and TM7) and RED/NIR (TM3 and TM4) is a feature of the Tasseled Cap Transform (Crist and Cicone, 1984), which these authors referred to as 'wetness' and was assumed to relate primarily to soil reflectance properties. Cohen and Spies (1992) concluded that 'Wetness, a feature of the TM Tasseled Cap, was the spectral variable most highly correlated to all [evergreen forest] stand attributes'. However, these workers also compared spectra from ground radiometer measurements of shaded and unshaded forest compartments. They found that the 'wetness' index responds to both the amount of water *and* shadows in the ground scene. In other words, it is possible to get similar wetness values for a simply structured, dense sunlit canopy, as for a more structurally complex one with more shadow, but less water-filled leaf area. This led these authors to suggest that the term 'wetness' be dropped and replaced with one such as maturity index, since more mature stands usually have more shadow and less leaf area (Cohen, 1994).

Other workers have suggested that the 1300 - 2500 nm wavelength region is inadequate for measuring the water concentration of whole plants or canopies because atmospheric absorption by water is very strong in this region (Peñuelas *et al.* (1997). Therefore, these workers suggest that a reflectance trough in the NIR region at 950-970, which corresponds to a weaker water absorption band, is better for the purpose. The usual relation between greenness and moisture of vegetation was corrected for by normalising the water index (900/970) by the NDVI. This also eliminated the seasonal variations in NDVI of some species. However, these workers did not consider the ability of derivative spectroscopy to reduce background noise, nor did they consider the structural effects of the canopy on the SWIR region.

A further application of the SWIR to forest canopies has been in the measurement of forest volume for managed stands. Ardo (1992) found a good correlation between Landsat TM 5 and forest compartment volume within plantations within Sweden (r^2 = -0.79). He concluded that the relationship is strongest for lower volume compartments. Similarly, Gemmell (1995) found that TM 4 and TM 5 were strongly inversely related to stand timber volume for mixed conifer species in British Columbia, with TM 5 having the greatest dynamic range. Gemmell (1995) also found that these bands were more sensitive to lower forest volumes and to the proportion of shadow and exposed ground in the stand. Both these studies found topographic effects small in relation to the effects of forest cover on reflectance.

The literature relating forest stands to Landsat TM 5, and the SWIR wavelengths in general, would tend to support the conclusion made by McCoy (1997) that uncorrected TM band 5 was most sensitive to pine regeneration. Fiorella and Ripple (1993) reported that their previously suggested 'structural index', which is a simple ratio of TM 4/TM 5, had a high correlation to age of regenerating Douglas-fir stands (r = 0.96). TM SWIR and thermal bands have improved discrimination of tropical forest regeneration areas over the ability of NIR/VIS indices (Boyd *et al.*, 1996). Jolly *et al.* (1996) found TM band 5 led to the best identification of clear-cut pine stands in south-west France. Finally, Jakubauskas (1996) found visible and SWIR TM bands to be correlated with height, basal area, biomass and LAI in successional stages of Yellowstone lodgepole pine. He concluded that the spectral reflectance properties of 'successional forest stands over time is a function of the combined effects of the overstory canopy, the amount of shadow within a canopy, and the understory'.

4.2.3 Measuring Vegetation Amount (LAI)

The previous sections described work that has related measured reflectance to vegetation or canopy parameters, such as percentage cover or Leaf Area Index (LAI). However, the establishment of such relationships is dependent on reliable and accurate measures of vegetation amount (Curran 1980; 1988). This section describes and assesses the various means of measuring LAI; no doubt the most comprehensive single measure of vegetation amount and one that is routinely used for physiological and ecological vegetation studies.

Percentage cover was shown to relate well to certain reflectance indices in the previous chapter, but by definition, percentage cover is a one-dimensional estimate of vegetation amount. LAI is a description of total foliage amount since it is the projected one-sided (half the total) leaf area per unit of ground area (usually m^2/m^2) (Jarvis and Leverenz, 1983). It is 'one of the primary measures used in remote sensing and process-based models to characterise plant canopies' (Chen *et al.*, 1997). However, it has been recognized that a one-sided projected area in one direction does not account for radiation interception by pine shoots and needles that are orientated in various directions, and are not necessarily flat. In other words, the ratio of total to *mean* projected area (i.e. not in one direction only) is not 0.5. To avoid this problem, LAI has been redefined as one half the total green-leaf area per unit of ground (Chen and Black, 1991; 1992; Fassnacht *et al.*, 1994; Stenberg *et al.*, 1994). Since the total green-leaf area definition is more appropriate for pine canopies, it is the definition of LAI used in this study.

A number of authors have reviewed the direct and indirect methods used for obtaining estimates of forest LAI (e.g Norman and Campbell, 1989; Chason *et al.*, 1991; Chen *et al.*, 1997; Gower *et al.*, 1999). Indirect methods largely involve optical measurements, which are used to measure canopy gap fraction, and thereby estimate canopy LAI. The most extensively reported apparatus in the literature relating to the LAI of forest canopies is the LAI-2000 Plant Canopy Analyzer (PCA)

(Li-Cor Inc., Lincoln, Nebraska). The PCA estimates LAI from measured relative light interception using a gap fraction formula as the contact frequency (Sampson and Allen, 1995). The gap fraction is defined as 'the percentage of sky seen from beneath the canopy' (Chen *et al.*, 1997). The PCA samples incident light at five distinct zenith angle classes for radiation wave bands in the blue region. Foliage density is estimated by integrating the relative light fraction over each zenith angle class with a known beam path length. An estimate of LAI is obtained by integration over each sampled zenith angle class, with the assumption that the inverse of the cosine of the mean angle for each class approximates a relative beam path length. One advantage of the PCA is that it calculates the light extinction coefficient of the canopy using the measured relative light intercepted. Other radiative methods require that the light extinction coefficient be estimated separately.

The Li-Cor PCA has been used by a number of researchers for a range of forest environments including deciduous species (Chason *et al.*, 1991; Eschenbach and Kappen, 1996; Strachan and McCaughey, 1996), Douglas fir (Chen and Black, 1991; Smith *et al.*, 1993) and a range of pine species (Gower and Norman, 1991; Gong *et al.*, 1992; Deblonde et al, 1994; Fassnacht *et al.*, 1994; Stenberg *et al.*, 1994; Sampson and Allen, 1995; Chen, 1996b; Chen *et al.*, 1997 and Gower *et al.*, 1999). Its popularity can be attributed to the relative ease with which measurements can be made, its speed, and therefore its cost effectiveness. However, originally designed for cultivated crop canopies, a number of problems have emerged to complicate its application to forest environments. Firstly, the PCA cannot separate woody or reproductive plant material from leaf plant material, so that it actually measures Plant Area Index (PAI), a less ecologically meaningful quantity than LAI (White *et al.*, 2000). To calculate LAI from PAI, local empirical corrections have been established (e.g. Gower and Norman, 1991; Deblonde et al, 1994; Fassnacht *et al.*, 1994; Chen, 1996b). Secondly, it has been consistently reported that the PCA underestimates conifer LAI, which has been attributed to the aggregation of needles at the shoot level (pines) or the branch level (Douglas fir). This is because the PCA uses a fisheye lens to project a hemispheric image of the canopy onto silicon detectors so that this projected image does not account for plant parts that shade each other

(Gower and Norman, 1991). These workers corrected the PCA LAI estimates by multiplying by the 'total-projected-needle area to shoot-silhouette-area ratio' which significantly improved the PCA estimates of LAI. However, since the work of Gower and Norman, several workers have improved the correction factor to account for non-random leaf area distribution in conifers (Smith *et al.*, 1993; Deblonde *et al.*, 1994; Fassnacht *et al.*, 1994; Stenberg *et al.*, 1994; Gower *et al.*, 1999).

Other instruments that utilise canopy transmittance to indirectly estimate LAI include DEMON (CSIRO, Centre for Environmental Mechanics, Canberra, Australia) and the Sunfleck Ceptometer (Decagon Devices, Pullman, WA, USA). Whitford *et al.* (1995) described the use of DEMON, which, unlike the PCA requires completely cloud-free conditions and does not sense light over various angles simultaneously. The Sunfleck Ceptometer has also been used to estimate LAI for forest canopies (e.g. Pierce and Running, 1988; Smith, 1993; Nel and Wessman, 1993). This instrument uses the average sunfleck fraction and photosynthetically active radiation of both diffuse and direct light, measured by a series of light sensors along a rod. However, since it samples only a small portion of the canopy, it requires a large number of measurements to describe the whole canopy (Fassnacht *et al.*, 1994). White *et al.* (2000) concluded that 'while transmittance methods can give consistent relative measurements at a given site, quantitatively accurate measurements require site-specific correction factors'. Furthermore, it has been suggested that indirect methods are unsatisfactory for more open stands with low LAI (Whitford *et al.*, 1995), for mixed stands (Gower and Norman, 1991) or for stands with varying canopy structure (Smith *et al.*, 1993).

Direct methods of measuring LAI are generally considered to be more accurate and are therefore used as the basis for assessing the accuracy of indirect methods. This may work well for crop plants that can be readily harvested and measured, but in practice direct LAI estimation of forest, and of conifers in particular, is more problematic. The tendency in the literature to assess indirect methods against direct methods, whose accuracy is not precisely known, must also call into question the accuracy assessment of indirect methods themselves. Nonetheless, aside from

directly measuring every leaf or needle, allometric relationships are perhaps the most commonly used direct method for tree LAI calculation (e.g. Mecuccini and Grace, 1995; Nemani *et al.*, 1993). Relationships are usually established between leaf area and basal area (e.g. Whitford *et al.*, 1995) or tree girth (Danson and Plummer, 1995), or sapwood area (Gower *et al.*, 1999). This may be effective for relatively homogeneous stands, where a small sample of trees can be destructively sampled. However, as Gower *et al.* (1999) point out, 'Using general allometric equations to estimate LAI for a specific stand can result in moderate to large errors because numerous abiotic and biotic factors influence the allometry coefficients'. This suggests that increased sampling would be required across a more heterogeneous semi-natural stand.

4.2.4 Statement of Aims

The aims of this research are as follows:

1. To develop a method of measuring the plot LAI of pine regeneration.
2. To produce estimates of plot LAI.
3. To extend the field radiometric data collected for the earlier MRes. study in terms of both season and wavelengths measured.
4. To use correlation analysis to explore the relation between SWIR wavelengths and percentage cover and LAI.
5. To assess the influence of seasonal changes in canopy colour on the strength of the correlation between selected indices and percentage cover and LAI.

4.3 Methods

4.3.1 Field Spectral Measurements

Following the earlier measurements in March, May, June and July 1997 for the MRes. study, measurements were continued over the sample plots at Inshriach through the 1997 and 1998 growing seasons. A GER 1500 ™ instrument continued to be used for the September, October 1997 and August 1998 sampling dates, but a GER 3700 ™ instrument was used in May and July 1998 in order to extend the sampling into the SWIR. Tables 4.1 and 4.2 summarize the instruments used and the measurement conditions.

Table 4.1 Field spectroradiometer specifications.

	GER 1500	GER 3700
Dispersion	1.5 nm	1.5 nm: 300-1050 nm 6.5 nm: 1050-1900 nm 9.5 nm: 1900-2500 nm
Digitisation	16 bits	16 bits
Channels and sensor type	512 Si	512 Si, 128 Pbs, 64 Pbs
Scan time	10 ms minimum	50 ms minimum
Memory	500 spectra in solid state memory or computer	computer
Spectral range	300-1100 nm	300-2500 nm
Resolution	3 nm	3 nm 300 - 1050 nm As for dispersion 1050- - 2500 nm
Detection	Si photodiode array	Si photodiode array and 2 Pbs arrays in the SWIR
FOV	15°	10°
Control	laptop computer/manual	laptop computer
Weight	4 Kg	6.4 Kg

The GER 1500™ spectroradiometer is a lightweight, highly portable instrument that has the advantage of a very fast scan time and a solid state memory for about 500 scans, making it very rapid to use. Its lighter weight makes it more suitable for fixing to a pole or a tripod to gain extra height and this instrument was suspended at 2 m above ground level. The GER 3700™ contains three separate detectors; the Si photodiode array is the same as the GER 1500™ for VIS/NIR wavelengths. Two further integrated PbS detectors allow scans to extend into the SWIR with wider dispersion.

Table 4.2 Measurement dates and conditions

Date	Instrument	Sky conditions	Clock time	Solar time	Altitude angle	Azimuth angle†
31 Mar 97	GER 1500	Overcast, uniform	10:50 - 14:35	11:01 - 14:46	35.87 - 27.92	18.19 - -48.48
16 May 97	GER 1500	Clear , hazy after 13:00	10:48 - 13:33	10:07 - 12:52	46.66 - 50.84	40.63 - -19.68
01 Jun 97	GER 1500	Some haze, clear by 14:00	12:07 - 15:05	11:24 - 14:22	54.37 - 46.45	14.17 - -51.59
05 Jul 97	GER 1500	Overcast, uniform	11:53 - 14:44	11:03 - 13:54	54.14 - 49.80	22.46 - -43.33
23 Sep 97	GER 1500	Clear, with some haze developing	11:50 - 15:35	11:13 - 14:58	31.92 - 22.54	13.87 - -49.40
31 Oct 97	GER 1500	Overcast, changeable light	10:15 - 13:39	09:46 - 13:10	13.54 - 17.15	33.21 - -17.96
14 May 98	GER 3700	Thin cirrus - sun obscured	13:40 - 16:31	12:59 - 15:50	50.00 - 33.04	-22.07 - -72.41
22 Jul 98	GER 3700	Overcast, variable light	11:33 - 16:14	10:41 - 15:22	50.43 - 37.79	29.46 - -66.82
31 Aug 98	GER 1500	Clear, some cumulus	13:07 - 15:45	12:22 - 15:00	41.29 - 30.30	-07.26 - -54.11

† The solar azimuth angle is the angular distance between due South and the projection of the line of sight to the sun on the ground. A positive solar azimuth angle indicates a position East of South, and a negative azimuth angle indicates West of South

A purpose-built adjustable stand was used to suspend the GER 1500™ at 2 m above ground level to give a nominal field-of-view of approximately 0.4 m. The GER 3700™ was supported on a tripod at 1.6 m above ground level to give a nominal field-of-view of approximately 0.3 m diameter. The radiometric data were collected as close to the solar noon as practicable in order to minimise the effects of shadowing

in the plots and to vary the Sun-target-sensor geometry as little as possible. All scans were normalised to radiance measured from a Spectralon™ reference panel and measurement procedures outlined by Milton (1987) and Milton *et al.* (1995) were followed. Particular care was taken to maintain the sensor alignment in the sun-target plane, with the operators as far down-sun of the target as practicable. Panel reference measurements were recorded for each target scan when the light was changeable, but between every five to ten scans when the light was more stable and uniform.

Each 5 x 5 m plot was measured using a systematic 1 m grid sampling system as illustrated in Figure 4.1.

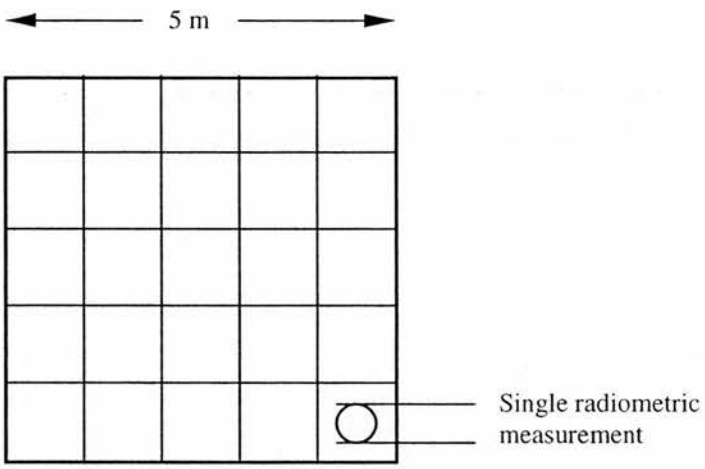

Figure 4.1 The 25-grid sampling system within each sample plot

Absolute reflectance was obtained for each reflectance measurement by multiplying reflectance by factors relating the reference panel to a National Physics Laboratory reflectance standard. The twenty-five spectra in each plot were averaged in each wavelength to give a mean overall reflectance spectrum for each plot on each sampling date. First-order derivative spectra were calculated using quadratic polynomial functions fitted by least squares over a 9 nm bandwidth interval (Saviztky and Golay, 1964).

4.3.2 Vegetation Measurements

The plot measurements involving the dimensions and location of each sapling within each plot were carried out during the MRes. study (see previous chapter). These measurements were used to calculate percentage cover. The position and distribution of each sapling is illustrated in Figure 2.2. Vegetation measurements carried out for the present study focussed on obtaining an accurate estimate of LAI. Fieldwork undertaken to measure LAI took place during April 1998.

The review of methods used to measure LAI is given in the previous section. Clearly, the easiest measurements to take are the indirect optical estimates of LAI, but the vegetation at Inshriach was considered unsuitable for reliable estimates using this method for several reasons. Firstly, optical methods have been tested almost exclusively within continuous forest stands and there is some evidence to suggest that indirect methods are unsatisfactory for more open stands with low LAI (Whitford *et al.*, 1995). Secondly, for younger regeneration, the base of the sapling crowns is often indistinguishable from the heather understorey, making it very difficult to obtain optical measurements of just the sapling LAI alone. Primarily for these reasons, optical methods were considered impractical for the study area.

Direct methods were also problematic, as they generally require destructive sampling to derive a site-specific allometric relationship. Destructive sampling was not permitted due to the conservation status of the study area, but also it would have been difficult to establish a robust relationship for such a heterogeneous canopy. Given that the plots were relatively small, and the trees not full size, the best option was considered direct measurement of leaf area on random samples from each plot.

A sampling strategy was devised that attempted to take account of the tree shape variation and particular architecture of the saplings. The structure of Scots pine saplings is essentially a hierarchical one (Kellomäki and Strandman, 1995); the elements of the architecture are stems, whorls, branches, shoots and needles. The

shoot has been described as the basic unit of branch and crown structure (Ross *et al.*, 1996) and therefore, sampling at the shoot level in the hierarchy was considered most appropriate. New shoots extend during each growing season, with needle-fall occurring after three to five years to leave the shoot bare as the bark forms. At any given time therefore, needles exist on at least three orders of shoot on the saplings, and sometimes on a fourth. Sampling took place in spring 1998, before that year's new shoot extension, so that first-order shoots held fully developed needles from the previous year's growth, and second-order shoots from the growing season before that, and so on. An inventory of the number of all orders of shoots from randomly selected saplings in each plot was considered an adequate sampling strategy (J. Kupiec, personal communication).

In order to account further for the variation in crown shape within each plot, the sampling was stratified using the basic crown descriptors of height and width. Figure 4.2 illustrates a plot of height against width for each sapling within each plot in order to group them according to crown dimensions. Prior to a field visit, random numbers were generated to give Cartesian coordinates to select saplings using their location within each plot. This procedure was carried out until at least one sapling from each class in each plot had been selected (Figure 4.2). Upon arriving at the plots, the saplings selected in this way were identified using the maps of sapling positions (Figure 2.2), and by reference to their measured crown characteristics.

The number of each order of shoot was counted on each sapling and since very few fourth-order shoots contained needles, these were included in the third-order shoot count. Further measurements were taken so that the needle density and mean needle length of the shoots at different positions in the crown could be recorded. Needle length and shoot length vary, so that in general, shoots in the upper part of the crown that receive more light were longer, with longer needles. More shaded shoots lower within the crown, tended to have shorter shoots and needles. This within-tree variation was recorded by measuring the shoot characteristics of each level, or whorl, within the crown.

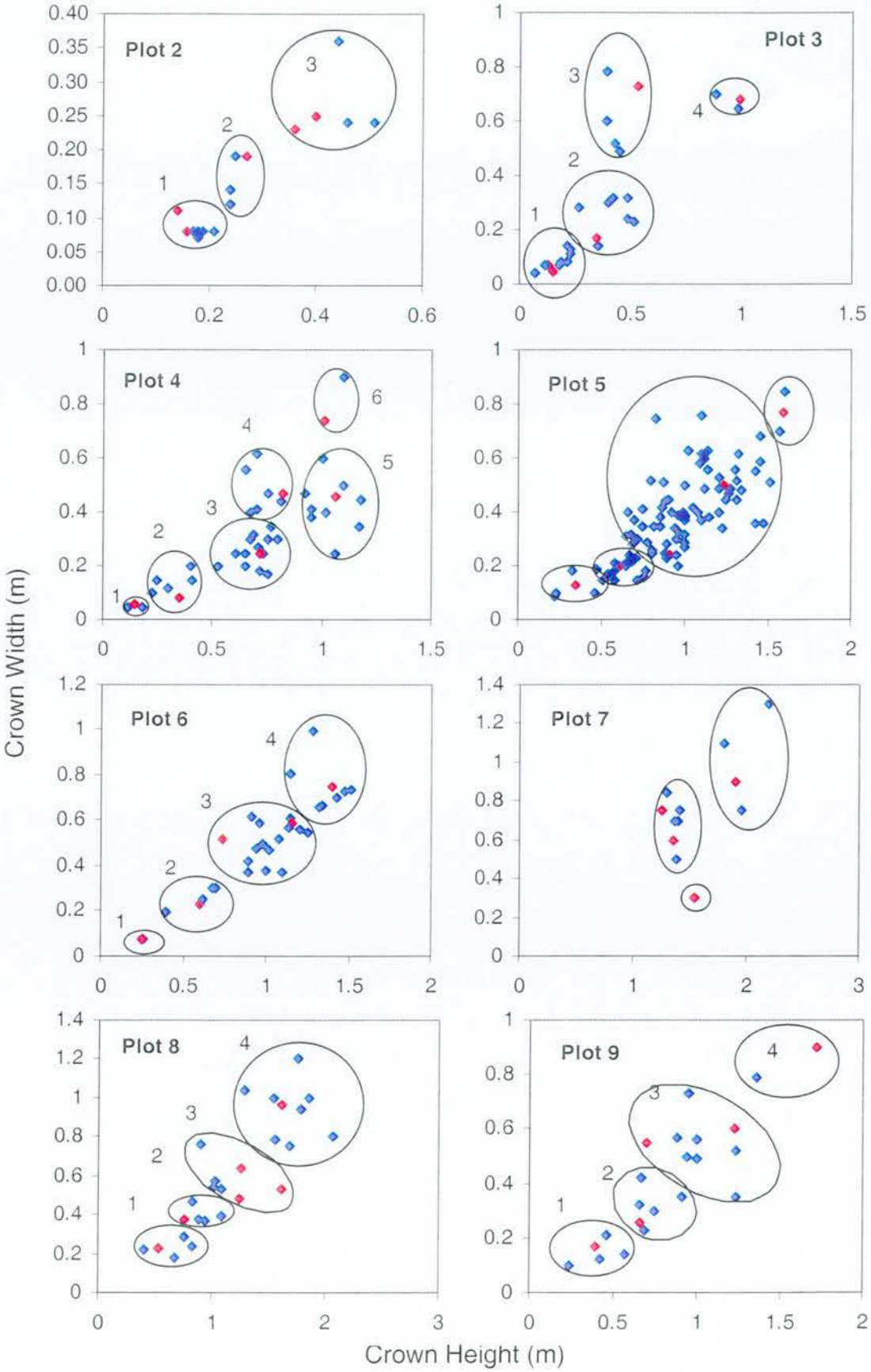

Figure 4.2 The stratified-random sampling of saplings within each plot using crown height/width and random numbers to select individuals within each class (shown in red) based on their coodinates. For plot 1, Scots pine LAI = 0.

On a sample of shoots from different locations within the crown, shoot needle density was found to be consistently close to 0.5 needles/mm. This value was used for all shoots sampled in order to estimate needle numbers from shoot length measurements.

After obtaining the number of each order of shoot within each whorl of the sample saplings, and obtaining an estimate of the number of needles on each shoot from shoot length, the remaining problem was to estimate the total surface area of a single pine needle. Measuring the total surface area of a pine needle may be achieved most easily by either measuring the projected-one-sided area using a planimeter, or, by a volume displacement method. Neither of these methods is particularly precise and both would require destructive sampling, which was not an option in this case. The planimeter can yield large inaccuracies for thin needles that may be twisted and not flat (Chen *et al.*, 1997; Flower-Ellis and Olsson, 1993). Volumetric methods convert measurements of needle volume to hemi-surface area using simplified geometric equations that assume a regular shape in needle cross section.

The method used in the present study takes advantage of a regression relationship established between the length of Scots pine needles and their surface area by Flower-Ellis and Olsson (1993). These workers sampled needles from young (15 year-old) Scots pine saplings grown in Sweden, from which they took six transverse sections using a freezing microtome to give 30 μm sections. The sections were magnified and projected onto a transparent screen using a projection microscope and the perimeter of the images were traced. Area-weight conversion factors were used to calculate needle volume and surface area. The result of this work was to produce a derived regression equation for predicting the surface area of a needle from its length;

$$A_t = 4.0196\ (\text{LENGTH mm}) - 10.6973$$
$$R^2 = 0.965,\ n = 30$$

where A_t = total surface area of one needle. According to Flower-Ellis and Olsson (1993), application of this regression to material of more southerly origin than Sweden is likely to lead to an over-estimation of LAI. However, any error due to

geographical variations is likely to be slight compared with other methods of estimating LAI, and the regression on needle length has a number of distinct advantages;

- it requires only needle-length measurements,
- other methods are considerably more time consuming,
- it achieves an estimate of needle area that allows comparison between plots as required, since any error will be systematic,
- needle length measurements were possible without needle/shoot removal, using calipers

The advantages of the whole method of estimating sapling LAI are as follows;

- there is no assumption of randomly distributed leaves as for optical methods,
- there is no confusion with the proportion of woody material (only the green 'leaf' area is being estimated),
- there is no destruction of samples is required, and
- there is rapid processing of data from field sampling using a simple spreadsheet.

The main disadvantages may be listed as follows;

- it is time consuming to count the number of shoots on each sapling and to measure shoot lengths and needle lengths,
- there is uncertainty over the applicability of the Swedish regression model for needle area.

Measuring the degree of uncertainty in using the Swedish regression model was difficult since no other method offers the same degree of accuracy (apart from a direct replication of the Swedish study). However, the needles from seven shoots were measured for length to 0.5 mm and for needle area using a Li-Cor LI-3000 leaf area meter by way of comparison. The leaf area meter was found to produce results 32% lower than the regression method. However, given the inaccuracies inherent in the leaf area meter, through narrow leaf samples, non-flat and twisted samples, it was expected that this method would significantly underestimate needle area.

4.4 Results and Interpretation

This section presents the results of linear correlation analysis using the measured reflectance and first-order derivative spectra from each sampling date. The relation between percentage cover and LAI of pine sapling in the sample plots, and measured reflectance is presented and interpreted in the context of seasonal changes in canopy colour and the potential of the indices used for monitoring changes in pine sapling amount.

Reflectance spectra measured with the GER 1500™ instrument are illustrated in the previous chapter, but measurements taken with the GER 3700™ in May and July 1998 are illustrated in Figure 4.3. Data centred around 1400 nm and 1900 nm were omitted as these regions represent wavelengths associated with maximum absorption of atmospheric water vapour. The visible and NIR reflectance up to about 1000 nm mirrors the results obtained with the GER 1500™ instrument, which was to be expected since the same detector is used over this range. Unfortunately, longer wavelengths proved very noisy with this instrument, with measurements above 1800 nm, in particular, considered less reliable. The water absorption features at around 970 and 1200 nm are much less noisy.

The main difference between the averaged plot spectra for the two months is the greater variation between plot NIR reflectance in May, over that in July 1998. This is likely due to the differing sky conditions on these two dates, rather than any significant change in plot characteristics over this short period. Figure 4.4 illustrates the derivative spectra for these dates, in which the noise at longer wavelengths is more pronounced.

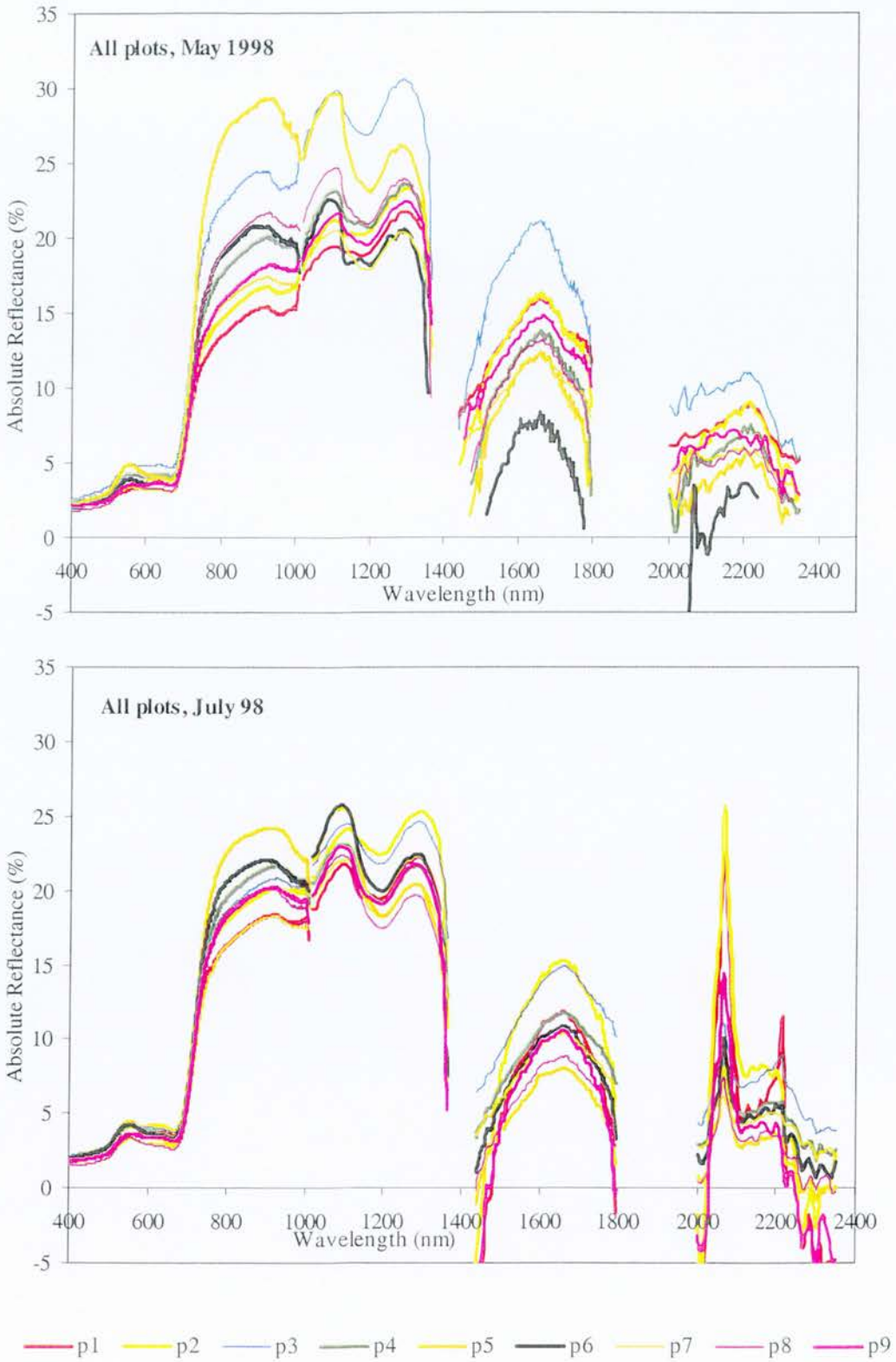

Figure 4.3 GER3700™ averaged reflectance spectra for each plot in May and July 1998.

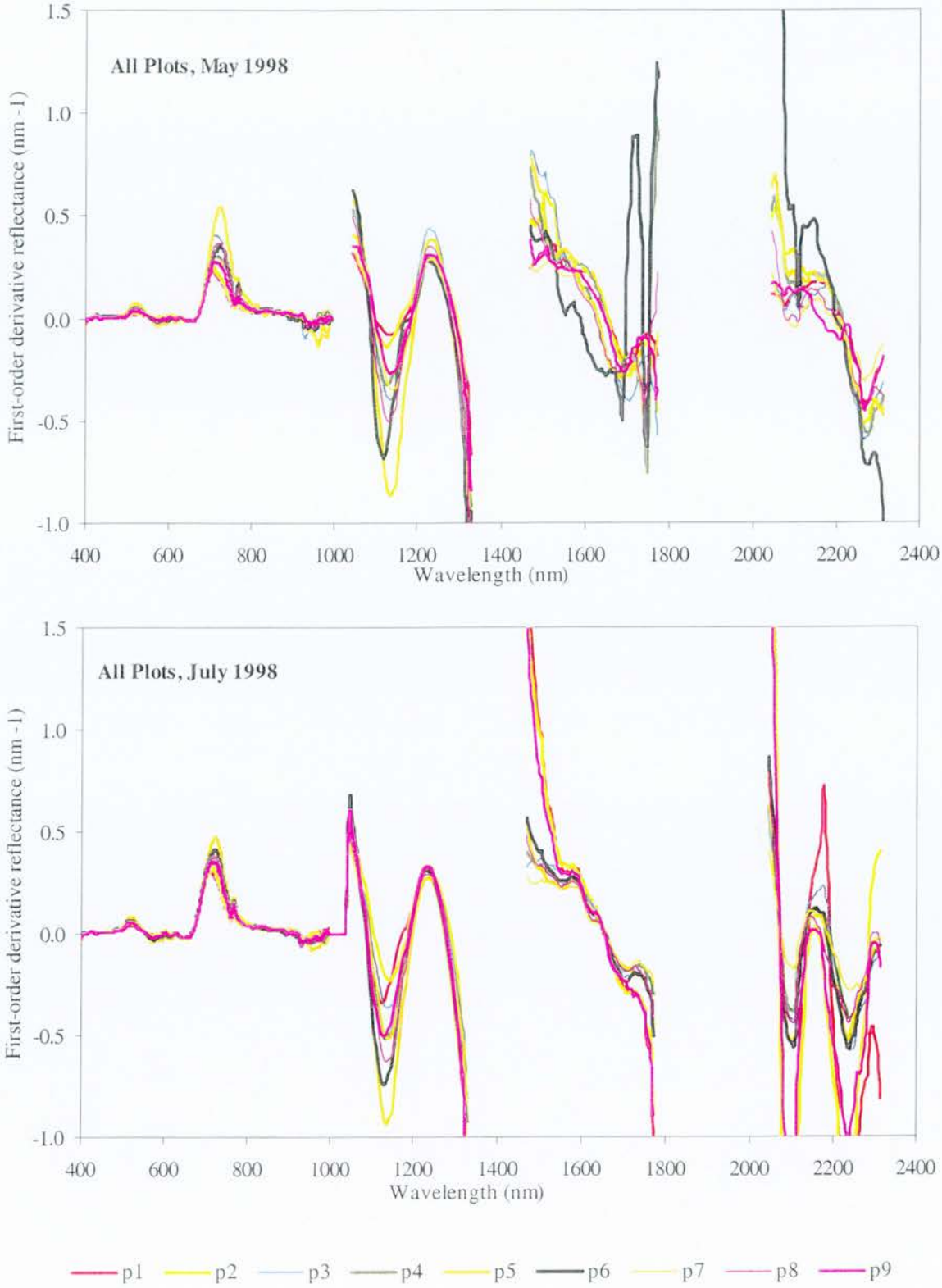

Figure 4.4 GER3700™ averaged first-order derivative reflectance spectra for each plot in May and July 1998.

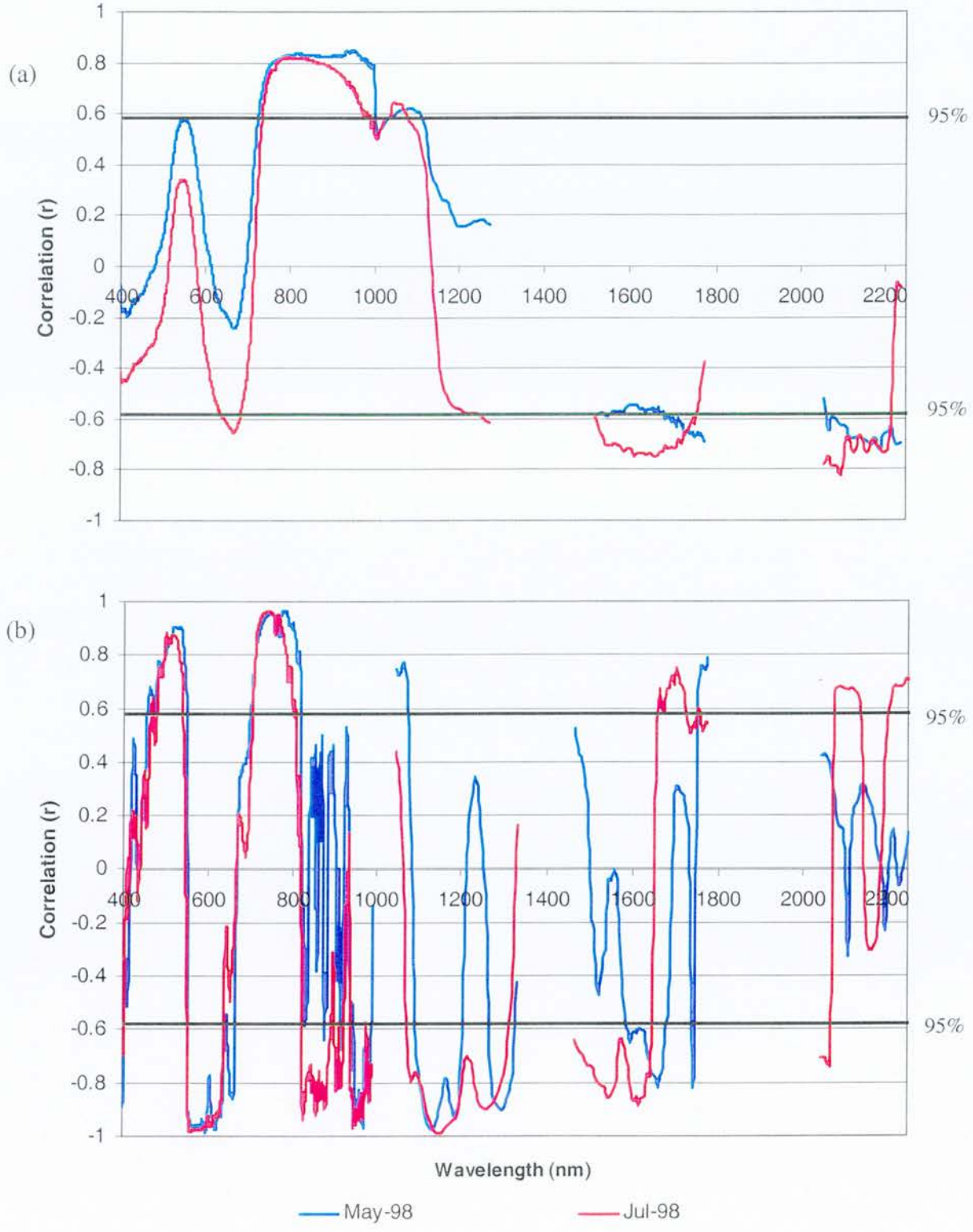

Figure 4.5 Correlograms showing the correlation of LAI at each wavelength (May and July data), for (a) reflectance and (b) first-order derivative reflectance. Confidence limits at 95% = ± 0.58 and 99% = ±0.75, (n = 9).

4.4.1 Relation between Reflectance and LAI

The correlograms in Figure 4.5 illustrate the strength of the relation between LAI and reflectance at each wavelength for the May and July 1998 data. The correlograms are useful indicators of the wavelength regions most sensitive to changes in LAI. Correlograms relating reflectance to percentage cover were also computed and produced very similar results to those for LAI in Figure 4.5. Within the visible and NIR, the reflectance correlogram curves (Figure 4.5 (a)) are similar to those generated for the previous MRes. study, albeit for percentage cover only, in that case. However, the curves above about 1000 nm in Figure 4.5 (a) provide new information on the potential of longer wavelengths for monitoring pine regeneration.

There remains a relatively high positive correlation with LAI throughout the NIR plateau until about 1100 nm; a point on the reflectance curve (Figure 4.3) at the top of the central peak on the NIR plateau. At longer wavelengths, the correlation becomes negative, and significant at the 95% confidence limit at about 1250 nm, centred on 1630 nm and on 2150 nm. Like the reflectance curve, the correlogram is noisier but consistent at longer wavelengths.

The region centred on 1630 nm corresponds to Landsat TM 5, which, it has been suggested, was the TM band corresponding best to stages of pine regeneration at Inshriach (McCoy, 1997). McCoy also reported the greatest dynamic range for reflectance in this region. The reflectance curves illustrated in Figures 4.3 (a) and (b) would appear to support this conclusion, particularly for the May data. Unlike the NIR, reflectance is greater for low-density plots than for higher density ones at the 1630 nm peak. The most likely explanation for this observation, is the effect of leaf water absorption, which would decrease reflectance in this region. However, the trend is not clear-cut, with medium density plots having very similar reflectance at this peak. This is likely due to the combined effects of tree size, proportion of shadow cast and plot density, in addition to the plot parameters measured (percentage cover and LAI). The reason for the greater range of reflectance values in the May data over the July data is likely due to the brighter sky conditions in May, giving a

higher reflectance for lower density stands in the SWIR. The trends observed around the 1630 nm peak are also identifiable in the MIR, 2150 nm region, but are less clear due to the lower dynamic range, lower absolute reflectance values and greater noise.

It was found that a combination of NIR reflectance with the SWIR as a simple SWIR/NIR ratio improved the correlation with LAI of both the NIR and SWIR alone (Table 4.3). However, the improved correlation coefficients from this ratio, still fell short of those achieved using the NIR/Red and NDVI ratios (Table 4.4).

Table 4.3 Correlation coefficients (r) between LAI and NIR/SWIR indices

	May 98	July 98
$SWIR_{1630}/NIR_{850}$	-0.93	-0.88
NIR_{850}	0.83	0.82
$SWIR_{1630}$	-0.56	-0.73

Table 4.4 Correlation coefficients (r) between selected indices and % cover (PC) of pine and Leaf Area Index (LAI).

	Mar-97		May-97		Jun-97		Jul-97		Sep-97		Oct-97		May-98*		Jul-98*		Aug-98	
	PC	LAI	PC	LAI	PC	LAI	PC	LAI	PC	LAI	PC	LAI	PC	LAI	PC	LAI	PC	LAI
Reflectance																		
Green peak	0.40	0.39	0.40	0.50	-0.22	-0.05	0.65	0.76	0.48	0.60	-0.17	-0.01	0.44	0.57	0.13	0.34	0.64	0.70
Red Trough	-0.86	-0.75	-0.78	-0.81	-0.85	-0.76	-0.57	-0.45	-0.91	-0.87	-0.79	-0.69	-0.41	-0.24	-0.79	-0.64	-0.69	-0.79
NIR	0.80	0.91	0.66	0.64	0.76	0.87	0.87	0.92	0.75	0.80	0.57	0.67	0.74	0.83	0.68	0.82	0.91	0.89
NIR/Red	0.97	0.97	0.88	0.91	0.97	0.97	0.95	0.94	0.90	0.93	0.95	0.93	0.97	0.96	0.98	0.95	0.90	0.96
NDVI	0.97	0.96	0.93	0.95	0.97	0.95	0.93	0.90	0.96	0.95	0.91	0.87	0.97	0.94	0.97	0.93	0.91	0.94
R_{752}/R_{722}	0.97	0.96	0.97	0.98	0.97	0.97	0.97	0.97	0.96	0.96	0.93	0.90	0.98	0.98	0.96	0.94	0.96	0.98
1st Derivative																		
R peak $_{719}$	0.92	0.98	0.85	0.90	0.91	0.97	0.90	0.94	0.85	0.89	0.77	0.83	0.83	0.89	0.85	0.94	0.94	0.94
L peak $_{703}$	0.65	0.78	0.59	0.68	0.76	0.86	0.82	0.88	0.59	0.67	0.47	0.58	0.58	0.67	0.39	0.56	0.83	0.81
R - L diff.	0.95	0.94	0.98	0.95	0.96	0.97	0.95	0.97	0.94	0.95	0.92	0.92	0.97	0.99	0.95	0.96	0.98	0.98
R/L ratio	0.95	0.94	0.99	0.96	0.97	0.98	0.96	0.96	0.97	0.95	0.92	0.88	0.97	0.97	0.95	0.93	0.96	0.95
D_{730}/ D_{700}	0.96	0.96	0.99	0.97	0.97	0.97	0.96	0.97	0.97	0.96	0.93	0.89	0.97	0.98	0.95	0.92	0.96	0.97
Green peak	0.96	0.97	0.89	0.92	0.83	0.92	0.89	0.94	0.83	0.89	0.59	0.68	0.85	0.90	0.77	0.88	0.83	0.89
Green trough	-0.98	-0.98	-0.94	-0.96	-0.92	-0.97	-0.93	-0.96	-0.91	-0.95	-0.87	-0.91	-0.95	-0.96	-0.92	-0.98	-0.89	-0.93
Grn. Dif.	0.97	0.97	0.92	0.94	0.88	0.96	0.89	0.92	0.87	0.93	0.74	0.81	0.91	0.94	0.86	0.94	0.85	0.91
D_{1150}													-0.93	-0.95	-0.97	-0.99		
REP	0.81	0.77	0.83	0.17	0.84	0.21	0.81	0.67	0.86	0.64	0.80	0.70	0.91	0.38	0.87	0.66	0.83	0.72

Significance levels are 0.58 (95%), 0.75 (99%) and 0.88 (99.9%); n = 9.
NIR/Red = R_{800}/R_{670}, NDVI = $[R_{800}-R_{670}/R_{800}+R_{670}]$.
** GER 3700 used to include the NIR and SWIR up to 2500 nm. GER 1500 used on all other sampling dates.*

4.4.2 Relation between First-Derivative Reflectance and LAI

The first-order derivative correlogram curves illustrated in Figure 4.5 (b) are also very similar to those generated for percentage cover in the previous MRes. study for the visible and NIR wavelengths. There was highly significant correlation at about 400, 520, 600, 750, 850, and 960 nm. Table 4.5 illustrates the correlation with LAI for these wavelengths, and describes their respective reflectance and first-derivative curve features.

Wavelengths around 1150, 1280, and 1630 in the NIR and SWIR were also found to correlate highly with LAI, although the correlation coefficient at 1150 nm was particularly high. This wavelength corresponds to the inflexion point of the descending limb of a reflectance trough on the reflectance curve, and is a distinct trough on the derivative curve. The 1150 nm derivative trough is more pronounced than the red-edge peak, since the reflectance curve is steeper at this point. In addition, there is a greater separation between the plots at the 1150 nm derivative trough than at the red-edge peak. The steepness of the reflectance trough's descending limb is likely to be related to canopy water content, which is directly related to LAI. Therefore, this feature may be useful for monitoring pine regeneration if it is relatively insensitive to clumping, shadow and atmospheric absorption.

Correlation coefficients for this first-derivative feature (D_{1150}) for both percentage cover and LAI are given in Table 4.4. Other workers have reported on the sensitivity of this derivative feature to canopy water content (Rollin and Milton, 1998) and to leaf water content (Danson *et al.*, 1992). However, Rollin and Milton (1998) also demonstrate that the exact wavelength position of first-derivative features will shift with the level of data smoothing. The present study applied a 9-point quadratic polynomial function and simplified least-squares procedure (Savitzky and Golay, 1964), which, it was felt, offered a compromise between loss of detailed spectral information and improvement in the signal-to-noise ratio through noise reduction.

Table 4.5 First-derivative spectral features correlating significantly with plot LAI

λ (nm)	*r* (July 1998)	1st derivative feature (Figure 4.4)	Reflectance feature (Figure 4.3)
400	-0.69*	Undefined feature	Leaf pigment absorption
520	0.88***	Peak	Left ascending limb of green reflectance peak
570	-0.98***	Trough	Right descending limb of green reflectance peak
710 - 760	0.94*** (mean)	Red-edge peak and descending limb	Top half of red-edge and transition to NIR plateau
850 - 890	-0.83** (mean)	Undefined feature	NIR plateau
950	-0.96***	Small trough	Water absorption trough (descending limb)
1150	-0.99***	Large trough	Water absorption trough (descending limb)
1280	-0.86**	Descending limb of peak at 1230 nm	Reflectance peak
1630	-0.85**	Undefined feature	Reflectance peak

Significance levels are 0.58 (95%), 0.75** (99%) and 0.88*** (99.9%); n = 9*

It is evident from Table 4.4 that in general, there is little difference between the strength of the correlations for percentage cover and LAI. A notable exception however, is the red-edge position (REP). REP is defined as wavelength of the maximum slope of the red-edge region between red-wavelength absorption and NIR reflectance. In relation to percentage cover, REP correlated significantly and consistently throughout the 1997 and 1998 growing seasons (Table 4.4), but less so with LAI. However, the previous chapter highlighted the potential confusion caused by the existence of two peaks on the derivative curve, and a switching in dominance between them as percentage cover increased.

The correlation between the REP and LAI calculated for the present study (Table 4.4) was lower than that for percentage cover, at every sampling date. This result contradicts results generally reported by other workers (e.g. Danson and Plummer, 1995). According to Ferns *et al.* (1984), the red-edge reflectance of a vegetation

canopy is controlled by chlorophyll concentration in the leaf and the degree of overlap between leaves. It can reasonably be assumed that the needle chlorophyll concentration will not differ considerably between the sample plots at Inshriach, but it is known that the spatial distribution of leaf area within the sample plots did (Figure 2.2). The value 'plot LAI' describes the amount of needle material within each plot, but does not take account of whether this material is clumped in one area, or distributed evenly.

Canopy structure has been shown to affect red-edge spectral parameters (Zarco-Tejada and Miller, 1999). The stronger correlation with LAI of the red-edge peaks (D_{719} and D_{703}) and their ratio, but the weaker correlation between LAI and REP, mirrors the results reported by Filella and Peñuelas (1994) for pepper plants. It would, therefore, be highly unlikely that REP will correlate well with LAI for heterogeneous canopies, such as a for natural pine regeneration.

4.4.3 The Effect of Season

One of the major problems when monitoring semi-natural landscapes for longer-term change, is the significant shorter-term seasonal changes in canopy colour, which may mask the longer-term changes of interest. Within the study plots, two seasonal changes were most apparent. Firstly, there was a flush of growth on the pine saplings as the current year's leader shoots extended; this was most apparent in July. The previous MRes. study included reflectance measurements up until July 1997, and it was concluded that this flush did not significantly affect the relationship between percentage cover and the wavelength indices selected for correlation. This conclusion is supported by the correlation coefficients for July 1998 (Table 4.5), which are also consistent with those for the rest of that season, and the previous year.

Secondly, the present study explored the effects of the flowering heather understorey in late August and early September by extending the sampling through the 1997 growing season. At this time of year, the heather flowers transform the understorey to a pink colour. Again, from the correlation coefficients presented in Table 4.4, the September 1997 and August 1998 values are consistent with those from other months. It is suggested therefore, that whilst the understorey canopy colour alters in late summer, it does not affect the relation between these indices and percentage cover or LAI of the pine overstorey.

Miller *et al.* (1997) studied the seasonal variation in understorey reflectance and their effect on vegetation indices for a range of conifer sites in North America. Interestingly, they found the least seasonal variation in reflectance occurred at young jack pine sites, with no significant effect on the relation between spectral vegetation indices and LAI. It is likely that in older stands, the composition of the understorey becomes modified by the overstorey, so that the understorey-only reflectance is not such a valid representation of reflectance for 'zero pine LAI'. Certainly, for the regeneration at Inshriach, the structure and species composition of the understorey community was consistent across the site, irrespective of the presence or absence of a regenerating pine overstorey.

4.5 Conclusions

The relation between measured reflectance in the VIS, NIR and SWIR wavelengths and pine sapling amount was investigated using correlation analysis, in order to assess their potential for monitoring regeneration. Two measures of pine sapling amount were calculated from detailed measurements of the saplings within nine sample plots at Inshriach. Percentage cover offered a relatively quick, one-dimensional estimate of pine sapling amount using only individual sapling crown diameter measurements. Conversely, LAI proved to be time consuming to measure, using the number and length of the basic canopy elements (needles and shoots) to estimate the LAI of whole sample trees, and thereby, of the whole plots. A regression model was used to convert needle length to needle area. A relationship of 0.5 needles per millimetre of shoot was established by sub-sampling, which enabled the number of needles per shoot to be estimated from shoot-length measurements.

Reflectance of each sample plot was measured on nine sampling dates, covering the 1997 and 1998 growing seasons. The wavelength range measured in May and July 1998 extended beyond the NIR into the SWIR by use of a different field radiometer, a GER 3700™. The GER 3700™ allowed the correlation analysis to include the SWIR for these months, and to test the sensitivity of this wavelength region to pine sapling amount. All reflectance measurements were transformed to absolute reflectance and to first-derivative reflectance.

Reflectance and first-order derivative indices that correlated strongly with percentage cover of pine in the previous MRes. study were used in the present study for the new data collected from September 1997 onwards, and were also used to test the correlation with LAI. For all the indices considered, except for REP, correlation with LAI was very similar to that with percentage cover. In the case of REP, correlation at each sampling date was significantly lower with LAI than with percentage cover. This was attributed to the clumpy distribution of green needles within some of the plots and the uneven distribution of the overstorey pine LAI.

Whilst other studies have shown correlation between REP and LAI, these have used field areas of relatively uniform plantation forestry. It is concluded that REP is not suitable for monitoring semi-natural forests because of their uneven LAI distribution, the potential confusion caused by the sudden switching of the dominant peak position, but also due to the uncertainties introduced by data smoothing. The REP, being over a relatively short wavelength range (approximately 25 nm), will be sensitive to variations in the degree of smoothing applied in different studies. Other derivative indices, such as those in the red-edge are less reliant on exact wavelength position, and more on derivative values.

Reflectance data collected in the SWIR in May and July 1998 correlated significantly in the regions of 1250, 1630 and 2150 nm. These regions are all associated with absorption of radiation by leaf water. The region of 1630 nm corresponds to Landsat TM 5, which, it has been suggested is the band most sensitive to pine regeneration. Correlation with LAI was improved in the SWIR (1630 nm) by combining it as a ratio with reflectance at the NIR (850 nm). This has the potential advantage of combining the sensitivity of the SWIR to canopy water content (and therefore LAI), with the relative insensitivity of the NIR to atmospheric water absorption, greater radiation received and the NIR sensitivity to canopy structure (and therefore also, LAI). However, the $SWIR_{1630}/NIR_{850}$ ratio correlation with LAI was still not as strong as the more traditional SVR or NDVI indices, which utilise the visible and NIR wavelengths.

Correlograms relating percentage cover and LAI to first-order derivative spectra indicated significant correlation with wavelengths in the region of 400, 520, 600, 750, 850, 960, 1150, 1280 and 1630. The strongest correlation in the SWIR region was at 1150, which corresponds to the inflexion point on the descending limb of the water absorption trough in this region.

Results from the correlation analysis also suggest that the relation between percentage cover and LAI and the selected indices are unaffected by seasonal changes in understorey and overstorey canopy colour. It should be stressed that in

terms of monitoring changes in pine sapling amount, the indices illustrated here that demonstrate high correlation with pine sapling amount, are only applicable to landscapes with the same relatively simple understorey. This will be particularly true for the D_{1150}, which is essentially just responding to total canopy water content and would be affected by variations in soil conditions and species compositon.

These results highlight the complexities of interpreting spectra of semi-natural regions of forest. Caution is required when relating absolute reflectance values to just one structural variable, such as LAI or percentage cover, because there may be other important variables of influence. At Inshriach, the density, distribution (i.e. clumping factor), understorey condition, or sky conditions all conspire to confound the relationship of interest. However, these results have shown that, within the wavelength range investigated, certain wavelengths and combinations of wavelengths offer greater potential for measuring pine sapling amount than others.

4.6 References

ALDAKHEEL, Y. Y. and DANSON, F. M., 1997, Spectral reflectance of dehydrating leaves: measurements and modelling. *International Journal of Remote Sensing*, **18**, 3683-3690.

ARDO, J., 1992, Volume quantification of coniferous forest compartments using spectral radiance recorded by Landsat Thematic Mapper. *International Journal of Remote Sensing*, **13**, 1779-1786.

BELWARD, A. S., TAYLOR, J. C., STUTTARD, M. J., BIGNAL, E., MATHEWS, J., and CURTIS, D., 1990, An unsupervised approach to the classification of semi-natural vegetation from Landsat Thematic Mapper data: a pilot study on Islay. *International Journal of Remote Sensing*, **11**, 429-445.

BLACKBURN, G. A., 1998, Quantifying cholorphylls and carotenoids at leaf and canopy scales: An evaluation of some hyperspectral approaches. *Remote Sensing of Environment*, **66**, 273-285.

BONHAM-CARTER, G. F., 1988, Numerical procedures and computer program for fitting an inverted Gaussian model to vegetation reflectance data. *Computers & Geosciences*, **14**, 339-356.

BOYD, D. S., FOODY, G. M., CURRAN, P. J., LUCAS, R. M., and HONZAK, M., 1996, An assessment of radiance in Landsat TM middle and thermal infrared wavebands for the detection of tropical forest regeneration. *International Journal of Remote Sensing*, **17**, 249-261.

CARTER, G. A. and MILLER, R. L., 1994, Early detection of plant stress by digital imaging within narrow stress sensitive wavebands. *Remote Sensing of Environment*, **50**, 295-302.

CHASON, J. W., BALDOCCHI, D. D., and HUSTON, M. A., 1991, A comparison of direct and indirect methods for estimating forest canopy leaf area. *Agricultural and Forest Meteorology*, **57**, 107-128.

CHEN, J. M., 1996a, Evaluation of vegetation indices and a modified simple ratio for Boreal applications. *Canadian Journal of Remote Sensing*, **22**, 229-242.

CHEN, J. M., 1996b, Optically-based methods for measuring seasonal variation of leaf area index in boreal conifer stands. *Agricultural and Forest Meteorology*, **80**, 135-163.

CHEN, J. M. and BLACK, 1991, Measuring leaf area index of plant canopies with branch architecture. *Agricultural and Forest Meteorology*, **57**, 1-12.

CHEN, J. M. and BLACK, 1992, Defining leaf area index for non-flat leaves. *Plant, Cell and Environment*, **15**, 421-429.

CHEN, J. M., RICH, P. M., GOWER, S. T., NORMAN, J. M., and PLUMMER, S., 1997, Leaf area index of boreal forests: Theory, techniques, and measurements. *Journal of Geophysical Research*, **102**, No.D24, 29,429-29443.

COCHRANE, M. A., 2000, Using vegetation reflectance variability for species level classification of hyperspectral data. *International Journal of Remote Sensing*, **21**, 2075-2087.

COHEN, W. B., 1994, GIS applications perspective: current research on remote sensing of forest structure. In *Remote Sensing and GIS in Ecosystem Management*, edited by V. A. Sample (Washington: Island Press), pp. 91-107.

COHEN, W. B., and SPIES, T. A., 1992, Estimating structural attributes of Douglas-fir western hemlock forest stands from Landsat and SPOT imagery. *Remote Sensing of Environment*, **41**, 1-17.

CRIST, E. P., and CICONE, R. C., 1984, A physically-based transformation of Thematic Mapper data - the TM tasseled cap. *I.E.E.E. Transactions on Geoscience and Remote Sensing*, **22**, 256-263.

CURRAN, P. J., 1980, Multispectral remote sensing of vegetation amount. *Progress in Physical Geography*, **4**, 315-341.

CURRAN, P. J., 1983, Multispectral remote sensing for the estimation of green leaf area index. *Philosophical Transactions of the Royal Society of London* A, **309**, 257-270.

CURRAN, P. J., and WARDLEY, N. W., 1988, Radiometric leaf area index. *International Journal of Remote Sensing*, **9**, 259-274.

DANSON, F. M., and CURRAN, P. J., 1993, Factors affecting the remotely sensed response of coniferous forest canopies. *Remote Sensing of Environment*, **43**, 55-65.

DANSON, F. M., and PLUMMER, 1995, Red-edge response to forest leaf area index. *International Journal of Remote Sensing*, **16**, 183-188.

DANSON, F. M., STEVEN, M. D., MALTHUS, T. J., and CLARK, P. J., 1992, High spectral resolution data for monitoring leaf water content. *International Journal of Remote Sensing*, **13**, 3045-3054.

DATT, B, 1999, Visible/near infrared reflectance and chlorophyll content in Eucalyptus leaves. *International Journal of Remote Sensing*, **20**, 2741-2759.

DEBLONDE, G., PENNER, M., and ROYER, A., 1994, Measuring Leaf Area Index with the LI-COR LAI-2000 in pine stands. *Ecology*, **75**, 1507-1511.

DEMETRIADES-SHAH, T. H., STEVEN, M. D., CLARK, J. A., 1990, High resolution derivative spectra in remote sensing. *Remote Sensing of Environment*, **33**, 55-64.

ESCHENBACH, C., and KAPPEN, L., 1996, Leaf area index determination in an alder forest: a comparison of three methods. *Journal of Experimental Botany*, **47**, No. 302, 1457-1462.

FASSNACHT, K. S., GOWER, S. T., NORMAN, J. M., and McMURTRIE, R. E., 1994, A comparison of optical and direct methods for estimating foliage surface area index in forests. *Agricultural and Forest Meteorology*, **71**, 183-207.

FERNS, D. C., ZARA, S. J., and BARBER, J., 1984, Application of high resolution spectroradiometry to vegetation, *Photogrammetric Engineering and Remote Sensing*, **50**, 1725-1735.

FILELLA, I., and PEÑUELAS, J., 1994, The red edge position and shape as indicators of plant chlorophyll content, biomass and hydric status. *International Journal of Remote Sensing*, **15**, 1459-1470.

FIORELLA, M., and RIPPLE, W. J., 1993, Analysis of conifer forest regeneration using Landsat Thematic Mapper data. *Photogrammetric Engineering and Remote Sensing*, **59**, 1383-1388.

FLOWER-ELLIS, J. G., and OLSSON, L., 1993, Estimation of volume, total and projected area of Scots pine needles from their regression on length. *Studia Forestalia Suecica*, **19**, 19 pp.

FOODY, G. M., 1990, Representation of inter-class gradients in heathland vegtation from ATM data. *Proceedings of the Airborne Remote Sensing Campaign, Keyworth, Nottingham, December 1990.*

GATES, D. M., KEEGAN, H. J., SCHLETER, J. C., and WEIDNER, V. R., 1965, Spectral properties of plants. *Applied Optics*, **4**, 11-20.

GAUSMAN, H. W., ESCOBAR, D. E., EVERITT, J. H., RICHARDSON, A. J., and RODRIGUEZ, R. R., 1978, Distinguishing succulent plants from crop and woody plants. *Photogrammetric Engineering and Remote Sensing*, **44**, 487-491.

GEMMELL, F. M., 1995, Effects of forest cover, terrain, and scale on timber volume estimation with Thematic Mapper data in a rocky-mountain site. *Photogrammetric Engineering and Remote Sensing*, **51**, 291-305.

GITELSON, A. A., KAUFMAN, Y.J., and MERZLYAK, M. N., 1996, Use of a green channel in remote sensing of global vegetation from EOS-MODIS. *Remote Sensing of Environment*, **58**, 289-298.

GITELSON, A. A., and MERZLYAK, M. N., 1994, Spectral reflectance changes associated with autumn senescence of *Aesculus hippocastanum* L. and *Acer platanoides* L. leaves. Spectral features in relation to chlorophyll estimation. *Journal of Plant Physiology*, **148**, 494-500.

GITELSON, A. A., and MERZLYAK, M. N., 1997, Remote estimation of chlorophyll content in higher plant leaves. *International Journal of Remote Sensing*, **18**, 2691-2697.

GONG, P., PU, R., and MILLER, J. R., 1992, Correlating leaf area index of Ponderosa pine with hyperspectral CASI data. *Canadian Journal of Remote Sensing*, **18**, 275-292.

GONG, P., PU, R., and YU, B., 1997, Conifer species recognition: An exploratory analysis of *in situ* hyperspectral data. *Remote Sensing of Environment*, **62**, 189-200.

GOWER, S. T., KUCHARIK, C. J., and NORMAN, J. M., 1999, Direct and indirect estimation of Leaf Area Index, fAPAR, and Net Primary Production of terrestrial ecosystems. *Remote Sensing of Environment*, **70**, 29-51.

GOWER, S. T., and NORMAN, J. M., 1991, Rapid estimation of leaf area index in conifer and broad-leaf plantations. *Ecology*, **72**, 1896-1900.

GUYOT, G., BARET, F., and JACQUEMOUD, S., 1992, Imaging spectroscopy for vegetation studies. In *Imaging Spectroscopy: Fundamentals and Prospective Applications*, edited by F. Toselli and J. Bodechtel (Dordrecht: Kluwer Academic Publications), pp.145-165.

HOPE, A. S., KIMBALL, J. S. and STOW, D. A., 1993, The relationship between tussock tundra spectral reflectance properties and biomass and vegetation composition. *International Journal of Remote Sensing*, **14**, 1861-1874.

HORLER, D. N. H., and AHERN, F. J., 1986, Forestry information content of Thematic Mapper data. *International Journal of Remote Sensing*, **7**, 405-428.

HORLER, D. N. H., DOCKRAY, M., and BARBER, J., 1983, The red edge of plant leaf relectance. *International Journal of Remote Sensing*, **4**, 273-288.

HUBBARD, N. K., and WRIGHT, R., 1982, A semi-automated approach to land cover classification of Scotland from Landsat. *Proceedings of the Annual Conference of the Remote Sensing Society, Liverpool, 15-17 December, 1982*, (Durham: Remote Sensing Society), pp. 212-221.

HUNT, E. R., and ROCK, B. N., 1989, Detection of changes in leaf water content using near- and middle-infrared reflectances. *Remote Sensing of Environment*, **30**, 43-54.

JAKABAUSKAS, M. E., 1996, Canonical correlation-analysis of coniferous forest spectral and biotic relations. *Remote Sensing of Environment*, **56**, 118-132.

JARVIS, P. G., and LEVERENZ, J. W., 1983, Productivity of temperate, deciduous and evergreen forests. In *Physiological Plant Ecology 4, volume 12D*, edited by O. L. Lange *et al.* (New York: Springer Verlag), pp. 233-280.

JOLLY, A., GUYON, D., and RIOM, J., 1996, Use of middle-infrared Landsat Thematic Mapper data for representation of clearcuts in the Landes region. *International Journal of Remote Sensing*, **17**, 3615-3645.

JONES, A. R. and WYATT, B. K., 1988, Improved automated classification of upland environments using high resolution satellite data. In *Ecological Change in the Uplands* edited by M. B. Usher and D. B. A. Thompson, British Ecological Society Special Publication Series (Oxford: Blackwell), pp.109-118.

KELLOMÄKI, S. and STRANDMAN, H., 1995, A model for the structural growth of young Scots pine crowns based on light interception by shoots. *Ecological Modelling*, **80**, 237-250.

KNIPLING, E. B., 1970, Physical and physiological basis for the reflectance of visible and near-infrared radiation from vegetation. *Remote Sensing of Environment*, **1**, 151-154.

LICHTENTHALER, H. K., GITELSON, A. A., and LANG, M., 1996, Non-destructive determination of chlorophyll content of leaves of a green and an aurea mutant tobacco by reflectance measurements. *Journal of Plant Physiology*, **148**, 483-493.

LUCAS, N. S., CURRAN, P. J., PLUMMER, S. E., and DANSON, F. M., 2000, Estimating the stem carbon production of a coniferous forest using an ecosystem simulation model driven by the remotely sensed red edge. *International Journal of Remote Sensing*, **21**, 619-631.

MALTHUS, T. J., 1995, A proposed standard format for the exchange of spectroradiometric data. In *Proceedings of the 21st Annual Conference of the Remote Sensing Society, 11-14 September, Southampton* (Nottingham: Remote Sensing Society), pp. 571-577.

MALTHUS, T. J., ANDRIEU, B., DANSON, F. M., JAGGARD, K. W., and STEVEN, M. D., 1993, Candidate high spectral resolution infrared indices for crop cover. *Remote Sensing of Environment*, **46**, 204-212.

MALTHUS, T. J., and MADEIRA, A. C., 1993, High resolution spectroradiometry: Spectral reflectance of field bean leaves infected by *Botrytis fabae*. *Remote Sensing of Environment*, **45**, 107-116.

MARTIN, M. E., NEWMAN, S. D., ABER, J. D. and CONGALTON, R. G., 1998, Determining forest species composition using high spectral resolution remote sensing data. *Remote Sensing of Environment*, **65**, 249-254.

McCOY, J., 1997, *Landsat TM imagery with ground spectral radiometer data for monitoring regeneration of Scots pine.* Unpublished MSc. Thesis, Department of Geography, University of Edinburgh.

MENCUCCINI, M. and GRACE, J., 1995, Climate influences the leaf area/sapwood area ratio in Scots pine. *Tree Physiology*, **15**, 1-10.

MILLER, J. R., WHITE, H. P., CHEN, J. M., PEDDLE, D. R., McDERMID, G., FOURNIER, R. A., SHEPHERD, P., RUBINSTEIN, I., FREEMANTLE, J., SOFFER, R., and LeDREW, E., 1997, Seasonal change in understory reflectance of boreal forests and influence on canopy vegetation indices. *Journal of Geophysical Research*, **102**, No. D24, 29,475-29,482.

MILTON, E. J., 1987, Principles of field spectroscopy. *International Journal of Remote Sensing*, **8**, 1807-1827

MILTON, E. J., ROLLIN, E. M., and EMERY, D. R., 1995, Advances in field spectroscopy. In *Advances in Environmental Remote Sensing*, edited by F. M. Danson and S. E. Plummer (Chichester: Wiley & Sons) pp. 9-32.

MORAN, J. A., MITCHELL, A. K., GOODMANSON, G., and STOCKBURGER, K. A., 2000, Differentiation among effects of nitrogen fertilization treatments on conifer seedlings by foliar reflectance: a comparison of methods. *Tree Physiology*, **20**, 1113-1120.

NEL, E. M. and WESSMAN, C. A., 1993, Canopy transmittance models for estimating forest leaf area index. *Canadian Journal of Forest Research*, **23**, 2579-2586.

NEL, E. M., WESSMAN, C. A., and VEBLEN, T. T., 1994, Digital and visual analysis of thematic mapper imagery for differentiating old growth from younger spruce-fir stands. *Remote Sensing of Environment*, **48**, 217-229.

NEMANI, R., PIERCE, L., RUNNING, S., and BAND, L., 1993, Forest ecosystem processes at the watershed scale: sensitivity to remotely-sensed Leaf Area Index estimates. *International Journal of Remote Sensing*, **14**, 2519-2534.

NORMAN, J. M., and CAMPBELL, G. S., 1989, Canopy structure. In *Plant physiological ecology: Field methods and instrumentation*, edited by R. W. Pearcy, J. Ehleringer, H. A. Mooney, and P. W. Rundel (London: Chapman and Hall), pp. 301-323.

PEÑUELAS, J., PIÑOL, J., OGAYA, R., and FILELLA, I., 1997, Estimation of plant water concentration by the reflectance of Water Index WI (R900/R970). *International Journal of Remote Sensing*, **18**, 2869-2875.

PIERCE, L. L., and RUNNING, S. W., 1988, Rapid estimation of coniferous forest leaf area index using a portable integrating radiometer. *Ecology*, **69**, 1762-1767.

PIERCE, L. L., RUNNING, S. W., and RIGGS, G. A., 1990, Remote detection of canopy water stress in coniferous forests using the NS001 Thematic Mapper simulator and the Thermal Infrared Multispectral Scanner. *Photogrammetric Engineering and Remote Sensing*, **56**, 579-586.

RIGGS, G. A., and RUNNING, S. W., 1991 Detection of canopy water stress in conifers using the airborne imaging spectrometer. *Remote Sensing of Environment*, **35**, 51-68.

ROLLIN, E. M., and MILTON, E. J., 1998, Processing of high spectral resolution reflectance data for the retrieval of canopy water content information. *Remote Sensing of Environment* **65**, 86-92.

ROSS, J., KELLOMÄKI, S., OKER-BLOM, P., ROSS, V., and VILIKAINEN, L., 1986, Architecture of Scots pine crown: phytometrical characteristics of needles and shoots. *Silva Fennica*, **20**, 91-105.

SAMPSON, D. A., and ALLEN, H. L., 1995, Direct and indirect estimates of Leaf Area Index (LAI) for lodgepole and loblolly pine stands. *Trees*, **9**, 119-122.

SAVITZKY, A., and GOLAY, M. J. E., 1964, Smoothing and differentiation of data by simplified least squares procedures. *Analytical Chemistry*, **36**, 1627-1639.

SHAW, D. T., MALTHUS, T. J., and KUPIEC, J. A., 1998, High-spectral resolution data for monitoring Scots pine (*Pinus sylvestris* L.) regeneration. *International Journal of Remote Sensing*, **19**, 2601-2608.

SMITH, N. J., 1993, Estimating leaf area index and light interaction coefficients in stands of Douglas-fir (*Pseudotsuga menziesii*). *Candian Journal of Forest Research*, **23**, 317-321.

SMITH, N. J., CHEN, J. M., and BLACK, T. A., 1993, Effects of clumping on estimates of stand leaf area index using the LI-COR LAI-2000. *Canadian Journal of Forest Research*, **23**, 1940-1943.

STENBERG, P., LINDER, S., SMOLANDER, H., and FLOWER-ELLIS, J., 1994, Performance of the LAI-2000 plant canopy analyzer in estimating leaf area index of some Scots pine stands. *Tree Physiology*, **14**, 981-995.

STRACHAN, I. B., and McCAUGHEY, 1996, Spatial and vertical leaf area index of a deciduous forest resolved using the LAI-2000 Plant Canopy Analyzer. *Forest Science*, **42**, 176-181.

TAYLOR, J. E., 1993, Factors causing variation in reflectance measurements from Bracken in Eastern Australia. *Remote Sensing of Environment*, **43**, 291-301

TEILLET, P. M., STAENZ, K., and WILLIAMS, D. J., 1997, Effects of spectral, spatial, and radiometric characteristics on remote sensing vegetation indices of forested regions. *Remote Sensing of Environment*, **61**, 139-149.

TREITZ, P. M., HOWARTH, P. J., SUFFLING, R. C. and SMITH, P., 1992, Application of detailed ground information to vegetation mapping with high spatial resolution digital imagery. *Remote Sensing of Environment*, **42**, 65-82.

TRODD, N. M., 1993, Characterising semi-natural vegetation: continua and ecotones. *Proceedings of the Remote Sensing Society Conference* (Nottingham: Remote Sensing Society).

VOGELMANN, J. E., ROCK, B. N., and MOSS, D. M., 1993, Red edge spectral measurements from sugar maple leaves. *International Journal of Remote Sensing*, **14**, 1563-1575.

WARDLEY, N. W., MILTON, E. J., and HILL, C. T., 1987, Remote sensing of structurally complex semi-natural vegetation - and example from heathland. *International Journal of Remote Sensing*, **8**, 31-42.

WEAVER, R. E., 1987, Spectral separation of moorland vegetation in airborne Thematic Mapper data. *International Journal of Remote Sensing*, **8**, 43-55.

WHITE, M. A., ASNER, G. P., NEMANI, R. R., PRIVETTE, J. L., and RUNNING, S. W., 2000, Measuring fractional cover and leaf area index in arid ecosystems: Digital camera, radiation transmittance, and laser altimetry methods. *Remote Sensing of Environment*, **74**, 45-57.

WHITFORD, K. R., COLQUHOUN, I. J., LANG, A. R. G., HARPER, B. M., 1995, Measuring leaf area index in a sparse eucalypt forest: a comparison of estimates from direct measurement, hemispherical photography, sunlight transmittance and allometric regression. *Agricultural and Forest Meteorology*, **74**, 237-249.

WOOLLEY, J. T., 1971, Reflectance and transmittance of light by leaves. *Plant Physiology*, **47**, 656-662.

ZARCO-TEJADA, P. J., and MILLER, J. R., 1999, Land cover mapping at BOREAS using red edge spectral parameters from CASI imagery. *Journal of Geophysical Research*, **104**, No. D22, 27,921-27933.

5.0 OPTICAL MEASUREMENTS OF PINE NEEDLES

5.1 Introduction

Vegetation canopy modelling in remote sensing research has played an important role in understanding the physical basis of light interaction with vegetation surfaces. Some workers have claimed that the future of remote sensing depends on the use of physical models and advances in computer science and technology (Myneni *et al.*, 1995). Despite such claims, there is little evidence in the literature that much effort is made to measure in detail, the optical properties of the most basic canopy elements; leaves, needles, twigs and so on. Such measurements are particularly important for the more complex models, which often scale-up the assumed interaction of light at leaf level, to that at the canopy level.

The reason for the apparent reluctance to collect such primary data for modelling studies is likely due to the measurements being time consuming and difficult to perform accurately. Reasonable estimates of leaf reflectance may be obtained by averaging repeated spectroradiometric measurements in the laboratory. However, there are a number of problems with this approach. For example, it does not allow leaf transmittance measurements, or take account of the hemispherical reflectance, only the specular, and it is difficult for small leaf samples, narrow leaves and needles that do not fill the field of view. Clearly, such considerations are important if the complexity of light interaction within canopies is to be meaningfully modelled.

This chapter considers the possible ways in which these problems may be confronted. A method is described and tested for measuring the optical properties of needles and narrow leaves. Finally, results of reflectance and transmittance

measurements of Scots pine needles are presented and their validity as primary variables for radiative transfer models is discussed.

5.2 Previous work

Investigations into the optical properties of leaves have been carried out for over one hundred years and the interaction of plants with radiant energy has been of interest to 'the botanist, forester, geographer, biophysicist, biochemist, ecologist, hydrologist, agronomist, photogrammist and others' (Gates *et al.*, 1965). The primary interest has been the understanding of the changes in optical properties relating to changes in leaf physiology. In remote sensing terms, this has promised the opportunity to predict and measure leaf physiological states. However, if laboratory measurements are to assist in the interpretation of data from sensors more remote from the vegetation canopy, then both reflectance and transmittance should be measured on the same sample under the same conditions. This is because the remote sensor will measure the result of light interactions taking place not at the single leaf level, but at the canopy level. Despite the importance of transmittance within the canopy, there has always been a limited amount of published transmittance data for single leaves (Myers and Allen, 1968). One notable exception is the extensive work of Gausman, which has illustrated the role of leaf structure on the measured optical properties of crop leaves (e.g. Gausman *et al.*, 1970; 1984; Gausman, 1977; 1983). For needles, there has been a limited amount, even, of published reflectance data, and transmittance data for needles have been essentially non-existent in the literature (Williams, 1991).

Another omission, particularly in the earlier measurements prior to 1930, was the contribution of diffuse light to the measurements. Glossy leaves may tend to follow Fresnel's law for specular reflection, whilst more diffuse reflectance from matt leaves approximate Lambert's cosine law (Myers and Allen, 1968). For most leaves though, light interaction with their surfaces consists of a diffuse and a specular element, so that both must be measured. During the 1930s the Hardy instrument made by General Electric, was among the first to be used with an integrating sphere to measure the diffuse radiation from a sample (Myers and Allen, 1968) and is described by Kortüm (1969, p, 228). An integrating sphere allows the collection of

all diffuse light reflected from a leaf (or any sample) surface since the inside of the sphere is coated with a perfect reflecting diffuser. In other words, the inside of the sphere is an 'ideal reflecting surface that neither absorbs nor transmits light, but reflects diffusely, with the radiance of the reflecting surface being the same for all reflecting angles, regardless of the angular distribution of the incident light' (Labsphere Inc., date unknown).

A generalized theory for measurements made using an integrating sphere is given in Goebel (1967) and the various types and operating theory are detailed by Kortüm (1969 pp. 219-229). In summary, these equations allow the calculation of the difference between the intensity of the reflected flux when a gap in the sphere wall is filled with the sample (i.e. when the sphere is not a perfect diffuser) and when the sphere wall is complete. This is referred to as the substitution method (Kortüm, 1969). The gap is usually referred to as the sample port and may be plugged with a known reference standard; usually of the same coating material as the interior of the sphere. The difference between the measured intensity when the reference is in place and when the sample is in place gives the reflectance factor of the sample, whilst absolute reflectance is obtained if the standard is pre-calibrated. The principle is the same as for field spectroscopy when using a calibrated reflectance panel to standardise measurements; however, the sphere allows the total hemispherical reflectance to be measured from the sample.

A popular integrating sphere was the Ulbricht sphere, which required the sample to be suspended within it. Rabideau *et al.* (1946) were among the first to report the very low absorption of near infra-red light in leaves using an Ulbricht sphere. Modern integrating spheres are generally much easier to use and may be an internal accessory for a relatively low-cost laboratory spectrophotometer, or an external accessory for use in the field with a portable spectroradiometer.

The integrating sphere in conjunction with a spectroradiometer has been used extensively to characterise the reflectance and transmittance of a range of leaves. Early research focussed on the interaction of light with the leaf from a functional and physiological perspective. Gates *et al.* (1965) briefly describe the use of an

integrating sphere to measure the specular and diffuse radiation from a range of leaves. Two different spectrophotometers were used to obtain measurements from 400 nm to 2000 nm. In the absence of the sensitive measurement devices available today, Gates *et al.* (1965) made measurements of pine needles by 'forming mosaic samples' in order to obtain a strong enough signal for reflectance measurements. Since transmittance of pine needles is very low, and therefore 'a measurement which is very difficult to obtain', these workers assumed that pine needles do not transmit radiation at all. They note that absorptance in pine needles is greater than for other leaf types, but the estimates of absorptance are likely to be inflated somewhat by the assumption of zero transmittance.

Extensive measurements on a variety of crop types were made by Woolley (1971) using a double-beam spectrophotometer with an integrating sphere over a wavelength range of 450 to 2700 nm. The sample leaves were held in place within the sphere on a black sample holder, which allowed measurements with different angles of incidence. Woolley measured surface reflectance over a range of incidence and viewing angles for visible wavelengths and concluded that over half of the visible light reflected by glossy leaves was specular. However, he also concluded that 'reflectance and transmittance characteristics of leaves....can be explained by the fact that a leaf is a good diffuser over the entire wavelength range, containing materials which absorb at specific wavelengths, and bounded by slightly roughened plane surfaces. Most of the diffusion was attributed to the interfaces between air and wet cell walls'.

A Perkin Elmer spectrophotometer fitted with and integrating sphere was used to measure the hemispherical reflectance of the upper surface of a range of leaves by Horler *et al.* (1983). The purpose of this work was to obtain detailed measurements of reflectance to compare chlorophyll concentrations of leaves with the red-edge parameter. Ferns *et al.* (1984) also concentrated on the red-edge and stressed the importance of high spectral resolution spectra for improving information about such vegetation spectral features. In their laboratory measurements of a pea canopy, hemispherical directional reflectance was measured by dividing the irradiance received by an integrating sphere, by the light received from the target through a slit

in the base of the sphere. Hemispherical directional reflectance (reflectance factor) 'is the ratio of radiance reflected from a surface in a given direction to that incident upon it' (Duggin, 1980). A more particular definition is given by Williams and Wood (1987) after Nicodemus *et al.* (1977) as 'the ratio of the radiant flux actually reflected by a sample surface to that which would be reflected into the same reflected-beam geometry by an ideal (lossless) perfectly diffuse (Lambertian) standard surface irradiated in exactly the same way as the sample'.

The need to create conditions where the sample illumination characteristics are the same as those for the reference, even for whole plants, or tree branches, has led to the development of measurement systems that integrate each element. For example, Williams and Wood (1987) describe an apparatus containing the spectrometer or radiometer, sphere, the illumination source, the reference standard and the viewing angle on one support structure. However, this apparatus provided no means of acquiring transmittance measurements.

More recently, spectral measurements of both canopies and individual leaves have become more practicable and less cumbersome. Field spectroradiometers such as the Li-Cor 1800 have their own integrating spheres as accessories and a lamp as a light source. More sensitive detection devices mean that smaller spheres can be used and fibre optic cables allow more flexible remote detection for such accessories. These instruments and ones like them, have been widely used for reflectance and transmittance measurements of leaves (e.g. Lorenzen and Jensen, 1991; Lichtenthaler *et al.*, 1996; Gitelson and Merzlyak, 1996; 1997; Knapp and Carter, 1998). Figure 5.1 illustrates how an external integrating sphere such as the Li-Cor 1800-12s can be arranged to measure the reference standard, the reflectance factor and the transmittance of a leaf sample.

Whilst systems such as the Li-Cor one work well for measuring the optical properties of leaves, particular problems are encountered in the case of needles or leaves smaller than the size of the port entrance. Most importantly, needles do not completely cover the sample port of the integrating sphere so that it is not possible to get a pure target signal for either reflectance or transmittance. Secondly, needles are

not flat, or regular in shape, so that merely forming a matt of needles side by side does not present a uniform surface representative of a single needle. The irregular shape of the needles will also mean that some light will pass through small gaps, which is particularly confounding for transmittance measurements, especially in the visible wavelengths where transmittance is low (Daughtry *et al.*, 1989).

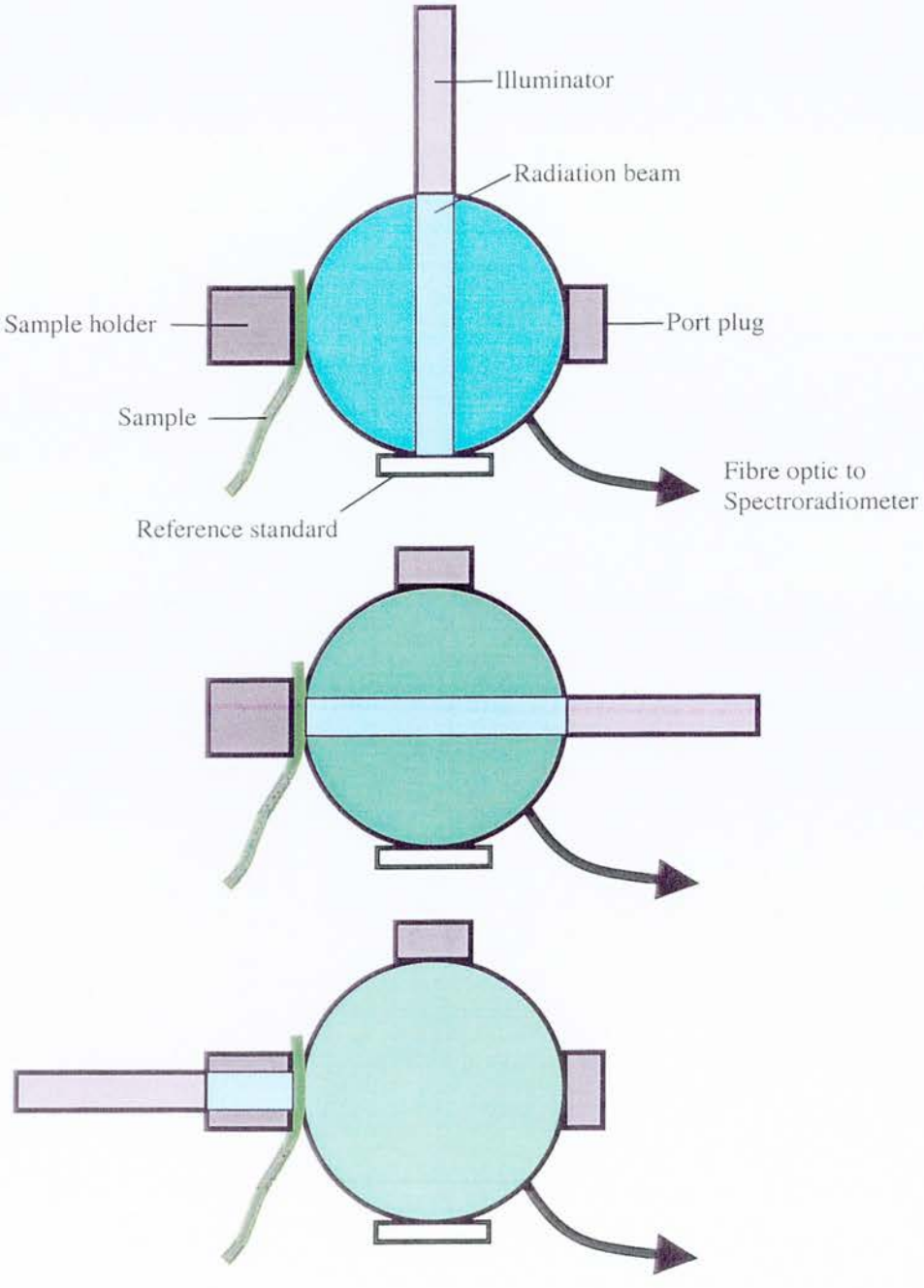

Figure 5.1 The Li-Cor 1800-12s external integrating sphere in its three configurations for reference (top), reflectance (middle) and transmittance (bottom) modes. Redrawn from Daughtry et al. (1989)

These workers also observed an increase in reflectance due to multiple scattering between adjacent surfaces when needles were placed side by side. One option is to treat the shoot instead of the needle as the basic optical element in a pine canopy. However, gaps will still exist between needles on a shoot, and transmittance measurements would still be very difficult and inaccurate.

Daughtry *et al.* (1989) described a technique for measuring the reflectance and transmittance of pine needles that tackled these problems. These workers outlined three cases for the measurement of both reflectance and transmittance of narrow leaves and needles using the Li-Cor 1800 apparatus. Case 1 was simply for a leaf sample that completely covered the sample port of the integrating sphere, and followed the arrangement outlined in Figure 5.1. Case 2 was for needles that were long enough to reach across the sample port and Case 3 for needles that were shorter than the diameter of the sample port. For Case 2, needles were laid side by side at about a needle-width apart. Reflectance and transmittance measurements were acquired in the usual manner. However, the proportion of the beam of light that passes through the needle gaps was calculated by measuring reflectance and transmittance after the needles were painted with an opaque matt black paint. This gap proportion was calculated as the ratio of flux at 680 nm transmitted through the blackened sample to the flux at 680 nm transmitted through the sample port with no sample in place. The 680 nm wavelength was chosen because transmittance through green leaves is close to zero in this part of the spectrum, due to absorption by chlorophyll. Case 3 was an extension of Case 2 for needles of pine species that were shorter than the diameter of the sample port of the integrating sphere (14.5 mm in the case of the Li-Cor 1800-12s). The needles were arranged in the same way, but were supported on transparent tape, with the reflectance and transmittance of the tape being measured first and taken into account when calculating the optical properties of the needle samples.

These authors stressed the importance of taking care that the needles are placed into exactly the same position over the sample port before and after painting. This was achieved by using holders for the needle samples made from a square of aluminium

sheet 0.7 mm thick, with a 22 mm diameter hole. The needles were taped over the hole and the sample holder was aligned by marks on the sample holder and the integrating sphere. The method was tested by measuring whole leaves and comparing the results with measurements of strips of whole leaves arranged in the same way as the needle samples. It was concluded that the method proved repeatable, although transmittance was slightly underestimated (typically 6%), whilst reflectance was slightly overestimated (typically 4%).

The method of Daughtry *et al.* (1989) formed the basis of optical measurement methods for needles in subsequent studies. For example, Williams (1991) used the 'Case 3' method and the Li-Cor apparatus (Figure 5.1) when comparing needle, branch and canopy level optical properties for a range of conifer species. He makes the point that the greatest drawback with the method 'was the time-consuming tedious task of painting the needles black without getting paint on the transparent tape medium'. Reflectance of twig samples was made by removing the needles and placing sections of twig side by side, and positioning in front of the sample port of the Li-Cor external integrating sphere. Since twigs are opaque, transmittance data were not obtained for these samples. In a related study, Rock *et al.* (1994) measured the needle and branch optical properties of two coniferous species to study the differences between first-year and second-year needles and how branch reflectance properties are related to needle-level changes. Needle reflectance and transmittance measurements were made using the method of Daughtry *et al.* (1989), and the Li-Cor 1800 apparatus.

The effect of different fertilization treatments on the optical properties of Douglas Fir seedlings was investigated by Dungan *et al.* (1996). For leaf optical properties these workers used the 'Case 2' method, but modified for the double beam Perkin-Elmer Lamda-9 spectrophotometer used. The spectrophotometer was equipped with a 15 cm diameter integrating sphere and measurements were made from 400 - 2500 nm. The difference between a single and double-beam spectrophotometer and their associated spheres is discussed in the following section. Dungan *et al.* (1996) reported that the abaxial (bottom) needle surface reflectance was greatest in the

visible, while adaxial (top) surface reflectance was greatest at 800-1400 nm. The lower reflectance at the top surface of the needles was attributed to the increased absorption by chloroplasts preferentially grouped near to this surface.

The Daughtry method has been improved on recently as a result of work during the The Boreal Ecosystem-Atmosphere Study (BOREAS). Mesarch *et al.* (1999) introduced modifications to improve both ease of measurement and accuracy. Firstly, they showed that improvements in estimates of transmittance could be made by reducing the gap fraction (GF) typically used (usually needles placed one needle-width apart; GF approximately 0.3-0.6). Processed Ektachrome slide film was used as a test material to compare whole film transmittance against film strips with different sized gaps. It was concluded that samples with smaller GFs (0.05-0.15) produced mean transmittance values similar to those of the uncut film, with standard deviations < 1.5%, whilst GFs over 0.3 produced increasingly poor estimates of 'true' film transmittance. However, the authors recommended that a larger GF be used for reflectance measurements, because of a slight over-estimation caused by multiple scattering between adjacent surfaces when needles are placed close together.

The second improvement made by Mesarch *et al.* (1999) related to both the estimation of the GF itself and the time consuming painting procedure. GF was estimated directly by imaging the sample and simply counting the proportion of non-needle to needle pixels in the image. This was done by placing a mask with a hole the same dimensions as the light beam over the sample of needles and taking a photograph with a solid state camera and frame grabber to capture a digital image. It was concluded that whilst this method did not improve on the accuracy of the painting method, it was much less time consuming and allowed the adaxial and abaxial, surfaces to be measured for the same sample.

5.3 Method Development and Testing

This section details the method used to obtain detailed optical measurements of Scots pine needles. The approach taken follows the image analysis and gap fraction (GF) technique detailed in Mesarch *et al.* (1999), and described in the previous section.

5.3.1 Materials

The spectrophotometer used in the present study was a medium-cost dual-beam UV/Vis/NIR Perkin-Elmer Lamda-40. A Labsphere RSA-PE-20 50 mm integrating sphere internal accessory was used to obtain hemispherical reflectance factor measurements and transmittance measurements. The sphere has two 11 mm diameter ports directly opposite each other and the accessory is aligned with a series of mirrors so that the rectangular sample beam of the spectrophotometer passes through the centre of each port (Figure 5.2). The spectrophotometer can record scans in the 300 to 1200 nm wavelength range. The inside of the sphere and the reference plug were both made from Spectralon ™.

Whilst the Labsphere integrating sphere accessory comes equipped with sample holders for solid targets that cover the sample port (such as whole leaves) and a cell sample holder for liquid samples, there is no means of holding a needle sample in place with positional accuracy. Additionally, the sample beam is not the same shape as the sample port and no information was available on the beam dimensions at the reflectance port and at the transmittance port. Two problems with the equipment available therefore, had to be overcome.

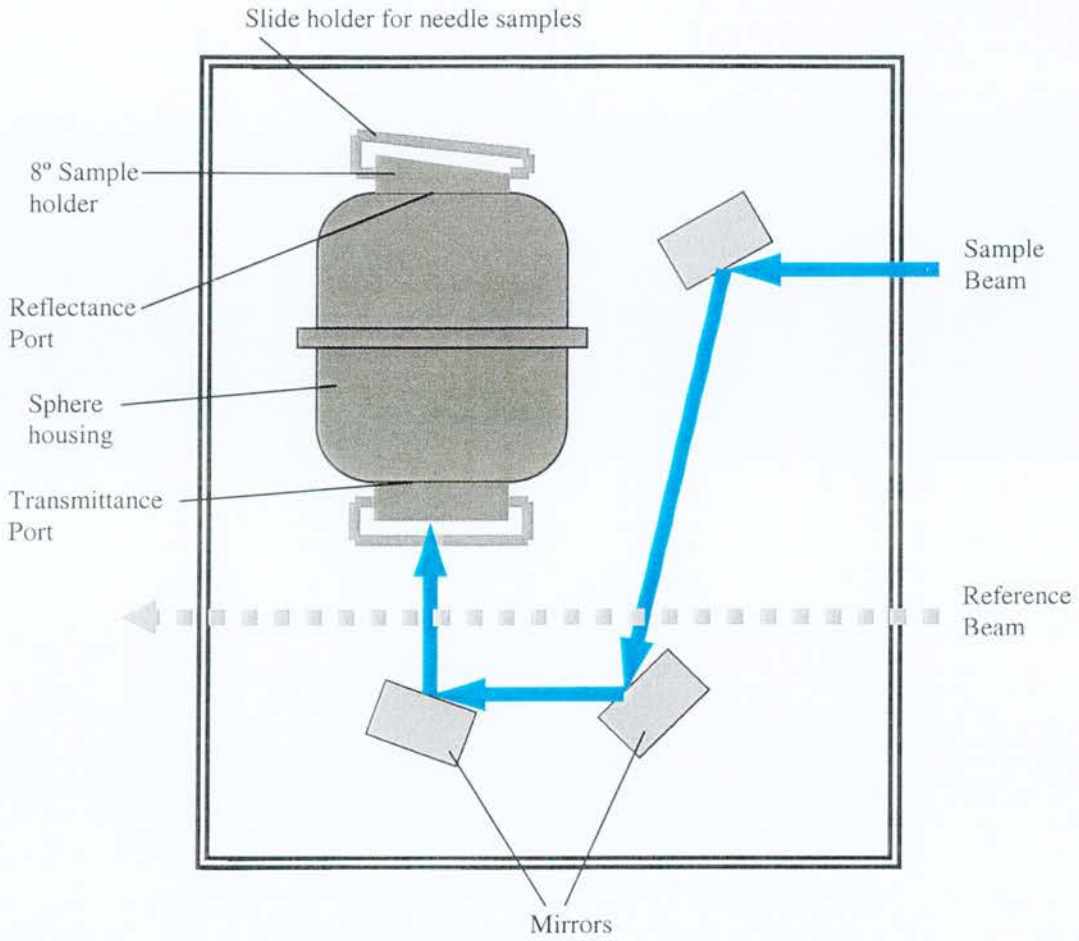

Figure 5.2 Schematic of the Labsphere RSA-PE-20 internal integrating sphere accessory for the Perkin-Elmer Lamda 40 spectrophotometer. The 8° sample holder was used to capture the specular component of reflectance within the sphere.

Firstly, the GF method is reliant on the ability to estimate the proportion of the sample of adjacent needles irradiated by the spectrophotometer's radiation beam. The method of Mesarch *et al.* (1999) requires a mask to be placed over the sample of adjacent needles so that this proportion can be measured. It was therefore necessary to use a sample holder that could be placed at the sphere entrance ports in *exactly* the same location every time. This was achieved by making a holder that could be moved up against the entrance ports and receive a 35 mm slide mount, in much the same way as a slide may be dropped into a manual slide projector. The needles were

taped to a piece of black card, cut to the same dimensions as a 35 mm slide mount and with a hole in the centre. Black card was used instead of actual slide mounts, because the window area was found to be larger than was necessary on slide mounts. Figure 5.2 illustrates the position of the sample holders; one at the reflectance port and one at the transmittance port.

Secondly, and perhaps more fundamentally, the precise dimensions of the sample radiation beam had to be measured at the reflectance and transmittance entrance ports to enable GF to be accurately calculated. Whilst the radiation beam could be seen by setting the wavelength to a visible wavelength and dimming the lights, there was no precise way to measure its exact dimensions. Exposing photographic film to the beam was considered as a means of imaging the beam as it entered and exited the sphere. However, it was considered likely that light would diffuse along the film, leaving an undefined boundary to the image.

To avoid this effect, a silver-halide photographic emulsion (Liquid Light™, Rockland Colloid Corp., Piermont, NY) was tested. This emulsion is primarily used for making black-and-white enlargements onto virtually any material and has the advantage of high contrast. Speed and contrast of the emulsion were increased by first sensitising the emulsion with one part in ten of working developer. In a dark room environment, the emulsion was warmed to increase viscosity, before being spread evenly on to white card cut to fit the sample holders, and allowed to dry thoroughly. Once dried, the prepared cards were placed into the sample holder against the reflectance port of the integrating sphere. The card was exposed briefly (< 2 seconds) to the spectrophotometer radiation beam, set to white light.

Following exposure, the emulsion was processed in four steps. Firstly, the cards were developed with a standard paper developer at a working strength of one part developer to two parts of water. Secondly, excess developer was removed by quickly rinsing with cool water. A powdered hardening fixer was then used (Kodak Unifix™) before finally washing and drying. The process was repeated for cards placed at the transmittance port.

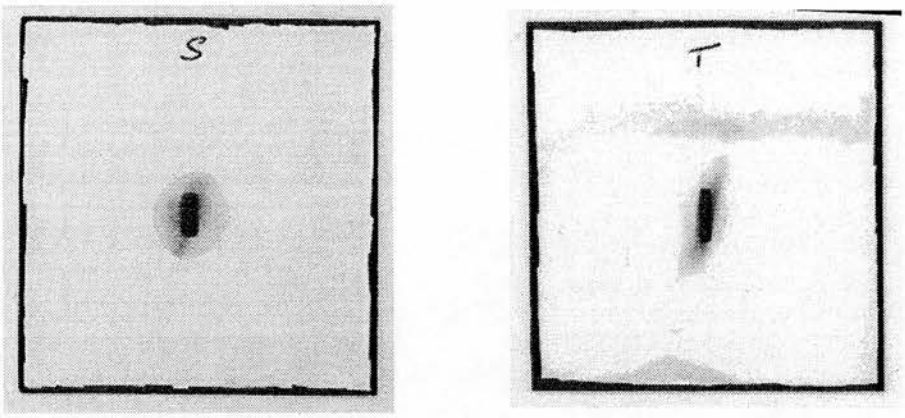

Figure 5.3 The Perkin Elmer Lamda 40 sample radiation beam dimensions at the sample reflectane port (S) and the transmittance port (T), imaged using photographic emulsion. The halo effect on the reflectance port image is due to diffuse light from within the integrating sphere.

Figure 5.3 illustrates the rectangular images of the radiation beam at the sample reflectance and transmittance ports. The emulsion images were used to make masks to overlay the needle samples before scanning to calculate the GF of each sample.

5.3.2 Method Testing

Prior to recording measurements of pine needles the method was tested by using unexposed but processed Ektachrome slide film in the same way as Mesarch *et al.* (1999). The processed film is an inert material with similar optical properties to leaves (i.e. low reflectance in the visible and relatively high transmittance in the NIR).

Figure 5.4 illustrates the transmittance of three samples of whole sections of unexposed, processed and developed film, compared with the same film cut into strips and corrected using the GF method. The film strips were placed close together to give small GFs, as recommended by Mesarch *et al.* (1999).

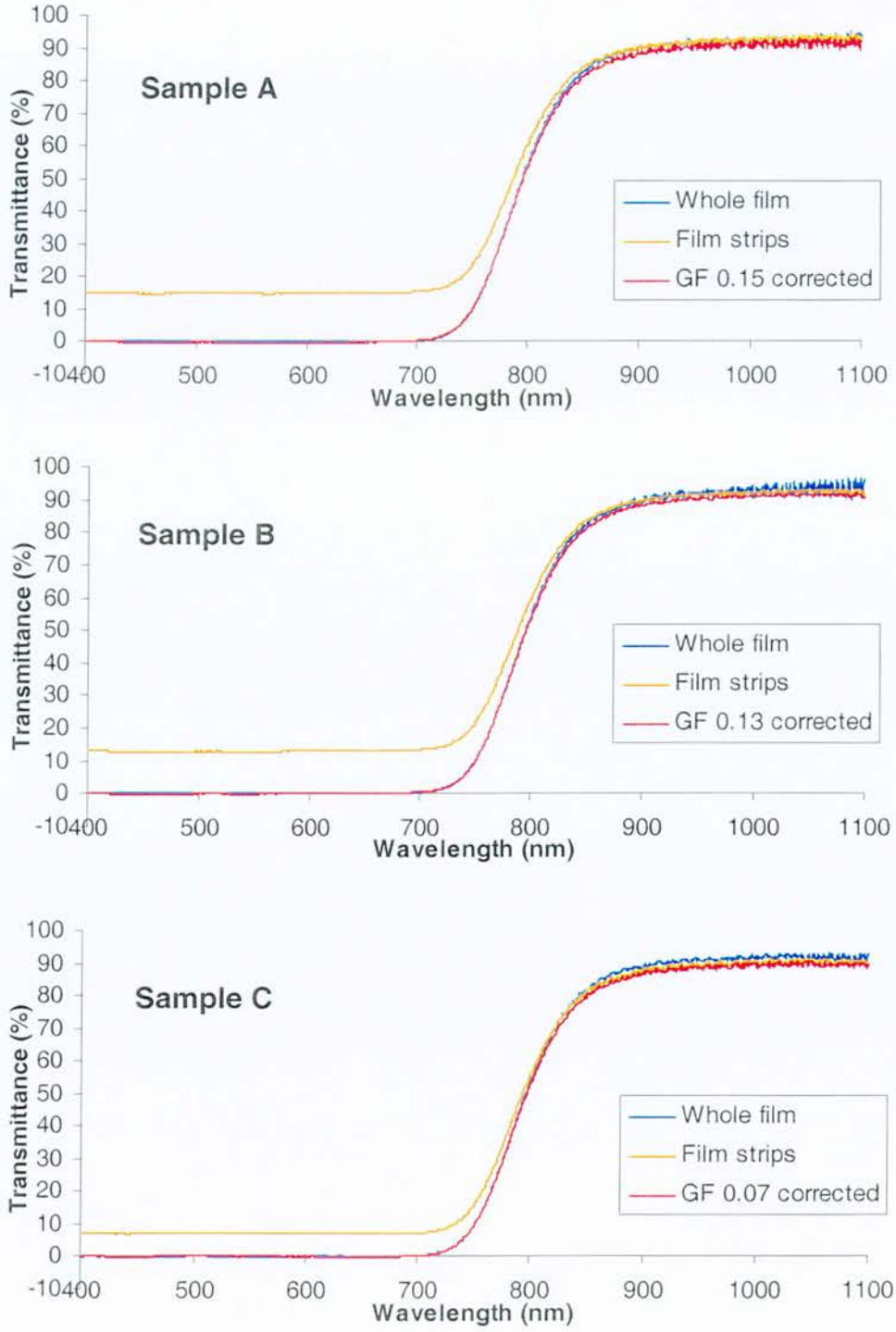

Figure 5.4 The whole film, film strips, and Gap Fraction (GF) corrected transmittance spectra for three samples of inert processed, unexposed Ektachrome film.

The transmittance corrected for the gaps was calculated by

$$\tau = \left[\tau_{total} - (\rho_{\omega} GF)\right] \frac{1}{(1 - GF)}$$

where

τ = transmittance through individual film strips or needles,

$\tau_{total} = T_{total}$ / REF - STR,

T_{total} = total transmitted radiation of the sample,

ρ_{ω} = reflectance of integrating sphere wall,

REF = reference radiation,

STR = stray light radiation,

GF = gap fraction,

while the equation for calculating film strip or needle reflectance per waveband is given as

$$\rho = \frac{\rho_{total}}{(1 - GF)}$$

where

ρ = reflectance of film strips, or individual needles,

$\rho_{total} = R_{total}$ - STR / REF - STR,

R_{total} = reflected radiation from the sample.

The reflectance of the integrating sphere wall (ρ_{ω}) with the reference in place is assumed to be equal to 1. The values of total reflectance (ρ_{total}) and total transmittance (τ_{total}) include both the contribution from the gaps and the film strips, or needles. In all calculations, the stray light term (STR) was ignored, since measurements were conducted within the spectrophotometer measuring compartment, which serves as a light trap.

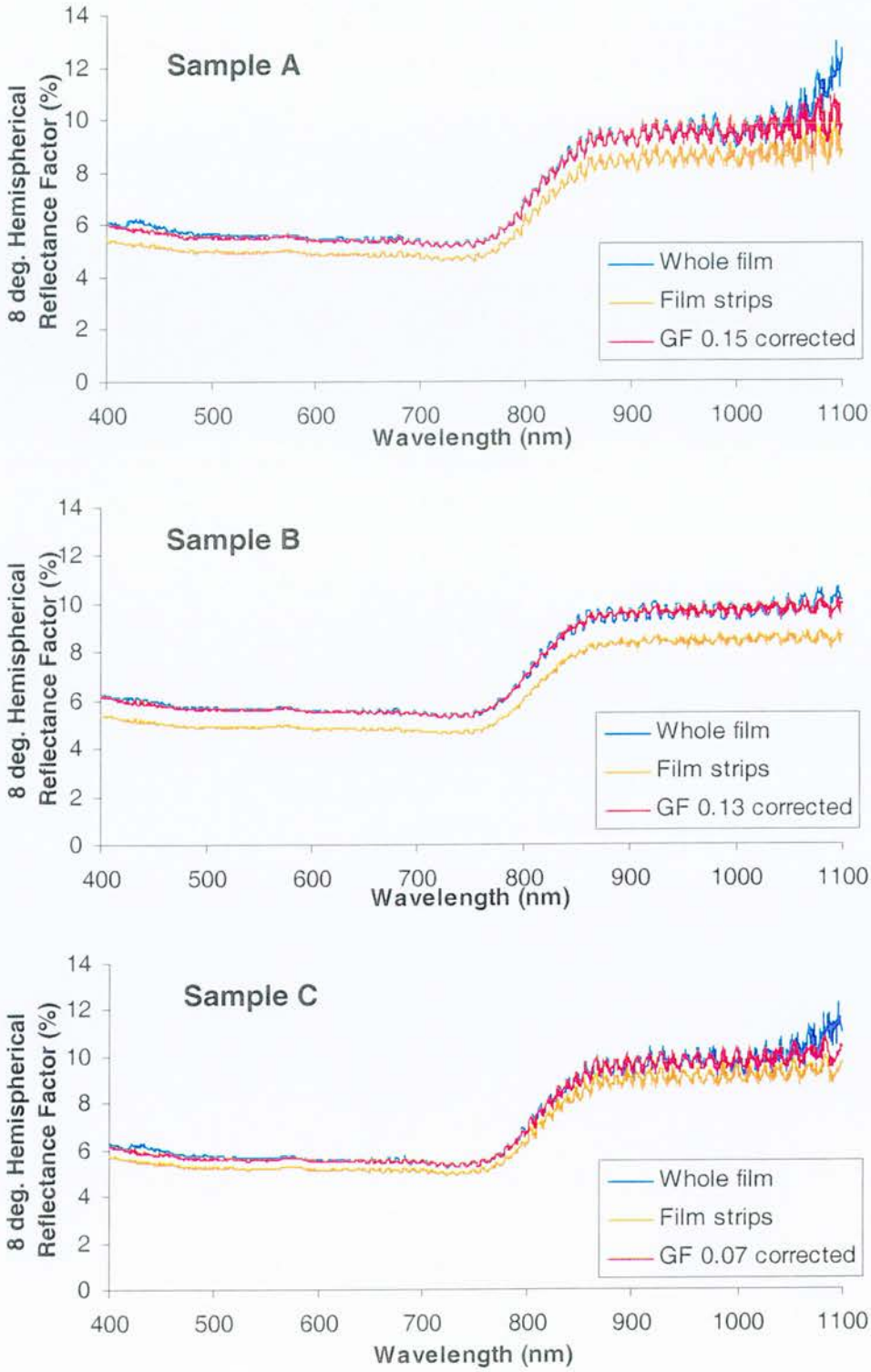

Figure 5.5 The whole film, film strips, and Gap Fraction (GF) corrected reflectance spectra for three samples of inert processed, unexposed Ektachrome film.

5.3.3 Error

Figures 5.4 and 5.5 illustrate that the image analysis and GF method accurately adjusts the film strip samples to the 'true' whole film transmittance and reflectance. When GF-corrected transmittance spectra were averaged across all samples, standard deviations were < 2% across all wavelengths; this is very similar to the results reported by Mesarch *et al.* (1999). The GF-corrected film strip reflectance spectra also closely estimated 'true' whole film reflectance, although these spectra were rather noisy. The noise may have been due to inadequate alignment and focussing of the sample beam. For subsequent measurements of pine needles, more care was taken to align the beam using the mirrors, prior to measurement acquisition.

Absolute error in reflectance measurements may occur when using single and dual-beam spectrophotometers operating with integrating spheres because of substitution errors. The dual-beam spectrophotometer used in the present study, for example, requires measurement of a reference standard, followed by the substitution of the sample for the reflectance measurement. However, the measured reflectance in this case is not equal to the relative reflectance of sample to standard 'because the conditions of irradiation for both measurements are different' (Kortüm, 1969, p.220). This error is magnified when the sample forms a large proportion of the sphere wall, as is the case for smaller spheres. Error is also compounded when the reflectance properties of the sample differ considerably from that of the standard.

In two cases, the substitution error can be ignored, simply because there is no substitution. The first is for external integrating spheres, where the illumination beam is moved between ports, but the properties of the sphere remain the same for transmittance, reference and reflectance measurements (see Figure 5.1). The second is for double-beam spectrophotometers, in which the sphere can contain both the sample and reference beam simultaneously.

Since the sphere used was relatively small, and since the reflectance properties of needles were considered to be very different from the Spectralon™ standard, it was

adjudged that substitution error would be large enough to warrant correction. Correction tables supplied by Labsphere were used, which compare the measured reflectance of Labsphere greyscale reflectance material measured in both a dual-beam and double-beam Perkin-Elmer spectrophotometer. The spectra acquired using the double-beam instrument was considered the 'true' reflectance since it contains no substitution errors. For the needle measurements (section 5.5), reflectance spectra were increased by about 4% across the wavelength range, using the Labsphere substitution error correction tables for Labsphere greyscale level 7. This level was selected because it most closely resembled the level of reflectance from the needle samples in the green visible wavelengths.

Substitution error also applies to transmittance measurements (Labsphere, 2000, p. 15) although correction tables were not available for transmittance. However, the low level of transmittance through pine needles no doubt reduces the substitution error to a negligible level. Mesarch *et al.* (1999) attribute the largest sources of error associated with this method to the resolution of the image and the alignment of the mask. Particular care was therefore taken when aligning the mask over the samples, prior to scanning.

5.4 Summary of method

In this section, each step of the method developed to measure needle reflectance and transmittance is described. Three stages are outlined; preparation, acquisition and processing.

5.4.1 Preparation

Instrument preparation required focussing and alignment of the radiation beam by mirror alignment. This was carried out by dimming the lights and setting the radiation beam to white light. The front panel of the spectrophotometer sample compartment was removed to allow easy viewing of the beam as it passed through the sample port. A thin piece of paper was placed in front of the reflectance port so that the cross-section and position of the beam relative to the port could be viewed at the same location as the needle samples would be placed. Using adjustment screws on each of the three mirrors the beam was first aligned so that is passed cleanly through the transmittance and reflectance ports and focussed so that the edges were as sharp as possible.

Masks were prepared by first measuring the radiation beam at both reflectance and transmittance ports using photographic emulsion to image the beam at these positions (section 5.3). The images were cut out from the cards coated with the emulsion to produce masks the same size as the needle sample holders.

Scots pine shoots were collected from the top third of the sunlit crown of six saplings at the Rothiemurcus study site. Only shoots from the top third of the crown were sampled as this portion of the crown contributes most to canopy reflectance. Shoots

were sealed in plastic bags with a little water and placed in cool boxes for transport back to the laboratory in Edinburgh. Samples were kept in the dark and at 5° C in a refrigerator over night to reduce chlorophyll breakdown. All measurements were completed within 48 hours of sample collection. Sample holders were made from black card with rectangular holes cut larger than the sample beam dimensions. Needles were selected at random from prior-year shoots and held in place side-by-side by adhesive tape.

5.4.2 Acquisition

All measurements were performed with room lights dimmed and a black cloth over the spectrophotometer sample compartment to eliminate any stray light from the outside. Scans were initiated and recorded using a PC running Uvwinlab™ software. Following a background correction scan performed with the Spectralon™ reference standard in place, five scans were recorded for each sample reflectance and transmittance measurement. Each scan took about two minutes to complete over the 400 - 1100 nm wavelength range. For some samples both the adaxial (top) and abaxial (bottom) needle surfaces were measured. Prior-year twig reflectance was also recorded by simply placing three or four twigs stripped of needles side-by-side at the reflectance port. Reflectance from a whole piece of bark from a sapling branch was also scanned. Neither of these canopy components required transmittance measurements since they are opaque.

5.4.3 Processing

The five spectra files were imported into Microsoft EXCEL™ and averaged. Standard deviations were found to be < 0.1% of the averaged values across the wavelength range, giving confidence to the stability of the instrument. GFs were calculated by first placing the masks over the needle samples and scanning them on a flatbed scanner at 600 dpi. Image files were then imported into Erdas IMAGINE™ to estimate the area of the gaps between needles in pixels. The images required a linear contrast stretch to be applied to adequately delineate the gap regions. GF was calculated as the total gap area (pixels) divided by the beam dimension area (pixels).

The GF values were applied to the averaged sample spectra according to the equations given in section 5.3. Finally, a correction for substitution error was applied as also discussed in section 5.3.

5.5 Results and Discussion

Twelve needle samples were prepared for transmittance measurements and twelve for reflectance measurements using the method described in the previous section. The needles were selected at random from shoots from four different trees, each sample being prepared from the same shoot. In addition, three samples from one tree were measured with their abaxial (bottom) surfaces facing the light source for both reflectance and transmittance. The reflectance of branch bark (twelve years old), and of twigs stripped of their needles was also measured in order to characterise other sources of canopy reflectance.

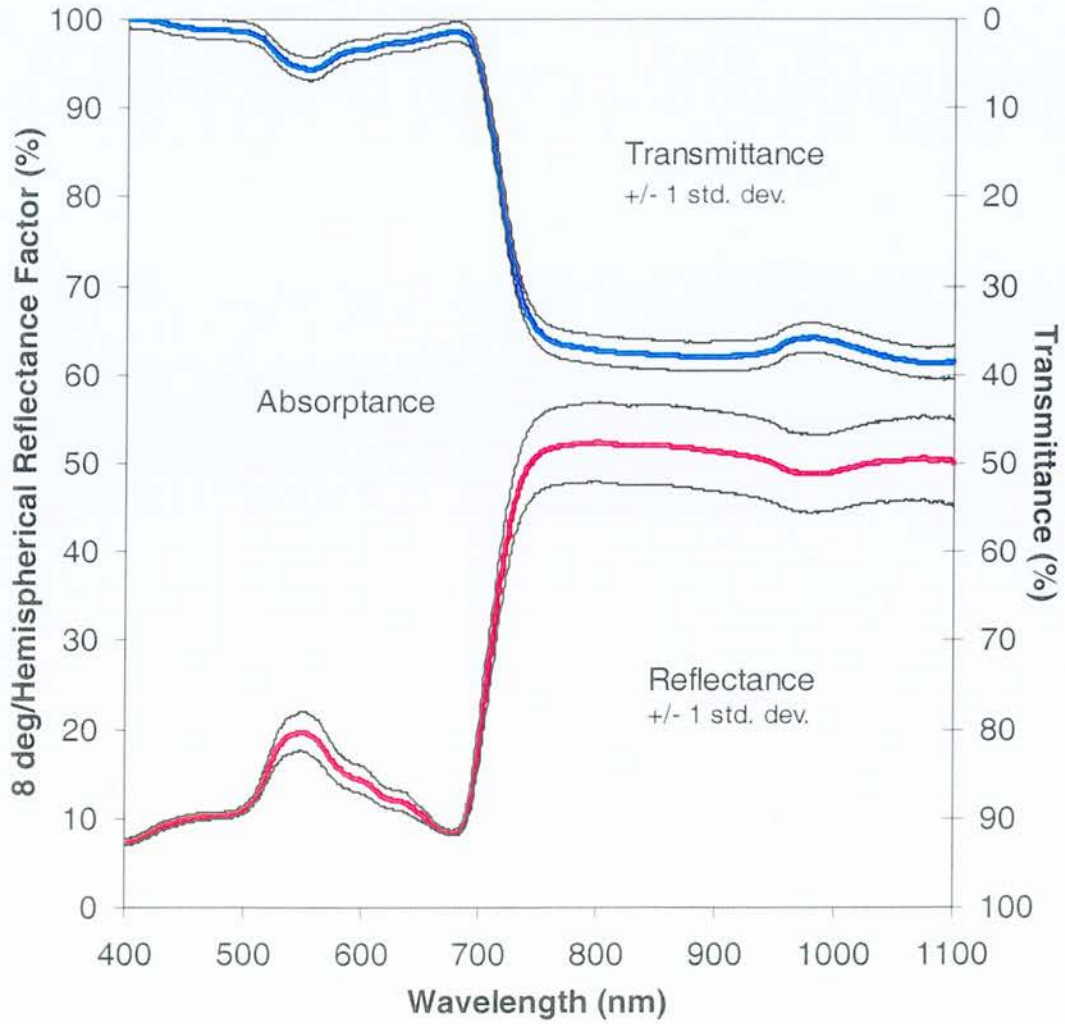

Figure 5.6 Optical properties of Scots pine needles (n=12)

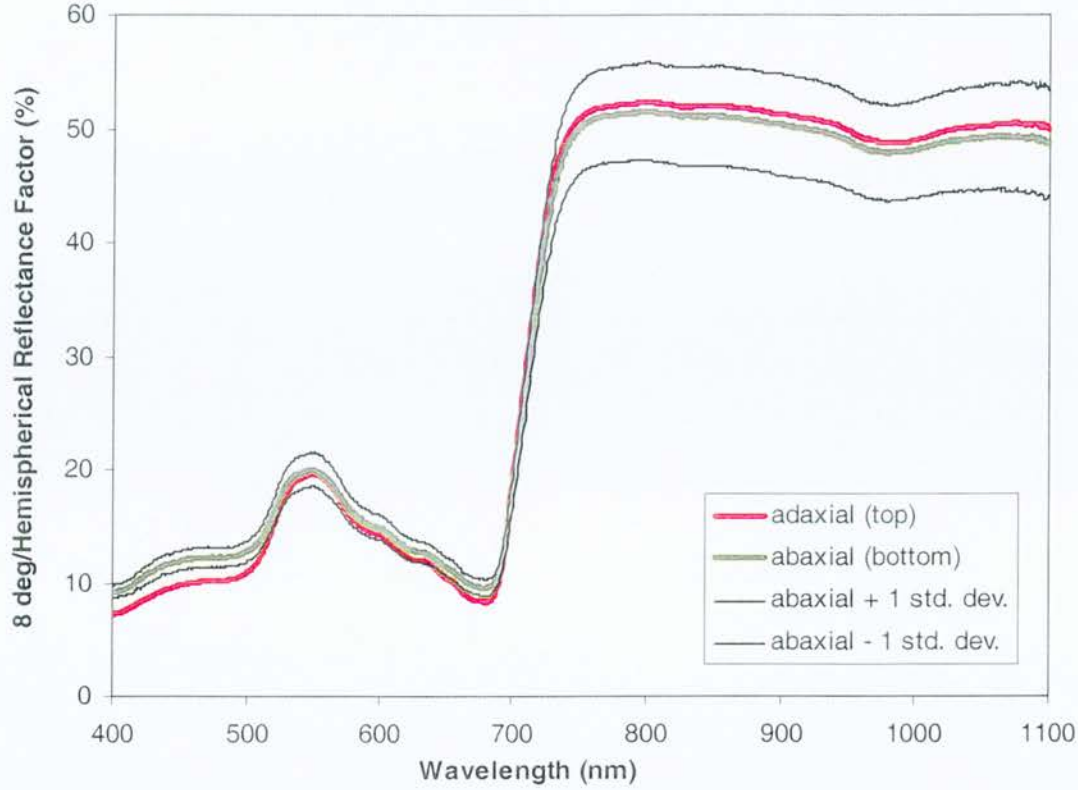

Figure 5.7 Comparison of averaged reflectance from needle adaxial and abaxial surfaces (n=3 for the abaxial spectra).

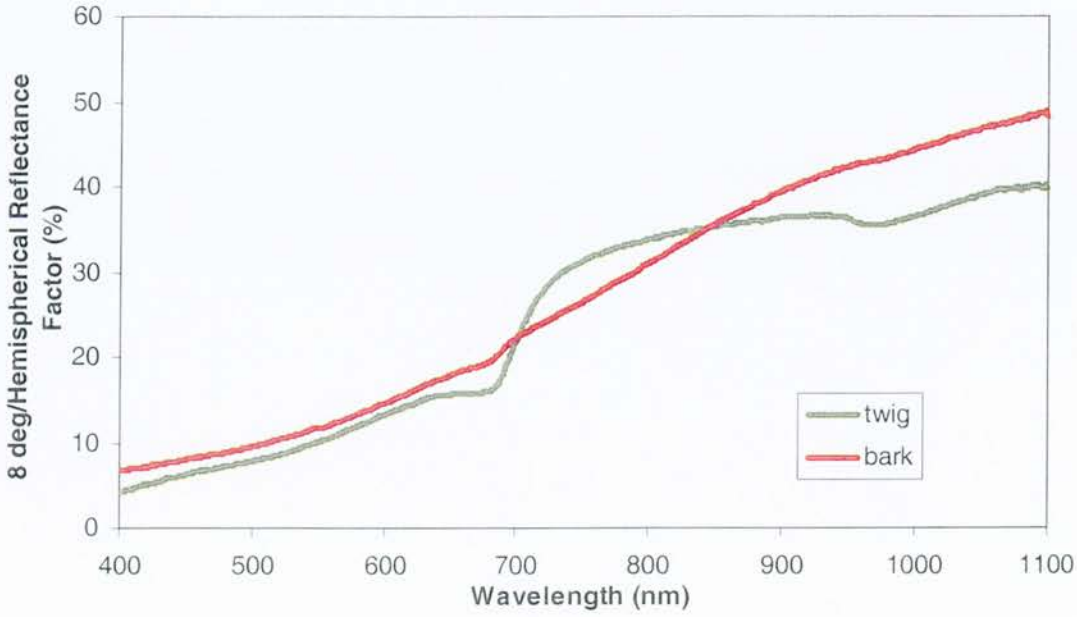

Figure 5.8 Averaged reflectance spectra for branch bark and first year twigs (shoots stripped of needles), n=3 in both cases.

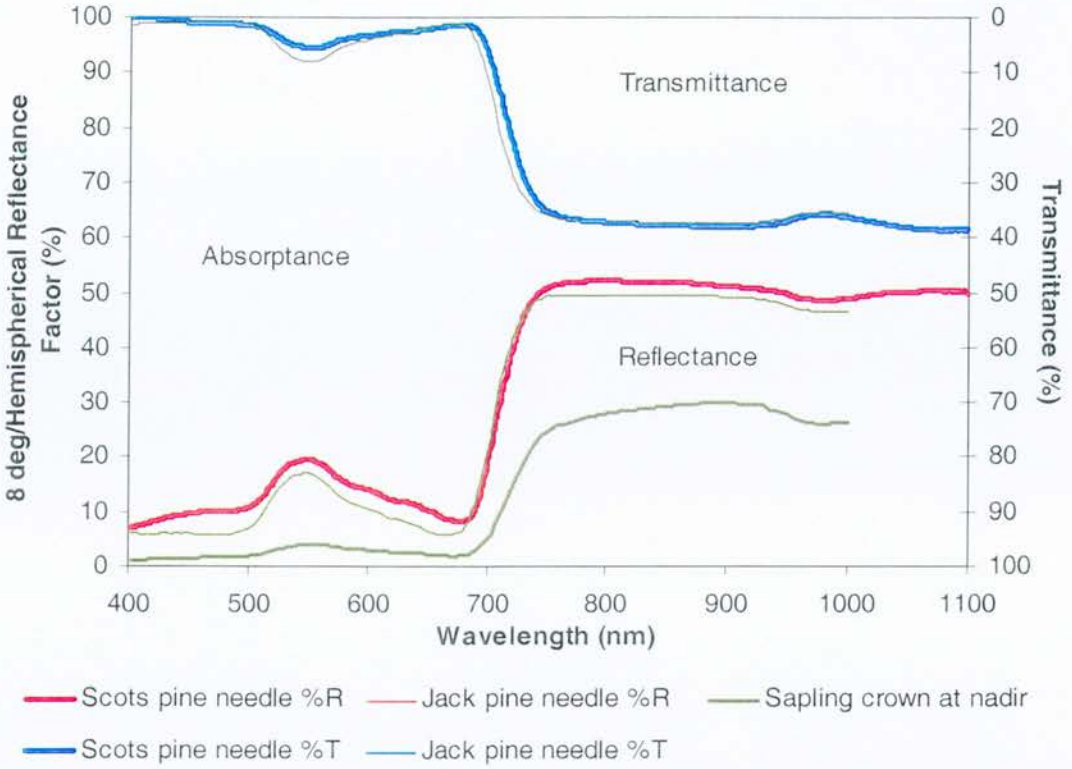

Figure 5.9 Reflectance and transmittance spectra of Scots pine and Jack pine needles (BOREAS). Scots pine sapling crown absolute reflectance measured at nadir with a GER 1500 spectroradiomter is also shown.

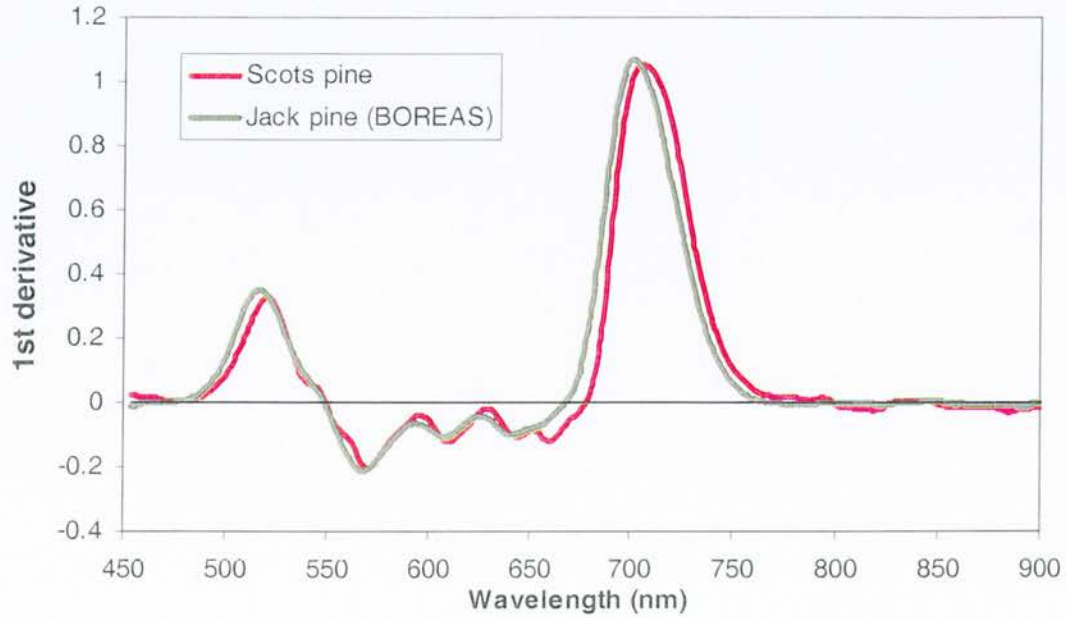

Figure 5.10 First-order derivative spectra of Scots pine and Jack pine needles to compare shape.

The averaged transmittance and reflectance spectra of the twelve samples are presented in Figure 5.6. Standard deviations were greatest for the NIR reflectance, which is likely due to both real variations in reflectance between samples and variations in GF. Similar to the results of Mesarch *et al.* (1999), it was found that measured reflectance in the NIR did increase very slightly with decreasing GF due to multiple scattering between adjacent surfaces. However, nine of the twelve reflectance samples had larger GFs (> 0.2) as recommended by Mesarch *et al.* (1999), so that the contribution from multiple scattering was largely minimised.

Reflectance in the NIR reached about 50%, dropping to < 9% at the chlorophyll absorption maxima in the blue and red visible regions. The transmittance spectra mirror the trends in the reflectance spectra, but at lower percentage levels. Transmittance in the chlorophyll absorbing regions of the visible wavelengths reach zero, and even become negative below about 450 nm. This is due to the errors inherent within the measurement method, particularly the error associated with GF estimation.

Figure 5.7 compares the reflectance from the upper and lower surfaces of three needle samples. One advantage of the image analysis technique over the painting method of Daughtry *et al.* (1989) is that it allows both sides of the same sample to be measured.(Mesarch *et al.* (1999). The spectra are very similar, although reflectance from the abaxial needle surface is slightly higher in the visible wavelengths. The same result was reported by Dungan *et al.* (1996) for Douglas Fir, and by Rock *et al.* (1994) and Williams (1991) for a range of conifer species. Dungan *et al.* (1996) attribute the lower adaxial reflectance values to the concentration of chloroplasts at the adaxial surfaces of leaves, and hence greater absorption at this surface.

As might be expected, the bark reflectance spectra illustrated in Figure 5.8 is featureless, and there is a steady increase in reflectance with wavelength and a relatively constant slope. The twig samples follow a similar trend, although there is clearly some degree of chlorophyll absorption at about 680 nm. This result was to be expected, since once stripped of their needles the twigs remained slightly green in

colour. The twig spectra are very similar to those reported by Williams (1991), who noted a general decrease in conifer twig reflectance with age. This was attributed to an increase in twig surface roughness with age. It is likely therefore, that younger twigs in particular contribute significantly to the interaction of light within the canopy, and thereby to measured canopy reflectance as a whole.

Illustrated in Figure 5.9 are the measured reflectance and transmittance spectra for Scots pine, compared with those of Jack pine. The Jack pine spectra were acquired as part of the North American BOREAS project in July 1994 (Mesarch *et al.*, 1998), using the Li-Cor apparatus. The comparison was considered valid since the species are similar and the BOREAS spectra were acquired using the same method of Mesarch *et al.* (1999). The Jack pine spectra illustrated here were acquired from samples collected from the sunlit side of the top third of the crown and at the same seasonal cycle as the samples collected for the present study[1]. The spectra are very similar for the two species, the main difference being greater reflectance values for Scots pine across the wavelength range. This may be due to the more glossy adaxial surfaces of Scots pine needles. There is very little difference in the intensity of either the green reflectance peaks or the chlorophyll wells, suggesting that chlorophyll concentrations are very similar for the two species. Despite the variations due to species and location, and those due to sensor differences, this comparison does confirm, in the absence of any other suitable Scots pine spectra, that the measurement method produced sensible results. The reflectance curve of a Scots pine sapling crown is also illustrated in Figure 5.9 for comparison. Overall percentage reflectance is much lower than for laboratory measured needle reflectance due to the greater absorption of radiation by the optically thick crown structure. The effect of shadow within the crown will also be incorporated in the sapling crown reflectance spectra.

---

[1] A guide document which includes more information about this dataset can be found at http://www-eosdis.ornl.gov/boreas/TE/te12lod/comp/TE12_Leaf_Optic.txt

The close similarity in the shape of the Scots pine and Jack pine spectra is evident from the first derivative curves presented in Figure 5.10. The features of the Scots pine spectra can be identified at slightly longer wavelengths than the Jack pine spectra. However, this comparison may not be valid since the Jack pine spectra were interpolated to a 5 nm resolution to aid comparison with other BOREAS data (Mesarch *et al.*, 1998), such that the exact position of peaks should be interpreted with some caution. For the Scots pine spectra, the chlorophyll absorption minima of the reflectance curve was at 679 nm, and the derivative spectra red-edge maxima was at 706 nm.

5.6 Conclusions

A method was developed and tested to allow the optical properties of needles and narrow leaf samples to be measured in a medium-cost laboratory dual-beam spectrophotometer fitted with an internal integrating sphere accessory. The method was based on the gap fraction (GF) method proposed by Daughtry *et al.* (1989) and modified by Mesarch *et al.* (1999) who proposed a method of independently estimating GF by image analysis. Both these previous studies utilized a field-portable spectroradiometer with an external integrating sphere accessory.

The GF/image analysis technique allows the reflectance and transmittance of samples that are narrower than the port diameter of the integrating sphere to be measured. A primary requirement of the method is that the dimensions of the sample beam at the sample reflectance and transmittance ports be precisely known. This was achieved in two ways. Firstly, a sample holder was constructed to accommodate the needles precisely in front of the radiation beam. Secondly, a method was developed to measure the exact dimensions of the radiation beam at both measurement ports. The beam was imaged onto a photographic emulsion.

A further modification of the method was required due to the substitution method of measurement used for dual-beam spectrophotometers. Substitution of the sample for the reference standard introduces a degree of error to measured reflectance since the reflectance properties of the sphere are altered. There is no error for apparatus that do not involve substitution, but rather comparison, such as the Li-Cor 1800 apparatus. For the comparison method it is the illumination source that is moved between ports for reference, reflectance and transmittance measurements and the reflectance properties of the sphere wall remain unchanged. Substitution correction tables published by Labsphere Inc. were applied to the measured reflectance spectra.

The method was tested by comparing the optical properties of whole pieces of unexposed, processed Ektachrome slide film with the GF-corrected spectra of strips of the same film. The film strips were arranged to simulate the same measurement position as that used for needle measurements. The GF/image analysis method was found to accurately correct the film strip samples to the 'true' whole film transmittance and reflectance. Standard deviations of averaged transmittance spectra were < 2% across all wavelengths, comparable to the results of Mesarch *et al.* (1999) who reported < 1.5% for the same film type. It was concluded that the largest source of error is likely to be in the alignment of the mask in order to image the GF and particular care was required for this part of the method.

Twelve samples of Scots pine needles were constructed for reflectance measurements, and twelve for transmittance measurements with smaller GFs. Variability between the optical properties of the samples was described by averaging the spectra and comparing the standard deviations. Standard deviations were greatest in the NIR wavelengths of the reflectance spectra. Variations in GFs and multiple scattering between adjacent needles at smaller GFs are thought to have contributed to this variability. The reflectance spectra of other canopy components (bark and twig) were also measured and it was concluded that twig reflectance is likely to contribute significantly to measured canopy reflectance.

Comparison of the averaged Scots pine spectra with those of Jack pine measured by the same method showed the optical properties of the two species of pine needle to be very similar. Scots pine reflectance was greater across the wavelength range and may be due to the more glossy needles. Scots pine needle spectral features, such as the green reflectance peak, the chlorophyll absorption well and the red-edge position, were red-shifted by 5-10 nm over the Jack pine spectra. Scots pine needle red-edge position was at 706 nm, and the chlorophyll absorption well was at 679 nm.

The measurement of both reflectance and transmittance of pine needles and narrow leaf samples is not commonly reported in remote sensing studies. Nevertheless, the current trend for canopy reflectance modelling in order to improve understanding of

the controls on light interaction within vegetation canopies clearly requires reliable leaf optical data. The importance of accurate reflectance and transmittance needle spectra for modelling forest canopy reflectance cannot be overstated, since it is the elementary optical unit within the canopy. The averaged reflectance and transmittance spectra presented in this chapter provide suitable data for reflectance modelling of young Scots pine canopies. The author is not aware of any other such detailed spectra for both reflectance and transmittance of Scots pine needles.

5.7 References

DAUGHTRY, C. S. T., RANSON, K. J., and BIEHL, L. L., 1989, A new technique to measure the spectral properties of conifer needles. *Remote Sensing of Environment*, **27**, 81-91.

DUGGIN, M. J., 1980, The field measurement of reflectance factors. *Photogrammetric Engineering and Remote Sensing*, **5**, 643-647.

DUNGAN, J., JOHNSON, L., BILLOW, C., MATSON, P., MAZZURCO, J., MOEN, J., and VANDERBILT, V., 1996, High spectral resolution reflectance of Douglas Fir grown under different fertilization treatments: experiment design and treatment effects. *Remote Sensing of Environment*, **55**, 217-228.

FERNS, D. C., ZARA, S. J., and BARBER, J., 1984, Application of high resolution spectroradiometry to vegetation. *Photogrammetric Engineering and Remote Sensing*, **50**, 1725-1735.

GATES, D. M., KEEGAN, J., SCHLETER, J. C., and WEIDNER, V. R., 1965, Spectral properties of plants. *Applied Optics*, **4**, 11-20.

GAUSMAN, H. W., 1977, Reflectance of leaf components. *Remote Sensing of Environment*, **6**, 1-9.

GAUSMAN, H. W., 1983, Visible light reflectance, transmittance, and absorptance of differently pigmented cotton leaves. *Remote Sensing of Environment*, **13**, 233-238.

GAUSMAN H. W., ALLEN, W. A., SCHUPP, M., WIEGAND, C. L., ESCOBAR, D. E., and RODRIQUEZ, R. R., 1970, Reflectance, transmittance and absorptance of light of leaves for 11 plant genera with different leaf mesophyll arrangements. *Texas A & M University, Texas Agricultural Experiment Station Technical Monograph 7, Sept. 1970*, pp38.

GAUSMAN, H. W., QUISENBERRY, J. E., BURKE, J. J., and WENDT, C. W., 1984, Leaf spectral measurements to screen cotton strains for characters affected by stress. *Field Crops Research*, **9**, 373-381.

GITELSON, A. A., and MERZLYAK, M. N., 1996, Signature analysis of leaf reflectance spectra: algorithm development for remote sensing of chlorophyll. *Journal of Plant Physiology*, **148**, 494-500.

GITELSON, A. A., and MERZLYAK, M. N., 1997, Remote estimation of chlorophyll content in higher plant leaves. *International Journal of Remote Sensing*, **18**, 2691-2697.

GOEBEL, D. G., 1967, Generalized integrating-sphere theory. *Applied Optics*, **6**, 125-128.

HORLER, D. N. H., DOCKRAY, M. and BARBER, J., 1983, The red-edge of plant leaf reflectance. *International Journal of Remote Sensing*, **4**, 273-288.

KNAPP, A. K., and CARTER, G. A., 1998, Variability in leaf optical properties among 26 species from a broad range of habitats. *American Journal of Botany*, **85**, 940-946.

KORTÜM, G., 1969, *Reflectance Spectroscopy; principles, methods, applications* (New York: Springer-Verlag) pp. 366.

LABSPHERE INC., date unknown, *RSA-PE-20 Integrating sphere instruction manual.* Labsphere Inc., P.O. Box 70, North Sutton, NH 03260, U.S.A., pp. 37.

LICHTENTHALER, H. K., GITELSON, A. and LANG, M., 1996, Non-destructive determination of chlorophyll content of leaves of a green and an Aurea mutant of tobacco by reflectance measurements. *Journal of Plant Physiology*, **148**, 483-493.

LORENZEN, B., and JENSEN, A., 1991, Spectral Properties of a barley canopy in relation to the spectral properties of single leaves and the soil. *Remote Sensing of Environment*, **37**, 23-34.

MESARCH, M. A., WALTER-SHEA, E. A., and HAYS, C. J., 1998. BOREAS TE-12 Leaf Optical Data for SSA Species. Available online at [http://www-eosdis.ornl.gov/] from the ORNL Distributed Active Archive Center, Oak Ridge National Laboratory, Oak Ridge, Tennessee, U.S.A.

MESARCH, M. A., WALTER-SHEA, E. A., ASNER, G. P., MIDDLETON, E. M., and CHAN, S. S., 1999, A revised measurement methodology for conifer needles spectral optical properties: evaluating the influence of gaps between elements. *Remote Sensing of Environment*, **68**, 177-192.

MYNENI, R. B., MAGGION, S., IAQUINTA, J., PRIVETTE, J. L., GOBRON, N., PINTY, B., KIMES, D. S., VERSTRAETE, M. M., and WILLIAMS, D. L., 1995, Optical remote sensing of vegetation: modeling, caveats, and algorithms. *Remote Sensing of Environment*, **51**, 169-188.

MYERS, V. I., and ALLEN, W. A., 1968, Electrooptical remote sensing methods as nondestructive testing and measuring techniques in agriculture. *Applied Optics*, **7**, 1819-1838.

RABIDEAU, G. S., FRENCH, C. S., and HOLT, A. S., 1946, The absorption and reflection spectra of leaves, chloroplast suspensions, and chloroplast fragments as measured in an Ulbricht sphere. *American Journal of Botany*, **33**, 769-777.

ROCK, B. N., WILLIAMS, D. L., MOSS, D. M., LAUTEN, G. N., and KIM, M., 1994, High-spectral resolution field and laboratory optical reflectance measurements of Red spruce and Eastern hemlock needles and branches. *Remote Sensing of Environment*, **47**, 176-189.

WILLIAMS, D. L., and WOOD, F. M., 1987, A transportable hemispherical illumination system for making reflectance factor measurements. *Remote Sensing of Environment*, **23**, 131-140.

WILLIAMS, D. L., 1991, A comparison of spectral reflectance properties at the needle, branch, and canopy level for selected conifer species. *Remote Sensing of Environment* **35**: 79-93.

WOOLLEY, J. T., 1971, Reflectance and transmittance of light by leaves. *Plant Physiology*, **47**, 656-662.

6.0 PINE CANOPY MODELLING

6.1 Introduction

Thomas and Huggett (1980) define a model as 'any simplified representation of reality'. There have been numerous attempts in remote sensing to simplify the complex reality of light interaction with vegetation. Two general approaches have been used (Hall *et al.*, 1995); 'empirical approaches that rely primarily on curve-fitting to correlate various measures of surface reflectance, including vegetation indices, to the biophysical characteristics of interest, and secondly, physical modeling approaches that attempt to forward model the relationship between leaf, canopy, and stand-level biophysical characteristics and reflected and emitted radiation'.

The simpler wholly empirical models have been more widely applied to large-scale estimates of vegetation characteristics using well-established indices such as the NDVI. Such models have the advantage of being easily invertible. 'Vegetation indices are a convenient way of summarizing the remote observations and are useful in mapping and event detection, and in some instances of estimating surface parameters' (Myneni *et al.* 1995). However, these simple models have been criticised because they assume that the relationship between signal and parameter is independent of all other vegetation parameters and light interaction processes. Asrar *et al.* (1989), for example state that 'this assumption is generally not valid, due to the complex nature of the interaction of solar energy with plant canopies'. Consequently, the main thrust of remote sensing research in recent years has attempted to produce models that account for this complexity. The result has been ever increasing

complexity within the models themselves, usually based on the physical principles of radiative transfer. Often, the models have attempted to tackle issues that are not explicitly remote sensing problems, such as the modelling of canopy or landscape structure, the result being different types of models combined. This approach has served to increase the general understanding of the relationships between remotely sensed data and parameters of interest. However, there is little evidence that these complex modelling efforts are being widely applied. For example, Holmgren and Thuresson (1998) conclude that 'forestry remote sensing research, through its increasing complexity and yet few benefits, is diverging from applied forestry research'.

This chapter begins with a review of model types and their applications. A hybrid computer simulation model called FLIGHT is then described and evaluated using pine needle spectra from the previous chapter. The modelled results are compared with averaged seasonal plot spectra for the nine sample plots at Inshriach. The roles of LAI and percentage cover are examined as controls on canopy reflectance for selected wavelengths, and the effects of changing crown density when LAI and percentage cover remain constant is explored. The modelled results are evaluated and discussed in the context of monitoring changes in areas of semi-natural pine regeneration.

6.2 Literature Review and Model Types

6.2.1 Model Types

Goel (1988) classifies the approaches to physical modelling of radiation into four types: 1) Geometrical models, 2) Turbid medium models, 3) Hybrid models and 4) Computer simulation models. This section summarises the description by Goel (1988) of earlier models within these categories, and considers their development by reference to more recent work. Models within these categories are based on either geometrical optics (involving rays and shadows) or radiative transfer theory, or the average canopy transmittance theory.

The first of the four model types are geometrical models, which assume the canopy to be made up of a ground surface, with geometrical objects or protrusions (sometimes perturbations) placed on it in a defined manner. For forest canopies, and perhaps the best known, the Li and Strahler (1985) model simulated images of cones on a plane. The aim was to design a model to estimate the size and density of trees from images of low-density timber stands, and took account of shadows. The model was inverted to obtain size and density parameters for a red fir and a mixed conifer site. Results were good for estimating cover, but not for tree size (e.g. Woodcock *et al.* 1997), although the main limitation of the model is that model inversion may be computationally intensive.

Turbid medium models are the second type of model categorised by Goel (1988). These models assume a homogeneous canopy, treating the canopy as a continuous medium split into layers, with constant optical and structural properties. Some are based on the radiative transfer equation, some use average canopy transmittance theory, or both. The Suits (1972) model was the first to account for solar viewing angles and explicitly related architectural and spectral parameters of the canopy and its elements to canopy reflectance. In general, the model captured qualitatively the

observed dependencies of canopy reflectance on solar/view directions and canopy parameters, such as LAI, average leaf inclination angle, and soil reflectance. However, most canopies do not meet the assumption of a homogeneous, continuous canopy in the Suits model. The model also assumes only horizontal and vertical vegetation elements.

The SAIL model (Verhoef, 1984) extended the Suits model to allow for any discrete distribution of leaf angles. It has been applied by a number of workers to crop canopies and has been found to be more realistic than the Suits model (e.g. Badhwar *et al.*, 1985; Goel and Deering, 1985). It has formed the basis of a number of vegetation canopy studies with varying success (e.g. Goward and Huemmrich; Kuusk, 1995), but its basic assumptions of canopy homogeneity limit its applications to many forest types. Pinty *et al.* (1990) concluded that sparse vegetation with low LAI values are not well represented by the model and inversion of the model to estimate forest LAI is unlikely to be successful (Rowland *et al.* 1998). Another discrete model is described by Norman *et al.* (1985) called Cupid, which has been used by other workers and employs essentially the same canopy parameters as for the SAIL model (e.g. Walthall *et al.*, 1985; 1997).

The third category of physical canopy reflectance models can be termed hybrid models. For the turbid medium approach, one of the key assumptions was that the individual foliage elements are randomly positioned. However, random distribution is not a good approximation for dense crowns of widely spaced rows, or widely separated individual trees in heterogeneous canopies. Instead, hybrid models identify subcanopies with an assumed regular shape like spheroid, ellipsoid, cylinder, or cube, but in these models, the interaction of the radiation with the vegetation elements within each subcanopy is modelled. Most hybrid models are a combination of the geometrical and turbid medium models, and are therefore the most complex and computer-intensive.

Earlier examples of hybrid models were extensions of previous turbid medium models. For example, for the Verhoef-Bunnik row model (Verhoeff and Bunnik,

1981), the row effect is described by modifying the coefficients in the Suits model for a homogeneous canopy. Results were fairly poor, especially for sparse canopies, because the model did not incorporate the specular reflectance effects and depth dependent distribution of vegetation elements. The Suits row model overcame some of the limitations of the Verhoef-Bunnik row model and was tested on a soybean-corn canopy. Further modifications were made in the Goel-Grier model, which used Suits' row model but added two features. Firstly, vegetation elements were allowed to have any inclination angle distribution and secondly, the canopy shape was better represented during various stages of growth. It was suggested that non-Lambertian behaviour of leaves may be an important effect to include within models that estimate the leaf angle distribution.

Norman and Welles (1983) modelled the canopy as a finite number of 3D geometrical figures such as ellipsoids or cylinders, spaced in one of many patterns - regularly spaced, densely grouped (including overlapping) at regular spacing, or sparse groups widely separated. The aim was to reflect more realistically the structure of a particular vegetation canopy. The foliage in each of these groups may be positioned randomly or non-randomly. Once the foliage has been distributed and the subcanopies spaced into a desired pattern, the attenuation of the incident solar beam as it travels the collection of subcanopies is calculated. For this purpose, the average transmittance theory is used. The computation of diffuse fluxes of energy for the layers was done using the Cupid model. Good results were obtained for a young corn canopy, but does not account for increased reflectance at the hotspot feature.

Another hybrid three-dimensional model is described by Kimes and Kirchner (1982). The conceptual framework is a rectangular solid of any dimension that is subdivided into cubical cells of unit dimensions. Each cell is identified by its x, y, and z coordinates and is associated with information about the scene component within the cell (the type of component - leaves, stems, soil, etc.) and the optical properties of components. The model calculates the fluxes between the cells. If a canopy could be considered as an array of subcanopies, then each of the subcanopies is represented

within a cube, with a continuity of flux from one cube to the neighbouring one. Although simulations have been carried out for forest canopies, the hotspot was not accounted for in this model and it assumes isotropic scattering for all interactions within the cells.

In an extension of their row model called TRIM, Goel and Grier (1988) decreased computation time of hybrid models and increased invertibility. TRIM used the canopy parameters of the SAIL model for homogenous canopies (leaf hemispherical reflectance, leaf hemispherical transmittance, LAI, azimuthally symmetric leaf angle distribution, soil hemispherical reflectance, and fraction of diffused skylight). The model was validated against corn canopies and assumes that subcanopies are distributed in a regular pattern. It is, therefore, most applicable to canopies whose architecture is in a repetitive pattern (Goel and Grier, 1988).

Other hybrid models for heterogeneous canopies have followed the geometrical route of Li and Strahler (1985). For forest canopy modelling, Nilson and Peterson (1991) compared model calculations with reflectance measurements collected with an airborne radiometer for 12 Scots pine-dominated boreal forests in Estonia, using linear regression. Parameters used for the model fell into three categories: 1) Forest parameters - stand density, tree height, crown length and radius, and trunk diameter; 2) Optical parameters - reflection and transmission coefficients and refraction index of needles, reflection coefficients for branches and trunks, and nadir reflectance factor for ground vegetation; 3) Structural parameters - LAI and branch area index, a grouping index for the tree pattern, and the mean linear dimension of foliage elements. Results showed good agreement in the red region, regardless of season, but poorest in the green and NIR regions in summer.

Computer simulation models are the fourth category of canopy reflectance models. These models are better at accounting for the dimensions of vegetation elements and the distance between them and their possible non-random distribution. For example, the Monte Carlo method treats canopy architecture in more realistic detail in order to calculate the canopy reflectance. Due to the large number of trials or repetitions and

number of trials or repetitions and the large number of variables required, the use of the Monte Carlo simulation method has been relatively limited. The earliest simulations, such as those by Oikawa and Saeki (1977 cited in Goel, 1988) helped to establish some general observations about the relationship between photon interaction and different parameters of canopy architecture. For example, for a constant leaf area index, the coefficient of penetration is larger for clumped leaf area densities than for random distributions of leaves. The Smith-Oliver model is a hybrid of analytical models and computer simulation models. It uses the Idso-de Wit model to determine the probabilities of the interaction of the incident and emergent fluxes within each canopy layer, whilst the probability of non-interception is implemented by the Monte Carlo procedure. Results were similar to the Suits Prime model, which is conceptually similar. The Ross-Marshak model (Ross and Marshak, 1988) is similar to the Oikawa-Saeki model for the architecture of the canopy. The canopy is taken to be infinite in the horizontal direction, consisting of identical test areas, with each area containing an equal number of plants, geometrically modelled. The model is used to study the effect of leaf dimensions, LAD, leaf shapes (round vs. elliptical), plant height and plant density, distances between leaves, and soil reflectance on the bidirectional canopy reflectance, for example, (Ross and Marshak, 1989).

The combination of a hybrid geometric optical/radiative transfer model with estimation of BRDF by Monte Carlo solution has also been applied to discontinuous forest canopies (e.g. North, 1996; Gerard and North, 1997). These simulations have demonstrated the importance of the geometric effects of forests on measured reflectance. For example, the simulations show that the red BRDF is mainly influenced by the illuminated ground component, and is sensitive to canopy cover, tree pattern distribution, and canopy gaps. The NIR BRDF is sensitive to canopy cover, crown-centre height distribution, and crown shape. One of the drawbacks of computer simulations can be the amount of computer resource required. Thompson and Goel (1998) developed a way of using the ray tracing Monte Carlo method with three orders of magnitude less photons required (which they refer to as the photon spread method), thereby considerably speeding up these type of models. They went

on to propose a model named SPRINT (Spreading of Photons for Radiation INTerception), which they describe as 'universal in the sense that it can emulate turbid medium, geometrical, hybrid, and computer simulation models' (Goel and Thompson, 2000). The model is designed for kilometre-level scenes with varied vegetation elements.

In this section, the main types of vegetation canopy models have been described and their various merits highlighted. The following section describes models developed for forest canopy modelling in more detail.

6.2.2 Recent Approaches to Forest Canopy Modelling

The limitations of many of the earlier modelling approaches when applied to more spatially and structurally complex canopies, such as forest canopies, has led to the realisation that many of the problems are not explicitly remote sensing ones. For example Myneni *et al.* (1995) state that 'research is required in the area of modeling tree architecture, especially for coniferous species, and quantifying spatial heterogeneity at landscape level'. Several attempts have been made to address this problem.

Cescatti (1997) suggests that there have been two extreme approaches to canopy modelling, neither of which is suitable for semi-natural canopies. He argues that geometrical description of crown shape is too approximate for describing crown asymmetry, and analytical description of crown architecture on the basis of empirical observation requires too many species-specific parameters. He developed a crown model, combined with a numerical solution for the computation of radiative transfer that 'represents a compromise between the simplicity of the uniform canopy model and the complexity of the architectural model.' The software, called FOREST can be used to describe complex canopies and for the analysis of the interaction between canopy structure and radiative fluxes.

Other authors pursue the combination of models based on canopy radiative transfer theory and geometric-optical modelling. For example, Asner and Wessman (1997) used this approach to consider the importance of different scales of observation (i.e. from leaf to landscape) on PAR absorption. They make the important conclusion that 'Landscape characteristics influence PAR absorption [and therefore, presumably canopy reflectance] beyond that which is exerted at the leaf level, but are not divorced from leaf and canopy characteristics'. Therefore, the spatial distribution of canopies may be more important to reflectance than canopy LAI, but at the same time this relationship is not unaffected by LAI. Gerard and North (1997) used the FLIGHT model for analyzing the effects of gaps in forest canopies on the

bidirectional reflectance distribution function (BRDF). The ray tracing/Monte Carlo method used in the FLIGHT model has been made considerably less computationally expensive by the SPRINT model of Goel and Thompson (2000), by employing the concept of photon spreading to speed up the calculations of BRDF. This has enabled them to propose their model for the analysis of the effects of complex forest structure on BRDF for kilometre-scale simulated scenes.

The importance of spatial arrangement in forest canopies has led to a further development in modelling studies that includes measures of image texture. Bruniquel-Pinel and Gastellu-Etchegorry (1998) simulated images with the discrete anisotropic radiative transfer model (DART) and quantified texture with variograms. The study investigated how image texture is influenced by crown diameter, distance between trees and rows, tree positioning, LAI and tree height. Viewing and illumination configurations, spectral domain and spatial resolution were also investigated in relation to image texture. The model results were tested against high-resolution airborne data. These workers stress the importance of using accurate radiative transfer models when studying canopy texture with image simulations and of crown diameter to image texture. They also stress the importance of understorey reflectance, especially when forest canopy LAI is low.

In a similar study, St-Onge and Cavayas (1995) simulated artificial images using a three-dimensional canopy model and a geometrical-optical model. They determined prediction equations for crown diameter, tree height, and stand density, based on image texture. The equations were applied to high-resolution (36 cm) airborne images. Good results were obtained for tree height, crown diameter, and stand density.

Using an empirical approach, Wulder *et al.* (1998) noted that since internal stand conditions, such as mutual shadowing, will actually result in a decrease in NDVI as LAI increases, image texture should be a useful additional source of information for predicting LAI in forested stands. Using ***casi*** data over forests in Canada, they established linear regression models between LAI and NDVI and found that the

relationship was indeed improved by introducing image texture. It was argued that in cases where the spectral information is heterogeneous, such as mixed-wood stands, the textural information is of greater information content than the spectral information. Information content of heterogeneous stands was best extracted with second-order texture measures and semivariance moment texture. This approach was also used in the present study (see Chapter 7). Multivariate models for the prediction of LAI provided the greatest amount of information when including texture values calculated from differing spectral channels. Coops and Culvenor (2000) pointed out that 'Recent studies, however, indicate the spatial pattern of trees within a scene can have a considerable effect on both the magnitude and distribution of canopy reflectance, especially at high sun-view zenith angles'.

With respect to Scots pine, modelling efforts within forestry have sought to account for crown architecture. A general yield model (Edwards and Christie, 1981) is based on plantations from 10 years and a top height of 6 m, but probably has little relevance to naturally regenerating saplings. Kellomäki and Kurttio (1991) developed an empirical model for the structural development of the crown system of young Scots pine, based on shoot length. Data were for 'stand grown' young pine in Finland. The model is a geometric one, which simulates the growth and structure of a young Scots pine grown in a stand, the tree being representative of the whole tree population in terms of a mean tree. It was noted that prevailing light conditions within the crown have a strong effect on the structural process of the crown system and the model was extended in Kellomäki and Strandman (1995) to include the effect of direct and diffuse radiation intercepted by a parent shoot during the previous season, thereby deriving its length. The authors state the advantage of this modelling approach using modular growth as making possible 'the modelling of the spatial distribution of the foliage in the crown system with no predetermined statistical distribution. Furthermore, the grouping of needles in the crowns of conifers can be effectively introduced into the model in the form of a detailed description of the shoot structure.'

Chen and Leblanc (1997) modified the Li-Strahler model to include not only within-crown architecture, but also the non-random distribution of trees (or grouping of trees) within boreal spruce forest. They refer to their model as 'four-scale' because it accounts for four scales of structural complexity. In other words, turbid media models, such as SAIL are one-scale; models with randomly-distributed discrete objects containing turbid media are two-scale (e.g. Li and Strahler, 1992); those describing non-random discrete objects containing turbid media are three-scale (e.g. Gerard and North, 1997); and finally, the four-scale model describing non-random discrete objects, but with internal structures such as branches and shoots. The purpose of the four-scale model was to better account for the effects of mutual shading of shoots, branches and trees, the distributions of which were all defined probabilistically. The model is therefore, necessarily, mathematically complex. Also the effect of multiple scattering is not taken into account, which will most likely affect predicted reflectance in the NIR. A summary of the main model types and their characteristics is given in Table 6.1

Table 6.1 Summary of canopy reflectance model types and their characteristics.

	Examples	Advantages	Disadvantages	Theoretical Basis
Geometrical	Li and Strahler (1985; 1986; 1992); Li *et al.* (1996); Jupp *et al.* (1986)	Accounts for shadow /large scale structure Generally invertible Best for sparse canopies with high leaf densities	Does not account for changes in reflectance due to solar and view angle differences. Ignores effects of microstructure, leaf optical properties and diffuse radiation.	Represents forest structure using 3-D shapes on a uniform ground surface.
Turbid Medium	Suits (1972); Verheof (1984)	Easily invertible Requires few input parameters Best for homogeneous canopies	Assumes a homogenous canopy layer, so works less well for complex forest canopies. Discrete versions are computationally expensive and not easily invertible.	Canopy is a 1-D opaque layer, or layers, with constant optical and structural properties.
Hybrid	Norman and Welles (1983); Nilson and Peterson (1991); Li *et al.* (1995); Chen and Leblanc (1997); Ni *et al.* (1999)	Allows calculation of BRDF and diffuse component Useful for inhomogeneous canopies	Greater complexity, so not easily invertible	Combines geometrical with turbid medium (discrete geometrical objects consisting of turbid media).
Computer Simulation	Ross and Marsak (1989); North (1996); Govaerts and Verstraete (1998); Lewis (1999); Goel and Thompson (2000)	Accounts better for canopy structure, especially at leaf/needle scale. Good for BRDF calculation Allows for non-random leaf distributions.	Greater complexity, so not easily invertible. Requires more detailed forest structural data, which is often difficult to obtain.	As for hybrid models, but can simulate random variables more realistically.

6.2.3 Statement of Aims

The FLIGHT model was used to model canopy reflectance for a range of scenarios with the following specific aims:

1. To evaluate the performance of the model against the mean seasonal reflectance (MSR) of the sample plots.
2. To examine the effects of changing LAI and percentage cover (PC) using the measured tree statistics from a sample plot.
3. To examine the effects of changing tree height (crown density) at different stand densities when LAI and PC remain constant.
4. To further understand the main controls on the indices selected for correlation analysis with LAI and percentage cover in Chapters 3 and 4.

6.3 Model Description and Methods

The Forest LIGHT Interaction Model (FLIGHT), described in North (1996) was used to simulate reflectance from a regenerating pine canopy over a heather understorey. The model is particularly suited for this forest type because it accounts for crown shape and a canopy with gaps. All four components of a scene in such a landscape are each explicitly modelled, namely; sunlit crown, shaded crown, sunlit understorey and shaded understorey (Fig 6.1).

A three-dimensional scene was specified as a 'box' (5 m^3) with a sky-plane, a wall plane and a ground-plane. Within the box the number of trees, crown shape (conical), and mean crown size were specified. Tree positions were estimated from a statistical distribution and allowed to overlap with each other and with the vertical planes of the bounding box.

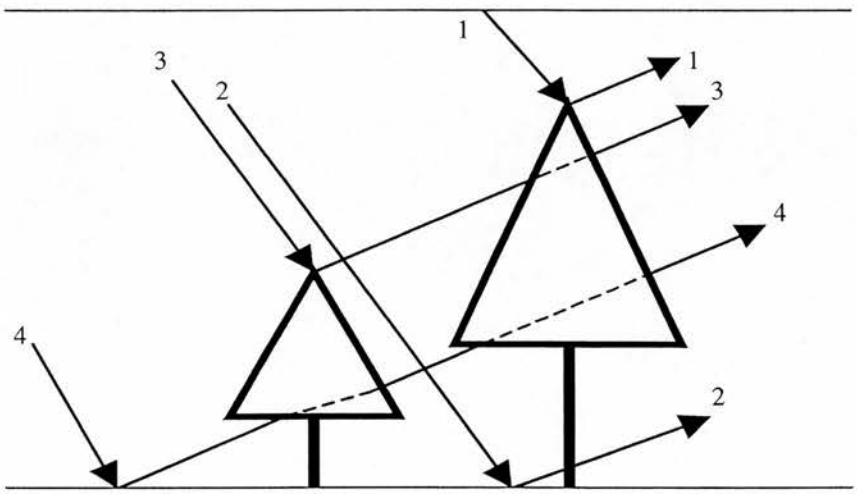

Figure 6.1 The ray tracing method used by the model, accounting for illuminated crown (1); illuminated ground (2); shaded crown (3) and shaded ground (4). Redrawn from Gerard and North (1997).

A deterministic ray-tracing procedure was used to calculate the proportion of sunlit and shaded crown and understorey, which deals with the problem of overlap and mutual shading. The model casts a ray (or photon of light) from the view direction towards the tree crowns and understorey through a grid cell, where it falls upon one of the four scene components (sunlit crown, shaded crown, sunlit understorey or shaded understrorey). The outgoing ray is cast in the direction of solar illumination, now assigned to one of the four scene components. The reflectance value of the forest scene at a given wavelength is calculated as the combination of each scene component reflectance multiplied by the fraction of that component visible. If a ray intersects one of the box walls, it re-enters from the opposite wall as if the same forest structure existed beyond the bounds of the box (North, 1996; Gerard and North, 1997).

The interaction of the photons within the tree crowns is modelled using a Monte Carlo solution of radiative transfer. The solution allows for the interactions of photons with both the understorey and the tree crowns and a photon can undergo a number of scattering events before exit. The simulation also takes into account within-crown structural parameters, such as foliage area density and leaf angle distribution (LAD). A spherical LAD was used in the present study, since this significantly simplifies the calculation and has been shown to produce valid results for conifers (North, 1996). Finally, the model also allows inclusion of a proportion of diffuse sky radiance by using anisotropic scattering functions. This was important when comparing the model to field data, since some of the data were collected when the diffuse sky component was a significant part of overall irradiance.

The model is written in Fortran and was compiled and run on a UNIX operating system, run by a Sun multiprocessor server. The FLIGHT program was modified to represent both the sample plot dimensions and the number of trees within each plot. Soil reflectance was represented by the mean seasonal reflectance (mean of all field measurements on all sampling dates) of Plot 1, containing only the heather understorey. This was considered a valid approach since the heather community provided a complete understorey cover within each of the sample plots and was

shown not have a seasonal effect on pine overstorey reflectance (Chapter 4). Miller *et al.* (1997) also concluded that 'jack pine sites may reasonably be represented by seasonally independent understorey reflectance spectra without serious error introduced in inverse canopy modeling'. The young jack pine sites are very similar in structure to those at the Scots pine study sites. The optical properties of the primary scattering elements within the crown (i.e. the needles) were represented by the reflectance and transmittance measurements of Scots pine needles collected from the study area, and detailed in Chapter 5.

The model also allows the trunk to be modelled, but this was not considered necessary, as in the young trees, the trunk was barely visible within the tree crown or heather understorey. However, the effect of including shoot reflectance was tested. A separate parameter file held the model parameters and canopy structural variables, which were set as detailed in Table 6.2.

The solar zenith angle was set to 45°, which was representative at this latitude. The number of photons was set to 1,000,000 (C. Rowland, pers. comm.). Increasing the number of photons increased the model run time, without any improvement in modelled spetra. Since the number of wavebands used did not greatly affect model run time, the number of wavebands used was 601, or 1 nm intervals over the 400 to 1100 nm wavelength range.

Table 6.2 Model parameters and canopy variables used to constrain the FLIGHT model.

Parameter/variable	Description	Value used
MODE	Mode of operation: forward (f), image (i), or solid object mode (s)	f
ONED_FLAG	Dimension of the model: 3D (0), 1D (1)	0
SOLAR_ZENITH	Source zenith angle (-ve value means diffuse beam only)	45°
SOLAR_AZIMUTH	Source azimuth angle	0
NO_WVBANDS	Number of wavebands simulated	601
NO_PHOTONS	Number of photon paths simulated	1,000,000
TOTAL_LAI	Mean one-sided total foliage area index	Various
FRAC_GRN	Fraction of green leaves in foliage by area	1.0
FRAC_SEN	Fraction of senescent/shoot material in foliage by area	0.0
LAD[1-9]	Leaf angle distribution, giving angle between normal to leaves and vertical, expressed as fraction lying within 10° bins	Spherical
SOILROUGH	Soil roughness index (0 = Lambertian)	0
AER_OPT	Aerosol optical thickness at 555 nm (-ve means direct beam only)	1.0
FRAC_COV	Fraction of ground covered by vegetation (overstorey)	Various
CROWN_SHAPE	Ellipse (e) or cone (c)	(c)
Exy, Ez	Crown radius, Crown height	Various
MIN_HT, MAX_HT	Min. and max. height to first branch	Various

6.4 Results and Discussion

6.4.1 Comparison with Mean Seasonal Reflectance (MSR)

The use of the FLIGHT model was compared with MSR for each plot by recreating as accurately as possible, the structure of the sample plots. This was carried out using the model canopy structural variables of LAI, LAD, fraction of cover, crown shape, crown height, and height of the first branch from the ground; all of which (except for LAD) had been measured within each sample plot. All the plot reflectance data, collected at nadir with the field spectroradiometer, were averaged to give mean plot reflectance spectra, which included any seasonal variation. Inevitably, MSR also included variation from the different illumination conditions and Sun zenith/azimuth angles on each of the field visits. As the MSR for each plot consisted of some 225 spectral scans, it was considered a reasonable summary of plot reflectance. Figure 6.2 illustrates the MSR for each of the sample plots containing pine saplings, together with their respective standard deviations and modelled results.

In general, the modelled spectra fall within the range of field spectral measurements as indicated by the standard deviation curves. A notable exception is the NIR portion of the modelled Plot 5 curve, which falls outside and below the MSR for this plot. The most likely explanation for this discrepancy is that the model fails to account for all the structural detail of the plot; for example, shoot clumping. The modelled NIR is slightly lower than the MSR for plots containing younger regeneration, but slightly greater than the MSR for plots 7 and 8, which contain older, larger saplings.

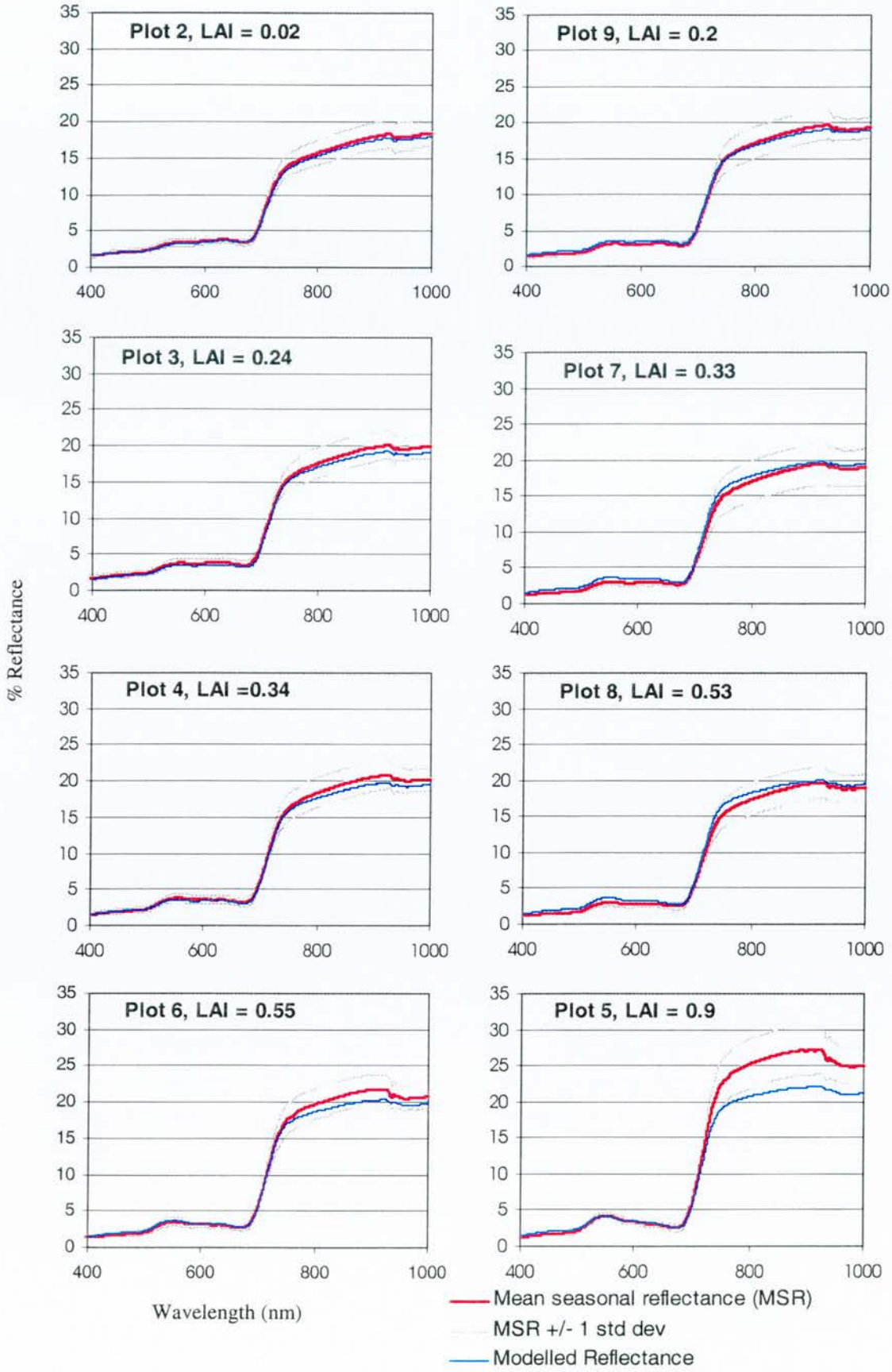

Figure 6.2 Modelled reflectance (FLIGHT) compared with MSR (Mean Seasonal Reflectance) for each plot containing pine saplings.

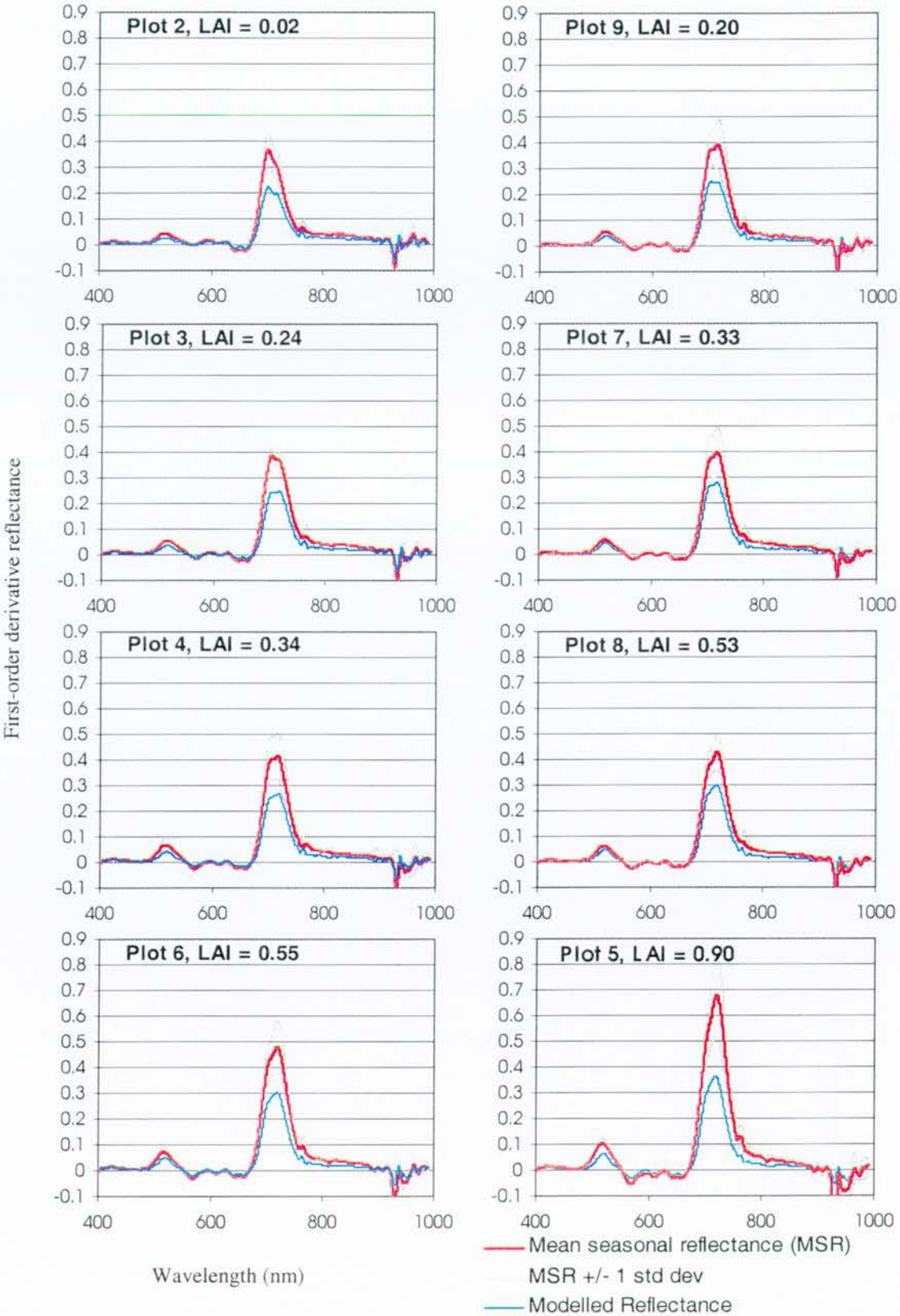

Figure 6.3 First-order derivative modelled reflectance compared with MSR

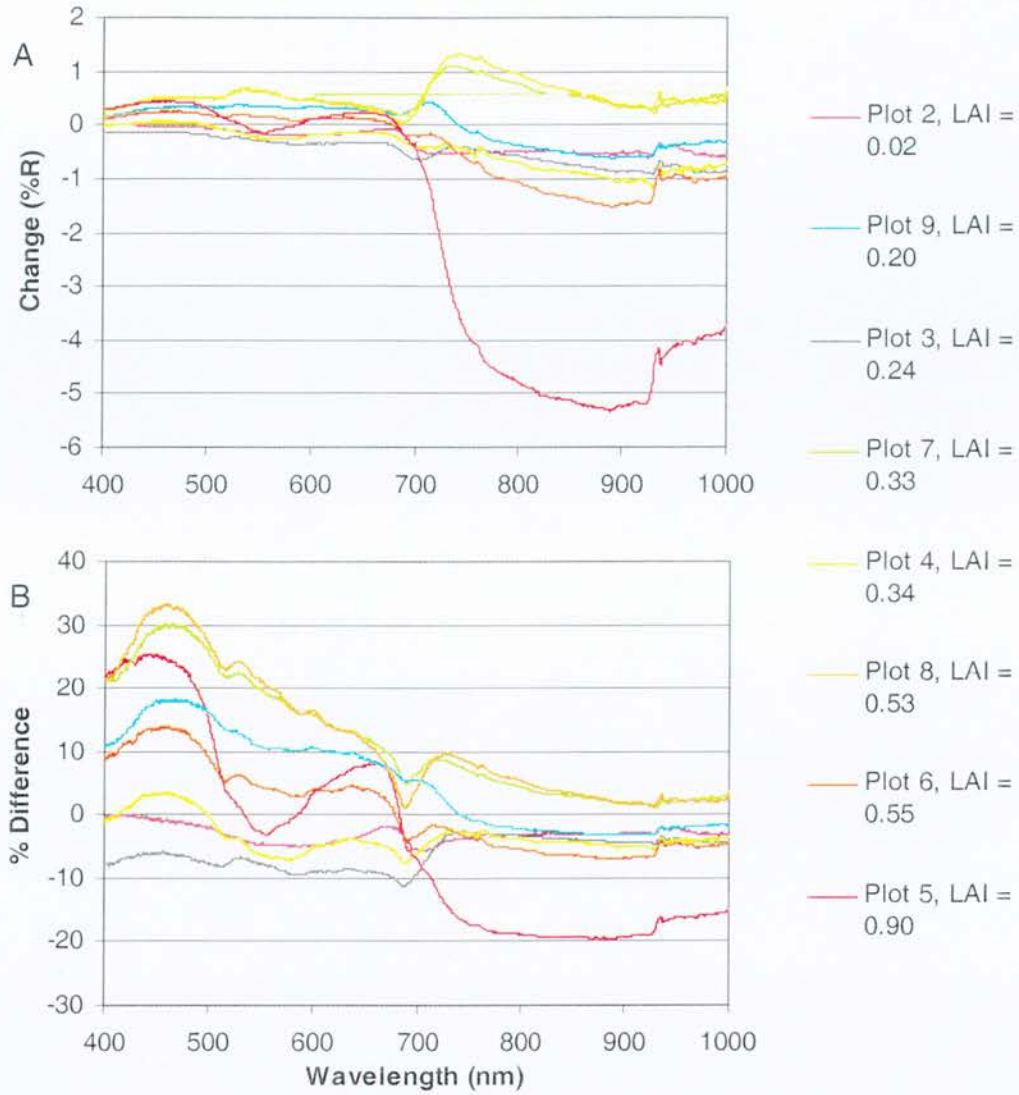

Figure 6.4 Change (%R) (a) and Percentage difference (b) between MSR and Modelled reflectance.

The model also accurately simulates the shape of the MSR plot spectra as illustrated by the derivative modelled and MSR curves in Figure 6.3. In particular, the shape of the red-edge feature (with switching dominance of the shoulder at longer wavelengths with increasing LAI) is also evident in the modelled derivative curves. However, despite the overall concordance in shape, the modelled reflectance curve is clearly slightly flatter at the green and red-edge slopes, as illustrated by the lower derivative peaks.

Figure 6.4 (a) illustrates the change in modelled reflectance from MSR at each wavelength for each plot in absolute percentage reflectance values. The greater modelled reflectance in the NIR for plots 7 and 8, but lower NIR for plot 5 is more clearly apparent than in Figure 6.2. However, Figure 6.4 (b) shows the percentage difference at each wavelength and it is clear that the greatest percentage deviation from the MSR is in fact in the blue wavelength region, particularly for plots 7, 8 and 5. The percentage difference in this wavelength region is much less for plots 2, 3 and 4. This suggests that the deviations are not a consistent error within the model, but may be due to the errors associated with measuring plot structural parameters, or the way these parameters are treated within the model itself.

The model was run to simulate the reflectance of plot 5 again, but including the laboratory-measured shoot and bark spectra (Chapter 5). The correct proportions of shoot and bark material viewable at nadir for each plot were not known, but estimates were made according to values in the literature (e.g. Nilson and Peterson, 1991). Including the laboratory measurements of shoot and bark optical properties did not improve the modelled reflectance of plot 5. The shoot and bark spectra are relatively flat, having the effect of reducing the magnitude of the modelled plot reflectance features, such as the green reflectance peak and red-edge slope. Since the model treats the individual tree crowns as containing a turbid media of random canopy elements, it does not account for the non-random arrangement of shoots within the pine canopy. Shoot and bark optical properties were omitted from further model simulations.

6.4.2 Changing LAI

The effect of changing LAI with a constant percentage cover of pine saplings (PC) was explored using the sapling size measurements of plot 5. Table 6.3 and Figure 6.5 illustrate the results of this analysis on selected wavelengths for both reflectance and derivative modelled spectra. These wavelengths were chosen for their known sensitivity to canopy variables, and from the results obtained in Chapters 3 and 4.

The green reflectance peak (R550) declines after reaching a LAI value of 1.5, whilst the red reflectance trough (R680) decreases consistently with increasing LAI (Figure 6.5 (a)). This negative relationship between red reflectance and LAI has been widely reported in the literature (e.g. Tucker, 1977; Ripple, 1985; Peterson *et al.*, 1987; Spanner *et al.*, 1990). The NIR reflectance (R850) however, increases until LAI 2.0, and then decreases with increasing LAI. This is likely due to the unrealistically high values of LAI contained within the relatively small volume of sapling crown within the plot.

Red-edge position (REP), defined as the wavelength position of the maximum value of the first-order derivative red-edge peak, is shown to be sensitive to increasing LAI (Figure 6.5 (b)). This result has been demonstrated by other workers (e.g. Danson and Plummer, 1955; Lucas *et al.*, 2000), and through modelling studies (e.g. Guyot *et al.*, 1992). As expected, there is a progression in REP to longer wavelengths with increasing LAI, but the wavelength range is relatively small (719 to 723 nm) for a large variation in modelled LAI (0.9 to 5.0), and the REP for LAI 1.5 and 2.0 is the same.

Derivative indices representing the slopes of the green reflectance peak (D520 and D570) are shown to be insensitive to increasing LAI (Figure 6.5 (c)). The derivative value at 703 nm (D703), demonstrates a negative relationship with LAI. DREPmax represents the largest derivative value on the red-edge peak and identifies the REP. DREPmax demonstrates a positive relationship with LAI up to a value of 2.0, but decreases slightly at LAI 3.0 and 5.0.

Table 6.3 The effect of increasing LAI in plot 5 (PC = 0.51)

	MSR	LAI 0.90	LAI 1.5	LAI 2.0	LAI 3.0	LAI 5.0
R550	4.30	4.19	4.19	3.99	3.85	3.53
R680	2.79	2.88	2.71	2.52	2.44	2.23
R850	26.54	21.44	22.93	23.29	22.81	22.65
D520	0.104	0.058	0.062	0.059	0.057	0.053
D570	-0.052	-0.030	-0.033	-0.032	-0.031	-0.029
D703	0.521	0.289	0.292	0.284	0.270	0.253
DREPmax	0.680	0.346	0.380	0.395	0.375	0.382
REP	720	719	721	721	722	723

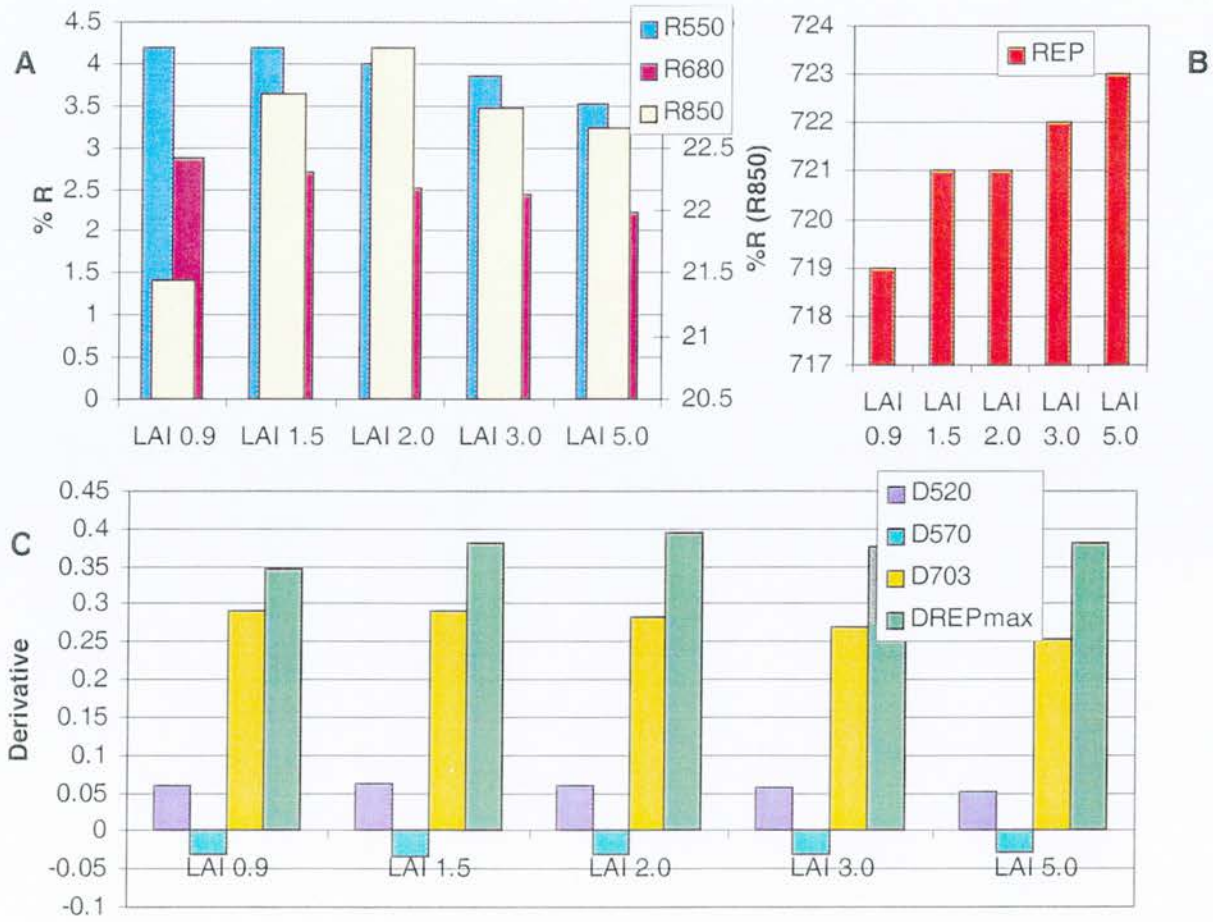

Figure 6.5 Charts to show the modelled values of Reflectance (a), REP (b), and Derivative reflectance (c) for selected wavelengths with increasing LAI.

These results for the two red-edge peak features correspond to the observations made in Chapters 3.0 and 4.0; namely, that the peak at the longer wavelength becomes more dominant with increasing pine sapling amount. The next section details the response of these modelled spectral features to increasing PC, whilst LAI remains constant.

6.4.3 Changing Percentage Cover (PC)

Table 6.4 The effect of increasing PC in plot 5 (LAI = 0.9 and 5.0)

	LAI = 5.0				LAI = 0.9			
	PC = 0.30	PC = 0.51	PC = 0.70	PC = 0.90	PC = 0.30	PC = 0.51	PC = 0.70	PC = 0.90
R550	3.04	3.25	3.95	4.68	3.50	4.21	4.52	5.01
R680	2.20	1.76	1.76	1.85	2.62	2.70	2.67	2.73
R850	19.08	21.57	25.63	30.97	19.37	21.63	22.58	23.32
D520	0.042	0.053	0.070	0.085	0.047	0.623	0.069	0.080
D570	-0.022	-0.032	-0.044	-0.056	-0.022	-0.033	-0.040	-0.047
D703	0.221	0.237	0.281	0.337	0.251	0.299	0.319	0.342
DREPmax	0.302	0.383	0.485	0.611	0.308	0.362	0.393	0.413
REP	721	725	725	725	719	719	719	719

Table 6.4 and Figure 6.6 present the modelled results of increasing PC when LAI is high (5.0) and when it is relatively low (0.9). The NIR (R850) and green (R550) modelled reflectance features illustrated in Figure 6.6 (a) relate positively to increasing PC at both levels of LAI. R550 reflectance is lower at each PC level when LAI is high, which mirrors the result reported in the previous section where R550 declined with increasing LAI.

The positive relation between R850 and PC is much less pronounced when LAI is lower. With this in mind, and since in reality LAI is likely to be low (less than 1.0) for areas of regeneration up to about fifteen years in age, it may be concluded that areas of regeneration with similar LAI, but different PC values, will give similar NIR values. In other words, LAI is the principal control on NIR reflectance for areas of regeneration, with PC of less influence in this wavelength region.

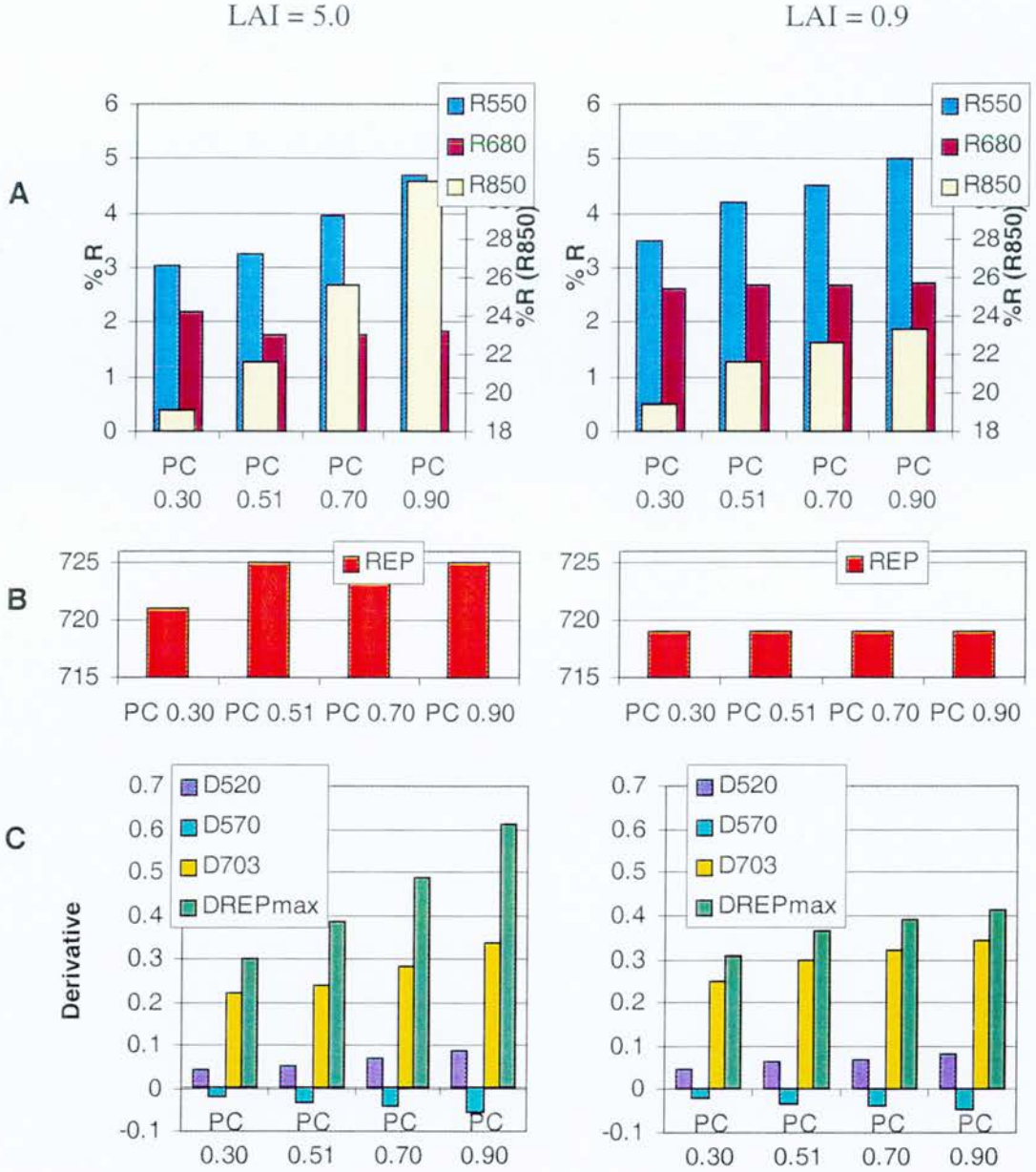

Figure 6.6 Charts to show the modelled values of Reflectance (a), REP (b), and Derivative reflectance (c) for selected wavelengths with increasing Percentage Cover (PC) at LAI = 5.0 and 0.9.

Reflectance at R680 is unaffected by changes in percentage cover, with no relationship evident, particularly when LAI is low. As for R850, these results suggest that the main control on reflectance at 680 nm is LAI. This is likely due to canopy chlorophyll content, which is unaffected by changing PC when LAI is kept constant. However, when LAI is high (5.0) and PC is low (0.30) there is an increase in R680. This may be explained by the greater proportion of illuminated ground

component when PC is low. Gerard and North (1997) have shown through modelling work with FLIGHT that red reflectance is controlled primarily by the illuminated ground component. The results in Figure 6.6 (a) suggest that R550 is more sensitive to PC, whilst R850 and R680 are more sensitive to LAI within areas of regeneration.

Figure 6.6 (b) illustrates the red-edge wavelength position (REP) at each PC level for both levels of LAI. The charts clearly show that REP is unaffected by changes in PC of pine, when LAI is constant. The only exception is when LAI is high (5.0) and PC is very low (0.30), although this is a somewhat unrealistic scenario. The insensitivity of REP to PC has been reported in several other studies (e.g. Ferns *et al.*, 1984 for laboratory leaf measurements; Gong *et al.*, 1992 for pine canopy measurements).

The modelled derivative reflectance values at selected wavelengths are illustrated in Figure 6.6 (c) for each level of PC and both levels of LAI. There is a clear positive relation between all these derivative reflectance values and PC, but as again, the relation is more pronounced and the values are greater at the higher LAI value.

These results have important implications for using reflectance and derivative reflectance at these wavelengths. The REP is clearly more suited to retrieving estimates of LAI since it is insensitive to variations in percentage cover. For semi-natural stands, where percentage cover is highly variable, this is a potentially useful relationship. However, there may be problems in identifying any relationship between REP and LAI due to its narrow wavelength range over a high range of LAI values. As has been shown in Chapters 3 and 4, the range of LAI values in the sample plots was relatively small (0.02 to 0.9) and this may explain the lower correlation found between REP and LAI for the study plots.

Conversely, derivative reflectance values around the green reflectance peak (D520 and D570) are more suited to measuring changes in PC because they are more sensitive to changes in PC than in LAI (compare Figures 6.5 (c) and 6.6 (c)). Derivative reflectance at DREPmax presents a similar case, although it shows a

positive relation to PC and a positive relation to lower values of LAI in particular. The shoulder of the red-edge derivative peak at D703 also demonstrated a greater sensitivity to PC than to the LAI values modelled, although changes in D703 were smaller than for DREPmax.

6.4.4 Changing Tree Size and Stand Density

The previous sections considered the effect of changing the plot structural parameters of LAI and percentage cover (PC) on modelled reflectance. However, a further source of variation occurs within regions of regeneration with respect to tree size. For any given area of regeneration, it may be possible to observe the same LAI and PC values, but different tree size and crown density. The model was used to explore the changes in reflectance and derivative reflectance for selected wavelengths by changing tree height, whilst keeping all other model parameters constant. This was carried out for three stand densities; one where a 5 x 5 m plot contained a single large tree, one containing ten smaller trees, and one with 100 trees (Figure 6.7 and Table 6.5).

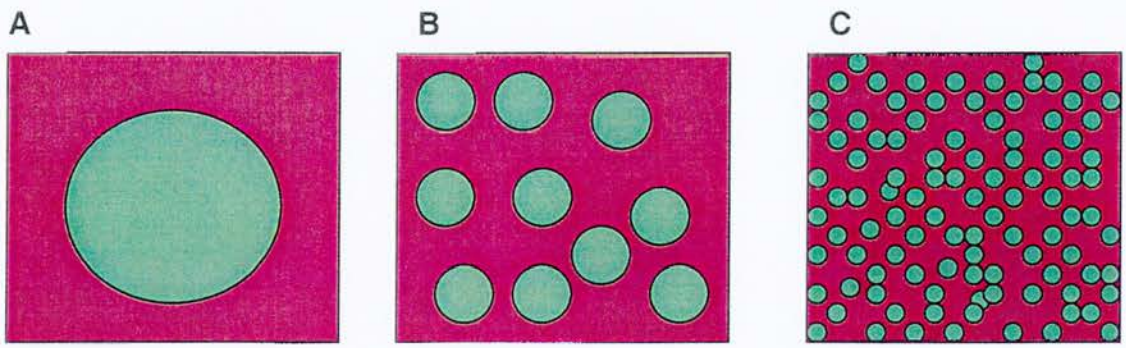

Figure 6.7 Plan view of three model scenarios to test the effect of changing tree height/crown density; one single large tree (a) ten smaller trees (b) and 100 trees (c).

Table 6.5 Model parameters for three scenarios to test the effect of changing tree height/crown density.

	A	B	C
No. Trees	1	10	100
Total LAI	3.0	3.0	3.0
Fraction of cover	0.5	0.5	0.5
Crown radius (m)	2.00	0.63	0.20
Crown height (m)	10, 9, 8, 7, 6, 5, 4, 3	3, 2.5, 2, 1.5, 1	1.3, 1.1, 0.9, 0.7, 0.5
Solar Zenith	45°	45°	45°

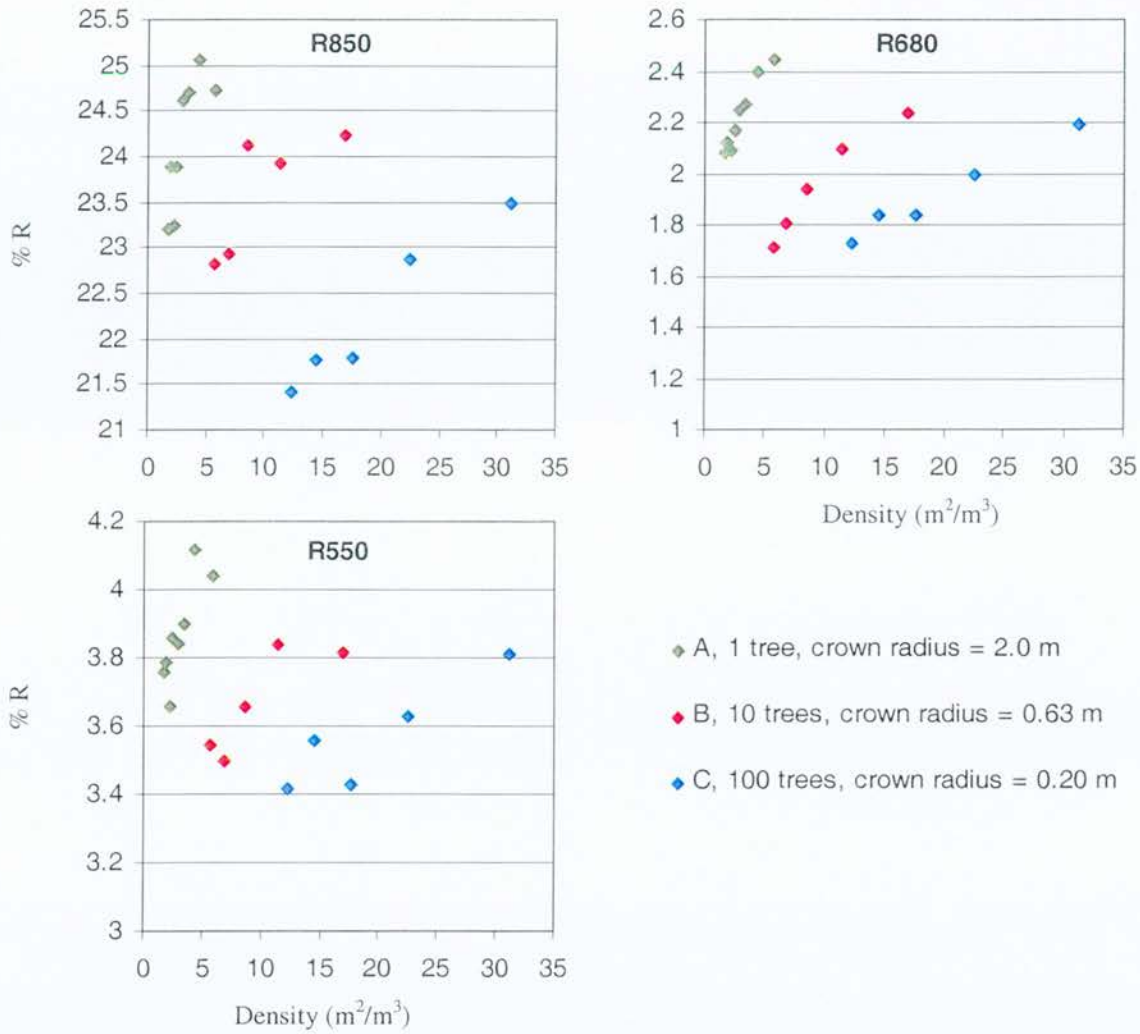

Figure 6.8 Modelled reflectance values at three wavelengths for three model scenarios with changing crown height/crown density.

As crown height was reduced, crown density increased within each model scenario, so that LAI and percentage cover remained constant. Crown density is plotted against percentage reflectance for each model scenario in Figure 6.8. In general, modelled reflectance increases with increasing crown density (or as crown height is reduced) for R850, R680 and R550. However, the dynamic range of reflectance values over the different levels of crown density is relatively small.

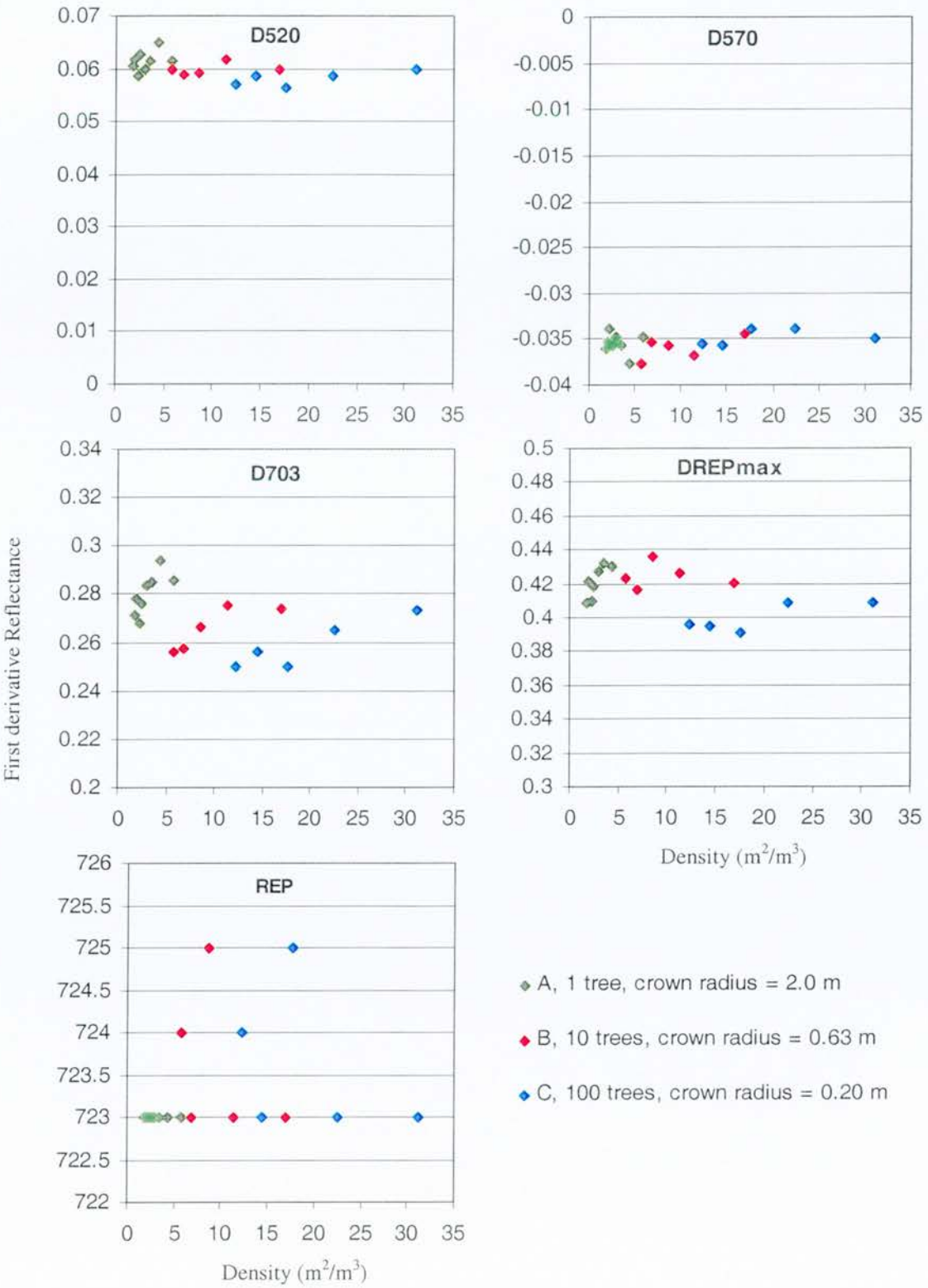

Figure 6.9 Modelled derivative reflectance values at three wavelengths for three model scenarios with changing crown height/crown density.

The modelled derivative reflectance values at selected wavelengths and the REP for each model scenario are illustrated in Figure 6.9. A general trend of increasing derivative reflectance with increasing crown density (or decreasing crown height) is evident for D703, and is very similar to the trend observed for the reflectance values in Figure 6.9. The influence of increasing crown density on D520, D570 and DREPmax is much less clear, partly due to the small values involved. Given the more significant influence on reflectance at these wavelengths of LAI and percentage cover it may be concluded that changes in crown height and crown density do not significantly affect modelled reflectance.

For the single tree scenario (A), REP is unaffected by crown height when LAI and percentage cover are constant. However, there is some movement in REP as the crown height is reduced for the multiple tree scenarios (B and C). This is likely due to the changing proportion of sunlit crown viewed as the degree of mutual crown shading alters with crown height. Clearly, the proportion of sunlit crown viewed is sensitive not just to changes in crown height, but also to viewing angle and Solar zenith angle.

These modelled data suggest that the influence of crown height and crown density is small in comparison to changes in LAI or percentage cover, particularly for the derivative spectra. The implication of this result is that spectral indices involving reflectance at these wavelengths will not distinguish between stages of regeneration or tree size in areas of similar LAI or percentage cover.

6.4 Conclusions

A hybrid geometric-optical model (FLIGHT) was used to simulate the mean seasonal reflectance (MSR) of the sample plots containing Scots pine saplings. The dimensions of the plots and the mean dimensions of the saplings within each plot were geometrically simulated by the model. Reflectance at nadir was calculated by tracing the path of photons cast into the simulated scene, using a Monte Carlo simulation procedure.

Modelled reflectance was within the variation of MSR across the wavelength range, except for the NIR in plot 5. Modelled reflectance was lower than MSR for plot 5, which was attributed to the fact that the model does not account for within-canopy scale structure, such as shoot clumping and the arrangement of needles on shoots. Inclusion of laboratory-measured shoot and bark optical properties did not improve the correspondence between modelled reflectance and sample plot MSR. The shape of the MSR spectra, however, as described by the first-order derivative, was well represented by the modelled first-derivative spectra. In particular, the switching of the dominant red-edge peak from shorter to longer wavelength with increasing percentage cover and LAI was well represented by the model. However, it is important to note that the same 9-point smoothing function was used for the MSR spectra as for the modelled spectra, which no doubt contributed to the similarities in shape. Rollin and Milton (1998) point out that different levels of smoothing can alter not only the exact wavelength of a spectral feature, but also its peak correlation with a canopy biophysical variable.

The model was used to explore the effect of changing LAI and percentage cover (PC) for scenarios using the sapling statistics for plot 5. LAI was varied between 0.9 and 5.0 and the reflectance (R550, R680, R850) and first-derivative reflectance (D520, D570, D703, DREPmax) values compared. These wavelengths were chosen for their known sensitivity to canopy variables, and from the results obtained in

Chapter 3 and 4. Red reflectance (R680) and red-edge derivative reflectance (D680) both declined with increasing LAI, whilst NIR reflectance (R850) increased with LAI only up to a LAI of 2.0. This value of LAI is likely to be near the maximum value obtained for regions of regeneration, with values as high as 5.0 remaining theoretical, and more realistic for older plantation forestry. DREPmax, the maximum value on the derivative red-edge peak, which is used to define red-edge position (REP), also increased with LAI, until reaching 2.0.

Derivative reflectance at D520 and D570, which represent the ascending and descending limbs of the green reflectance peak, were unresponsive to changing LAI, but related positively with PC. Modelled values at D520 and D570 were the only wavelengths that demonstrated a relation with PC, but none with LAI. This suggests that they could be utilised as indices for determining PC, irrespective of LAI. Results in chapter 4 however, indicated that correlations between LAI and PC at these wavelengths was equally strong, making them at odds with the model results. The modelled results serve to highlight the close correlation between these two canopy variables, which may have contributed to the similar correlation coefficients between them for measured derivative reflectance at these wavelengths.

The red-edge derivative features, DREPmax and D703 were also related positively to PC. There were clear positive relationships for PC with R850 and R550, but not with red reflectance at R680. Both R850 and R550 increased with increasing PC, but R680 was unchanging, particularly at the lower level of LAI.

REP was shown by the modelled results to be sensitive to LAI, but insensitive to changes in PC. REP may therefore be a candidate index for LAI retrieval within regions of regeneration. However, an important limitation to its application is the narrow range of wavelengths over which the shift in REP was observed. Since LAI within regions of regeneration will always be relatively low (less than 1.0) the narrow range of REP values for different areas of regeneration may not allow these regions to be reliably distinguished. However, the modelled results do support the conclusions made in Chapters 3 and 4; that the derivative red-edge peak values could

be used to measure changes in pine sapling amount. For example, the positive relation of DREPmax with LAI, and the negative relation of D703 with LAI is demonstrated by the model. This supports the logic of combining the two derivative values as an index for LAI (i.e. the ratio D719/D703). The main caveat with such an approach might be in obtaining image data with a suitably high radiometric resolution to allow these two features to be adequately distinguished.

In a similar way, the rationale for combining NIR reflectance with the reflectance at the red-wavelength trough is confirmed by the model since the NIR (R850) increases with LAI, whilst the R680 reflectance decreases with LAI. It is this mechanism of opposing relationships with increasing canopy structure and chlorophyll content that generate the high correlation between LAI and the NDVI and SR indices observed in Chapter 4.

The model was also used to explore the effects of changing tree height (and, by definition, crown density) by keeping LAI, crown radius and PC constant. In this way, the question of whether reflectance of one large tree could be distinguished from reflectance of many smaller trees, when LAI and PC are the same, was investigated. Results showed that the effect of changing crown height/density was much smaller than the effects of changing LAI or PC for the modelled data. Derivative reflectance at D520 and D570 were particularly insensitive to changes in crown height for all three levels of stand density (one single tree, 10 trees and 100 trees). For R850, R550, R680, D703 and DREPmax all showed a weak trend of increasing reflectance with increasing crown density (decreasing crown height). Since the model is better at representing stand-scale, rather than crown-scale structure, these trends can be explained in relation to changes in the proportion of shaded crowns and crown geometry within each modelled scenario.

REP was insensitive to decreasing crown height for the single tree scenario, but moved to longer wavelengths and back again for the scenarios with multiple crowns. It was suggested that the changing proportions of sunlit and shaded crowns

contributed to these wavelength shifts in REP and that changes in Sun/viewing-angle geometry would have a similar effect.

6.5 References

ASNER, G. P. and WESSMAN, C. A., 1997, Scaling PAR absorption from the leaf to landscape level in spatially heterogeneous ecosystems. *Ecological Modelling*, **103**, 81-97.

ASRAR, G., MYNENI, R. B. and KANEMASU, E. T., 1989, Estimation of plant-canopy attributes from spectral reflectance measurements. In *Theory and Applications of Optical Remote Sensing* edited by G. Asrar (New York: Wiley & Sons), p253.

BADHWAR, G. D., VERHOEF, W., and BUNNIK, J. J., 1985, Comparative study of Suits and SAIL canopy reflectance models. *Remote Sensing of Environment*, **17**, 179-195.

BRUNIQUEL-PINEL, V. and GASTELLU-ETCHEGORRY, J. P., 1998, Sensitivity of texture of high resolution images of forest to biophysical and acquisition parameters. *Remote Sensing of Environment*, **65**, 61-85.

CESCATTI, A., 1997, Modelling the radiative transfer in discontinuous canopies of asymmetric crowns. I. Model structure and algorithms. *Ecological Modelling*, **101**, 263-274.

CHEN, J., 1983, The recipricocity relation for reflection and transmission of radiation by crops and other plane-parallel scattering media. *Remote Sensing of Environment*, **13**, 475-486.

CHEN, J., 1985, Kubelka-Munk equations in vector-matrix forms and the solution for bidirectional vegetative canopy reflectance. *Applied optics*, **24**, 376-382.

CHEN, J. M., and LEBLANC, S. G., 1997, A four-scale bidirectional reflectance model based on canopy architecture. *IEEE Transactions on Geoscience and Remote Sensing* GE-**35**: 1316-1337.

DANSON, F. M., and PLUMMER, S. E., 1995, Red-edge response to forest leaf area index. *International Journal of Remote Sensing*, **16**, 183-188.

COOPS, N., and CULVENOR, D., 2000, Utilizing local variance of simulated high spatial resolution imagery to predict spatial pattern of forest stands. *Remote Sensing of Environment*, **71**, 248-260.

GERARD, F. F. and NORTH, P. R. J., 1997, Analyzing the effect of structural variability and canopy gaps on forest BRDF using a geometric-optical model. *Remote Sensing of Environment*, **62**, 46-62.

GOEL, N. S., 1988, Models of vegetation canopy reflectance and their use in estimation of biophysical parameters from reflectance data. *Remote Sensing Reviews*, **4**, 1-212.

GOEL, N. S., and DEERING, D. W., 1985, Evaluation of a canopy reflectance model for LAI estimation through its inversion. *IEEE Transactions on Geoscience and Remote Sensing*, **23**, 674-684.

GOEL, N. S. and GRIER, T., 1988, Estimation of canopy parameters for in homogeneous vegetation canopies from reflectance data: III. TRIM: A model for radiative transfer in heterogeneous three-dimensional canopies. *Remote Sensing of Environment*, **25**, 255-293.

GOEL, N. S. and THOMPSON, R. L., 2000, A snapshot of canopy reflectance models and a universal model for the radiation regime. *Remote Sensing Reviews*, **18**, 197-225.

GOVAERTS, Y. M., and VERSTRAETE, M. M., 1998, Raytran: A Monte Carlo ray tracing model to compute light scattering in three-dimensional heterogeneous media. *IEEE Transactions on Geoscience and Remote Sensing* **36**: 493-505.

GOWARD, S. N., and HUEMMRICH, K. F., 1992, Vegetation canopy PAR absorptance and the Normalized Difference Vegetation Index: An assessment using the SAIL model. *Remote Sensing of Environment* **39**: 119-140.

GUYOT, G., BARET, F., and JACQUEMOND, S., 1992, Imaging spectroscopy for vegetation studies. In F. Toselli and J. Bodechtel (eds), *Imaging Spectroscopy: Fundamentals and Prospective Applications*, (Dordrecht: Kluwer Academic Publications), 145-165.

HALL, F. G., TOWNSHEND, J. R., and ENGMAN, E. T., 1995, Status of remote sensing algorithms for estimation of land surface state parameters. *Remote Sensing of Environment* **51**: 138-156.

HUEMMRICH, K. F., and GOWARD, S. N., 1997, Vegetation canopy PAR absorptance and NDVI: An assessment for ten tree species with the SAIL model. *Remote Sensing of Environment* **61**: 254-269.

HOLMGREN, P. and THURESSON, T., 1998, Satellite remote sensing for forestry planning - A review. *Scandinavian Journal of Forest Research*, **13**, 90-110.

JACQUEMOUD, S., BARET, F., ANDRIEU, B., DANSON, F. M., AND JAGGARD, K., 1995, Extraction of vegetation biophysical parameters by inversion of the PROSPECT + SAIL models on Sugar Beet canopy reflectance data. Application to TM and AVIRIS Sensors. *Remote Sensing of Environment* **52**: 163-172.

JUPP, D. L. B., WALKER, J., and PENRIDGE, L. K., 1986, Interpretation of vegetation structure in Landsat MSS Imagery: a case study in distributed semi-arid Eucalypt woodland. *Journal of Environmental Management*, **23**, 35-57.

KELOMÄKI, S. and KURTTIO, O., 1991, A model for the structural development of a Scots pine crown based on modular growth. *Forest Ecology and Management* **43**: 103-123.

KELOMÄKI, S. and STRANDMAN, H., 1995, A model for the structural growth of young Scots pine crowns based on light interception by shoots. *Ecological Modelling* **80**: 237-250.

KIMES, D. S., and KIRCHNER, J. A., 1982, Radiative transfer model for heterogeneous 3-D scenes. *Applied Optics* **21**, 4119-4129.

KIMES, D. S., NORMAN, J. M., and WALTHALL, C. L., 1985, Modeling the radiant transfers of sparse vegetation canopies. *IEEE Transactions on Geoscience and Remote Sensing* **23**: 695-704.

KUUSK, A., 1994, A multispectral canopy reflectance model. *Remote Sensing of Environment* **50**: 75-82.

KUUSK, A., 1995, A fast, invertible canopy reflectance model. *Remote Sensing of Environment* **51**: 342-350.

LEWIS, P., 1999, Three-dimensional plant modelling for remote sensing simulation studies using the Botanical Plant Modelling system. *Agronomie*, **19**, 185-210.

LI, X. and STRAHLER, A.H., 1985, Geometrical-optical modeling of a conifer forest canopy. *IEEE Transactions on Geoscience and Remote Sensing*, **23**, 705-721.

LI, X. and STRAHLER, A.H., 1986, Geometrical-optical bidirectional modeling of a coniferous forest canopy. *IEEE Transactions on Geoscience and Remote Sensing*, **24**, 906-919.

LI, X. and STRAHLER, A.H., 1992, Geometrical-optical bidirectional reflectance modeling of the discrete-crown vegetation canopy: Effect of crown shape and mutual shadowing. *IEEE Transactions on Geoscience and Remote Sensing*, **30**, 276-292.

LI, X., STRAHLER, A.H., and WOODCOCK, C. E., 1995, A hybrid geometric optical-radiative transfer approach for modeling albedo and directional reflectnace of discontinuous canopies. *IEEE Transactions on Geoscience and Remote Sensing*, **33**, 466-480.

LI, Z. Q., CIHLAR, J., ZHENG, X. N., MOREAU, L., and LY, H., 1996, The bidirectional effects of AVHRR measurements over boreal regions. *IEEE Transactions on Geoscience and Remote Sensing*, **34**, 1308-1322.

LUCAS, N. S., CURRAN, P. J., PLUMMER, S. E., and DANSON, F. M., 2000, Estimating the stem carbon production of a coniferous forest using an ecosystem simulation model driven by the remotely sensed red edge. *International Journal of Remote Sensing*, **21**, 619-631.

MILLER, J. R., WHITE, H. P., CHEN, J. M., PEDDLE, D. R., McDERMID, G., FOURNIER, R. A., SHEPHERD, P., RUBINSTEIN, I., FREEMANTLE, J., SOFFER, R., and LeDREW, E., 1997, Seasonal change in understory reflectance of boreal forests and influence on canopy vegetation indices. *Journal of Geophysical Research*, **102**, No. D24, 29,475-29482.

MYNENI, R. B., MAGGION, S., IAQUINTA, J., PRIVETTE, J. L., GOBRON, N., PINTY, B., KIMES, D. S., VERSTRAETE, M. M., and WILLIAMS, D. L., 1995, Optical remote sensing of vegetation: modeling, caveats, and algorithms. *Remote Sensing of Environment* **51**: 169-188.

NI, W., WOODCOCK, C. E., and JUPP, D. L. B., 1999, Variance in bidirectional reflectance over discontinuous plant canopies. *Remote Sensing of Environment* **69**: 1-15.

NILSON, T. and PETERSON, U., 1991, A forest canopy reflectance model and a test case. *Remote Sensing of Environment* **37**: 131-142.

NORMAN, J. M. and WELLES, J. M., 1983, Radiative transfer in an array of canopies. *Agronomy Journal* **75**, 481-488.

NORMAN, J. M., WELLES, J. M., and WALTER, E. A., 1985, Contrasts among bidirectional reflectances of leaves, canopies, and soils. *IEEE Transactions on Geoscience and Remote Sensing*, **23**, 659-668.

NORTH, P. R. J., 1996, Three-dimensional forest light interaction model using a Monte Carlo method. *IEEE Transactions on Geoscience and Remote Sensing*, **34**, 946-956.

PETERSON, D. L., SPANNER, M. A., RUNNING, S. W., and TEUBER, K. B., 1987, Relationship of Thematic Mapper simulator data to leaf area index of temperate coniferous forest. *Remote Sensing of Environment* **22**, 323-341.

PINTY, B., VERSTRAETE, M. M., and DICKINSON, R. E., 1990, A physical model of the bidirectional reflectance of vegetation canopies. 2. Inversion and validation. *Journal of Geophysical Research*, **95**, 11,767-11,775.

RIPPLE, W. J., 1985, Asymptotic reflectance characteristics of grass vegetation. *Photgrammetric Engineering and Remote Sensing*, **38**, 1209-1212.

ROLLIN, E. M., and MILTON, E. J., 1998, Processing of high spectral resolution reflectance data for the retrieval of canopy water content information. *Remote Sensing of Environment* **65**, 86-92.

ROSS, J., and MARSHAK, A., 1988, Calculation of canopy bidirectional reflectance using the Monte Carlo method. *Remote Sensing of Environment*, **24**, 213-225.

ROSS, J., and MARSHAK, A., 1989, The influence of leaf orientation and the specular component of leaf reflectance on the canopy bidirectional reflectance. *Remote Sensing of Environment*, **27**, 251-260.

ROWLAND, C. S., DANSON, F. M., NORTH, P. R. J., and PLUMMER, S. E., 1998, Modelling the effect of heterogeneous canopy structure. *Proceedings of the 24th Annual Conference of the Remote Sensing Society, The University of Greewich, 9-11 September* (Nottingham: Remote Sensing Society), 649-655.

THOMAS, R. W. and HUGGETT, R. J., 1980, *Modelling in Geography; A Mathematical Approach* (London: Harper & Row), pp 3-10.

THOMPSON, R. L., and GOEL, N. S., 1998, Two models for rapidly calculating bidirectional reflectance of complex vegetation scenes: Photon spread (PS) and statistical photon spread (SPS) model. *Remote Sensing Reviews*, **16**, 157-207.

SPANNER, M. A., PIERCE, L. L., PETERSON, D. L., and RUNNING, S. W., 1990, Remote sensing of temperate coniferous forest leaf area index: The influence of canopy closure, understorey vegetation and background reflectance. *International Journal of Remote Sensing*, **11**, 95-111.

ST-ONGE, B. A. and CAVAYAS, F., 1995, Estimating forest stand structure from high resolution imagery using the directional variogram. *International Journal of Remote Sensing*, **16**, 1999-2021.

STRAHLER, A. H., WOODCOCK, C. E., and SMITH, J. A., 1986, On the nature of models in Remote Sensing. *Remote Sensing of Environment*, **20** 121-139.

SUITS, G. H., 1972, The calculation of the directional reflectance of vegetative canopy. *Remote Sensing of Environment*, **2** 175-182.

TUCKER, C. J., 1977, Asymptotic nature of grass canopy reflectance. *Applied Optics*, **16**, 1151-1157.

VERHOEF, W, 1984, Light scattering by leaf layers with application to canopy reflectance modeling: The SAIL model. *Remote Sensing of Environment*, **16**, 125-141.

VERHOEF, W., and BUNNIK, N. J. J., 1981, Influence of crop geometry on multispectral reflectance determined by the use of canopy reflectance models. *Proceedings of the International Colloquium on Signatures of Remotely Sensed Objects, Avignon, France, 8-11 September*, 273-290.

WALTHALL, C. L., 1997, A study of reflectance anisotropy and canopy structure using a simple empirical model. *Remote Sensing of Environment*, **61**, 118-128.

WALTHALL, C. L., NORMAN, J. M., WELLES, J. M., CAMPBELL, G., and BLAD, B. L., 1985, Simple equation to approximate the bidirectional reflectance from vegetative canopies and bare soil surfaces. *Applied optics*, **24**, 383-387.

WOODCOCK, C. E., COLLINS, J. B., JAKABHAZY, V. D., LI, X., MACOMBER, S. A., and WU, Y., 1997, Inversion of the Li-Strahler canopy reflectance model for mapping forest structure. *IEEE Transactions on Geoscience and Remote Sensing*, **35**, 405-414.

WULDER, M. A., LEDREW, E. F., FRANKLIN, S. E., and LAVIGNE, M. B., 1998, Aerial image texture information in the estimation of northern deciduous and mixed wood forest Leaf Area Index (LAI). *Remote Sensing of Environment*, **64**, 64-76.

7.0 SPATIAL ANALYSIS

7.1 Introduction

A changing landscape may be detected within remotely sensed images as a simultaneous spectral and spatial modification of the measured signal, for any system used. It follows that the changing physical properties of elements within the landscape will be detected as changing spectral and spatial detail within the whole image. Thus far, the present study has paid particular attention to the spectral properties of pine regeneration. This chapter seeks to explore the utility of the spatial dimension of images in relation to different stages of pine regeneration and their physical characteristics.

The exploration of the spatial dimension of remotely sensed images has been relatively recent and has been considered from a number of viewpoints. Initially, studies focussed on the importance of appropriate scales of observation (e.g. Woodcock and Strahler, 1987; Atkinson and Danson, 1988; Curran, 1988). This has remained an important theme of research since varying the spatial resolution of the sampling system (i.e. effective pixel or ground resolution) will vary the scale of landscape information being studied (Marceau *et al.*, 1994a). More recent studies have concentrated on studying the spatial arrangement of particular landscape types through the emerging discipline of landscape ecology (e.g. Rossi *et al.*, 1992; Simmons *et al.*, 1992; Lobo *et al.*, 1998; Aubry and Debouzie, 2000). Significantly, in terms of the present study, the spatial structure of images has been investigated recently in relation to forest landscapes (e.g. Cohen *et al.*, 1990; St-Onge and Cavayas 1995, 1997; Wulder *et al.*, 1998; Treitz and Howarth, 2000). The common theme throughout this research has been the application of the semivariogram as a means of quantifying and describing spatial structure and as the basis of a set of spatial analysis tools collectively termed geostatistics. The way in which

geostatistics have been applied to remote sensing is reviewed by Curran and Atkinson (1998).

This chapter begins by describing the semivariogram and its theoretical basis as a measure of texture. Previous work is reviewed in the context of forest research in particular. A summary of the important points from the literature relating to the spatial analysis of Scots pine regeneration is followed by a clear statement of the aims of the present study. The methods and data sources used are described, followed by a presentation of the results. Finally, the results are discussed and critically evaluated in detail and in the context of other research.

7.2 The Semivariogram

Central to the use of geostatistics in image analysis is the semivariogram (Curran, 1988), a second order statistic which provides a means of displaying and quantifying spatial continuity, or image texture. The semivariogram is constructed by first pairing all values of a spatially continuous variable (Z), at a location (**x**), separated by a vector (**h**). Each pair is then plotted as a scatterplot with the value of Z(**x**) on the x-axis and the value of Z(**x**+**h**) on the y-axis. For any spatially continuous variable one would expect that when **h** is smaller, pairs of values would plot close to the x = y line on the scatterplot. As the separation distance increases, the similarity between pairs decreases, and the points on the scatterplot appear less dense and further away from the x = y line. A set of scatterplots can be drawn, each with a different separation distance. The closeness of a set of paired values to this diagonal line is conventionally described by the correlation or covariance. However, in geostatistics the moment of inertia is used, given by half of the expected squared difference between the x and y coordinates of each pair of points on the scatterplot (Oliver and Webster, 1991):

$$\gamma(\mathbf{h}) = \frac{1}{2}\mathbf{E}\left[\{Z(\mathbf{x}) - Z(\mathbf{x}+\mathbf{h})\}^2\right],$$

where Z(**x**) and Z(**x** + **h**) are the reflectance values at two locations, **h** is the lag between them and E is the expectation. However, since we are sampling from the population of reflectance values (z) at a particular position ($\mathbf{x}_i$) and comparing a number of finite observations, $M(\mathbf{h})$, the equation should be rewritten as an estimate:

$$\hat{\gamma}(\mathbf{h}) = \frac{1}{2\mathrm{M}(\mathbf{h})}\sum_{i=1}^{\mathrm{M}(\mathbf{h})}\{\mathrm{z}(\mathbf{x}_i) - \mathrm{z}(\mathbf{x}_i+\mathbf{h})\}^2$$

and the resulting semivariogram is called the experimental semivariogram.

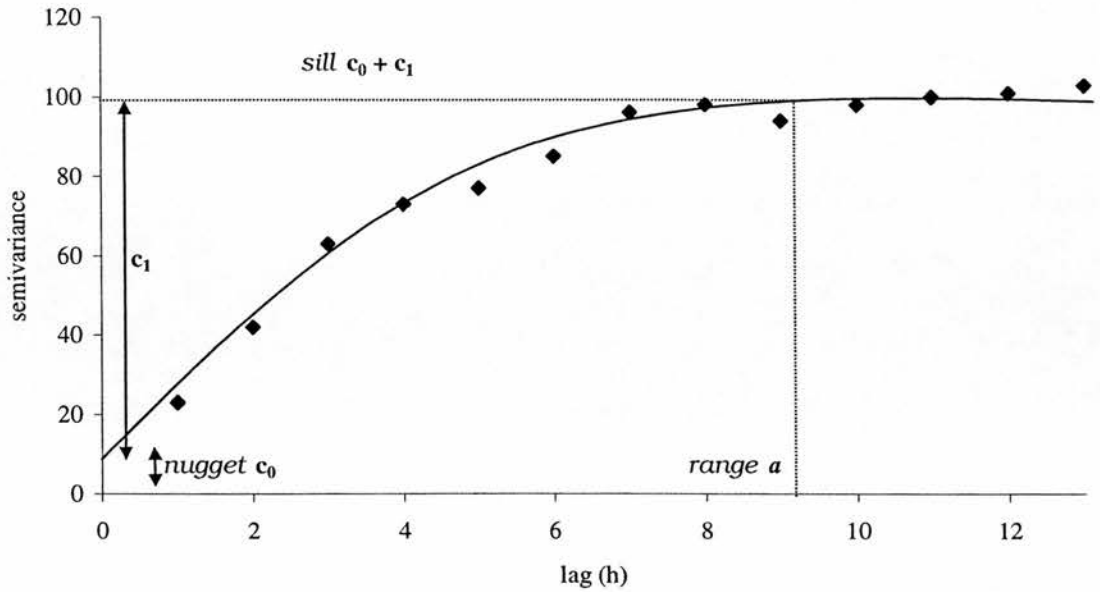

Figure 7.1 An example of an experimental semivariogram and its parameters. Each point represents an averaged value from a separate h-scatterplot.

The moment of inertia (or semivariance) for each scatterplot can be plotted against **h** to produce the semivariogram (Figure 7.1). In practice, the h-scatterplots are not usually drawn and it is common to go directly to the semivariogram to describe spatial continuity (Isaaks and Srivastava, 1989), which is what will be presented in this chapter.

Since **h** is a vector having direction as well as distance, semivariograms are often constructed for a variety of directions to allow spatial continuity to be summarized in different directions. This is required when considering anisotropy or pattern in the spatial structure of the variable's surface. The separation distance (or lag **h**) between sample points can also be reduced to produce a more detailed semivariogram.

Figure 7.1 illustrates some of the main features used to describe the semivariogram and Table 7.1 summarizes the terms and symbols used to describe the semivariogram. As the separation distance increases, so does the semivariance value. This increase levels off once points become a certain distance apart; at this distance, points further away cease to be more different from points closer together. The distance at which the semivariogram levels off is called the range (**a**). The sill (**c**) is simply the semivariogram value at which the range is reached and is theoretically equivalent to the variance of the sample (Burrough, 1995, p230). Since the value of a sample location is the same when compared with itself, or $\gamma(\mathbf{h}) = 0$ when $\mathbf{h} = 0$, the semivariogram would be expected to pass through the origin. However, due to sampling variability and random noise there may be a nugget effect (Figure 7.1) where $\gamma(\mathbf{h}) > 0$ when $\mathbf{h} = 0$. This effect is less likely for regularly gridded data such as pixel values within an image. One of the reasons why geostatistical techniques work well in remote sensing studies is that a remotely sensed image provides a level of sampling not generally attainable in the field. In the next section, the application of the semivariogram to remote sensing research is explored, paying particular attention to image texture for forested environments.

Table 7.1 The terms and symbols used in the semivariogram and their definitions (from Curran and Atkinson, 1998).

Term	Symbol	Definition
Support	**y**	Areas, shape and orientation of space represented by each
Lag	**h**	Distance (and direction in two or more dimensions) between sampling pairs
Sill	**s**	Maximum value of $\gamma(\mathbf{h})$ model
Range	**a**	Point on x-axis where $\gamma(\mathbf{h})$ model reaches maximum. Places closer than the range are related statistically, places further apart are not.
Nugget variance	$\mathbf{c_0}$	Point where model intercepts the y-axis. Represents a component of the variation that is spatially uncorrelated
Structured variance	**c**	Sill minus nugget variance
Gradient	**m**	The slope for $\gamma(\mathbf{h})$ model with a linear component

7.3 The semivariogram, image texture and forests

7.3.1 Literature Review

The issue of scale in remote sensing has been a primary concern that led to the use geostatistics. The scale of an image prescribes the type of information attainable from it, and is therefore of fundamental importance. Woodcock and Strahler (1987) studied the influences that landscape structure plays in selecting the appropriate spatial resolution for a particular application of remote sensing. Their work formally demonstrated that spatial structure, or texture, is a function of the dimensions of the ground elements. Texture within images is therefore dependent on the degree of contrast between image scene elements. For pine forest for example, contrast is governed by the relative amounts of sunlit background, shaded background and sunlit and shaded crowns.

The degree of contrast, or image variance, is intimately linked to the spatial resolution of the image. This is because a pixel size smaller than the sunlit or shaded elements will allow them to be individually resolved, resulting in a highly textured image. This case is commonly referred to as high (H)-resolution (Woodcock and Strahler, 1987) since the pixel size is high resolution with respect to the scene elements of interest. The converse is low (L)-resolution, in which the pixel size is larger than the average size of scene elements, leading to an overall image-variance reduction and a more homogeneous, less textured image. The H- and L-resolution shorthand is often used to refer to the resolution of the image in relation to the scene elements of interest, such as trees in a forest environment.

In relation to forest environments, several studies have employed geostatistics to describe their spatial structure. The importance of the relationship between sampling size (pixel size) and the size of scene elements and landscape structure motivated several workers to consider the idea of optimal spatial resolution. One approach has been to use local variance, which is the variance between neighbouring pixel's DNs

(Hyppänen, 1996). Woodcock and Strahler (1987) used local variance/resolution graphs produced from increasingly coarse resolution images to estimate optimal resolutions for a variety of landscape types. The inflection point on the graph was interpreted as the pixel size that minimizes the autocorrelation between neighbouring pixels, or maximum variance between neighbouring pixels. Marceau *et al.* (1994b) also used local variance in airborne MEIS-II data to explore the idea of optimal resolution for varying forest types. They suggested the use of digitized aerial photographs as a means to identify optimal spatial resolutions for different tree species using this approach.

However, as Atkinson and Danson (1988) point out, the local variance method requires an averaging of (usually) nine pixels, so that the value of neighbouring pixels is not being directly considered. A better statistic, these authors argue, is the semivariance at lag 1, or when the semivariance is maximised between neighbouring pixels. This may be found by progressively degrading the image to coarser resolutions and determining at which resolution $\gamma(\mathbf{h}=1)$ is maximum. This can be done by either regularizing a semivariogram from a high resolution image, or by calculating semivariograms for a progressively degraded high resolution image (Atkinson and Danson, 1988; Atkinson, 1997). The easiest way to envisage the idea of $\gamma(\mathbf{h}=1)$ at maximum is to consider two extremes. In the first, the pixel size is much smaller than the scene elements (trees, for example), so that there is a high level of spatial dependence in the pixel values (the H-resolution case). This may be useful for relating the semivariogram to crown diameter. The second extreme case, is where the pixel size is much larger than the average tree size (the L-resolution case), so that much of the information is lost due to averaging (mixed pixels). The second case may be more suited to characterising compartment reflectance. The optimal resolution as defined by Atkinson and Danson (1988), is a compromise between the two, so that both averaging and spatial information are optimised. Like Woodcock *et al.* (1988), Atkinson and Danson also highlighted the close relationship between the range parameter of the semivariogram and the diameter of the elements within a scene. For a more open canopy, the range may be related more to the spacing between crowns than to the diameter of the crowns themselves. The

relationship between the range and crown size is therefore likely to hold only for continuous stands, since gaps in the canopy reveal a larger scale of dependence than that between individual tree crowns (Lévesque and King, 1999).

Cohen *et al.* (1990) investigated the utility of semivariograms for assessing conifer canopy structure using digitised aerial videography (1m), as well as SPOT HRV (10m) and Landsat TM (30m) data. They found the range of the semivariogram for young stands to be about 5m for the aerial imagery. These stands have a continuous canopy layer of uniform trees and the range was thought to be approximately equal to the tree crown diameter. The sills were reported as relating to contrast in the imagery (i.e. variance), which relates to percent canopy cover and layering in the stands. This relationship is assumed to hold because the variance of measured reflectance from a uniform canopy will be lower than from one that is multilayered. Treitz and Howarth (2000) came to a similar conclusion when reporting that the sill increased with density of understorey for experimental semivariograms calculated from high resolution CASI imagery of Canadian boreal forest.

Another feature of variable canopy layers was a waveform in the semivariogram at longer lags, due to the regular pattern of change in variance over a non-uniform canopy. Cohen *et al.* (1990) also found that variability decreased as lower spatial resolution SPOT and TM images were used. At the same time, the ability to distinguish between different cover types also reduced, as the semivariograms became flatter and the sills lower and closer together. It was concluded that semivariograms computed from transects with a 1m lag described spatial pattern most clearly, but matrix-semivariograms (omnidirectional) related better to crown size. Most importantly however, the study suggested that the variance as described by the sill variance value, perhaps in combination with the range value as indices, could be used to discriminate between stands of varying structure.

McGwire *et al.* (1993) investigated the use of semivariograms to describe the relationship between a linear regression model linking TM NDVI of savannah woodland with percentage cover. They also investigated the effect of varying pixel

size. Autocorrelation distances (the semivariogram range) were estimated from NDVI using a spherical model fitted to the experimental point semivariograms. Like Cohen *et al.* (1990), McGwire *et al.* (1993) found that trends in percentage cover became apparent as resolution decreased. However, trends were not detected for resolutions lower than the overall gradient of change (i.e. resolutions that only include one tree). This is because the variance is reduced at coarser resolutions through not being dependent on the presence/absence of trees. McGwire *et al.* (1993) showed that spatial structure and the resolution of a particular sensor are important considerations when applying remote sensing as a sampling scheme for monitoring or mapping purposes.

Hyppänen (1996) takes a similar view, and highlighted the importance of describing spatial autocorrelation before undertaking inventory using remote sensing for a particular purpose. This is because there is an optimal pixel size for different land use classes. Hyppänen used digitized aerial photography to compute semivariograms for pine forest in Finland. The study area contained homogeneous classes of Scots pine and Norway spruce of different age classes. The youngest Scots pine compartments (tree height 1.3 – 7m) were found to have a range (limit of dependence) at 4m with a corresponding crown diameter of 2.1m. The relationship between range and crown diameter, and the sill and vertical layering was similar to that found by Cohen *et al.* (1990).

Another approach to investigating the possible links between the semivariogram as a measure of image texture and forest structure is to model the forest environment of interest. The first to do this were Woodcock *et al.* (1988) who created a coniferous forest scene consisting of four elements: illuminated tree crown and background, and shaded tree crown and background. They also considered the effect of varying 'acquistion parameters' (*sensu* Bruniquel-Pinel and Gastellu Etchegorry, 1998) which include sun-sensor geometry and spatial resolution. Woodcock *et al.* (1988) stressed that spatial variation in images can be predicted based on scene and sensor parameters. St-Onge and Cavayas (1995) looked at the influence of tree size and density on the spatial structure of high resolution images of forest stands. They used

a three-dimensional canopy model and a geometrical-optical model to create artificial images and analysed the influence of one parameter at a time and of spatial resolution, on image texture. Applying these results to 0.36m airborne imagery, they obtained good correspondence between semivariogram parameters and tree density and crown diameter. St-Onge and Cavayas (1995) also highlighted the differing results obtained for directional semivariogram in the parallel and perpendicular directions in relation to the Sun azimuth angle. In more open canopies, longer shadows in the parallel direction produced longer range estimates, whilst range estimates from the semivariogram in the perpendicular direction more closely approximate mean crown size.

Bruniquel-Pinel and Gastellu-Etchegorry (1998) used the discrete anisotropic radiative transfer model (DART) to generate artificial images of forest plantation. Results from their study suggest a 'complex dependency of variogram characteristics (range, sill, amplitude of oscillations) on biophysical and acquisition parameters'. It was concluded that tree crown diameter was the most influential biophysical parameter on semivariogram characteristics.

7.3.2 Summary and statement of aims

There is much evidence in the literature to show that geostatistics can be a useful tool for describing and quantifying the spatial dimension of images. Curran and Atkinson (1998) go so far as to refer to the 'powerful synergy between geostatistics and remote sensing'. Previous work has stressed the importance of scale in both remote sensing and geostatistics and scale has often been explicitly investigated, either in relation to the support size used to sample a scene, or by varying the scene elements themselves in modelling studies. There is also a synergy between landscape ecology and remote sensing since a major problem in ecological research is in determining the scale at which to attempt to measure change (Simmons *et al.*, 1992). Geostatistics would therefore seem to provide a much-needed link between remote sensing and landscape research; entirely appropriate to the remote sensing of Scots pine regeneration. Previous work has illustrated the importance of applying geostatistical methods at a scale appropriate to the scene elements under investigation. Provided the landscape is not completely homogeneous, there will be spatial correlation at all levels of the landscape spatial hierarchy. The semivariogram may have a similar form over a range of scales (support sizes) but that does not mean that the semivariogram characteristics relate to the objects under study. From the literature, particularly the work by Woodcock and Strahler (1987), it is clearly necessary to have a support size smaller than, or equal to, the average tree crown width (H-resolution with respect to the individual trees). A support size larger than the individual trees should provide information on the spatial structure of a group of trees, or regeneration clump (H-resolution with respect to a clump, but L-resolution with respect to individual trees).

Interpretation of the semivariogram characteristics has been clearly related to the dimension of individual elements within a scene, as well as to overall structure. The range parameter (autocorrelation distance) may relate to crown size but can be confused by sun and sensor geometry. The influence of shadow within forest scenes is a particularly important source of variation that is dependent on sun and sensor geometry. The range parameter may also relate less well to crown size in more open

canopies, which has implications for less dense regions of regeneration. The sill parameter is related to overall image variance and should increase as percentage cover decreases, since the background vegetation will introduce more variation. Most previous work has been carried out on regular plantation forestry and how far these relationships carry as the canopy becomes more random (or natural) has not been tested.

These observations lead to a number of questions, which can be formulated into a number of hypotheses with associated aims for the research:

Research hypotheses

1. An image of the study area providing suitable contrast between tree crown and background, and H-resolution with respect to the trees, or tree clumps, will allow the spatial structure of natural regeneration to be described through the semivariogram characteristics.
2. The range parameter will relate to tree crown size, whilst the sill will allow separation of regeneration stages due to changing scene variance. Scene variance will be driven by the degree of shadow and by tree density.
3. Different stages of regeneration will have different optimal spatial resolutions for characterising spatial structure.

Research aims

1. To acquire imagery at a suitable spatial and spectral resolution to distinguish between different stages of regeneration using measures of spatial structure.
2. To compute both directional and omnidirectional semivariograms for a variety of regeneration stages.
3. To consider the effect of changing spatial resolution on the semivariogram, and propose an optimal spatial resolution for monitoring natural pine regeneration.
4. To compare semivariogram characteristics with measured structural variables; crown diameter, crown spacing, tree density and percentage cover.

7.4 Methods

7.4.1 Data Selection

In order to describe the spatial dependence within relatively small areas of regeneration, themselves containing relatively small individual trees, it was considered necessary to use an image source providing a very fine resolution. Initially, airborne *casi* data were considered, since it would provide the opportunity to carry out the spatial analysis on an image of NDVI, or some other index selective for the pine canopy. However, the nominal ground resolution of 2 m x 2 m achieved would clearly be L-resolution with respect to saplings in most regeneration stages, and would therefore likely not adequately describe spatial dependence. It has been suggested that such L-resolution data cannot fully capture forest stand parameters (Jupp *et al.*, 1988). Additionally, there was a large uncertainty in the registration of the *casi* imagery, particularly in relation to the small areas of interest.

However, as Holopainen and Wang (1998) point out, the 'recent rapid development of digital technology has offered the possibility of using high-resolution digital or digitized aerial photographs for numerical interpretation of forest parameters'. The visual interpretation of aerial photos has been used for many years for the purpose of forest management (Cohen *et al.*, 1996), but the conversion of such analogue data into digital form is now relatively inexpensive. Data storage issues have also largely been resolved, even at the desktop PC level.

Digitized colour infrared aerial photography has been used in several landscape spatial analysis studies, such as to analyse the spatial complexity of a landscape (Weiler and Stow, 1991), identifying spatial patterns in natural landscapes (Lacaze *et al.*, 1994), or for separation of forest stands (Holopainen and Wang, 1998; Wang *et al.*, 1998). In the present study, true colour aerial photography was used, with the green band brightness DN values principally used as the variable of interest. This was considered to be a valid approach since the green band DN values associated with sunlit sapling crowns contrasted strongly with those of shaded and background

scene elements (P. Lewis, pers. comm. 1999). Furthermore, the principal background components are bare soil and heather, which have much higher blue and red-band brightness values respectively, in comparison to pine crown. The strong contrast between the major scene elements was expected to strengthen the characterisation of regeneration spatial dependence through the semivariogram.

7.4.2 Data acquisition

Aerial Photography

The true-colour aerial photographs were acquired on 18 May 1999, between 08:35 and 09:35 GMT (09:35 and 10:35 BST). The platform used was the NERC Airborne Remote Sensing Facility Piper PA31 350 Chieftain twin-engined aircraft. Details of the camera are given in Table 7.2 below.

Table 7.2 Details of the NERC-ARSF camera

CAMERA MAKE	WILD RC 10
LENS TYPE	UNIVERSAL AVIOGON II (RC 10)
FOCAL LENGTH	153.438 mm
APERTURE	F4
FILM TYPE	AGFAPAN 25 PROFESSIONAL

The photographs were taken at an altitude of 1470 m and runs were in a North to South orientation over Rothiemurcus and Northeast to Southwest over Inshriach. The Sun's altitude angle at 10:00 BST was 38.5° and the solar azimuth angle was 116.5° from North. There was no cloud cover, with excellent visibility and wind-still at ground level, although turbulence was reported at the flying altitude. The nominal scale of the photographs was 1:6,500.

Digital capture

Initially, the photographs were scanned on an Epson GT-1200 A3 colour flatbed scanner at a nominal resolution of 1200dpi. However, it was later realized that the true maximum resolution of the scanner was 800dpi, and higher resolutions were obtained only through interpolation. Since younger pine regeneration clumps consist of saplings of less than 1m in diameter, it was considered necessary to achieve as

high a resolution as possible in order to characterise the spatial dependence adequately. In order to digitally capture the photographs at a higher resolution a Zeiss 80mm lens was used in conjunction with a digital camera back giving a resolution of 7,000 x 7,000 pixels.

The digital camera was manoeuvred and adapted with extension tubes to capture images at 1200dpi of about two thirds of the photograph area. The resulting pixel size (ground resolution) was 0.14m. Details of the digital camera and capture set-up are given in Table 7.3 below.

Table 7.3 Details of the digital camera used to digitize the air photos

Digital camera back	Phase One PowerPhase 6x6 Uninterpolated files 42bit internal colour depth, 14 bit per colour precision
Resolution	7,000 x 7,000 pixels
Capture area	56mm x 56mm frame
Capture software	Phase One version 3.1.1 for Power Mac
Camera body	Hasselblad 501CM
Lens	Zeiss 80mm (plus extensions for close-up work)
Capture	Power Mac g4 400Mhz/Apple21" Studio Monitor with ColorSync
Lighting	2 Photon Beard 'Highlight' studio lights: cool running, flicker free, balanced fluorescent lamps.

Orthorectification

Initially, the data processing and analysis was carried out using unrectified scanned aerial photographs. Whilst the results of this work largely met the initial aim to distinguish between the spatial dependence of different stages of regeneration, it did not adequately consider the orientation of the photographs relative to the Sun's position. The shadow component of the scenes varied in orientation making the directional semivariograms difficult to compare. The lack of orthorectification also introduced an element of spatial uncertainty, since any distortion remained throughout the analysis.

In order to orthorectify the photographs to a high level of precision, differential GPS data were obtained for points within each of the Rothiemurcus and Inshriach study areas. Two Ashtech Z-12 GPS receivers with antenna (0.132m radii) were obtained on loan from the NERC Geophysical Equipment Pool. One receiver (base station) was placed on Ord Ban hill, less than 4km from each study area. The antenna was attached to a triangulation point on the hill, with a precisely known National Grid reference and WGS84 latitude and longitude.

The base station recorded its own position at an epoch interval of 20 seconds during both days that measurements at each study site were recorded. The second receiver served as the rover (remote) station with the same epoch interval, recording measurements for 20 minutes at each point. Ground Control Points (GCPs) were selected from colour photocopies of the air photographs taken into the field and were features that were easily visible, but at the same time as small as possible. Features chosen included boulders and small patches of vegetation or bare soil notable for their high contrast with their surroundings. Care was taken not to select features in hollows or under tree canopies, which would obstruct or reduce the sky-view. Care was also taken to orientate the antenna in the same direction as the base station (magnetic North was used), and the antenna height above each feature was also recorded to include in the post-processing. The rover antenna was placed on a general-purpose adjustable tripod and carefully levelled using a tribach. The rover

station was operated in static mode requiring longer logging times at each position than when using kinematic mode, but giving results that are more accurate. Kinematic mode also requires the known point, or base station to be nearby, which was not practicable in this case. All GCPs were logged with between 8 and 11 satellites locked.

Tree data

Data were also acquired on the physical properties of the areas of regeneration to be sampled from the digitized photographs. Crown spacing and crown diameter were measured in the field by sampling along random transects and taking a mean value. For regions sampled containing mature trees, these measurements were estimated from the digitized photographs after orthorectification. Percentage cover of the sunlit heather, sunlit tree crown, bare soil and shadow within each area sampled was calculated from a supervised classification, which is discussed further in the results section.

7.4.3 Data processing

Differential GPS

The GCP data were downloaded from the receivers and processed using the Ashtech PRISM™ software supplied with the instruments. Table 7.4 summarizes the results together with residual mean square errors for each calculation.

Table 7.4 The results of the differential GPS software PRISM™

Rothiemurcus Day 328						
Station	Lat.	Long.	NG East	NG North	Ortho ht.	RMS (m)
BASE	57.15419946	3.83373398	289168.976	808529.692	428.2	
ROT1	57.16489854	3.77024667	293041.2111	809609.4875	285.0	0.126
ROT2	57.16207988	3.77047132	293019.4786	809296.093	295.8	0.004
ROT3	57.16150645	3.77778562	292575.5011	809243.7195	284.6	0.013
ROT4	57.15817422	3.77313438	292847.1304	808865.5515	283.4	0.010
ROT5	57.15692799	3.76992166	293037.8308	808721.826	293.7	0.011
ROT6	57.15644681	3.76317259	293444.6345	808657.7149	306.8	0.008
ROT7	57.15932771	3.76406686	293398.8448	808979.762	304.7	0.011
ROT8	57.16311775	3.76400438	293413.5383	809401.4818	293.2	0.010

Inshriach Day 329						
Station	Lat.	Long.	NG East	NG North	Ortho ht.	RMS (m)
BASE	57.15419946	3.83373398	289168.976	808529.692	428.2	
INS1	57.13720797	3.83795985	288863.7061	806635.9662	270.2	0.005
INS2	57.13357707	3.84093665	288672.6644	806236.7128	281.6	0.006
INS3	57.13077681	3.85296511	287936.262	805944.8036	292.7	0.006
INS4	57.12803198	3.84761988	288251.4899	805630.5214	277.5	0.011
INS5	57.12867462	3.8382743	288819.077	805686.7974	293.4	0.007
INS6	57.13171442	3.83438346	289063.6715	806018.6822	289.3	0.004
INS7	57.13813691	3.83058078	289313.0036	806727.3482	278.6	0.003

Orthorectification

Files from the digital camera capture were not used in the orthorectification because the viewing area required to obtain maximum resolution did not allow all fiducials to be included within the image. The file sizes of the digital camera files were also half as big again as the scanner files, making them less manageable within the software.

Orthorectification was carried out on the scanned airphotographs using ERDAS IMAGINE OrthoBASE™ software, which is dedicated for the purpose. Data input included the camera focal length, average flying height, principal point offset, lens distortion parameters and corner fiducial coordinates (calibration data supplied by NERC-ARSF). Four consecutive photographs covered the area of interest at Inshriach and three for Rothiemurcus with a typical overlap of 70 - 80% for consecutive photographs. Once the fiducial marks had been measured, their positions were carefully adjusted so that the global RMS error for the orientation solution did not exceed 0.3 pixels and was typically less than 0.1 pixels. The RMS error in this case reflects the degree of correspondence between the calibrated fiducial mark positions and the measured fiducial mark positions. The GCPs calculated from the GPS measurements were registered on each photograph.

The software then performs a tie point procedure using an image correlation technique for identifying corresponding image positions of ground points and taking their respective images measurements. It was found that this automatic procedure often produced many tie points for certain areas and few for others, particularly for areas of mature forest. Tie points were added manually for these areas to provide a more even spread across the overlap area of the images, as well as adjusting the coefficient limit for the correlation and the search window size. Up to 200 tie points were established for each image. At this stage each photograph was referenced on an XY coordinate system, so an aerial triangulation was used for defining the mathematical relationship between the images and the ground in 3D. This resulted in X, Y and Z coordinates being assigned to all the tie points in the desired coordinate system. Again, RMS error values were reported in order to assess the accuracy of

the triangulation procedure. Finally, orthorectification was performed which removed the scale variation and geometric errors inherent in the imagery caused by sensor orientation and topographic relief displacement. The Digital Elevation Model (DEM) required for orthorectification was obtained by repeating the tie point and triangulation process to generate hundreds of reference points. The X, Y and Z coordinates from these points were extracted to a data file and then used to create an elevation surface within ERDAS IMAGINE™. Finally, each image was resampled to 0.5m using the nearest neighbour method.

Sample sub-scene collection

Following the orthorectification of the scanned images and the higher resolution digital camera image capture, regions were selected from the photographs to represent a range of forest types, including different stages of regeneration. Details of the land cover types collected are detailed in Table 7.5.

Table 7.5 The land-cover types selected for sub-scene sampling

Land-cover type/description	Filename	Spatial pattern	No. of samples*
Young Plantation	YP	Rows	1
Old Growth	OG	Clumpy	3
Dark heather background only	DH	Smooth	3
Young regeneration, high density	HD	Smooth	3
Young regeneration, low-med. density with light coloured heather background	LD	Clumpy/speckled	3
Young regeneration, medium density, with dark coloured heather background	MD	Clumpy	3
Older regeneration	OR	Clumpy	3
Older regeneration 1	OR1	Clumpy	3

*A sample is a 20 x 20m sub-scene image extracted from each land-cover region; see text for full explanation and Figures 7.2 and 7.3.

The young plantation (YP) sample (ten years), was selected from a plantation adjacent to the Inshriach study site and was chosen as a control sample because of its regular spatial pattern and relatively uniform individual tree size. In particular, it was expected that the stripy pattern of the regular rows would result in periodicity within the directional semivariograms. All the other samples were taken from semi-natural growth, ranging from young regeneration to mature old growth Scots pine. Another source of variation, apart from age and density, was in the background vegetation. Although almost exclusively heather, it was noted that on drier knolls the heather is sparser, resulting in a much lighter coloured background. In order to compare the effect of these background variations in colour, regions of regeneration with dark and light (dense and thin) heather cover were selected. The sparser heather cover appears lighter on the photographs because of both the reflective woody stems and the lichen *Cladonia impexa*, which is more abundant on the drier knolls. Images from the digital camera were extracted for each land-cover type and registered to the orthorectified images, using a pixel matching procedure.

For each of the semi-natural growth land-cover types, three sub-scene sample images were randomly located and extracted in order to account for some of the variation within each type. The size of these sub-scene sample images was restricted by both the total number of pixels that represented a reasonable computing time for the semivariograms and, by one that would fit within the area of each land-cover type. A sub-scene sample image of approximately 20 x 20 m contained 20,736 pixels from the 0.14m digital camera images. The digital camera images were resampled to lower resolutions in order to compare the effect of changing scale on the computed semivariograms. The highest resolution remained at 0.14m since this was the highest achievable resolution from the digital camera images, followed by 0.2m, 0.5m and 1m. In summary, 7 semi-natural land-cover types were identified, each being sampled 3 times at 4 different scales. In addition a relatively regularly spaced young plantation was sampled once at 5 different scales, so that a total of 89 sample sub-scenes were extracted for spatial analysis using the semivariogram. A summary of the image data used for the spatial analysis is presented in Figure 7.2 and 7.3 at the end of this section.

Geostatistical Analysis

Each of the 89 sample sub-scene image files were converted to ASCI format and edited to the correct format for the UNIX based GSLIB software (Deutsch and Journel, 1998). Each input file contained five variables; OS National Grid coordinates in the X and Y planes, brightness values for the red, green and blue image data layers. All three data layers were included since it took no more computer resource than when running the software for green DN alone. The output files were manipulated by changing the details within a parameter file. These parameters include the type of output required (e.g. semivariogram, correlogram, madogram and other such functions), together with pixel size (for directional output), lag distance, number of lags and directional details for directional semivariograms. Directional semivariograms were computed in four directions; 0° (South to North), 90° (W to E), 45° (SW to NE), 135° (NW to SE).

The output files were imported into Microsoft EXCEL™ in order to construct the experimental semivariograms for visual interpretation. Visual interpretation included noting the overall form of the semivariogram, which includes the classic spherical bounded form (Figure 7.1), or an unbounded form where there is spatial dependence, but no range is reached over the distance measured. Other forms include periodic semivariograms which have a regular or irregular wave form, or a flat semivariogram indicating no spatial dependency in the data (data are randomly distributed) and all the sill is nugget variance.

When the semivariogram is to be used for spatial interpolation using methods such as kriging, it is usual to fit a model to the semivariogram curve and the range and sill parameters are derived as model parameters. In the present study, range and sill estimates are based on 'an eyeball estimate of curve form' (Franklin and McDermid, 1993). This was thought to be no more precise than the model fitting procedure since there is subjectivity both in the choice of model and in its fitting.

7.4.4 Summary of Methods

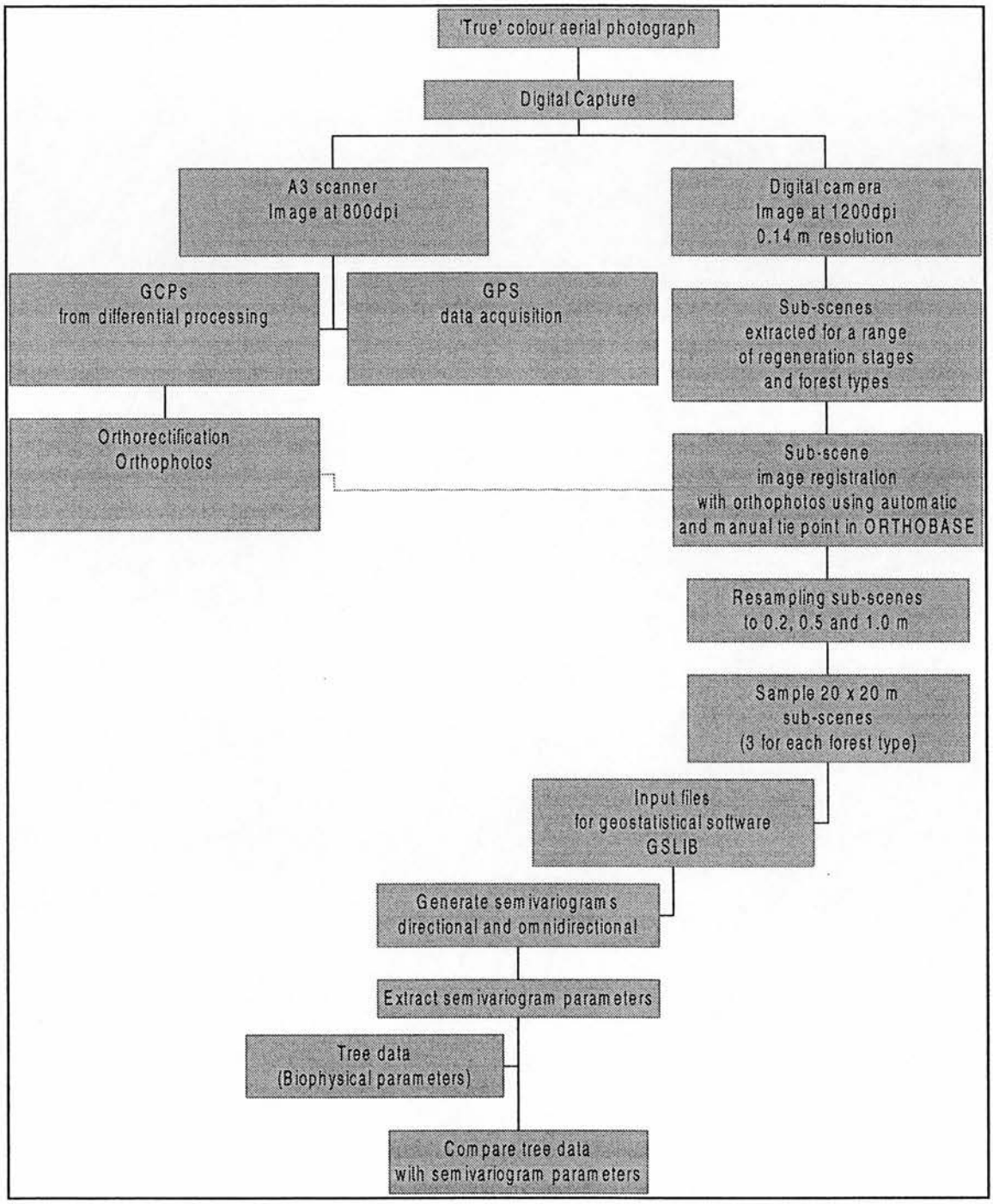

Figure 7.2 Summary of Methods

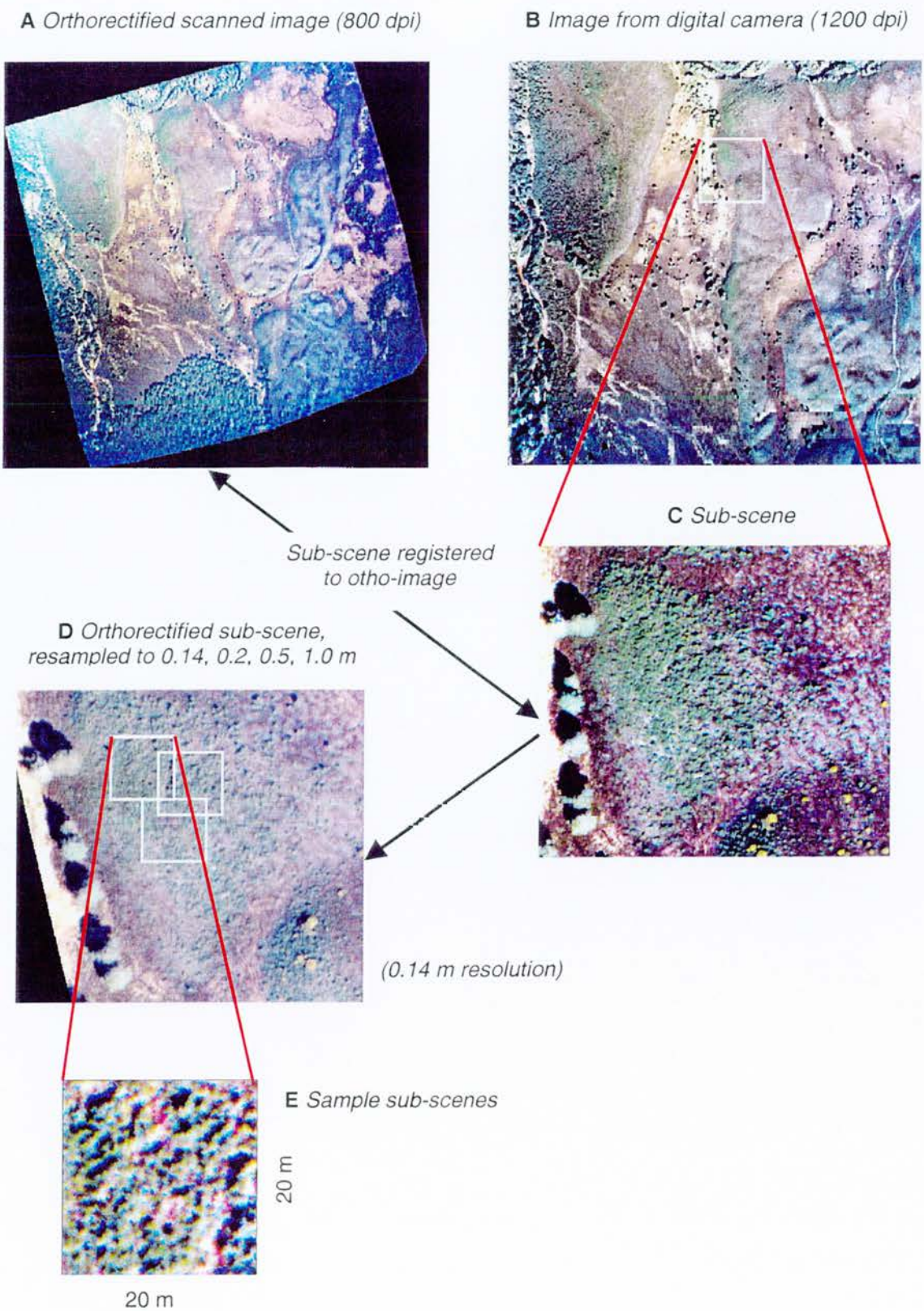

Figure 7.3 Summary of the image data used for the spatial analysis

7.5 Results

This section presents the results of the data acquisition and processing detailed in the previous section. Firstly, the physical data relating to the canopy structure within each sample area are presented. Secondly, the results from the geostatistical analysis are detailed, together with examples of some of the experimental semivariograms calculated. Finally, the relationships between the biophysical and semivariogram parameters are explored.

7.5.1 The Biophysical Data

Table 7.6 presents the biophysical data for each sample sub-scene. The Young Plantation (YP) was deliberately selected for its more regular spatial pattern. Sample YP serves as a useful test of the ability of the semivariogram calculated on the green band DN to relate to the regular canopy structure. The biophysical parameters presented in Table 7.6 are therefore also the yardstick by which all other samples are compared. The greatest contrast is found between the High Density young regeneration (HD) and YP, particularly for the number of individuals and tree density. Samples HD a, b and c have about 500 individuals packed into the 20 x 20m sample square giving a density of around 13,000 ha^{-1}, compared with just 96 individuals and 2,400 ha^{-1} in sample YP. The high density of natural regeneration is often observed ocurring on disturbed ground or on top of freely drained knolls where Scots pine seedlings are able to out-compete faster growing grasses and herb species. The effect is a tightly packed, uniform canopy, which is only about 1 m high in the case of HD. This canopy structure gives a smooth texture within the image compared to canopies with lower percentage cover and density. The smoother texture is a result of a reduced shadow and background component within canopies of greater crown closure, or percentage cover. A smooth texture is also observed for the Dark Heather (DH) sample, which was sampled in order to consider the spatial properties of the understorey vegetation cover.

As the naturally regenerating Scots pine develops, the canopy structure may become more clumpy due to the more evident variations in growth between individuals and between groups of individuals. Samples of Lower Density (LD) and Medium Density (MD) demonstrate this appearance and have notably fewer individuals and lower density. Samples LD and MD are most similar to YP in respect of individual crown parameters (Table 7.6), but the spatial structure is random as opposed to systematic.

Older Regeneration samples (OR and OR1) also have a clumpy appearance, but contain many fewer individuals than younger regeneration samples. The extreme cases of this trend are the Old Growth (OG) samples, which have the fewest individuals and much lower densities.

The image characteristics of green band DN mean and variance are included within Table 7.6 to illustrate the effect of the various biophysical differences between samples on these statistics. Similar trends were evident in the blue and red bands. Most notable is the greater image variance in green band DN for the samples with older trees. This is due to the greater degree of shadow and mutual shading of tree crowns in older natural stands. This idea is supported by the fact that the smoother HD samples have the lowest image variance values. The exact proportions of sunlit and shaded elements within each sample canopy are considered in more detail in the next section.

Table 7.6 Sample sub-scene biophysical and image characteristics

Description	Sample	Spatial pattern	Count (No.of trees)	Density (ha^{-1})	% cover	Mean crown Ø (m)	Mean spacing (m)	Mean height (m)	Green DN mean	Green DN variance
Young plantation	YP	Rows	96	2400	44	1.2	0.95	1.40	107	1750
Old growth	OG	Clumpy	10, 8, 8 *	250, 196, 197	40, 49, 57	4.4, 4.9, 5.4	1.9, 2.0, 1.9	8.20	93, 103, 102	2255, 2619, 2049
Dark heather	DH	Smooth	na	na	na	na	na	na	na	na
Young regen.	HD	Smooth	536, 524, 448	13400, 13100, 11250	55, 55, 59	0.39, 0.48, 0.5	0.22, 0.22, 0.18	1.00	131, 132, 139	327, 342, 273
Young regen.	LD	Clumpy/ speckled	84, 86, 101	2100, 2150, 2525	29, 15, 21	0.95, 0.43, 0.47	1.06, 1.48, 1.14	1.52	140,134, 129	503, 347, 463
Young regen.	MD	Clumpy	133, 149, 102	3325, 3725, 2600	36, 30, 29	0.55, 0.45, 0.57	0.86, 0.62, 0.75	1.58	118,118, 129	593, 597, 772
Older regen.	OR	Clumpy	77, 81, 111	1900, 2025, 2775	47, 30, 27	1.06, 1.03, 0.72	0.44, 0.76, 0.50	2.10	97, 100, 98	1141, 976, 885
Older regen	OR1	Clumpy	32, 38, 43	796, 950,1075	34, 33, 35	2.11, 1.88, 1.70	1.32, 0.53, 0.79	3.20	84, 85, 90	1070, 930, 900

* *3 values relate to samples a, b and c, respectively*

7.5.2 The Sample Image Characteristics

As noted in the previous section and in 7.3.1, image variance is driven by image contrast, which for forest canopies is governed by the varying amounts of sunlit and shaded elements. In order to consider the effect of these varying proportions of sunlit and shaded elements on semivariogram characteristics, each was measured using a supervised classification. Three main scene elements were identified within the samples; sunlit crown, sunlit heather and shadow. The sunlit components were trained by delineating areas that were identifiably green crown or brown/purplish heather. Any area too dark to identify between crown and heather was included in the shadow/shaded training set. The training classes were adjusted and added to, until the classified image resembled the pattern of the original images as closely as possible. The number of pixels in each class were used to estimate the percentage of each. Where appropriate, a fourth class for bare soil was included and could be easily identified as very bright or white in colour due to the very high reflectivity of the sandy soils within the study area. The results of these classifications are presented in Table 7.7, and in Figure 7.4 on the following pages.

The YP sample has a similar proportion of sunlit crown to shadow (Table 7.7) with the spatial pattern of plantation rows clearly illustrated in Figure 7.4. The relatively regular sequence of sunlit crown and shadow is apparent in the East to West direction, occasionally interspersed with patches of sunlit heather. This sequence is evident in most of the samples, but the direction is more in line with the Sun angle (approximately South East to North West) and is more random. The greatest proportion of shadow is found in the older stands and is related to tree height and crown width. The result is that the Old Growth (OG) samples have very little sunlit heather; most of the background vegetation being under shadow. For younger regeneration samples however, the proportion of shadow is lower, despite variations in density. The main variation in the younger stands is in the amount of sunlit heather, which is related to tree density. The classification of the sample sub-scenes worked well, although greater variations in scene element brightness for the OG samples probably caused these to be the least accurate.

Table 7.7 Percentage of scene elements in each sample using a supervised classification

Cover type	YP	OG	OG	OG	DH	DH	DH	HD	HD	HD	LD	LD	LD	MD	MD	MD	OR	OR	OR	OR 1	OR 1	OR 1
Sample	-	a	b	c	a	b	c	a	b	c	a	b	c	a	b	c	a	b	c	a	b	c
Sunlit Crown	44	40	49	57	-	-	-	55	55	59	29	15	21	36	30	29	47	30	27	34	33	35
Sunlit Heather	19	18	3	7	87	90	89	16	18	20	51	61	52	44	41	45	21	37	28	20	20	30
Shadow	36	42	48	36	12	6	7	29	27	21	20	24	28	20	29	24	32	32	44	46	47	35
Bare soil	-	-	-	-	2	4	4	1	<1	<1	<1	1	<1	1	1	1	<1	1	1	-	-	<1

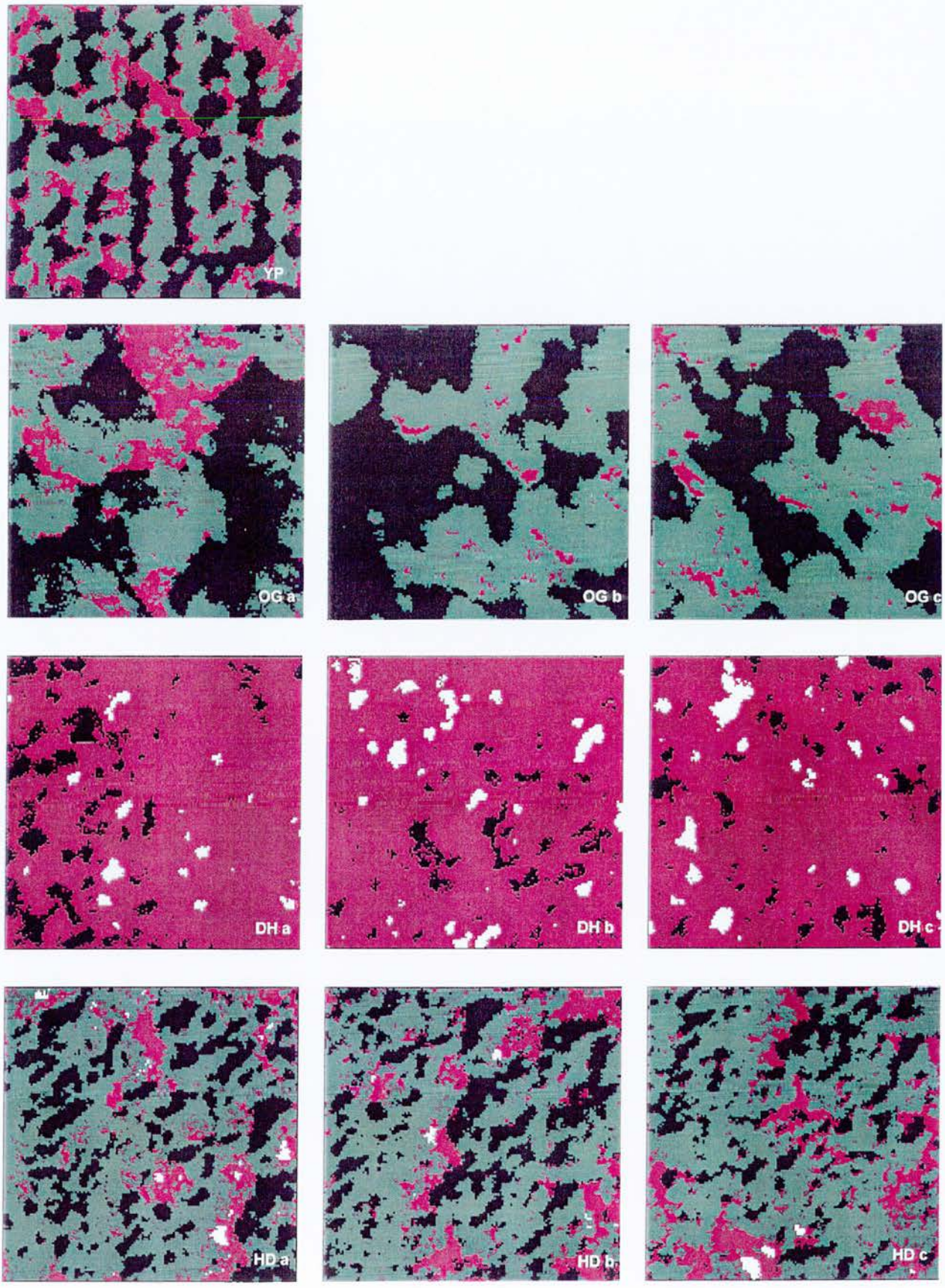

Figure 7.4 The classification results for each of the sample sub-scenes. Green = sunlit crown, maroon = sunlit heather, black = shadow, white = bare soil. Contd. over/...

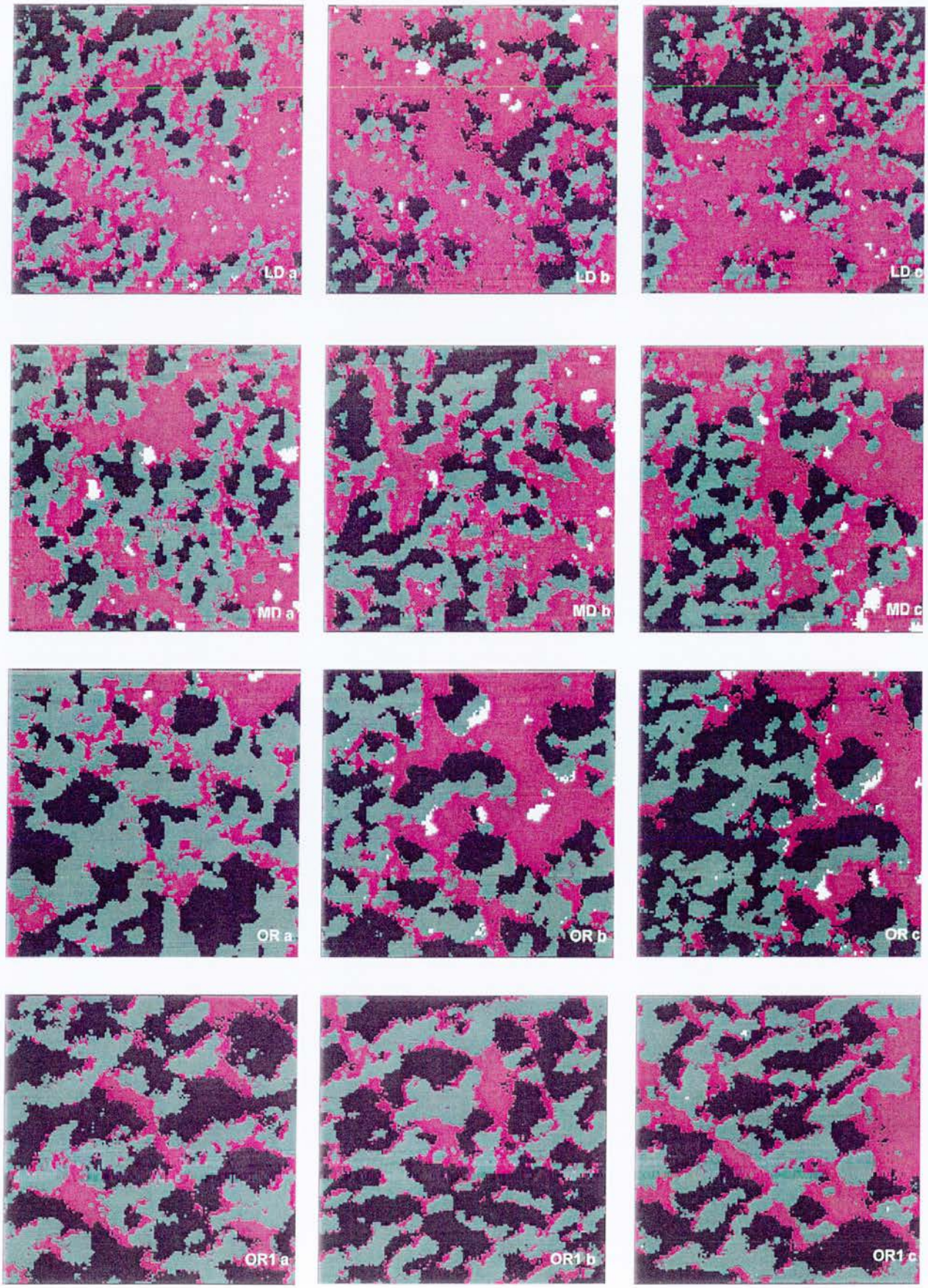

Figure 7.4 .../contd. The classification results for each of the sample sub-scenes.

7.5.3 Semivariogram Characteristics - Young Plantation (YP)

In the previous section, the spatial arrangement of the sub-scene sample images was illustrated in the classified images presented in Figure 7.4. This section and section 7.5.4 present the results of the semivariogram computations using the GLIB software. Both omnidirectional and directional (West to East; South to North; SW to NE and NW to SE) semivariograms were computed in order to give an overall impression of spatial dependence (omnidirectional) and a description of spatial pattern and anisotropy (directional). The effect of decreasing image resolution was also explored and is included in the following presentation of the semivariograms.

Young plantation (YP) omnidirectional semivariograms

Figure 7.5 presents the omnidirectional semivariograms for YP for all three image layers; red, green and blue bands. All three semivariograms have very similar forms, indicating that all three bands have the same spatial structure across the image. This form is described as the 'classic' semivariogram form (Curran, 1988). The principal difference between the bands is in the sill, which is similar for the red and green but much lower in the blue. The higher sill values for the red and green bands indicate higher overall image variance for these layers than for the blue layer. This may be explained by reference to Table 7.7, which shows that the image is principally green crown and shadow, with some purplish heather. The sill is reached rapidly and represents the limit of spatial dependence (or autocorrelation) at the range; approximately 2.0 m for all three bands. There is also some cyclicity after the sill has been reached, which is more noticeable in the green and red semivariograms, but is neither regular, nor particularly pronounced.

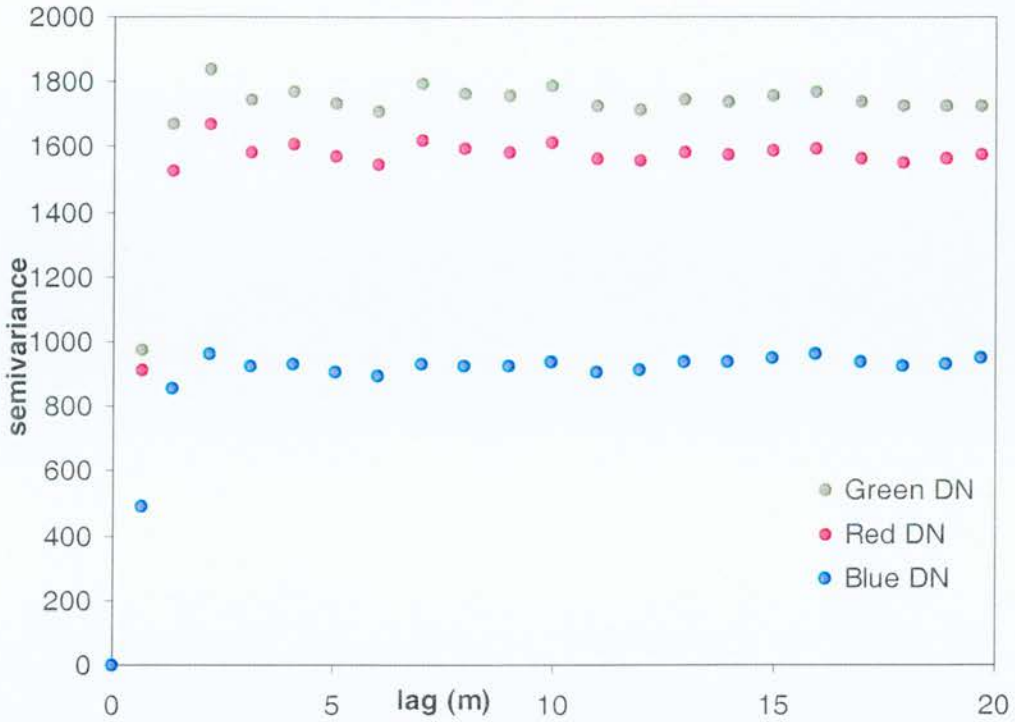

Figure 7.5 Young Plantation (YP) omnidirectional semivariograms for all three image bands (0.14 m resolution).

There is a peak at the fourth lag[1] (2.15 m), which is no doubt due to the sharp and regular contrast between the tree crowns and the adjacent shadow. At the fifth lag (3.09 m) pixel values are more similar to each other again. This 'hole effect' is commonly found for spatial patterns with recurring values (Isaaks and Srivastava, 1989 p.156).

[1] Note that the first lag distance is 0, however, subsequent lags do not equal the image pixel size (0.14 m in this case) since omnidirectional semivariograms are not computed on the basis of a regular grid, but on point data; the centre of each pixel being a sample point. Pairs of point values are compared in all directions, within a degree of angular tolerance, so that the average separation distance between points for any lag is not equal to the pixel size, or multiples of it.

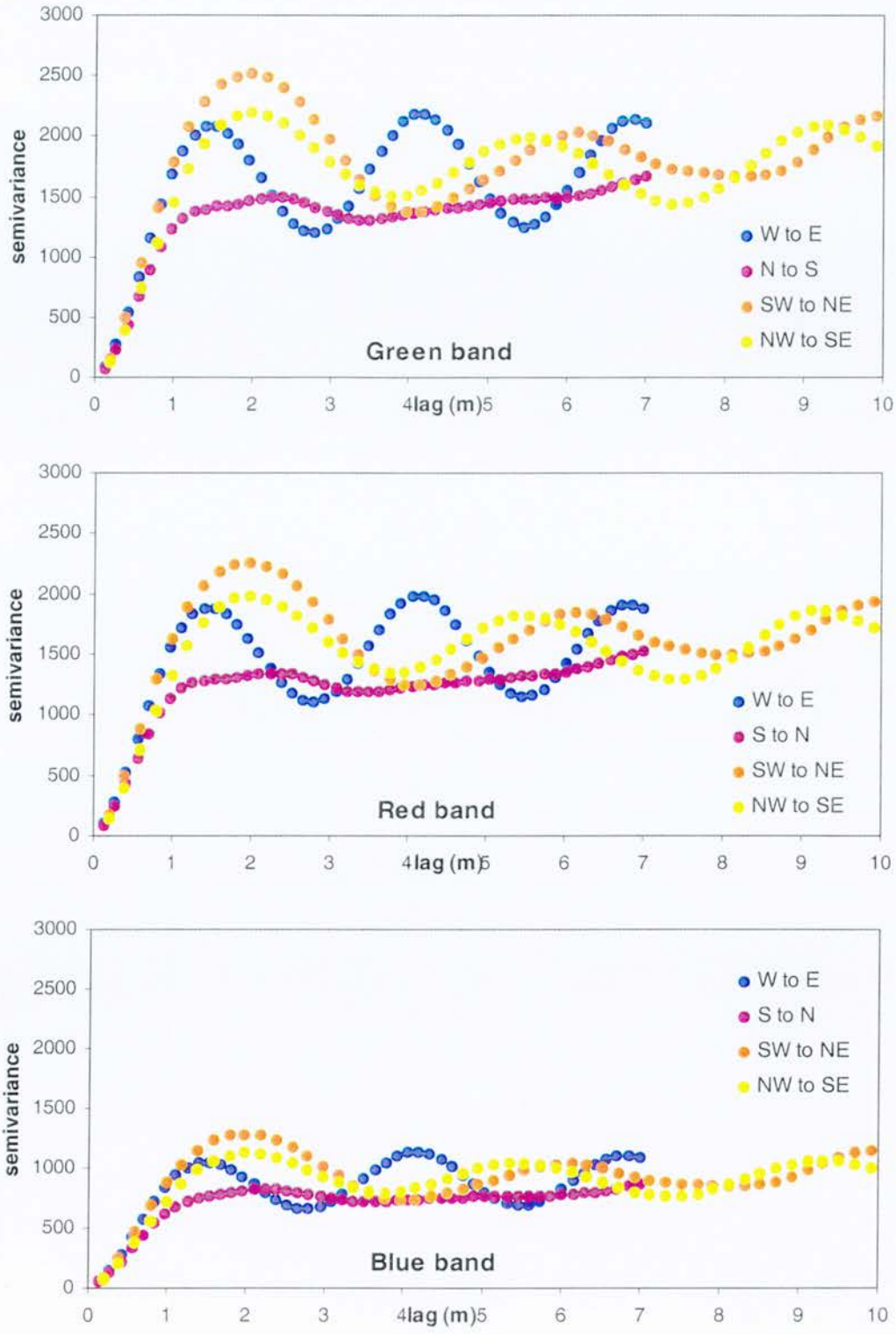

Figure 7.6 Young Plantation (YP) directional semivariograms for all four principal directions (0.14 m resolution)

Young plantation (YP) directional semivariograms

Figure 7.6 illustrates the four directional semivariograms computed for each band in the YP sub-scene sample images. These semivariograms were computed over 50 lags, or over 7 m (50 x 0.14 m) in the W to E and N to S directions. The lag spacing is larger than 0.14 m for the diagonal directions because the diagonal distance between the centre of the square pixels is greater than the 0.14 m horizontal or perpendicular distance.

Most notable, is the similarity in semivariogram form for each band and it clearly makes little difference which band is used for the computation. There is a slight difference in the level of the sills; the blue band being the lowest. This is the same as for the omnidirectional semivariograms in Figure 7.5. There would appear to be no gain in information by constructing semivariograms for all three bands, so all further semivariograms were constructed using the green band alone.

The regular periodicity in the W to E directions is most prominent in the green band due to the greater sill values. In other words, overall image variance is greatest for green pixel DN values, so that patterns are stronger in the green band semivariograms. The pronounced and regular periodicity in the W to E direction relates to pixel values compared across the plantation rows (see Figure 7.4). The distance between peaks is 1.6 m and the first peak is at 2.6 m, which is approximately the same as the range.

There is a strong contrast between the W to E and N to S directional semivariograms since N to S is along the rows and spaces, rather than across them. The range is not strictly reached in the N to S direction as the semivariogram is unbounded. Semivariance is lower due to the reduced variability of pixel values in this direction. It is worth noting that it makes little difference if the semivariograms are computed in the opposite directions (i.e. E to W, or S to N etc.) since the same pixel-pair differences will be averaged. The periodicity is evident in the diagonal directions, but is less regular. There is also a greater distance between peaks due to the greater

distance between rows in the diagonal direction. The anisotropy in this image is clearly apparent in the directional semivariograms since their forms differ depending on direction. These results indicate that the semivariograms calculated on the basis of pixel DN values do reflect the spatial pattern of the plantation image.

Changing spatial resolution (Young plantation)

Figure 7.7 presents the green band omnidirectional semivariograms for each resolution. The form of the semivariograms remained the same as resolution is decreased from 0.14 to 0.5 m, but there was a slight change once the pixel size reached 1.0 m. At this point, the sill value dropped slightly from 1750 to 1630. This observation can be explained by noting that generally, when resolution increases neighbouring pixels become more similar, thereby reducing variance. However, in the YP sample the point on the semivariograms at which this semivariance reduction was most marked was at the lag distance of 2 m. This was the distance over which similar brightness values would be expected to occur, since it was equal to the mean distance between the centre of tree crowns and the centre of row spaces. Image variance was minimised at this lag because the pixel size approximates both the mean crown diameter and the mean spacing between crowns (1.2 m and 0.95 m, respectively), each recurring at approximately this lag distance. This results in a slight alteration in the form of the semivariogram at the 1.0 m pixel resolution.

The form of the semivariogram changes at the 2.0 m resolution and the peak in semivariance shifted to a lag distance of 4 m (Figure 7.7). At 2.0 m the pixel size was L-resolution with respect to the main scene elements (the 1.2 m trees and 0.95 m gaps) and each pixel value is more likely to represent a mixture of these elements. Nevertheless, very similar values for both the range and the sill are obtained at the lowest resolution, as at the highest resolution.

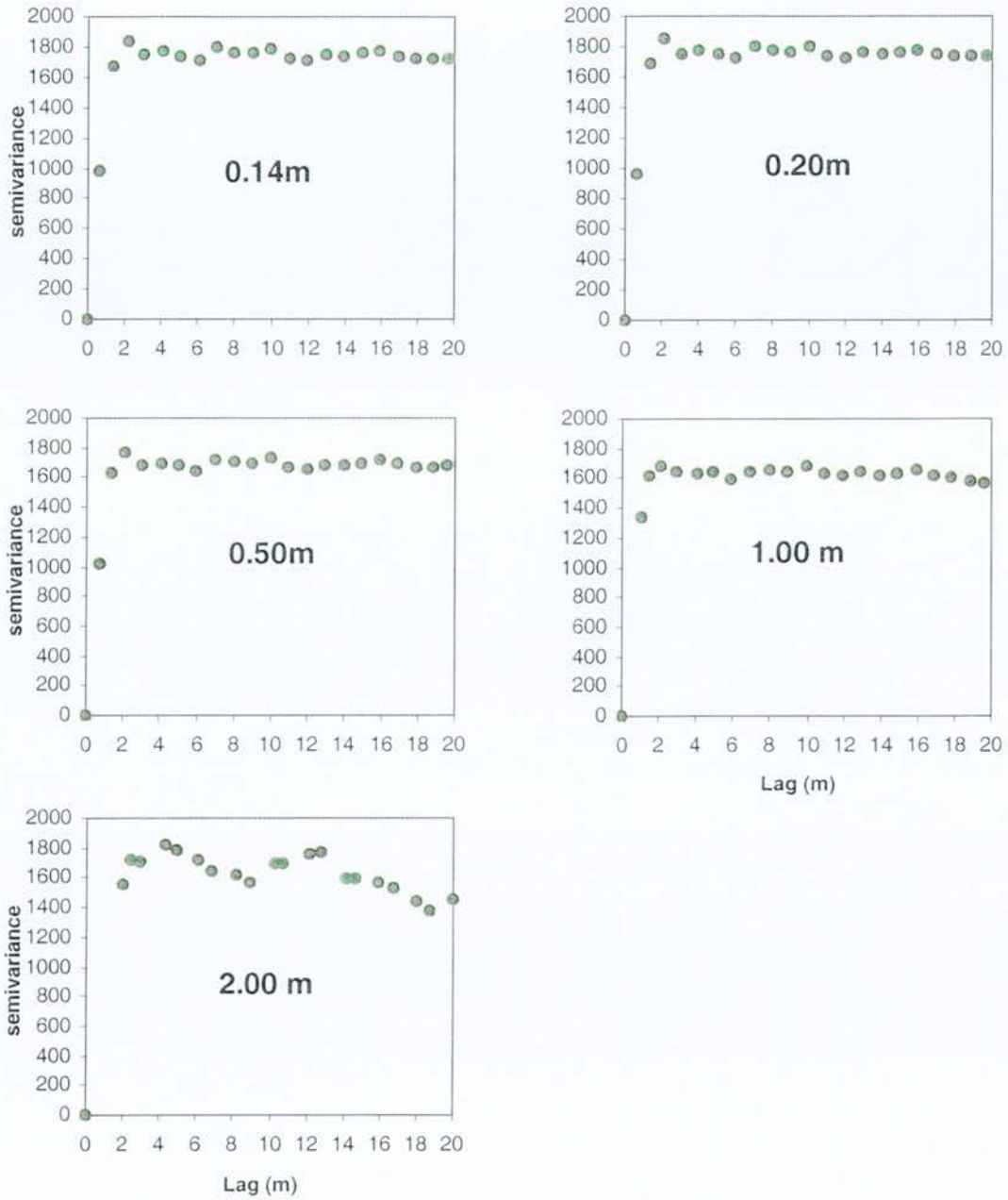

Figure 7.7 Young Plantation (YP) omnidirectional semivariograms (green band DN) for each spatial resolution. The pixel size of the images captured with the digital camera represent the greatest resolution (0.14 m). The lower resolutions were obtained by progressively degrading the original image using a bilinear resampling method.

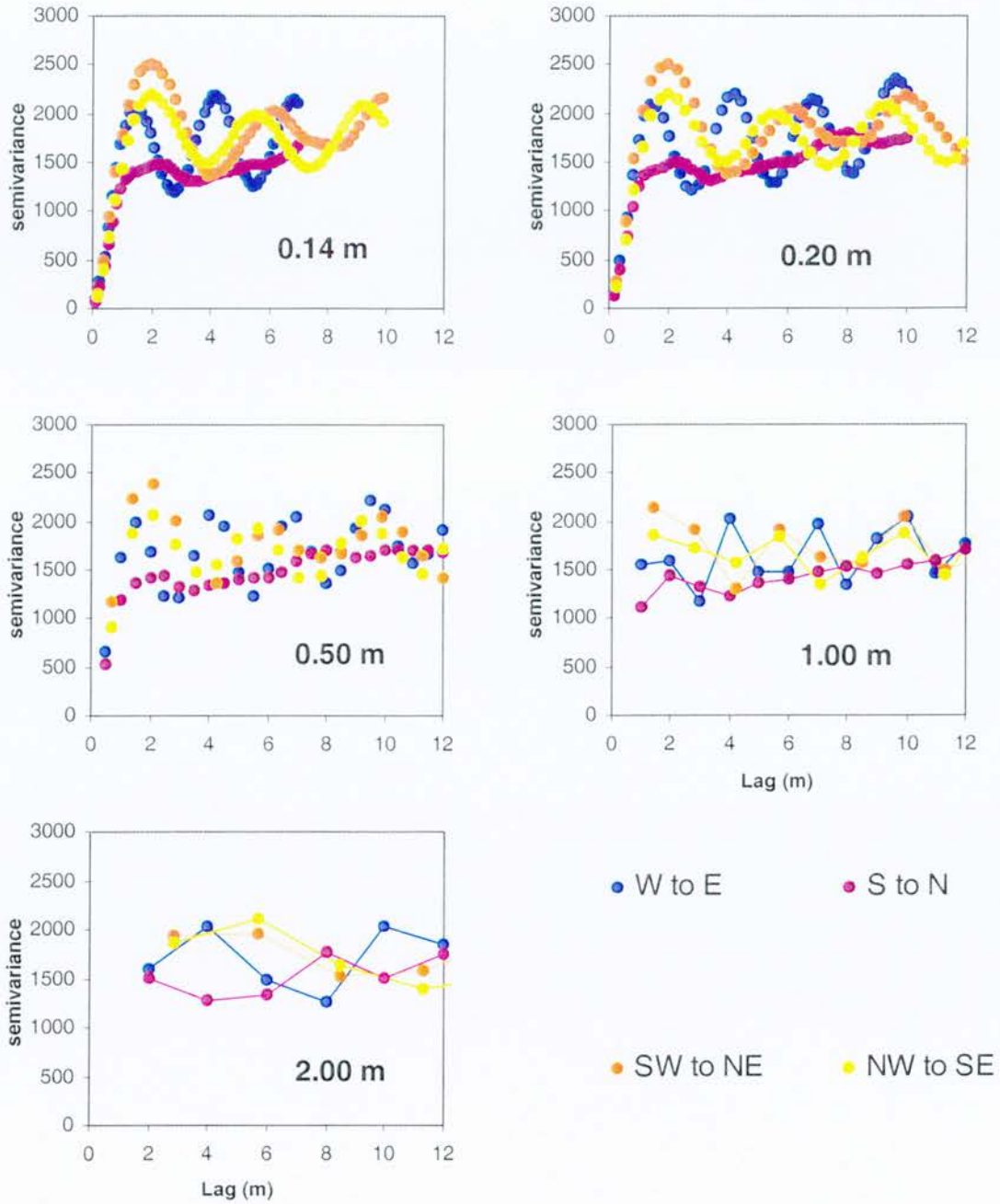

Figure 7.8 Young Plantation (YP) directional semivariograms (green band DN) for each spatial resolution. Lines are drawn to aid the eye and are not modelled fits.

Illustrated in Figure 7.8 are the directional semivariograms for the YP samples at each resolution. As for the omnidirectional semivariograms in Figure 7.7, the directional semivariograms alter in form as the pixel size approaches the average crown and crown spacing dimensions. The periodicity is strongly evident at resolutions up to 0.5 m, but less clear as it approaches the mean crown size at 1.0 m. The sill is slightly reduced at the 1.0 m resolution (from about 1830 to about 1680) for the reasons previously discussed in relation to the omnidirectional semivariograms at different resolutions. The lowest resolution sample at 2.0 m, demonstrates some periodicity in the E to W direction, but on a different scale to the periodicity at higher resolutions. A larger sample over a wider area would be required to explore this feature further, but any results would relate to landscape pattern at a different scale than the one currently under study. In other words, at 2.0 m, the scene elements of interest are no longer sapling crowns, but rather sapling crowns with background.

The semivariograms in the S to N direction are notably different to those in other orientations, with no periodicity. Strictly, these semivariograms do not have a range value since the sill value is never reached. The unbounded nature of the semivariograms in this direction indicates a lack of spatial autocorrelation since the pixels in rows and in spaces between rows have very similar values in this orientation, no matter what the lag distance is. Clearly visible in the 0.14 and 0.2 m directional S to N semivariograms is a step at about 2.2 m, which is very similar to the range measured in the remaining three directions. Following this step, the semivariogram continues to approach a sill value asymptopically. This apparent anomally would suggest that there is a degree of spatial autocorrelation at this lag distance in the N to S direction and may be explained by the slight irregularity in the stripy pattern of the YP sample (see Figure 7.4).

The directional semivariograms illustrate two important points about spatial analysis using the semivariogram. Firstly, the omnidirectional variogram can be thought of as an average of semivariograms calculated through a range of directions. The omnidirectional semivariogram is therefore a useful summary of overall spatial

structure within an image. Secondly, where directional anisotropy exists, the omnidirectional semivariogram may not reflect these trends. In the case of the YP sample, the range parameter most closely approximates mean crown size in the W to E directional semivariogram (Table 7.8), particularly when resolution approximates mean crown diameter at the 1.0 m image pixel resolution.

Summary of Young Plantation (YP) Semivariogram Characteristics

Table 7.8 summarizes the semivariogram characteristics for the YP sample. All the values have been extracted by eye, rather than by fitting a model, for reasons detailed in 7.4.3. For each resolution, the individual directional semivariogram parameter values were averaged to compare with the omnidirectional values. This comparison demonstrates that the omnidirectional semivariogram does indeed function as an averaged directional summary of the spatial structure of the images, since mean directional and omnidirectional parameter values are very similar. Range values are very similar in the diagonal directions, and are slightly greater than the range values in the W to E direction for all but the 2.0 m resolution. This is likely due to the greater distance between sample values in the diagonal direction and is a functional of the square pixel grid data, rather than the dimensions of the scene elements. The range parameter for the N to S direction should be treated with caution since strictly, no range parameter exists for a semivariogram form that approaches the sill asymptopically. The directional semivariograms have very similar range and sill parameters at each sample resolution, except for the 1.0 m resolution, which approximates crown size, particularly in the E to W direction.

Periodicity is present in all H-resolution cases, demonstrating that regular spatial patterns have a strong influence on semivariogram form. In the W to E and the diagonal directions, the lag distance to the first semivariogram peak closely approximates both mean spacing and mean crown diameter in these directions (0.95 and 1.2 m respectively). The mean lag distance between peaks is greater than the lag distance to the first peak, and may be related to crown diameter and crown spacing combined.

Table 7.8 Summary of semivariogram parameters for each YP sample resolution.

Direction/ resolution	Range (m)	Sill (DN)	Periodicity	Mean lag distance between peaks (m)	Lag distance to first peak (m)
YP 0.14 m					
W to E	1.5	1800	Regular	2.6	1.6
N to S	-	-	Unbounded	-	-
SW to NE	2.0	2030	Irregular	-	2.0
NW to SE	2.0	1990	Regular	3.7	2.0
Mean directional	1.8	1830	-	-	1.9
omnidirectional	2.0	1750	-	-	2.2
YP 0.20 m					
W to E	1.5	1770	Regular	2.7	1.5
N to S	-	-	Unbounded	-	-
SW to NE	2.0	2040	Regular	4.0	2.0
NW to SE	2.0	2000	Regular	3.6	2.0
Mean directional	1.8	1830	-	-	1.8
omnidirectional	2.0	1750	-	-	2.1
YP 0.50 m					
W to E	1.5	1690	Regular	2.5	1.5
N to S	-	-	Unbounded	-	-
SW to NE	2.0	2000	Regular	4.0	2.0
NW to SE	2.0	1800	Regular	7.6	4.0
Mean directional	1.8	1740	-	-	3.7
omnidirectional	2.1	1700	-	-	2.1
YP 1.00 m					
W to E	1.0	1550	Regular	3.0	1.0
N to S	-	-	Unbounded	-	-
SW to NE	1.4	1900	Regular	5.0	1.4
NW to SE	1.4	1860	Regular	4.2	1.4
Mean directional	1.3	1680	-	-	1.3
omnidirectionlal	2.0	1630	-	-	2.1
YP 2.00 m					
W to E	4.0	2000	-	-	-
N to S	2.0	1500	-	-	-
SW to NE	2.8	1950	-	-	-
NW to SE	3.0	1870	-	-	-
Mean directional	3.0	1830	-	-	-
omnidirectionlal	2.5	1720	-	-	-

7.5.4 Semivariogram Characteristics - Semi-natural samples

The previous section presented in some detail, the results of the semivariogram computations for the YP sample. This enabled the effect of the regular pattern and regular tree and spacing characteristics to be observed on the semivariogram form. This section presents the results of the semivariograms computed for the more randomly distributed semi-natural vegetation cover types. Firstly, the effect of differing proportions of scene elements (shadow, heather and crown) in the images on the sill value is considered for the omnidirectional semivariograms. The range and sill parameters are then compared for each cover type. The difference between samples and the effect of changing resolution is also presented.

The sill values

As for the YP samples in the previous section, there was very little difference in the form of the omnidirectional semivariograms between the red, green and blue bands for each land cover type. However, there was notable variation in the level of the sill value between bands. Samples with medium to high density of pine regeneration resulted in higher sill values for the green band than for the red or blue band. However, the red band sill values were similar to the green band sill values when pine density or pine cover was low (Figure 7.9). It is clear from Figure 7.9 that the absolute sill values are not directly related to the amount of pine in the sample area since the sill value for the low density sample (LD) is greater than that for the high density (HD) sample. This is due to variations in background reflectance. In this case, the LD sample was deliberately taken from an area where the heather was lighter in colour in order to compare with the dark coloured heather samples (DH). The lighter colour is partially due to a greater lichen component within more freely drained areas; usually on top of knolls.

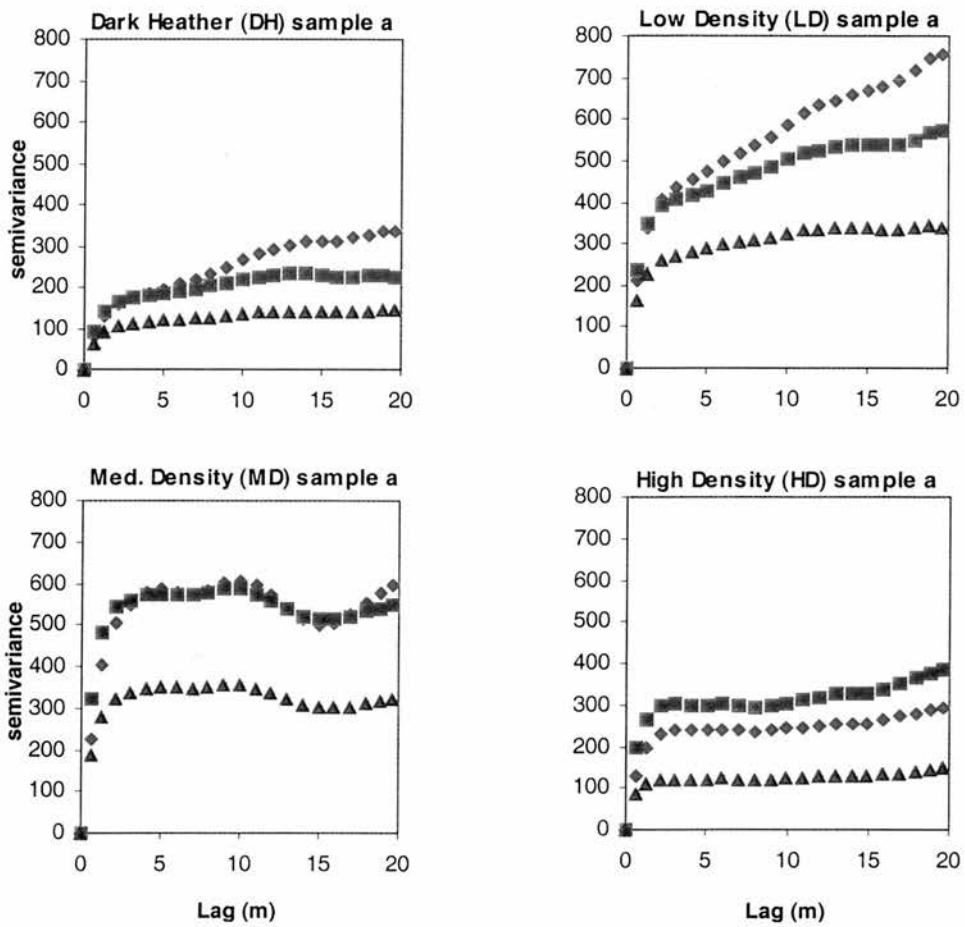

Figure 7.9 Omnidirectional semivariograms (0.14 m resolution) to illustrate the relationship between different bands (colours are representative) and density of pine regeneration.

Contrast is lower for the HD sample due to its uniform appearance. Whilst any relationship between the amount of pine regeneration and absolute sill values may be influenced by these other images characteristics, Figure 7.9 does illustrate some consistency between the relative sill values of different bands, and the amount of pine. To illustrate this point further, the sill values of the green and red bands were expressed as the ratio green/red and plotted against percentage cover of pine (Figure 7.10). There is a clear relationship between the amount of pine in a 20 m sample plot and this ratio. Figure 7.10 also illustrates that the different stages of regeneration and the different cover types are largely separable within this plot.

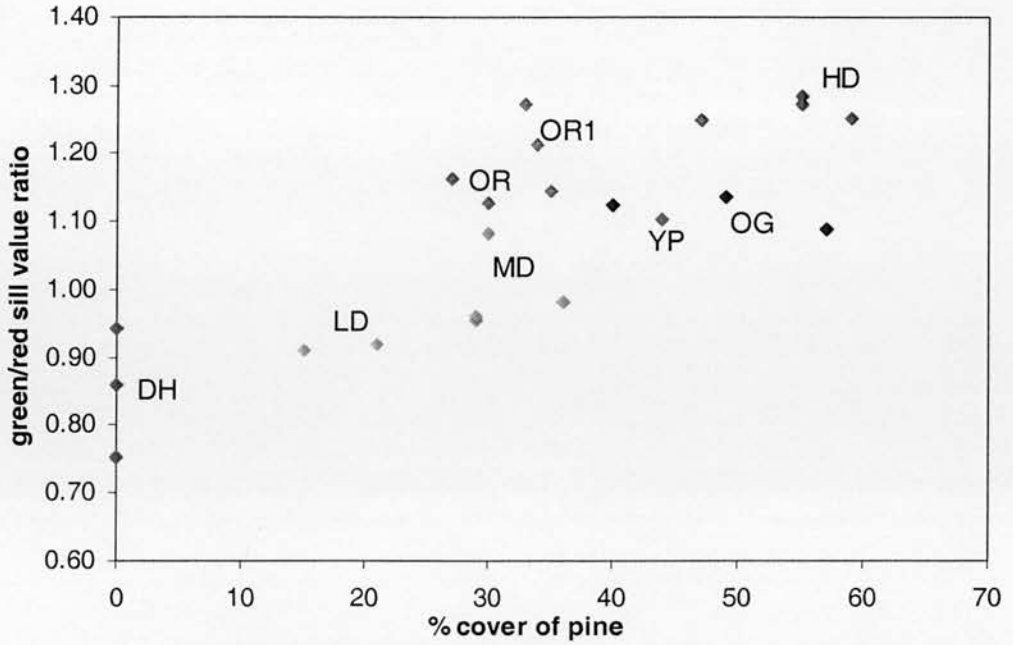

Figure 7.10 The relation between amount of pine and the ratio of the green band sill value to the red band sill value (0.14 m resolution images).

In general, the greater the percentage cover of pine, the greater the ratio of green/red semivariance sill values. For young regeneration at lower to medium percentage cover the ratio was less than one and for older regeneration at medium percentage cover the ratio was between 1 and 1.27. Young regeneration at higher percentage cover produced a ratio of more than 1.29.

The sill value of one image band alone may not relate directly to the amount of pine within a sample area, but Figure 7.11 illustrates that different stages of regeneration are separable on this basis. The sill value, which approximates DN variance was highest for the old growth samples (OG a, b and c) in which there is a higher contrast between shadow and sunlit crowns. Sill values are lowest for the less textured, smoother images; high density young regeneration (HD) and darker heather (DH) samples have the lowest sill values. Notably, the older regeneration samples (OR and OR1), which were purposely selected from different parts of the photographs, have very similar sill values and are distinct from other regeneration stages.

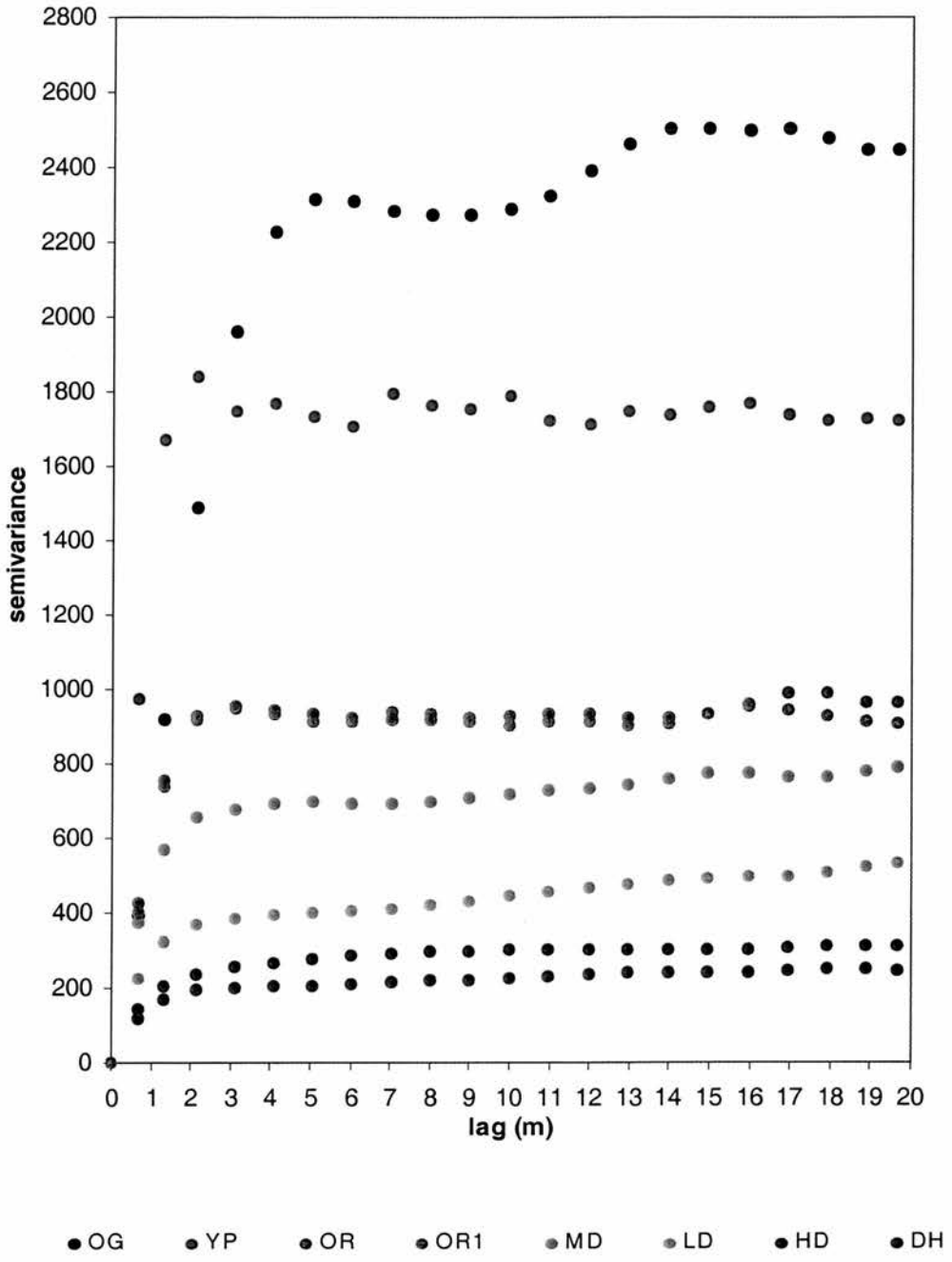

Figure 7.11 Mean green band omnidirectional semivariograms for each land cover type (0.14 m resolution) to illustrate the separability of regeneration stage on the basis of image texture, or the sill value which approximates DN variance.

Range values

Range values for the omnidirectional semivariograms varied very little with changing resolution for all the cover types. There was however, variation in range values between cover types as expected. Figure 7.12 summarizes the range values for each cover type and for each resolution and illustrates four principal results, which require highlighting and interpretation.

Firstly, there was no real difference between each of the resolutions used; there appeared to be similar range values produced at the lowest resolution to those at the highest resolution. This result held for every cover type and irrespective of mean crown diameter. In general, semivariogram form varied very little with resolution suggesting that there is as much relevant spatial information held within and image of 1.0 m as one of just 0.14 m.

Secondly, omnidirectional range values do not relate well to the mean crown diameter of regeneration cover types (HD, LD, MD, OR and OR1) but do approximate the young plantation and old growth mean crown diameters more closely. The low density (LD) cover type produced semivariograms in which a sill was not reached (unbounded), rendering estimates of the range unrealistic. The form of the LD omnidirectional semivariograms is illustrated in Figure 7.9. Whilst the range parameter cannot be strictly estimated from such a semivariogram form, it can be noted that there is a lag distance at which there is a change in the degree of spatial dependence. This lag distance is at about 4 m, which is similar to the range values for the other regeneration cover types. It is suggested that for this low density cover type, the light coloured heather background is dominant but relatively uniform, but the saplings with their associated shadow slightly modify a semivariogram that would otherwise exhibit little or no spatial dependence.

Thirdly, directional semivariogram range values relate better to mean crown diameter than the omnidirectional ones, but particularly in the SW to NE direction, which was perpendicular to the Sun's rays at the time of photo acquisition. This effect is

particularly noticeable for the medium density (MD) cover type. Figure 7.13 illustrates the relationship between the estimated mean range values and the mean crown diameters for each cover type in the SW to NE direction, at the 0.14 m resolution. The relationship is a strong one, but the deviation from the 1:1 line in Figure 7.13 indicates a systematic over-estimation of crown diameter by the range value. It is suggested that the over-estimation was due to the tendency of individual saplings to merge crowns with neighbours to give a clumpy structure. The range therefore related more to the clump dimensions than to the measured mean individual crown sizes within each cover type. In sample plots where individual tree crowns are more evenly spaced (YP and OR1), the range value more closely estimates the crown diameter. A similar monotonic relationship also existed between the range values and percentege cover and tree density for the regeneration samples, but was much weaker.

Lastly, the dark heather (DH) cover type with no trees exhibits two possible range values caused by a possible sill at two levels, and a step in the semivariogram at larger range value at 14 m. The larger range value is dominant in the omindirectional semivariogram, but the smaller one is more pronounced in the directional semivariograms (Figure 7.12). This emphasises the different roles of the omni- and directional semivariograms. The omnidirectional summarizes the overall spatial pattern of the DH image, which is less textured than the images with trees and hence the longer range value. The directional semivariograms highlight the smaller scale variations due to bare soil, and shadow effects due to hollows and individual heather bushes. In a similar way, the old growth omnidirectional semivariograms have a step form (see Figure 7.11), but since the first step was very pronounced, this was used to estimate the range value. The step feature would suggest that there is more than one limit of spatial dependence, or two scales of spatial dependence, but caution is required when interpreting the semivariogram form at longer lag distances. This is because the number of pixel pairs at longer lags is much less, resulting in a smaller sample size and greater uncertainty in the semivariogram form.

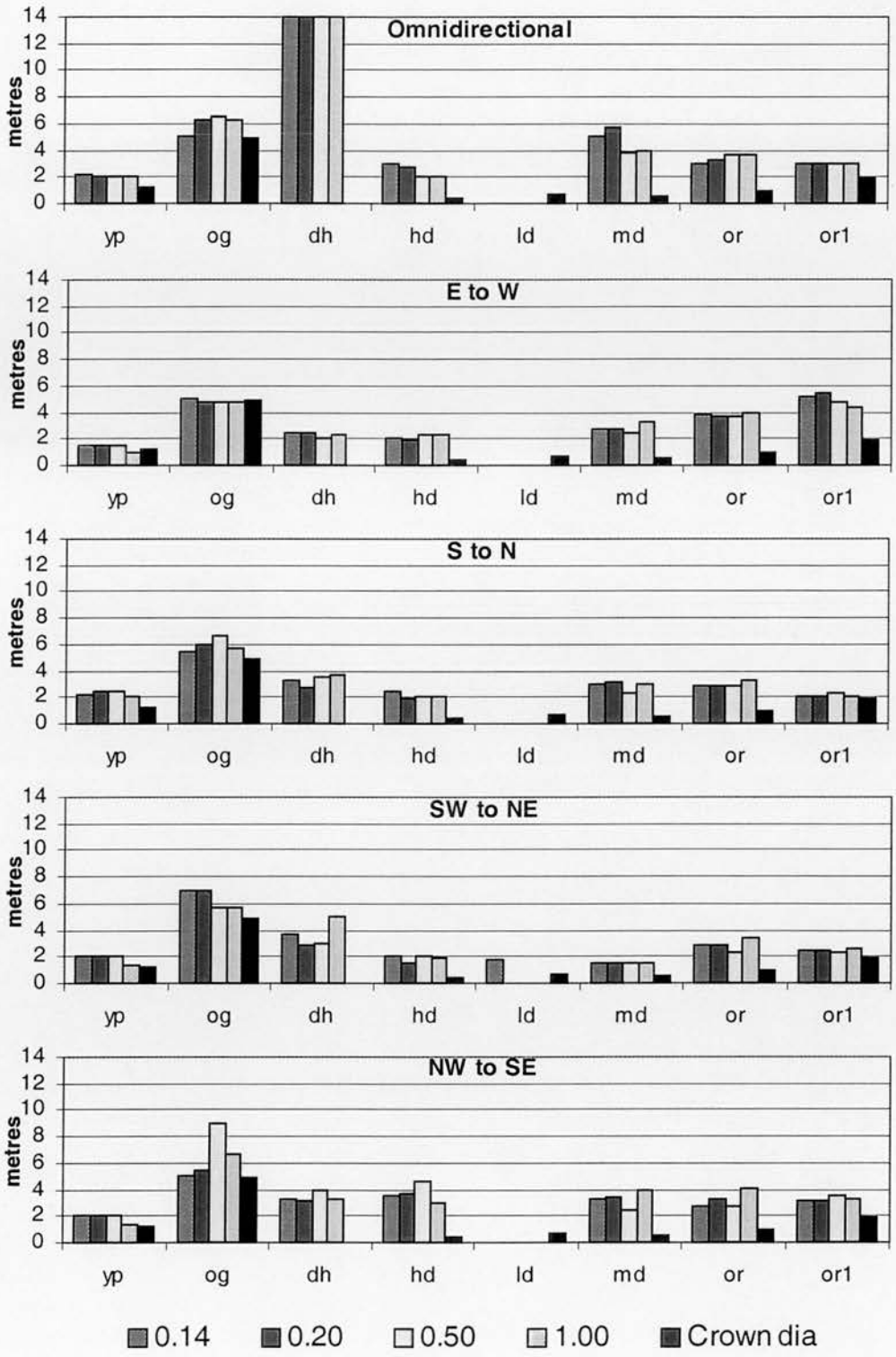

Figure 7.12 Semivariogram range paramater estimates for each cover type at each resolution compared with mean crown diameter (range values are the mean of samples a, b and c for the semi-natural cover types).

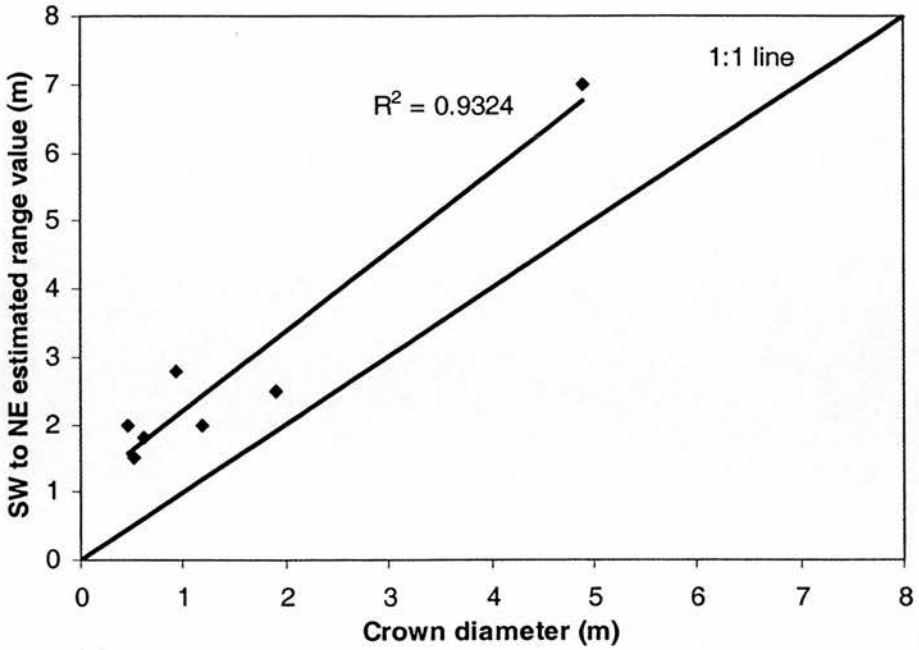

Figure 7.13 The relationship between mean estimated semivariogram range and mean crown diameter for each cover type, for the SW to NE direction.

Periodicity

Periodicity in the semi-natural semivariograms was irregular in comparison with the regular periodicity observed in the YP cover type, which was no doubt due to the more random distribution of trees. Like the YP samples, periodicity was strongest in the directional semivariograms and in the directions more perpendicular to the Sun's rays (E to W and SW to NE). The period between the top of each cycle was averaged for the three samples for each cover type for the SW to NE directional semivariograms. The results of this analysis show that periodicity is greater than the measured mean crown diameter, but that periodicity does increase with increasing crown diameter (Figure 7.14). This suggests that crown diameter does influence periodicity, but that random noise is also involved. Figure 7.14 also illustrates that resolution makes very little difference to periodicity, except for the 1.0 m resolution, which produces much greater periods for the younger regeneration samples. Comparing mean crown diameter plus mean crown spacing against periodicity

produced a very similar result to that shown in Figure 7.14 with the mean period still greater than measured mean crown diameter.

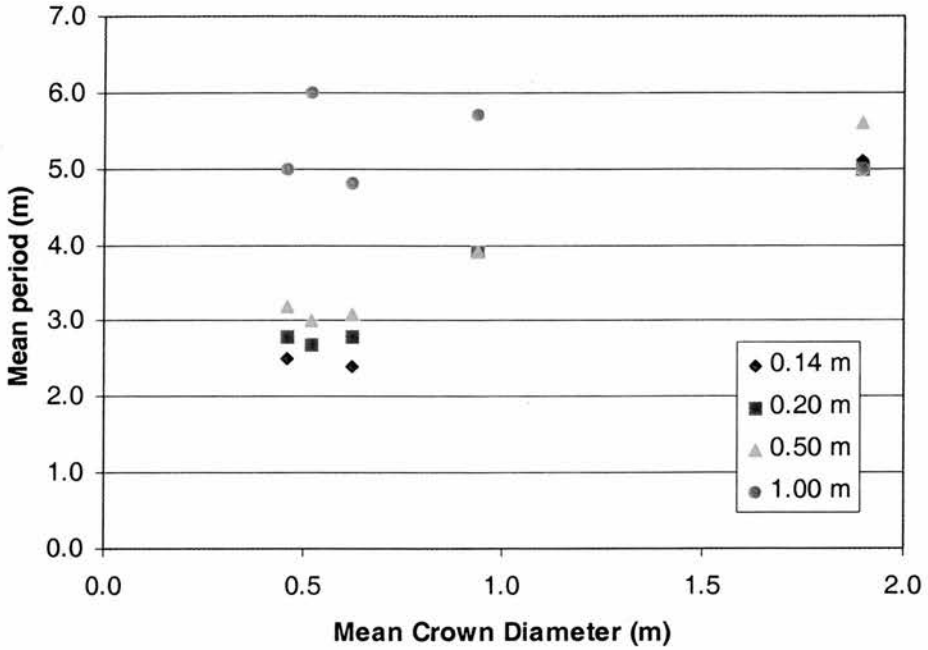

Figure 7.14 The relationship between mean semivariogram period and mean crown diameter for each regeneration cover type for the SW to NE directional semivariogram, and at each resolution.

7.6 Discussion

7.6.1 Using the Sill to Separate Regeneration Stage

The form of the omnidirectional and directional semivariograms was very similar for each of the image bands; red, green and blue. This has been reported in other studies (e.g. Atkinson and Danson, 1988), but like the results reported in Hyppänen (1996), whilst the form was similar, the largest variation between bands was in the level of the semivariance (and by definition, the sills). This variation is no doubt due to the varying influence of the scene elements on each image band. Green DN will be more influenced by the amount of pine in the sample plot, whilst blue and red DN by the proportion of shadow and heather understorey, respectively.

Variation in the sills between cover types has been attributed to factors within stands that increase stand complexity, such as vertical layering (e.g. Cohen *et al.* 1990) or tree height (Treitz and Howarth (2000). The results from the present study support these conclusions, since older regeneration images did have much higher semivariance than the younger regeneration samples, although percentage cover and density were also influencing factors. High density stands will always have a smoother texture than lower density stands, whatever the tree height or age. A similar conclusion was reached by Coops and Culvenor (2000), who showed that as percentage cover increased, the texture variance decreased consistently for modelled forest stands with varying tree spatial patterns.

The lower density and percentage cover for the Low Density (LD), Dark Heather (DH) and one of the Medium Density (MD) samples produced omnidirectional semivariograms with no clear spatial structure. These samples contained larger areas of relatively untextured continuous heather and lichen understorey resulting in an unbounded form of semivariogram (Curran, 1988). This form of semivariogram indicates that no range value was reached over the lag distance used for calculating

the semivariogram (Treitz and Howarth, 2000) and is a feature of more open canopies with larger gaps (Lévesque and King, 1999). According to Isaaks and Srivastava (1989), if the omnidirectional semivariogram has no structure, there is little point in calculating directional semivariograms. This proved to be the case in the present study, as all the directional semivariograms calculated for these samples with unbounded omnidirectional semivariograms, were also unbounded. This highlights a potential problem for interpreting semivariograms for areas of regeneration, since much regeneration is low density.

Despite these problems with defining absolute sill values for unbounded semivariograms, it was still possible to separate regeneration types based on semivariance. This was achieved by using the relative sill values of the green and red bands as a simple ratio (Figures 7.9 and 7.10). For cover types with unbounded semivariograms and no sill, the semivariance at a lag equivalent to the range of other regeneration types was used. This is not as arbitrary as it may seem, because although the unbounded semivariograms had no sill, there was a lag distance at which pixel values became much less spatially dependent. A sharp decrease in the slope of the semivariograms marked this point, which was at a similar lag distance to the range observed in other regeneration samples (see Figure 7.9).

7.6.2 Relating the Range Parameter to Tree Size

It was found that directional semivariogram range values relate better to mean crown diameter than those from omnidirectional semivariograms. For continuous stands the range has been shown to be approximately equal to tree crown diameter (Cohen *et al.*, 1990). However, in the present study the range was consistently greater than the mean crown diameter, which may be due to the fact that individuals tend to have inter-connecting crowns giving a clumpy structure that is greater than mean crown diameter. Coops and Culvenor (2000) explicitly studied the effect of spatial pattern on local variance and concluded that clumping or aggregation produces larger areas of low and high local variance. This in turn produces extremes of response in local variance when compared to scenes with a more random spatial pattern. The semivariogram has been shown to have similar properties to the local variance curve (Simmons *et al.*, 1992), so that the work of Coops and Culvenor (2000) does have relevance to the present study. Alternatively, the longer range parameter estimates could be due simply to the presence of gaps in the canopy and tree crowns of varying size (Treitz and Howarth, 2000). It seems likely that all these factors contribute to the over-estimation of mean crown size by the range parameter. This result highlights potential difficulties in directly relating the range parameter to crown size when considering the spatial structure of regions of regeneration.

Other studies have reported semivariogram range values greater than mean crown diameter. Treitz and Howarth (2000) collected Compact Airborne Spectrographic Imager (CASI) data over a range of forest types in Northwestern Ontario at an average spatial resolution of 0.73 m in the cross-track direction and 5.36 m in the along track direction. Range values were greater than mean crown diameter for each forest type. Hyppänen (1996) used digitized colour infrared aerial photography resampled to 1 m resolution to produce semivariograms for Scots pine and Norway spruce compartments in Finland. He found the range for young Scots pine compartments to be 4 m for a mean crown size of 2.1 m. This result is proportionally very similar to results in the present study, where the 1.0 m resolution SW to NE

semivariogram produced a mean range approximately twice the mean crown diameter for the regeneration samples.

Nevertheless, Figure 7.13 illustrates that a strong linear relationship exists between the range parameter and the perpendicular directional semivariogram (meaning perpendicular to the Sun azimuth angle). Other workers have found a strong linear relationship between the range and crown size (e.g. Cohen *et al.*, 1990; Lévesque and King, 1999). Notably, the strength of the relationship declines rapidly as pixel size exceeds the crown size of most of the regeneration samples for the SW to NE direction. The coefficient of determination (R^2) = 0.93 at 0.14 m (Figure 7.13), 0.97 at 0.20 m, 0.94 at 0.50 m, 0.79 at 1.00 m and no linear relationship at 2.00 m. However, the inclusion of the old growth (OG) sample perhaps falsely emphasises the linearity of the relationship since its range and crown size estimates are much larger than all the other samples. The OR1 sample also had a significantly larger mean crown diameter than younger regeneration samples. Nevertheless, for the 0.20 m pixel resolution an R^2 value of 0.99 described the strength of the relationship between range and crown diameter when the OG and OR1 samples were excluded.

The range parameter varied with direction of semivariogram; an effect most strongly illustrated in the YP sample because of the obvious directional anisotropy associated by the plantation rows. The range was shorter in the across-row direction (E to W) and much longer (or unbounded) in the along-row direction. St-Onge (1999) explains that 'The directional variation of the range reflects the anisotropy of texture, an indicator of the linearity and "orientedness" of the elementary image pattern'. For the regeneration samples the range was longer in the orientations parallel to the Sun's azimuth angle and shorter in the perpendicular orientations. This is a common feature in lower density stands in particular, since the shadow cast by an individual tree on the background will be longer in the parallel direction (St-Onge and Cavayas, 1995). The orientation of the shadows can be observed on the NW side of saplings in Figure 7.4, and within the lower density LD and MD samples in particular. The relation between crown size and range just described was strongest in the perpendicular direction, which supports the modelled results of St-Onge and Cavayas

(1995). These workers also used a ratio of the range in the parallel direction to the range in the perpendicular direction in an attempt to derive a complete measure of anisotropy from the range parameter. When the interest is primarily in the relation between texture and crown size, however, the range parameter in the direction perpendicular to the Sun azimuth is preferable (e.g. Lévesque and King, 1999).

7.6.3 Optimal Spatial Resolution

What is the optimal spatial resolution for monitoring Scots pine regeneration using remote sensing? Many workers have advocated the range parameter as a useful indicator of optimal spatial resolution (Curran, 1988; Woodcock *et al.*, 1988a; 1988b and Treitz and Howarth, 2000). This would seem logical since places closer than the range are related statistically, whereas places further apart are not (Curran and Atkinson, 1998). Using this rationale for the results from the present study, an image pixel resolution of about 2.0 - 3.0 m would represent a typical range value for regions of regeneration.

A second approach to the question of optimal resolution is outlined by Atkinson and Danson (1988). They defined the optimal resolution as a compromise between a pixel size smaller that the dominant scene objects and one that is much larger. In the former case, there is a higher level of spatial dependence in the pixel values and may be better for estimating crown size, whilst the latter may be more appropriate in characterising overall scene properties, such as reflectance. These workers described optimal resolution as lying 'between these two extremes of information duplication and information loss', which is the same as when the average difference between neighbouring pixels is maximised. In terms of the semivariogram, neighbouring pixels are those at a lag of one ($\mathbf{h} = 1$). The maximum semivariance at this lag, denoted as $\gamma(\mathbf{h} = 1)$, can be estimated by comparing this value over progressively lower pixel resolutions. This analysis was carried out for the present study and the resolutions considered were extended to include a 2.0 m pixel resolution for the regeneration samples (Figure 7.15).

Figure 7.15 illustrates that only the young plantation (YP) sample reaches a maximum semivariance at $h = 1$ over the range of resolutions used. The maximum is at the 1.0 m pixel resolution and is significantly greater than at other resolutions. This result can be explained clearly by the sequence of tree crown and row spaces that occur in sequence across the image. Since the mean crown size of 1.2 m and the mean spacing between crowns of 0.95 m closely approximates the 1.0 m pixel

resolution, neighbouring pixel variance is maximised at this spatial resolution. Interestingly, the across row (W to E) semivariogram range parameter at the 1.0 m resolution was also 1.0 m. This result suggests that for plantation with strong spatial patterns at least, optimal resolution can be estimated meaningfully from maximum semivariance at **h** = 1. Clearly though, the initial spatial resolution of the imagery used must be H-resolution with respect to the trees and spaces for this analysis to be reliably performed.

The Old Growth (OG) semivariance values at **h** = 1 continue to increase throughout the range of resolutions used. It can be reasonably assumed that further increases of image pixel size would produce further increases in semivariance at **h** = 1 until pixel size more closely approximates the mean crown diameter at about 5.0 m.

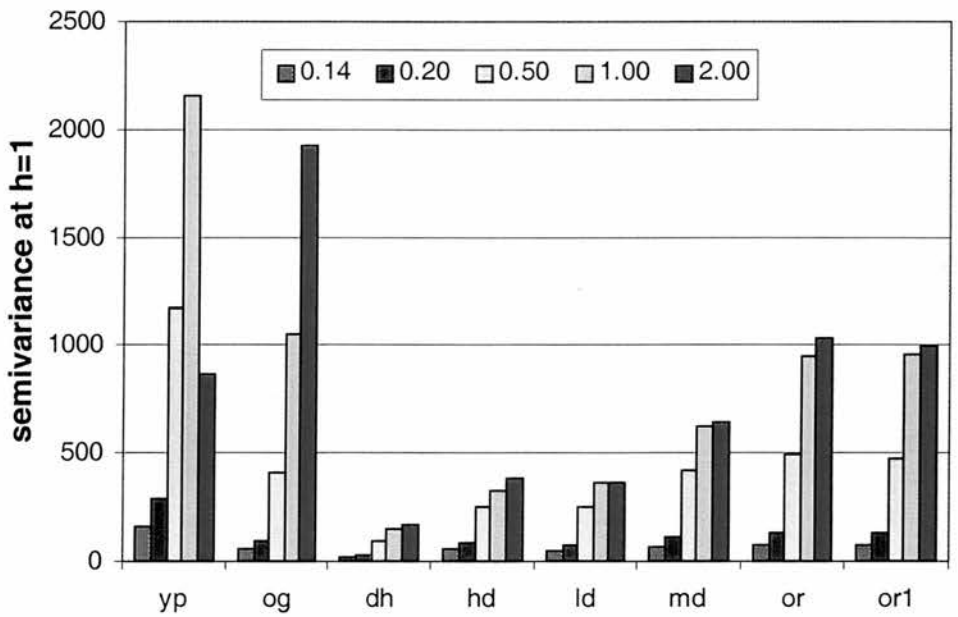

Figure 7.15 Comparison of semivariance at lag one ($\gamma(h=1)$) from SW to NE directional semivariograms for each resolution, to define 'optimal resolution' for each cover type.

Semivariance at **h** = 1 for the regeneration samples and the heather-only sample (DH) produced a very similar response to each other for changing image pixel resolution. The overall pattern was that maximum resolution at **h** = 1 was not reached, even at the 2.0 m pixel resolution. For the younger regeneration samples

(HD, LD and MD) maximum semivariance was approached from the 0.5 m pixel size, with a sharp increase between the 0.2 and 0.5 m pixel sizes. A similar pattern was observed for the older regeneration samples (OR and OR1), except that there is also a large increase in semivariance at h = 1 between the 0.5 and 1.0 m pixel sizes. Unlike the YP sample, there is no sharp decrease in semivariance at this lag once the pixel size reaches 2.0 m. This is no doubt due to the more random nature of the regeneration samples and associated irregular gap, crown and clump sizes.

An encouraging aspect of these results is that one resolution would appear to be adequate for distinguishing between regeneration stages based on semivariance. Figure 7.15 illustrates that a pixel size of 2.0 m should contain enough spatial information to achieve this. However, as previously discussed the relation between semivariance and regeneration stage is affected by density; denser stands such as HD having lower sill values than lower density stands such as LD. A similar conclusion was reached by Treitz and Howarth (2000) for Canadian boreal forest. A further caveat is that the relation between the range parameter and tree size was much stronger at higher resolutions, particularly at 0.2 m as discussed in the previous section. Higher resolutions also produce more points on the semivariogram providing a more detailed response. Therefore, as Atkinson and Danson (1988) point out, optimal resolution depends on the application, or the information required.

7.6.4 Monitoring Regeneration Using Spatial Analysis of Images

The ability of geostatistical analysis to describe within plot and between plot spatial characteristics through the semivariogram using aerial photophraphy has been demonstrated over the previous sections. However, it is recognized that demonstrating theoretical relationships and developing an operationally robust monitoring method may be some distance apart. A number of factors can be identified as potential caveats for monitoring that require some discussion.

The utility of digitized aerial photography as a source of spatial information has been demonstrated in the present study and is a significant result in terms of forest applications for several reasons. Aerial photography remains the most commonly used image source for forest applications (Bolduc, *et al.*, 1999; Holmgren and Thuresson, 1998) and certainly remains the most accessible image data source for environmental monitoring within Scotland. There is also the potential of using existing photography stretching back over the years to assist in our understanding of landscape monitoring (e.g. Hester *et al.*, 1996).

One potential problem however, is that photographs acquired on different dates will have varying acquisition parameters, making comparisons for monitoring purposes difficult. This is a particular problem when using the sill value from the semivariogram (Holopainen and Wang, 1998). These workers developed a calibration procedure in which window values for red, green and blue digitized colour photo bands were corrected to the principal point level with linear regression models. However, the authors admit that the method requires separate calibration for each stand type, which may prove impractical. Furthermore, a particular regeneration class, or stage, may not be represented near to the principal point, which is more likely to occur on large-scale photography. Variations in topography and its effect on textural analysis using the directional semivariogram have also been considered as a potential problem for geostatistical analysis of images, particularly when estimating the range parameter. However, St-Onge (1999) has shown that

topography affects texture mostly in sparse stands, and that absolute error when deriving estimates of tree size and density is low.

7.7 Conclusions

Geostatistical analysis of digitized aerial photographs using the semivariogram was used to characterise the textural properties of different stages of natural Scots pine regeneration. The three image data layers (red, green and blue) produced similar semivariogram forms within each forest type, but the relative sill values between red and green image bands related to percentage cover of pine. It was suggested that a simple ratio of green/red sill values could be used to distinguish between different densities of young regeneration. The sill values alone allowed separation of regeneration stage based on forest texture. However, comparison of the semivariogram sill value acquired on different dates would benefit from calibration to remove the effects of variations in Sun-sensor geometry and other acquisition parameters.

The range parameter from omnidirectional semivariograms did not relate well to crown size. This was probably due to the averaging effect of the omnidirectional semivariograms, coupled with the strong directional anisotropy in this type of image scene. The range parameter was influenced by the size of gaps in the canopy (percentage cover), tree size and the degree of clumpiness.

The range parameter derived from the directional semivariogram perpendicular to the Sun azimuth angle related well to crown size, particularly when pixel size approximated mean crown size. It is recommended that perpendicular directional semivariograms from H-resolution images are used for estimating within-plot structural variables, such as mean crown size. However, for separation of regeneration stage, an optimal spatial resolution, as defined by the method of Atkinson and Danson (1988), of between 1.0 and 2.0 m is recommended. This resolution is slightly L-resolution with respect to mean crown size within regeneration plots. When very strong directional anisotropy exists, as in the case of young forest plantation, the across-row directional semivariogram range most closely

approximated mean crown size, but this relationship was sensitive to image pixel resolution.

Results from this study highlight both the value and depth of information that can be derived from the spatial domain of images, but also the great potential for misinterpretation. This is particularly likely if only the omindirectional semivariogram is considered, or there is a lack of attention to scale factors. There remains a need for *a priori* information on the environment under study and some care when interpreting the semivariogram. These difficulties are clearly a barrier to some applications of geostatistical analysis, such as automated mapping which remains experimental (St-Onge, 1999). Nevertheless, for some forest applications, spatial characteristics as described by the semivariogram have proved superior to spectral measures (Bowers *et al.*, 1994).

7.8 References

ATKINSON, P. M., 1997, Selecting the spatial resolution of airborne MSS imagery for small-scale agricultural mapping. *International Journal of Remote Sensing*, **18**, 1903-1917

ATKINSON, P. M., and DANSON, F. M., 1988, Spatial resolution for remote sensing of forest plantations. In: *Proceedings of IGARSS '88 Symposium, Edinburgh, Scotland, 13-16 September 1988*, ESA Publishing Division, pp. 221-223.

AUBRY, P., and DEBOUZIE, D., 2000, Geostatistical estimation variance for the spatial mean in two dimensional systematic sampling. *Ecology*, **81**, 543-553.

BOLDUC, P., LOWELL, K., and EDWARDS, G., 1999, Automated estimation of localized forest volume from large-scale aerial photographs and ancillary cartographic information in a boreal forest. *International Journal of Remote Sensing*, **20**, 3611-3624.

BOWERS, W. W., FRANKLIN, S. E., HUDDAK, J., and McDERMID, G. J., 1994, Forest structural damage using image semivariance. *Canadian Journal of Remote Sensing*, **20**, 28-36.

BURROUGH, P. A., 1995, Spatial aspects of ecological data. Chaper 7 in Jongman, R. H. G., Ter Braak, C. J. F, and van Tongeren, O. F. R., editors, *Data analysis in community and landscape ecology* (Cambridge: Cambridge Universtiy Press).

COHEN, W. B., SPIES, T. A., and BRADSHAW, G. A., 1990, Semivariograms of digital imagery for analysis of conifer canopy structure. *Remote Sensing of Environment*, **34**, 167-178.

COHEN, W. B., KUSHLA, J. D., RIPPLE, W. J., and GARMAN, S. L., 1996, An introduction to digital methods in remote sensing of forested ecosystems: Focus on the Pacific Northwest, USA. *Environmental Management*, **20**, 421-435.

COOPS, N., and CULVENOR, D., 2000, Utilizing local variance of simulated high spatial resolution imagery to predict spatial pattern of forest stands. *Remote Sensing of Environment* **71**: 248-260.

CURRAN, P. J., 1988, The semivariogram in remote sensing: an introduction. *Remote Sensing of Environment*, **24**, 493-507.

CURRAN, P. J., and ATKINSON, P. M., 1998, Geostatistics and remote sensing. *Progress in Physical Geography*, **22**, 61-78.

DEUTSCH, C. V., and JOURNEL, A. G., 1998, *GSLIB: Geostatistical software library and user's guide,* 2nd Edition, Applied Geostatistics Series (New York; Oxford University Press).

HAY, G. J., NIEMANN, K. O., and GOODENOUGH, D. G., 1997, Spatial thresholds, image-objects, and upscaling: a multiscale evaluation. *Remote Sensing of Environment*, **62**, 1-19.

HESTER, A. J., MILLER, D. R., and TOWERS, W., 1996, Landscape-scale vegetation change in the Cairngorms, Scotland, 1946-1988: Implications for land management. *Biological Conservation*, **77**, 41-51.

HOLMGREN, P., and THURESSON, T., 1998, Satellite remote sensing for forestry planning - A review. *Scandinavian Journal of Forest Research*, **13**, 90-110.

HOLOPAINEN, M., and WANG, G., 1998, The calibration of digitized aerial photographs for forest stratification. *International Journal of Remote Sensing*, **19**, 677-696.

HYPPÄNEN, H., 1996, Spatial autocorrelation and optimal spatial resolution of optical remote sensing data in boreal forest environment. *International Journal of Remote Sensing*, **17**, 3441-3452.

ISAAKS, E. H., and SRIVASTAVA, R. M., 1989, *An Introduction to Applied Geostatistics* (Oxford: Oxford University Press).

JUPP, D. L., STRAHLER, A. H., WOODCOCK, C. E., 1988, Autocorrelation and regularization in digital images I: basic theory. *I.E.E.E. Transactions on Geoscience and Remote Sensing*, **26**, 463-473.

LACAZE, B., RAMBAL, S., and WINKEL, T., 1994, Identifying spatial patterns of Mediterranean landscapes from geostatistical analysis of remotely-sensed data. *International Journal of Remote Sensing*, **15**, 2437-2450.

LÉVESQUE, J., and KING, D. J., 1999, Airborne digital camera image semivariance for evaluation of forest structural damage at an acid mine site. *Remote Sensing of Environment*, **68**, 112-124.

LOBO, A., MOLONEY, K., OSCAR, C., and NONA, C., 1998, Analysis of fine-scale spatial pattern of a grassland from remotely-sensed imagery and field collected data. *Landscape Ecology*, **13**, 111-131.

MARCEAU, D. J., HOWARTH, P. J., and GRATTON, D. J., 1994a, Remote sensing and the measurement of geographical entities in a forested environment. I. The scale and spatial aggregation problem. *Remote Sensing of Environment*, **49**, 93-104.

MARCEAU, D. J., GRATTON, D. J., FOURNIER, R. A., and FORTIN, J., 1994b, Remote sensing and the measurement of geographical entities in a forested environment. 2. The optimal spatial resolution. *Remote Sensing of Environment*, **49**, 105-117.

McGWIRE, K., FRIEDL, M., and ESTES, J. E., 1993, Spatial structure, sampling design and scale in remotely-sensed imagery of a California savanna woodland. *International Journal of Remote Sensing*, **14**, 2137-2164.

OLIVER, M. A. and WEBSTER, R., 1991, How geostatistics can help you. *Soil Use and Management*, **7**, 206-216.

ROSSI, R. E., MULLA, D. J., JOURNEL, A. G., and FRANZ, E. H., 1992, Geostatistical tools for modelling and interpreting ecological spatial dependence. *Ecological Monographs*, **62**, 277-314.

SHAW, D. T., and MALTHUS, T. J., 1999, Spatial properties of natural Scots pine regeneration. *Proceedings of the 25th Annual Conference of the Remote Sensing Society, University of Wales, 8-10 September 1999* (Nottingham: The Remote Sensing Society), pp.849-856.

SIMMONS, M. A., CULLINAN, V. I., and THOMAS, J. M., 1992, Satellite imagery as a tool to evaluate ecological scale. *Landscape ecology*, **7**, 77-85.

St-ONGE, B., 1999, Topgraphic effects on the texture of high-resolution images measured by the semivariogram. *Photogrammetric Engineering and Remote Sensing*, **65**, 923-935.

St-ONGE, B. A., and CAVAYAS, F., 1995, Estimating forest stand structure from high resolution imagery using the directional variogram. *International Journal of Remote Sensing*, **16**, 1999-2021.

St-ONGE, B. A., and CAVAYAS, F., 1997, Automated forest structure mapping from high resolution imagery based on directional semivariogram estimates. *Remote Sensing of Environment*, **61**, 82-95.

TREITZ, P., and HOWARTH, P., 2000, High spatial resolution remote sensing data for forest ecosystem classification: an examination of spatial scale. *Remote Sensing of Environment*, **72**, 268-289.

WANG, G., POSO, S., WAITE, M.-L. and HOLOPAINEN, M., 1998, The use of digitized aerial photographs and local operation for classification of stand development classes. *Silva Fennica* **32**, 215-225.

WEILER, J. M. N., and STOW, D. A., 1991, Spatial analysis of land cover patterns and corresponding remotely-sensed image brightness. *International Journal of Remote Sensing*, **12**, 2237-2257.

WOODCOCK, C. E., and STRAHLER, A. H., 1987, The Factor of Scale in Remote Sensing. *Remote Sensing of Environment*, **21**, 311-332.

WOODCOCK, C. E., STRAHLER, A. H., and JUPP, D. L. B., 1988a, The use of variograms in remote sensing: I. Scenes models and simulated images. *Remote Sensing of Environment*, **25**, 323-348.

WOODCOCK, C. E., STRAHLER, A. H., and JUPP, D. L. B., 1988b, The use of variograms in remote sensing: II. Real digital images. *Remote Sensing of Environment*, **25**, 349-379.

WULDER, M. A., LeDREW, E. F., FRANKLIN, S. E., and LAVIGNE, M. B., 1998, Aerial image texture information in the estimation of northern deciduous and mixed wood forest Leaf Area Index (LAI). *Remote Sensing of Environment*, **64**, 64-76.

8.0 CONCLUSIONS

8.1 Summary and Conclusions

Gong *et al.* (1997) distinguish between two types of remote sensing research; those that use what they describe as the 'decomposed' approach (leaf/shoot/branch optical properties and scaling-up using models) and the *in situ* hyperspectral approach for species recognition and characterisation. These workers consider the latter approach to 'provide more insights into the practical use of remote sensing'. The present study commenced very much with this philosophy in mind, but later considered the 'decomposed' approach as a way of tackling questions that could only be answered with an unrealistic fieldwork effort. Interestingly, in their conclusion, Gong *et al.* (1997), clearly state that they will need to collect more field data under a wider range of conditions in order to answer their research hypotheses. No doubt, more data would also provide further insights into the use of remote sensing for monitoring Scots pine regeneration. However, this study has achieved its objective of addressing the current lack of information on the spectral and spatial properties of natural pine regeneration. In particular, the lack of detailed canopy and needle measurement for Scots pine has been addressed. The ground-based approach has also required careful consideration of how measures of pine sapling amount are best measured on the ground.

Percentage cover was relatively quick to measure compared to LAI. In this study it was only necessary to measure the diameter of the crown base of each sapling within the eight 5 x 5 m sample plots containing saplings. Percentage cover was then obtained by assuming a circular shape of the crowns in plan-view, calculating individual crown cover and summing these values for each of the saplings within the

sample plots. For estimating percentage cover over the whole study site a classification approach could be used for digitised aerial photography (as in Chapter 7), or airborne imagery. The main requirement would be that the spatial resolution is H-resolution with respect to the sapling crown sizes. Clearly, percentage cover estimates will be more accurate with a greater number of pixels within each sapling crown.

Since regeneration over a whole site is unevenly distributed, with higher density clumps and larger areas of lower density regeneration, a preferred approach would be to delineate these areas prior to classification. This would be a useful first-step for monitoring regeneration at any site and would lead to a base-map of regeneration at the site, which could be used for future monitoring efforts. Digitised large-scale colour aerial photographs, or aerial digital photography, could be interpreted visually for this purpose and incorporated directly into a GIS. Within these delineated areas a per-pixel classification would be improved using broad band colour-infrared (CIR) photography to classify saplings using a red/NIR vegetation index, and then predict percentage cover (e.g. Haddow *et al.*, 2000). However, individual tree counts would not be possible in the denser regions of regeneration because of the high degree of clumping and crown overlap within natural regeneration sites.

LAI is a more complete measure of sapling amount and canopy structure than percentage cover and is therefore a preferred measure with which to monitor regeneration. It is also more ecologically meaningful since it relates to physiological processes such as photosynthesis, transpiration, evapotranspiration and productivity (Nel and Wessman, 1993; Chen *et al.*, 1997). The estimation of LAI over a whole regeneration site would be more problematic than for percentage cover. The method developed and described in Chapter 4 involving exhaustive sampling of saplings and a scaling-up of needle surface area based on a regression on needle length enabled sample plot LAI estimation. It was concluded that other direct methods were either inappropriate for saplings or too time-consuming, whilst indirect methods involving optical measurements of canopy gaps would be too inaccurate for natural pine regeneration sites.

These conclusions provide a strong argument for the estimation of LAI at regeneration sites using remote sensing. This study has found that the NIR/Red and NDVI indices correlate strongly with pine sapling LAI. Since LAI at regeneration sites is relatively low in comparison with mature managed forest stands, these relationships were linear. Problems have been encountered when predicting LAI for stands with high LAI because such relationships are curvilinear and become asymptotic at higher LAI values (e.g. Nemani *et al.*, 1993; Turner *et al.*, 1999). This is because NIR reflectance decreases in older closed-canopy stands. In the SWIR, reflectance at 1630 nm was found to relate strongly and negatively with LAI. Since NIR reflectance relates strongly and positively with LAI, it was theorised that correlation might be improved by combining these opposing relationships. The ratio $SWIR_{1630}/NIR_{850}$, did improve the correlation with LAI of both the NIR and SWIR reflectance alone, but did not provide an improvement to the correlation with the NIR/Red and NDVI indices.

The ability to predict LAI using these simple ratios has advantages for monitoring regeneration because they require relatively simple image processing operations, and a low spectral resolution sensor could be used. For example, broad band CIR photography could be used for this purpose, particularly at floristically simple sites where confusion with other tree species and the influence of understorey reflectance is minimal.

High-spectral resolution data offers the potential for species discrimination and the employment of derivative spectroscopy for noise reduction. This may be particularly important at floristically more complex sites. Strong correlation was found between pine sapling LAI and the derivative red-edge peaks at 719 and 703 nm and on the derivative trough at 1150 nm. It was concluded that the red-edge peak at shorter wavelengths was controlled primarily by canopy chlorophyll content, whilst the peak at longer wavelengths was controlled by both canopy chlorophyll content and canopy structure. A ratio of derivative reflectance at these red-edge features, together with a ratio of derivative reflectance at the red-edge peak shoulders (D_{730}/D_{700}), also

correlated strongly with pine sapling LAI. D_{1150} had a strong negative correlation with LAI and percentage cover, and this feature was more pronounced than the red-edge feature, with greater separation between the values for each plot. The main control on this feature is likely to be canopy water content (e.g. Rollin and Milton, 1998), which is directly related to LAI. These derivative indices would be particularly suited for estimating LAI at regeneration sites because of their insensitivity to background reflectance and their selectivity for the pine signal.

Airborne hyperspectral imaging sensors would be most suitable for applying these indices to monitoring regeneration, although there may be issues relating to positional accuracy, radiometric calibration and atmospheric correction. The importance of well-calibrated imagery increases for monitoring applications, where measurement of change is required. The applicability of scaling-up these narrow-band indices to airborne imagery would need to be tested. A further problem might be the issue of the competing requirements for high spatial and high spectral resolution imagery. Positional accuracy is also likely to be compromised at the low air-speeds required to achieve a good signal-to-noise ratio with a combined high spatial resolution.

Seasonal variation in understorey canopy colour did not affect the strength of the correlation between percentage cover or LAI and the spectral wavelength and indices investigated. This was due the low productivity of the heather dominated understorey and the absence of other significant herb or grass species. However, in general, the collection of hyperspectral data over regeneration sites is likely to be most favourable in April or May in Scotland, before the new green growth of other species emerges.

The red-edge position (REP) did not correlate as strongly with LAI as the other red-edge indices. The reason for this was related to the relatively small differences in LAI between the sample plots. The lowest value in plot 2, which contained seedlings was just 0.02, whilst the highest LAI value in plot 5 was 0.90. At the lowest values of LAI, the red-edge peak is at the shorter wavelength component at 703 nm. At the

highest values it red-edge peak is at the longer wavelength component at 720 nm. However, there is not a smooth progression to longer wavelengths through the LAI values between the lowest and highest values. Rather, a switching of the dominant peak from the shorter wavelength component to the longer wavelength component was observed over this LAI range. The result was a poorer REP/LAI relation than might have been expected, given the results from previous work (e.g. Gong *et al.*, 1992) and the modelled results in the present study. The FLIGHT model confirmed that the main control on REP is LAI and that REP is insensitive to canopy cover. However, the LAI values investigated in relation to REP by Gong *et al.* (1992) and the modelling in the present study used a much wider range of LAI values than those in the sample plots. It is therefore concluded that REP is more appropriate for predicting LAI of older stands, and is not recommended for predicting LAI at regeneration sites. REP is also sensitive to the width of smoothing functions used in computing derivative spectra and this should be taken into account when comparing results from different studies for similar forest canopy types.

The modelled plot spectra generated using the FLIGHT model allowed comparison with the field spectral measurements. The main advantage of the modelling approach is the ability to analyse the influence of a single canopy structural parameter, whilst all other parameters remain constant; thereby creating scenarios that are very difficult to achieve in the field. Although the scenarios sometimes had unrealistic levels of LAI and percentage cover for regeneration sites, they did allow trends to be observed.

The model also validated the reasoning for the choice of vegetation indices proposed from the correlation analysis of field spectral data. The modelled results produced a positive relation between DREPmax (the maximum derivative value of the red-edge feature used to define REP) and LAI. Conversely, there was a negative relation between the modelled D703 reflectance and LAI. By combining the derivative red-edge value at the longer wavelengths with the component at shorter wavelengths the sensitivity to pine sapling LAI is maximised.

The model also confirmed that reflectance in the NIR (R850) increases with increasing LAI, whilst the R680 red reflectance decreases with increasing LAI. It was concluded that the mechanism of opposing relationships of increasing canopy structure giving increasing R850 values, and increasing chlorophyll content giving decreasing R680 values, generate the high correlation between LAI and the NDVI and SR indices. The modelled results also suggested that only the derivative values representing the limbs of the green reflectance peak were sensitive to percentage cover, but insensitive to LAI.

Although strong relationships between measured reflectance and pine sapling amount (as LAI) have been demonstrated in this study, there remained issues relating to the distribution of LAI within a sample area. Since information on the stage of regeneration is of use to conservation managers, it was considered important to try to distinguish between plots of similar LAI values, but differing tree size. The model was used to investigate the effects of changing tree number and crown size (and hence crown needle density), whilst keeping LAI, percentage cover and all other model parameters constant. Modelled results showed that the effect of changing crown height/crown needle density was much smaller than changing LAI or percentage cover. R850, R550, R680, D703 and DREPmax all showed a weak trend of increasing reflectance with increasing crown needle density.

The implication of these results is that it would be difficult to draw conclusions about the size of trees from spectral data alone. Furthermore, these results were consistent for different stand density scenarios, so that a single larger tree will be spectrally similar to many smaller trees for a sample area with the same LAI and percentage cover values. The weak trends that were observed are likely due to the changes in proportion of shaded crowns and crown geometry within each modelled scenario. Another important consideration is the model itself, which treats each tree crown as a turbid medium and the within-crown non-random structural parameters such as the arrangement of needles on shoots and the clumped distribution of shoots on branches was not explicitly modelled.

Modelled reflectance was compared with mean seasonal reflectance (MSR) of the sample plots. The shape of the plot MSR spectra, as described by the first-order derivative, was well represented by the modelled first-derivative spectra. Modelled reflectance values were generally overestimated in the blue region, and NIR was underestimated for plot 5 with highest density of regeneration. This was also likely due to the non-random arrangement of the needles and shoots which was not represented by the model.

Detailed measurements of the optical properties of Scots pine needles from the study area were used as the model input data. The measurement method used followed the gap-fraction/image analysis technique described by Mesarch *et al.* (1999), but was adapted for use with a medium-cost laboratory dual-beam spectrophotometer, fitted with an internal integrating sphere accessory. Error within the method was < 2% across the 400 to 1000 nm wavelength range of the instrument. It was concluded that the largest source of error was associated with the mask alignment when imaging the gap fraction of the sample and particular care is required at this task.

The reflectance and transmittance spectra of Scots pine needles were very similar to the measurements of Mesarch *et al.* (1999) for Jack pine. The main difference was that the Scots pine needle spectral features, such as the green reflectance peak, the chlorophyll absorption well and the red-edge position, were red-shifted by 5-10 nm over the Jack pine spectra. Scots pine needle REP was at 706 nm, and the chlorophyll absorption well was at 679 nm. For canopy reflectance models, where the primary data input are the optical properties of the smallest optical unit within the canopy (the leaf or needle), and which are then scaled-up to canopy reflectance, such measurements are fundamental to model accuracy. However, the influence on canopy reflectance of larger structural elements of the canopy, such as the arrangement of the needles, shoots and branches, as well as the arrangement of individual trees, are also important considerations.

The arrangement, shape and size of individual trees within an image scene also influence the textural properties of an image. Geostatistical analysis of digitized

colour aerial photographs was used to characterise the textural properties of different stages of natural Scots pine regeneration. The semivariogram sill value, which is related to overall image variance, allowed separation of regeneration stage based on forest texture. For this purpose, an optimal spatial resolution of between 1.0 and 2.0 m is recommended, which is slightly L-resolution with respect to the mean crown width of saplings within regeneration plots.

The range parameter was influenced by the size of gaps in the canopy (percentage cover), tree size and the degree of clumpiness. Perpendicular (i.e. to the Sun's rays) directional semivariograms from H-resolution images are recommended for estimating within-plot structural variables, such as mean crown size. When very strong directional anisotropy exists, as in the case of plantation forestry, the across-row directional semivariogram range most closely approximated mean crown size. However, since this relationship was sensitive to image pixel resolution, the analysis of multi-stage forest compartments may require a range of pixel sizes to relate the range parameter accurately to crown width, which may not be practicable.

There is clearly a great deal of information to be retrieved from the spatial domain of images. Of particular use, is the potential demonstrated in this study to identify regeneration stage, which was shown to be uncertain through spectral analysis. A major benefit of such spatial analysis techniques using digitized aerial photography is the relatively low processing requirement of the images. However, image calibration would be required where regeneration stretches across a whole photograph. This is because two similar forest types at different sides of a photograph may have different textural properties, due primarily to exposure fall-off (Holopainen and Wang, 1998). A further requirement is for good ground-positional accuracy and careful orthorectification of photographs.

Although aerial sources of data are recommended for site-specific monitoring, there may be a role to play from recent advancements in satellite imagery. For example, the Ikonos satellite offers spatial resolution as high as 1 m in panchromatic mode. Such data may allow spatial analysis of landscapes using methods like the

geostatistical approach taken in this study, whilst also providing greater spatial coverage than aerial data. Ikonos also produces 4 m multispectral data, which still needs to be explored for its potential in landscape monitoring. Given that the quality of satellite imagery is likely to improve, and the cost likely to decrease, there is potential for its use within routine forest monitoring. The low number of cloud-free days however, remains a particular problem when applying optical satellite imagery to monitoring landscapes in Scotland.

Monitoring of natural regeneration presents a major challenge for remote sensing because it combines many of the recurring problems encountered when seeking to use the technology for applied purposes. These include problems associated with scales of observation, mixed pixels, vertical stratification and lateral heterogeneity of the canopy, canopy gaps and clumping, graded boundaries and edge detection. This list, amongst others, must be added to whatever problems are already associated with remote sensing of managed forest compartments. This spiral of complexity has led to a fusion of remote sensing techniques with the emerging discipline of landscape ecology. In short, the solution to monitoring natural landscapes lies in an acceptance that an integration of disciplines is required, and this study has demonstrated that remote sensing techniques may provide an important contribution.

8.2 References

CHEN, J. M., RICH, P. M., GOWER, S. T., NORMAN, J. M., and PLUMMER, S., 1997, Leaf area index of boreal forests: Theory, techniques, and measurements. *Journal of Geophysical Research*, **102**, No.D24, 29,429-29443.

GONG, P., PU, R., and MILLER, J. R., 1992, Correlating leaf area index of Ponderosa pine with hyperspectral CASI data. *Canadian Journal of Remote Sensing*, **18**, 275-292.

GONG, P., PU, R., and YU, B., 1997, Conifer species recognition: An exploratory analysis of *in situ* hyperspectral data. *Remote Sensing of Environment*, **62**, 189-200.

HADDOW, K. A., KING, D. J., POULIOT, D. A., PITT, D. G., and BELL, F. W., 2000, Early regeneration conifer identification and competition cover assessment using airborne digital camera imagery. *The Forestry Chronicle* **76**, 915-928.

HOLOPAINEN, M., and WANG, G., 1998, The calibration of digitized aerial photographs for forest stratification. *International Journal of Remote Sensing*, **19**, 677-696.

MESARCH, M. A., WALTER-SHEA, E. A., ASNER, G. P., MIDDLETON, E. M., and CHAN, S. S., 1999, A revised measurement methodology for conifer needles spectral optical properties: evaluating the influence of gaps between elements. *Remote Sensing of Environment*, **68**, 177-192.

NEL, E. M. and WESSMAN, C. A., 1993, Canopy transmittance models for estimating forest leaf area index. *Canadian Journal of Forest Research*, **23**, 2579-2586.

NEMANI, R., PIERCE, L., and RUNNING, S., 1993, Forest ecosystem processes at the watershed scale: sensitivity to remotely-sensed Leaf Area Index estimates. *International Journal of Remote Sensing*, **14**, 2519-2534.

ROLLIN, E. M., and MILTON, E. J., 1998, Processing of high spectral resolution reflectance data for the retrieval of canopy water content information. *Remote Sensing of Environment* **65**, 86-92.

TURNER, D. P., COHEN, W. B., KENNEDY, R. E., FASSNACHT, K. S., and BRIGGS, J. M., 1999, Relationships between Leaf Area Index and Landsat TM spectral vegetation indices across three temperate zone sites. *Remote Sensing of Environment*, **70**, 52-68.

APPENDIX

Paper published in the International Journal of Remote Sensing, 1998, Vol. 19, No. 13, 2601-2608.

INT. J. REMOTE SENSING, 1998, VOL. 19, NO. 13, 2601–2608

High-spectral resolution data for monitoring Scots pine (*Pinus sylvestris* L.) regeneration

D. T. SHAW, T. J. MALTHUS

Department of Geography, University of Edinburgh, Drummond Street, Edinburgh EH8 9XP, Scotland, UK

and J. A. KUPIEC

The Environment Agency, National Centre for Environmental Data & Surveillance, Lower Bristol Road, Bath, BA2 9ES, England, UK

(*Received 6 February 1998; in final form 7 May 1998*)

Abstract. High-resolution field spectroradiometric measurements were used to investigate the spectral properties of naturally regenerating Scots pine (*Pinus sylvestris* L.) in relation to sapling cover and season. Ratios of reflectance (R_{757}/R_{722}) and first-derivative reflectance (D_{719}/D_{703} and D_{730}/D_{700}) in the red-edge region correlated most strongly with increasing sapling cover. The main control on these ratios was the contrast between the biomass of heather and pine saplings. At the site investigated, the strength of the correlation of reflectance ratios with sapling cover was not affected by seasonal changes in canopy colour.

1. Introduction

The measurement of change in the composition and quantity of semi-natural vegetation using remote sensing has been slow to develop. The main challenge has been that different habitat types may exhibit similar spectral properties, which also change with scale and season. The result is that quantitative ecological interpretation of canopy variables becomes confounded. Consequently, applications of remotely sensed data to semi-natural vegetation have been confined to mapping broad habitat types (e.g. Hubbard and Wright 1982, Belward *et al.* 1990). A threefold approach is required: increased habitat-type discrimination using high spectral resolution data; the determination of appropriate scales of observation and; an understanding of the nature and magnitude of changes in reflectance because of seasonal vegetation change.

For monitoring changes in natural Scots pine regeneration, high spectral resolution data collected at an appropriate spatial resolution has the potential to distinguish pine sapling cover from background reflectance, and to quantify the amount of cover. This Letter examines high spectral resolution spectroradiometric data for relations between reflectance and first-order derivative indices and increasing Scots pine sapling cover. Derivative spectroscopy was used to fully investigate the shape of the high spectral resolution spectra and to take advantage of the suppression of background signals (e.g. Demetriades-Shah *et al.* 1990). The effect of seasonal variation in understorey vegetation reflectance and its influence on the estimation of sapling cover is also examined.

2. Methods

The study area (Inshriach, 57° 08 N, 3° 51 W) lies at 280 m in the Spey valley on the western margin of the Cairngorm National Nature Reserve. The area is now managed for the re-establishment of native pine woodland, which is taking place by means of natural regeneration. Pine seedlings and saplings up to about 15-years old and 2 m in height are scattered throughout the area (Shaw 1997).

The sapling cover within nine 5 m by 5 m plots was estimated by measuring the width of foliage on each sapling as viewed from above. These measurements were summed to estimate the proportion of ground covered by saplings (as percentage cover) in each plot, as viewed by a sensor at nadir.

Measurements of canopy reflectance were obtained using a GER 1500™ spectroradiometer (300 nm–1100 nm range; 3 nm spectral resolution; 1·5 nm spectral sampling interval). A 15° foreoptic was used, and the spectroradiometer was mounted on a stand 1·5 m above the canopy to give a 0·4 m field-of-view. Twenty-five measurements were recorded systematically for each of the nine sample plots within a 25-cell grid, and normalised against a calibrated Spectralon™ reference panel. The sampling was repeated throughout 1997 on 31 March, 16 May, 1 June, 5 July, 23 September and 31 October. To reduce the effects of low Sun angle, shadow and longer atmospheric pathlengths, scans were recorded within two hours either side of the solar noon. Sky conditions were clear for sampling dates in May, June and September; overcast but unchanging light conditions in March and July and variable in October.

3. Results and discussion

3.1. *Reflectance and derivative spectra*

A mean of the 25 absolute reflectance spectra for each sample plot was used to represent the plot reflectance signatures at each sampling date. The mean plot spectra were further processed to first-order derivative spectra using quadratic polynomial functions fitted by least squares over a 9-nm interval (Savitzky and Golay 1964). The shape of the mean reflectance and derivative spectra revealed a clear distinction between plots with varying sapling cover (figure 1). In particular, the influence of pine was notable as increased near-infrared (NIR) and green wavelength reflectance, but decreased reflectance due to chlorophyll absorption in the red wavelengths.

The derivative spectra, which compare the variation in the shape of the reflectance spectra, illustrate two principal spectral features. Firstly, the inflection point of the ascending limb of the green reflectance peak is represented by a derivative maximum ($\lambda_{\sim 520\,\mathrm{nm}}$), whilst the inflection point of the descending limb is represented by a derivative minimum ($\lambda_{\sim 570\,\mathrm{nm}}$). Secondly, the red-edge inflection point was characterised by two maxima in the derivative spectra; ~ 703 nm (D_{703}) and ~ 719 nm (D_{719}). Figure 1 (*b*) illustrates that the second maximum (at the longer wavelength) becomes dominant with increased sapling cover. This trend is usefully described as a ratio of the two peaks (D_{719}/D_{703}) in relation to sapling cover.

A correlation matrix was used to compare the correlation coefficients for every simple wavelength ratio within the reflectance and derivative spectra that relate to changes in pine sapling cover. Within the reflectance data, the ratio of reflectance at 757 and 722 nm (R_{757}/R_{722}) had the highest correlation coefficient when data from four sampling dates were combined. Within the derivative data, the ratio of derivative reflectance at 730 and 700 nm (D_{730}/D_{700}) had the highest correlation coefficient for the combined data. These two indices were therefore selected for the study, in addition to those derived from the spectral features already identified in figure 1.

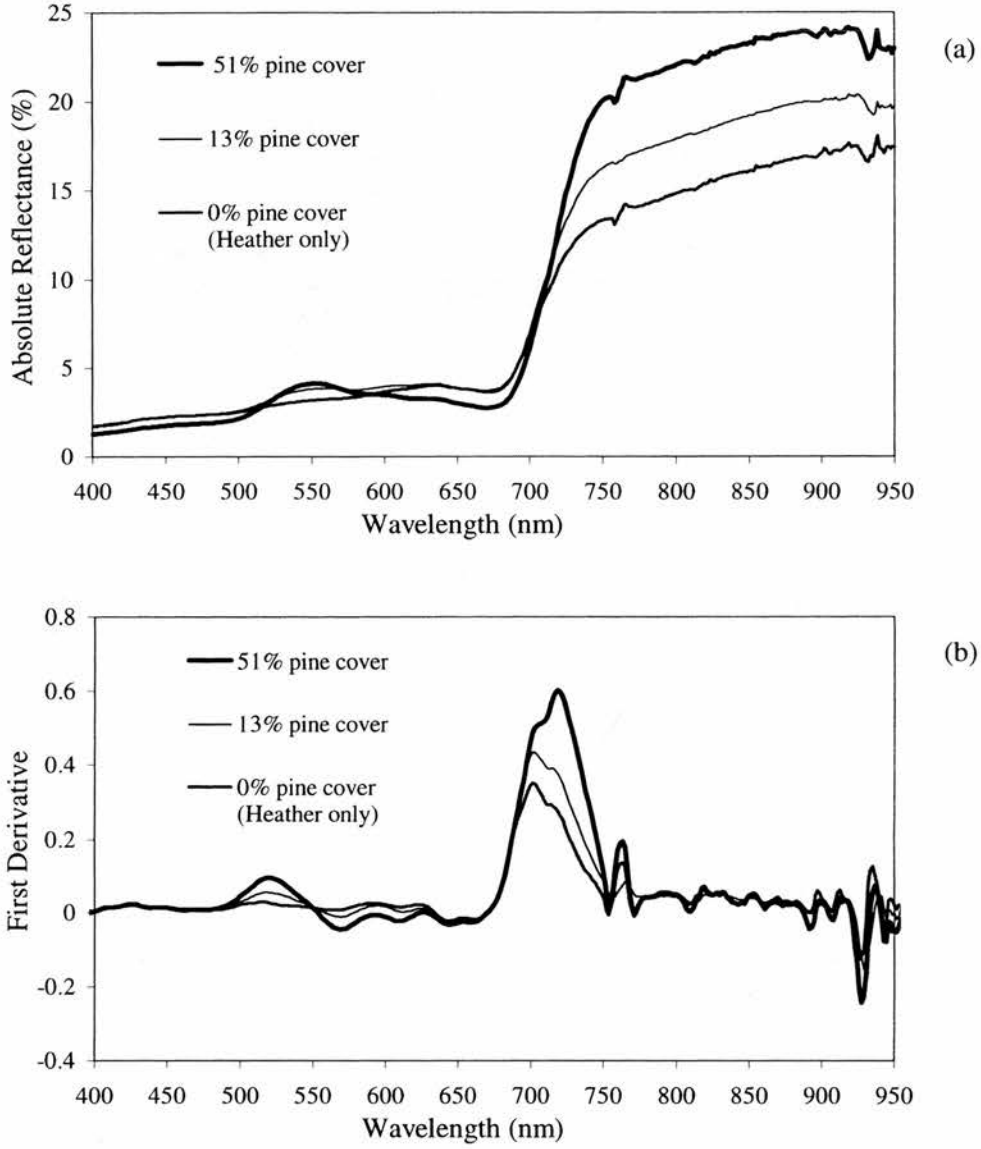

Figure 1. Typical mean (*a*) reflectance spectra, and (*b*) first-derivative spectra for plots with different degrees of sapling density ($n=25$). The 51% cover plot represents the greatest cover of regeneration measured. Measurements from March 1997.

3.2. *Relation between reflectance indices and sapling cover*

The NIR/Red and NDVI (Normalised Difference Vegetation Index) indices both had a strong correlation with sapling cover, but the ratio R_{757}/R_{722} had the strongest correlation at each sampling date (table 1). Correlation coefficients were less significant for the single values at R_{670} and R_{800}, than for indices involving combinations of wavelengths. This is to be expected, since indices involving combinations of wavelengths may reduce background variability in absolute reflectance (e.g. Malthus

Table 1. Linear correlation coefficients (r) between percentage cover of pine and plot mean reflectance for selected indices.

Wavelength (nm)	March	May	June	July	Sept.	October
Reflectance feature						
R_{550}	0·40 n.s.	0·40 n.s.	−0·22 n.s.	0·65*	0·48 n.s.	−0·17 n.s.
R_{670}	−0·86**	−0·78**	−0·85**	−0·57 n.s.	−0·91***	−0·79**
R_{800}	0·81**	0·66*	0·76**	0·87**	0·75**	0·57 n.s.
NIR_{800}/Red_{670}	0·97***	0·88***	0·97***	0·95***	0·90***	0·95***
NDVI	0·97***	0·93***	0·97***	0·93***	0·96***	0·91***
R_{757}/R_{722}	0·97***	0·97***	0·97***	0·97***	0·96***	0·93***
1st Derivative feature						
REP	0·73*	0·90***	0·82**	0·67*	0·75**	0·67**
$\lambda_{\sim 520}$†	0·96***	0·89***	0·83**	0·89***	0·83**	0·59*
$\lambda_{\sim 570}$†	−0·98***	−0·94***	−0·92***	−0·93***	−0·91***	−0·87**
D_{719}	0·92***	0·85**	0·91***	0·90***	0·85**	0·77**
D_{703}	0·65*	0·59*	0·76**	0·82**	0·59*	0·47 n.s.
D_{719}/D_{703}	0·95***	0·99***	0·97***	0·96***	0·97***	0·92***
D_{730}/D_{700}	0·98***	0·99***	0·99***	0·96***	0·99***	0·91***

*$p<0·05$; **$P<0·01$; ***$p<0·001$; n.s. not significant at the $p<0·05$ confidence level.
†Maximum and minimum values derived irrespective of wavelength but at approximately 520 and 570 nm respectively.
$n=9$ in each case.

et al. 1993). The reflectance peak at R_{550} had no significant correlation with sapling cover, except in July when the correlation was only weakly significant.

Several workers have reported that the relation between vegetation amount, such as Leaf Area Index (LAI) and vegetation indices such as the NDVI and NIR/red ratio, breaks down with decreasing canopy closure (e.g. Spanner *et al.* 1990, Baret 1995). This has been attributed to the confounding effects of understorey reflectance in more open stands. When considering areas of regeneration however, it may be more useful to think of the saplings as modifying the reflectance of the background matrix vegetation (Franklin 1986). It is likely that the contrast between the high chlorophyll content of the saplings and the low content of the heather maintains the strong relation between sapling cover and reflectance indices. Furthermore, the complex and clumped structure of the sapling foliage against the background heather contributes to the contrast in NIR reflectance for areas of different density observed in figure 1. These contrasts in both chlorophyll concentration and canopy structure explain the strong relation between sapling cover and vegetation indices for this essentially bimodal canopy. This theory is further supported by the strong linear relation with the R_{757}/R_{722} ratio at the red-edge (figure 2 (*a*)); a region governed by this influence of saplings on both the NIR and red reflectance.

Areas of regeneration with a more complex mix of species are likely to offer less reliable spectral measures of sapling density. For example, purple moor-grass (*Molinia caerulea* (L.) Moench), bracken (*Pteridium aquilinum* (L.) Kuhn), juniper (*Juniperus communis* L.) and blaeberry/bilberry (*Vaccinium myrtillus* L.) all display a similar spectral response to saplings in the red and NIR, depending on the season (data not shown).

3.3. *Relation between derivative indices and sapling cover*

Correlation coefficients presented in table 1 for derivative indices are high for both the green and red-edge spectral features. There is generally a slightly stronger relation between sapling cover and $\lambda_{\sim 520\,nm}$ than for $\lambda_{\sim 570\,nm}$, but the red-edge indices D_{719}/D_{703} and D_{730}/D_{700} have the strongest linear relation with sapling cover (figures 2(*b*) and (*c*)). The largest slope was obtained for D_{730}/D_{700}, making this a stronger model for cover estimation; there is a larger increment in reflectance for every increase in percentage cover.

Notably, the second red-edge peak (D_{719}), which is observed to increase with sapling cover, is more strongly correlated than the first peak (D_{703}). Clearly, the derivative reflectance at the second red-edge peak is controlled by the proportion of pine measured by the sensor. This is in agreement with previous work on biphasic red-edge features of both leaf and canopy spectra. For example, it has been suggested that the peak at the shorter wavelength is controlled primarily by chlorophyll concentration, whilst the second peak is controlled by both chlorophyll concentration and a leaf stacking component (Horler *et al.* 1983, Ferns *et al.* 1984, Boochs *et al.* 1990). In the context of the pine sapling canopy, the leaf stacking, or increased depth of green biomass, increases the contribution to NIR reflectance due to scattering.

Derivative spectra have been shown to eliminate the effects of background and non-target signals (Demetriades-Shah *et al.* 1990) but have also enabled the red-edge position (REP) to be studied in relation to leaf and canopy variables. For example, Danson and Plummer (1995) reported a strong relation between REP and LAI for coniferous plantations. Table 1 illustrates that REP (defined as the maximum derivative red-edge peak) had a strong positive relation with percentage cover of

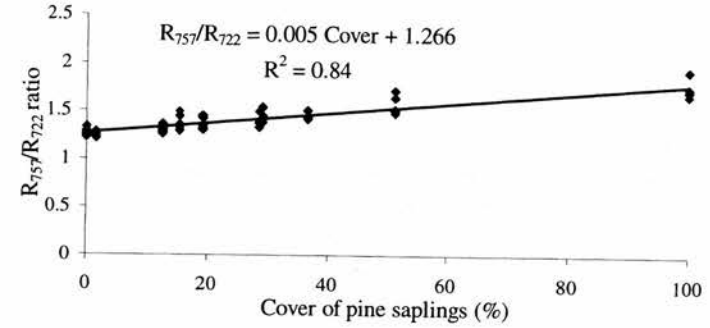
R_{757}/R_{722} = 0.005 Cover + 1.266
R^2 = 0.84
R_{757}/R_{722} ratio
Cover of pine saplings (%)

(a)

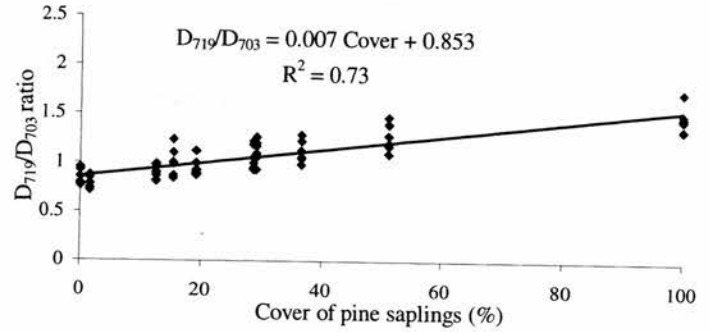
D_{719}/D_{703} = 0.007 Cover + 0.853
R^2 = 0.73
D_{719}/D_{703} ratio
Cover of pine saplings (%)

(b)

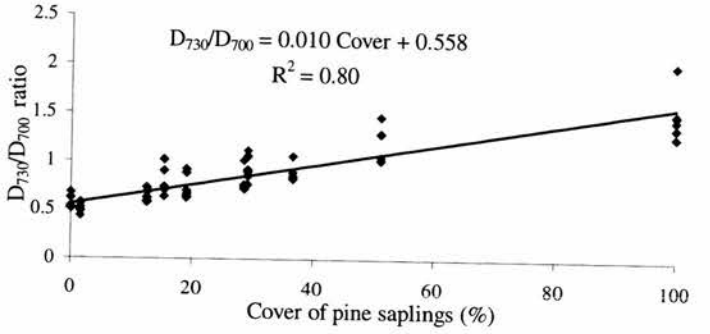
D_{730}/D_{700} = 0.010 Cover + 0.558
R^2 = 0.80
D_{730}/D_{700} ratio
Cover of pine saplings (%)

(c)

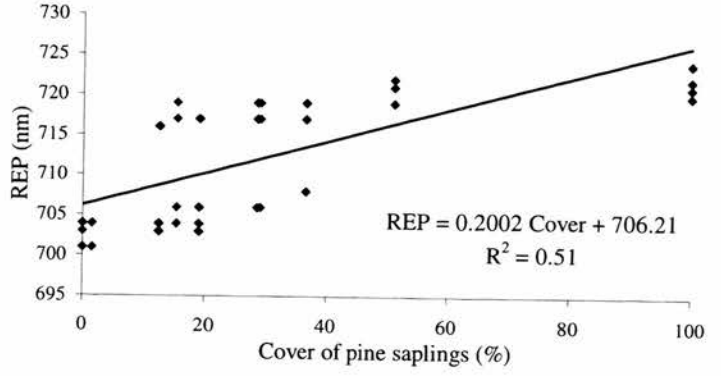
REP = 0.2002 Cover + 706.21
R^2 = 0.51
REP (nm)
Cover of pine saplings (%)

(d)

pine, although not as strong as the ratio derivative indices. Figure 2 (*d*) combines all the data in one linear regression and illustrates that a derivative maximum may exist at either ~704 nm, or at ~716 nm when pine cover is between about 15 and 40%. The definition of REP as the maximum derivative peak assumes that there is a linear progression from shorter wavelengths (~701 nm) to longer wavelengths (~720) with increasing cover. This is not the case since the peak position switches from shorter to longer wavelength is between 15 and 40% cover.

To predict percentage cover using REP without ambiguity, one alternative might be to use one regression for each peak; where REP is 706 nm or below, use the relation with the left peak and if 716 nm or above, use the relation with the right peak. However, the ratios D_{730}/D_{700} and D_{719}/D_{703} have several advantages over the REP for predicting cover of pine. Firstly, REP is affected by variable illumination conditions, whereas a ratio of reflectance at specific wavelengths helps to eliminate this effect. Secondly, the derivative peak ratios include information within both peak wavelength regions, regardless of cover value. Thirdly, the wavelengths at 719 nm and 703 nm are selected for the strong influence on reflectance that pine and heather have at these wavelengths. The ratio should therefore be selective for the target signal. Moreover, previous work suggests that REP is independent of cover (Horler *et al.* 1983), but sensitive to measures of canopy depth such as LAI (Ferns *et al.* 1984). It is suggested therefore, that for measuring changes in pine sapling cover within heather moorland, REP will be a less useful indicator than a red-edge ratio of reflectance values.

3.4. *Relation with seasonal change*

It had been expected that the seasonal greening of the heather would affect background reflectance and, therefore, the correlation between reflectance indices and pine cover. However, very little seasonal variation in the correlation coefficients was observed (table 1). This may be due in part, to the late growth phase of the heather at the study site and its concomitant low rate of biomass production (Gimingham 1972), coupled with the poor soils in the region. The saplings underwent a flush of growth in July, which may explain the only significant correlation with R_{550} in this month. However, none of the indices involving combinations of wavelengths were affected by this flush. Due to the floristic simplicity of the study area, perennial grass and herb species did not affect the correlation of the indices described with sapling cover. Future work will incorporate sampling in late August when the heather canopy colour alters due to flowering.

4. Conclusion

There is clear potential for monitoring changes in sapling cover using high spectral resolution indices in the red-edge spectral region. Reflectance at these wavelengths is particularly sensitive to the contrast between sapling and heather green leaf amount. It was found that the relative proportion of the two derivative red-edge maxima (D_{719}/D_{703}) and of the derivative red-edge shoulders (D_{730}/D_{700}), hold more

Figure 2. Relation between sapling cover and the ratios (*a*) R_{757}/R_{722}, (*b*) D_{719}/D_{703}, (*c*) D_{730}/D_{700}, and (*d*) Red-edge position (REP) with linear regression models fitted. Data from all sampling dates used. 100% cover was simulated using a mean of repeated measurements over a single healthy sapling on each sampling date.

information about the relative proportion of the species than the red-edge position or single wavelength indices. Further work will need to consider the appropriate scales of observation at which these indices should be applied.

Acknowledgments

This research was supported by NERC through MRes Award GT23/96/9/C and Studentship GT/97/84/EO. The GER 1500 was obtained on loan from the NERC Equipment Pool for Field Spectroscopy, whose assistance and advice is acknowledged. Fieldwork was supported by Scottish Natural Heritage.

References

BARET, F., 1995, Use of spectral reflectance variation to retrieve canopy biophysical characteristics. In *Advances in Environmental Remote Sensing*, edited by F. M. Danson and S. E. Plummer (Chichester: Wiley & Sons), pp. 33–52.

BELWARD, A. S., TAYLOR, J. C., STUTTARD, M. J., BIGNAL, E., MATHEWS, J., and CURTIS, D., 1990, An unsupervised approach to the classification of semi-natural vegetation from Landsat Thematic Mapper data: a pilot study on Islay. *International Journal of Remote Sensing*, **11,** 429–445.

BOOCHS, F., KUPFER, G., DOCKTER, K., and KÜHBAUCH, W., 1990, Shape of the red edge as vitality indicator for plants. *International Journal of Remote Sensing*, **11,** 1741–1753.

DANSON, F. M., and PLUMMER, S. E., 1995, Red-edge response to forest leaf area index. *International Journal of Remote Sensing*, **16,** 183–188.

DEMETRIADES-SHAH, T. H., STEVEN, M. D., and CLARK, J. A., 1990, High resolution derivative spectra in remote sensing. *Remote Sensing of Environment*, **33,** 55–64.

FERNS, D. C., ZARA, S. J., and BARBER, J., 1984, Application of high resolution spectroradiometry to vegetation. *Photogrammetric Engineering and Remote Sensing*, **50,** 1725–1735.

FRANKLIN, J., 1986, Thematic Mapper analysis of coniferous forest structure and composition. *International Journal of Remote Sensing*, **7,** 1287–1301.

GIMINGHAM, C. H., 1972, *Ecology of Heathlands* (London: Chapman and Hall).

HORLER, D. N. H., DOCKRAY, M., and BARBER, J., 1983, The red edge of plant leaf reflectance. *International Journal of Remote Sensing*, **4,** 273–288.

HUBBARD, N. K., and WRIGHT, R., 1982, A semi-automated approach to land cover classification of Scotland from Landsat. *Proceedings of the Annual Conference of the Remote Sensing Society, Liverpool, 15–17 December, 1982* (Nottingham: Remote Sensing Society), pp. 212–221.

MALTHUS, T. J., ANDRIEU, B., DANSON, F. M., JAGGARD, K. W., and STEVEN, M. D., 1993, Candidate high spectral resolution infrared indices for crop cover. *Remote Sensing of Environment*, **46,** 204–212.

SAVITZKY, A., and GOLAY, M. J. E., 1964, Smoothing and differentiation of data by simplified least squares procedures. *Analytical Chemistry*, **36,** 1627–1639.

SHAW, D. T., 1997, Remote Sensing for monitoring natural regeneration of Scots Pine (*Pinus sylvestris* L.) in the Cairngorms. Unpublished MRes. thesis, Department of Geography, University of Edinburgh.

SPANNER, M. A., PIERCE, L. L., PETERSON, D. L., and RUNNING, S. W., 1990, Remote sensing of temperate coniferous forest leaf area index: The influence of canopy closure, understorey vegetation and background reflectance. *International Journal of Remote Sensing*, **11,** 95–111.